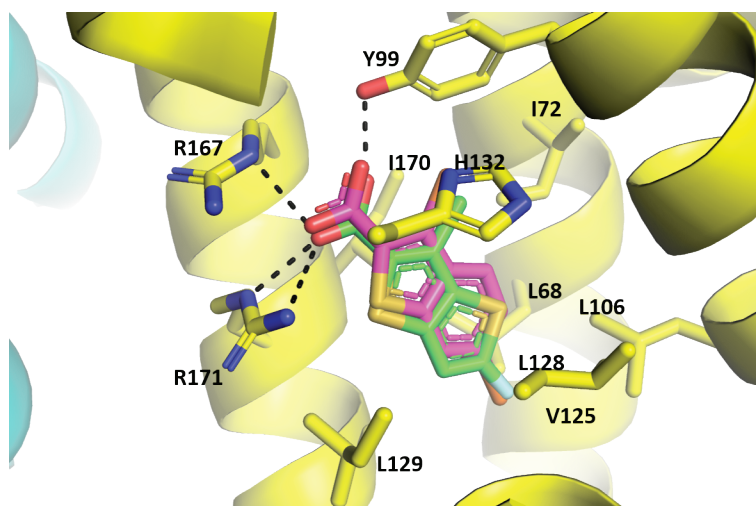


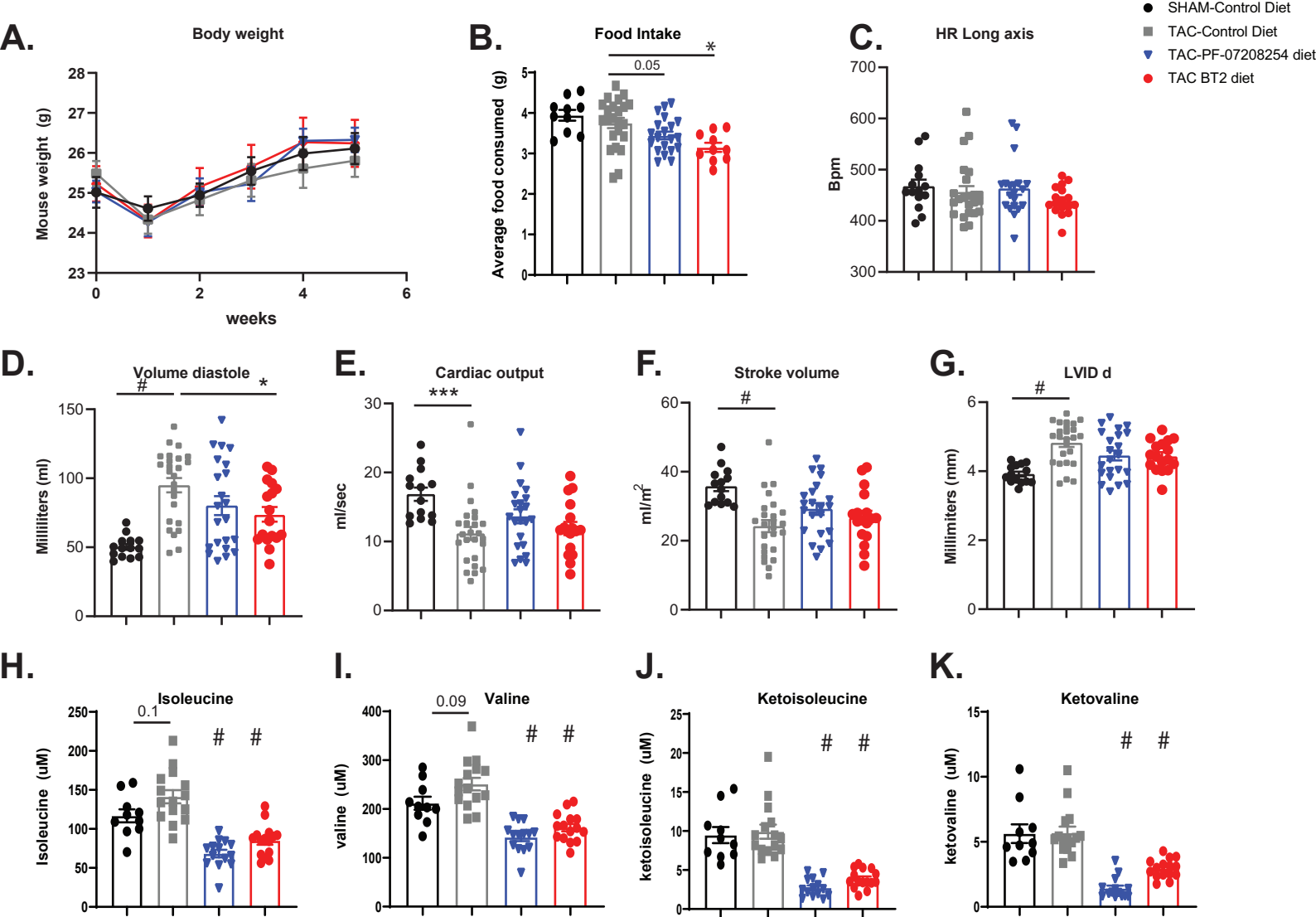
Supplementary Information

Small molecule branched-chain ketoacid dehydrogenase kinase (BDK) inhibitors with opposing effects on BDK protein levels

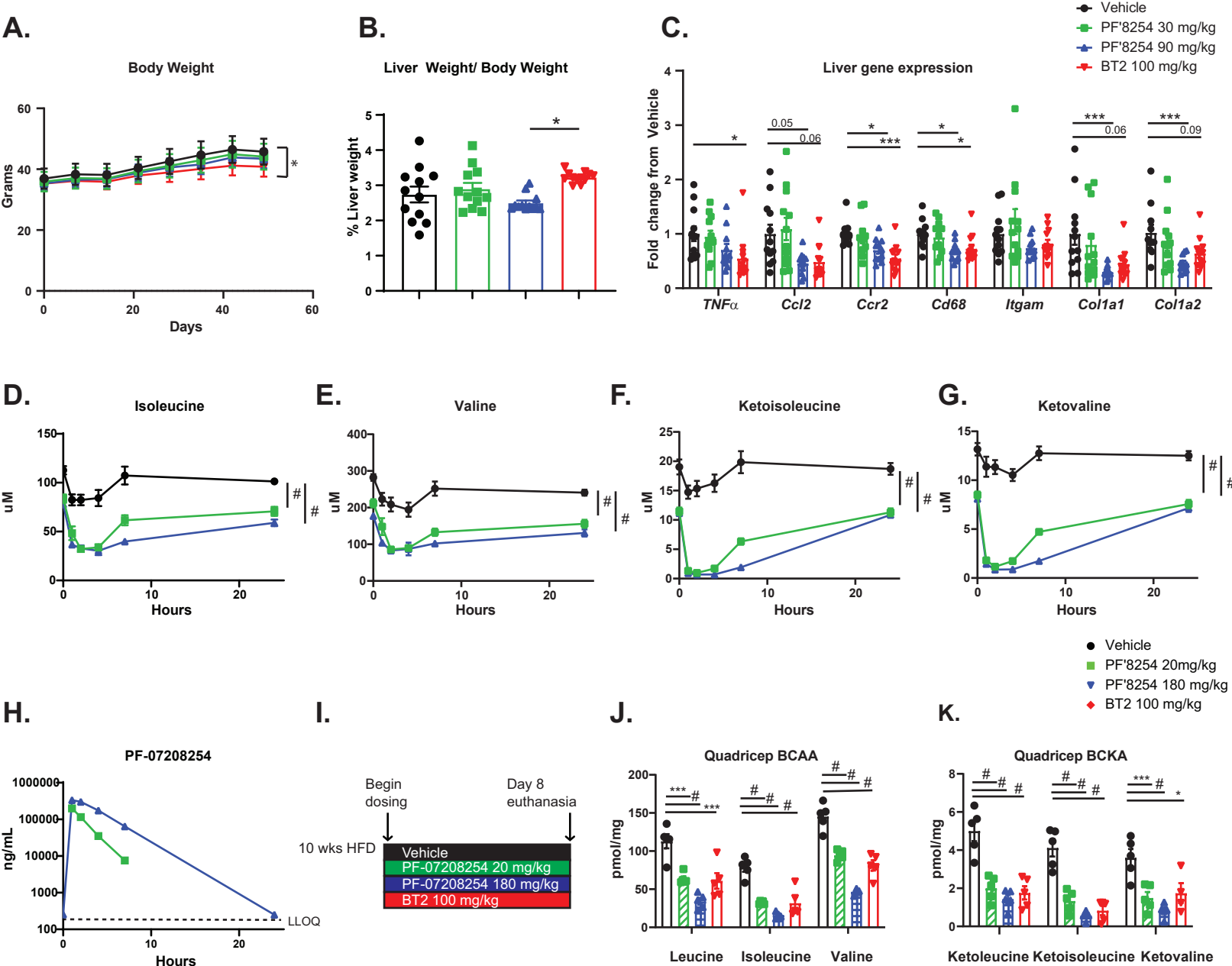
Rachel J. Roth Flach, Eliza Bollinger, Allan R. Reyes, Brigitte Laforest, Bethany L. Kormos, Shenping Liu, Matthew R. Reese, Luis A. Martinez Alsina, Leanne Buzon, Yuan Zhang, Bruce Bechle, Amy Rosado, Parag V. Sahasrabudhe, John Knafels, Samit K. Bhattacharya, Kiyoyuki Omoto, John C. Stansfield, Liam D. Hurley, LouJin Song, Lina Luo, Susanne B. Bretkopf, Mara Monetti, Teresa Cunio, Brendan Tierney, Frank J. Geoly, Jake Delmore, C. Parker Siddall, Liang Xue, Ka N. Yip, Amit S. Kalgutkar, Russell A. Miller, Bei B. Zhang, Kevin J. Filipski



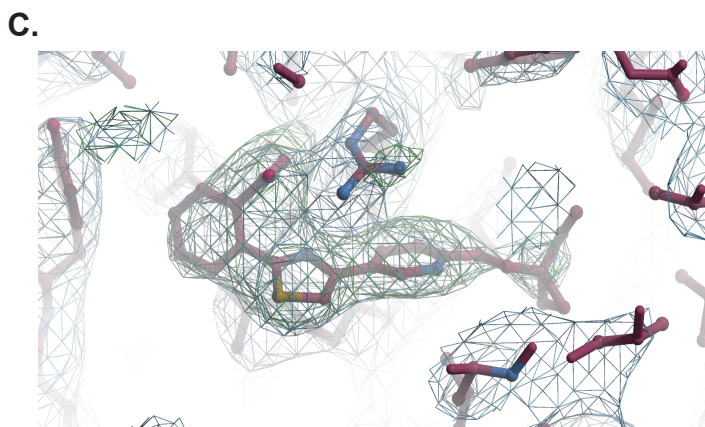
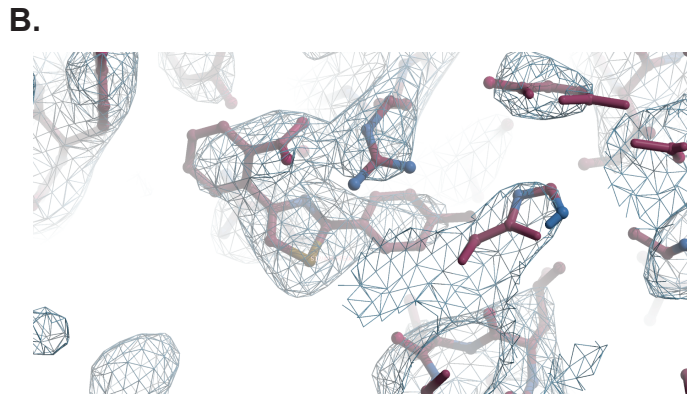
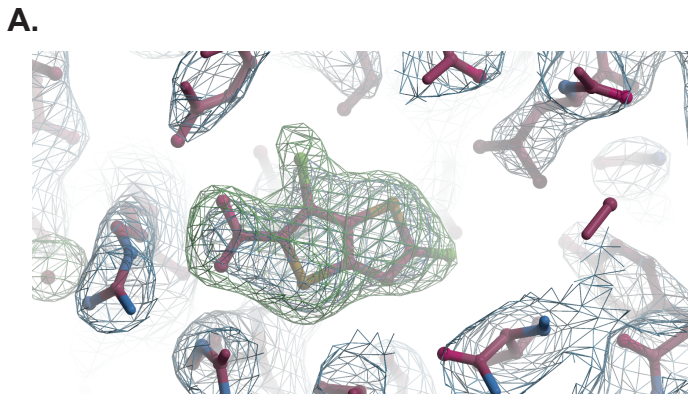
Supplementary Figure 1. Overlay of PF-07208254 and BT2 bound to hBDK from X-ray structures. PF-07208254 is shown in stick model with C atoms colored green. Superimposed is BT2 with C atoms colored in pink. BDK side chains that contact PF-07208254 are shown in sticks. Polar interactions are shown in dash.



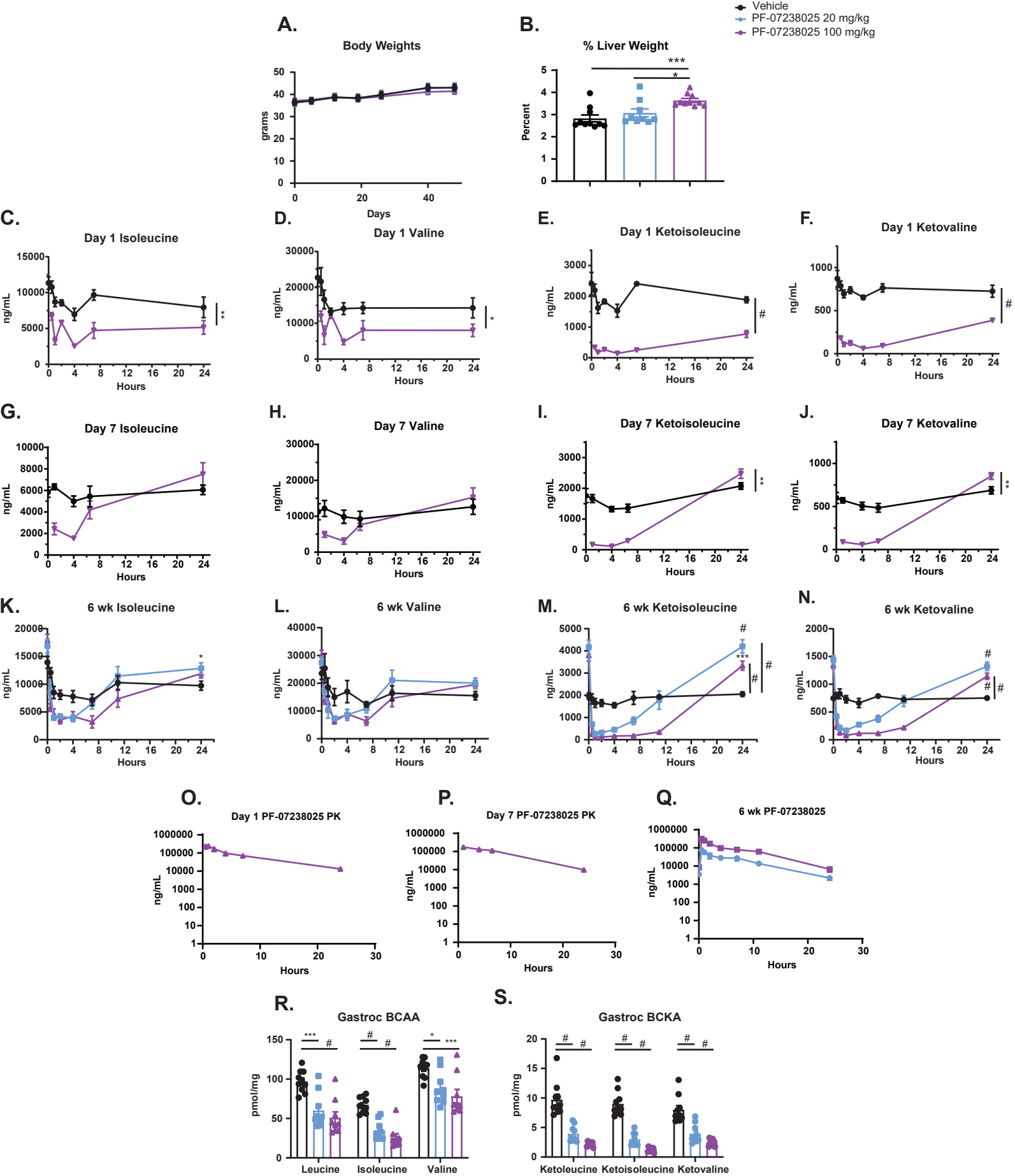
Supplementary Figure 2. PF-07208254 improves cardiac function in a TAC model and reduces BCAA and BCKA. Mice were subjected to TAC surgery as described in Figure 1A. **A.** Body weights throughout the study (N=10-23 animals/group; statistics performed using a longitudinal mixed effects model with a random intercept for each mouse and an AR(1) covariance structure). **B.** Average daily food intake (N=10-23 animals/group; $p=0.010$). **C-G.** Echocardiography endpoints (N=14-26 animals/group). **C.** Heart rate (HR). **D.** Volume at diastole (#; $p<0.0001$, *; $p=0.044$). **E.** Cardiac output (**; $p=0.001$), **F.** Stroke volume (#; $p<0.0001$), **G.** Left ventricular internal diameter at diastole (LVID;d) (#; $p<0.0001$). **H-K.** Plasma BCAA and BCKA were measured at day 38 (N=10-14 animals/group). **H.** Isoleucine (#; $p<0.0001$), **I.** Valine (#; $p<0.0001$), **J.** Ketoisoleucine (#; $p<0.0001$), **K.** Ketovaline (#; $p<0.0001$). Statistics performed for B-K by one-way ANOVA with Tukey post-hoc test. Data represent the mean \pm SEM. Source data are provided as a Source Data file.



Supplementary Figure 3. PF-07208254 improves metabolic endpoints and lowers BCAA/BCKA in HFD-fed mice. Mice were fed HFD and treated with PF-07208254 or BT2 as in Figure 2A. **A.** Body weights throughout the study (N=11-12; a longitudinal mixed effects model with a random intercept for each mouse and an AR(1) covariance structure was fit). **B.** Liver weight was measured as a percentage of body weight (N=12 animals/group; a pairwise Wilcoxon test was performed *; $p=0.014$). **C.** RNA was isolated from livers, and qRT-PCR was performed for several genes (N=12 animals/group; A one-way ANOVA with Tukey HSD test (*ccr2* *; $p=0.043$, ***; $p=0.001$) or a pairwise Wilcoxon test was performed (*tnfa* *; $p=0.017$, *ccl2*, *cd68* *; $p=0.015$, 0.043 , *itgam*, *col1a1* ***; $p=0.004$, *col1a2* ***; $p=0.002$). **D-H.** A PK/PD assessment was performed after 7 weeks of treatment in which mice are dosed with compound and timed bleeds are performed to measure BCAA, BCKA and drug levels (N=6-12 animals/group; a one-way ANOVA with Tukey HSD test was performed for D-G). **D.** Isoleucine (#; $p<0.0001$), **E.** Valine (#; $p<0.0001$), **F.** Ketoisoleucine (#; $p<0.0001$), **G.** Ketovaline (#; $p<0.0001$). **H.** PF-07208254 concentrations. **I-K.** HFD-fed mice were randomized into groups after 10 weeks on diet and treated for 8 days with PF-07208254 or BT2. Quadriceps muscle was isolated one hour post final compound dose, and BCAA and BCKA were measured (N=4-5 animals/group; a one-way ANOVA with Tukey HSD test was performed). **I.** Study design. **J.** BCAA (***; $p=0.001$, #; $p<0.0001$). **K.** BCKA (*; $p=0.019$, ***; $p=0.005$, #; $p<0.0001$). Data represent the mean \pm SEM. Source data are provided as a Source Data file.

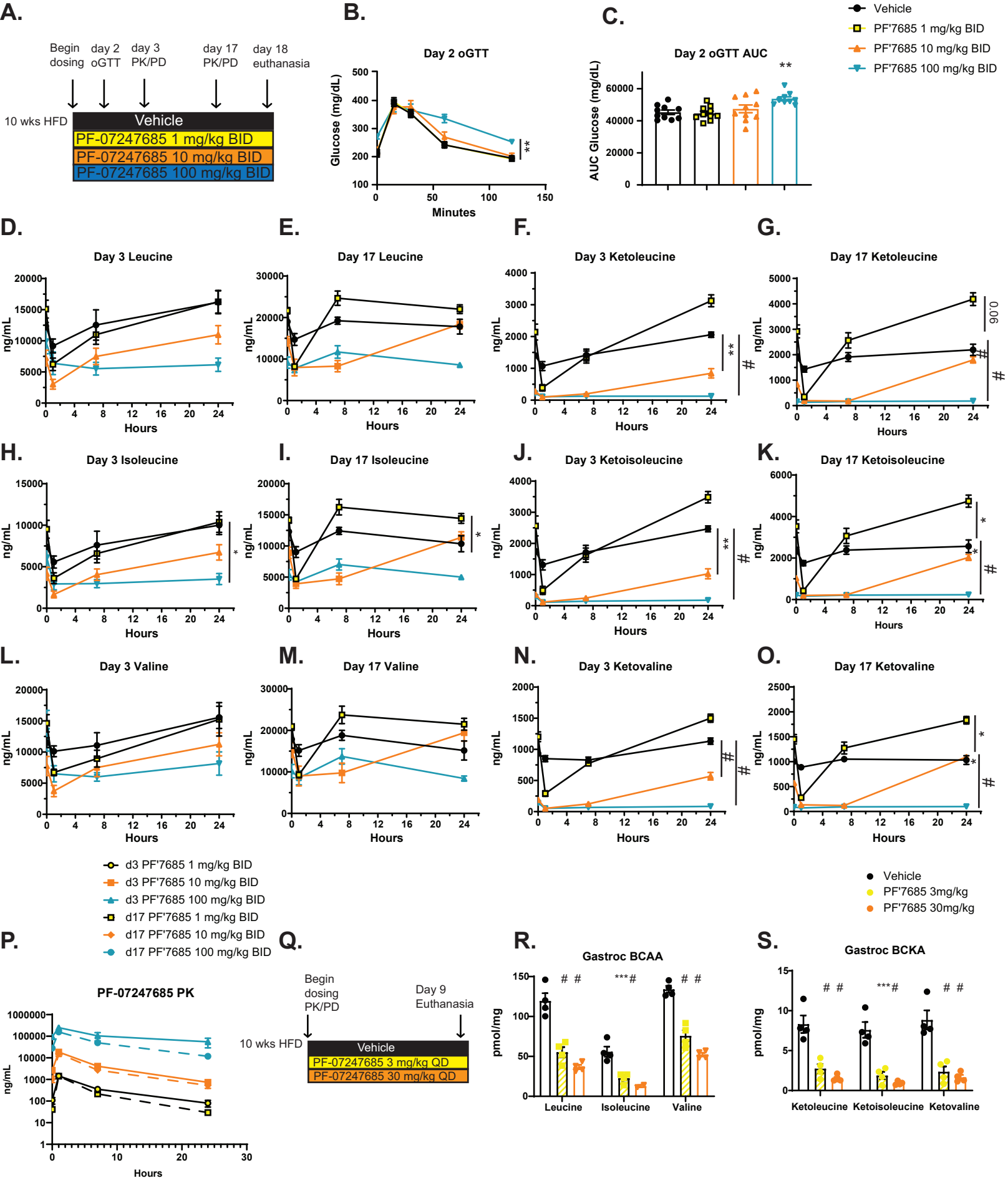


Supplementary Figure 4. OMIT maps for crystal structures. A. OMIT map for PF-07208254. To show model building quality, the final refined model was embedded in initial 2Fo-Fc (blue mesh) and Fo-Fc (green mesh) maps contoured at 1.2σ and 3.0σ , respectively, before the ligand was included in calculation. **B.** OMIT map for **S3**. To show model building quality, the final refined model was embedded in initial 2Fo-Fc (blue mesh) map contoured at 1.2σ , before the ligand was included in calculation. **C.** OMIT map for PF-07247685. To show model building quality, the final refined model was embedded in initial 2Fo-Fc (blue mesh) and Fo-Fc (green mesh) maps contoured at 1.2σ and 3.0σ , respectively, before the ligand was included in calculation.



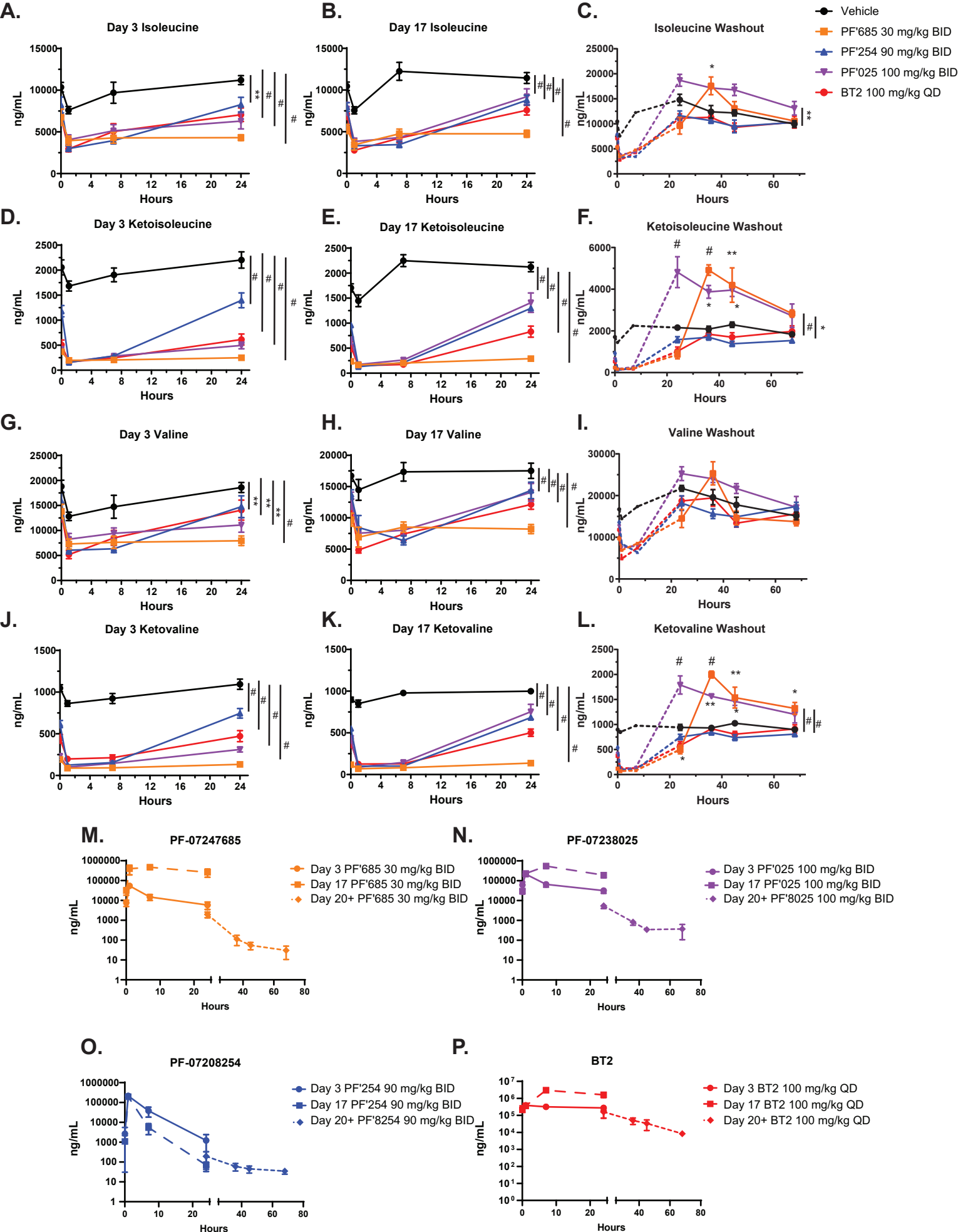
Supplementary Figure 5
Related to Figure 4

Supplementary Figure 5. Thiazole PF-07238025 does not improve metabolic endpoints after day 2, and BCAA/BCKA rebound occurs over time. Mice were fed HFD for 10 weeks, at which time animals were randomized into groups, and treated daily with vehicle or PF-07238025 for 8 weeks as in Figure 4D. **A.** Body weights throughout the study duration (N=9-10 animals/group; a longitudinal mixed effects model with a random intercept for each mouse and an AR(1) covariance structure was fit). **B.** % liver weight at euthanasia (N=9-10 animals/group; a one-way ANOVA with Tukey HSD test was performed, *, $p=0.03$, ***, $p=0.001$). **C-Q.** PK/PD assessments were performed on day 1 (N=4 animals/group), after 7 days (N=4 animals/group), or 6 weeks of treatment (N=5-10 animals/group), in which mice were dosed with compound, and timed bleeds were performed to measure drug levels, BCAA, and BCKA levels, as in Figure 4K-N. **A** one-way ANOVA with Tukey HSD test was performed on AUC and 24 hour time points for each analyte. **C.** Day 1 Isoleucine (**; $p=0.0059$), **D.** Day 1 Valine (*; $p=0.027$), **E.** Day 1 Ketoisoleucine (#; $p=2.16 \times 10^{-6}$), **F.** Day 1 Ketovaline (#; $p=0.0001$), **G.** Day 7 Isoleucine, **H.** Day 7 Valine, **I.** Day 7 Ketoisoleucine (**; $p=0.00055$), **J.** Day 7 Ketovaline (***, $p=0.0046$), **K.** Week 6 Isoleucine (*; $p=0.048$), **L.** Week 6 Valine, **M.** Week 6 Ketoisoleucine (#; $p<0.0001$, ***, $p=0.001$), **N.** Week 6 Ketovaline (#; $p<0.0001$). **O-Q.** Total PF-07238025 concentrations at **O.** Day 1, **P.** Day 7, and **Q.** Week 6. **R-S.** Gastrocnemius muscle was isolated 1 hour post final compound dose, and **R.** BCAA (isoleucine***; $p=0.001$, #; $p<0.0001$, valine***; $p=0.002$, *, $p=0.028$) and **S.** BCKA were measured (#; $p<0.0001$). Data represent the mean \pm SEM. Source data are provided as a Source Data file



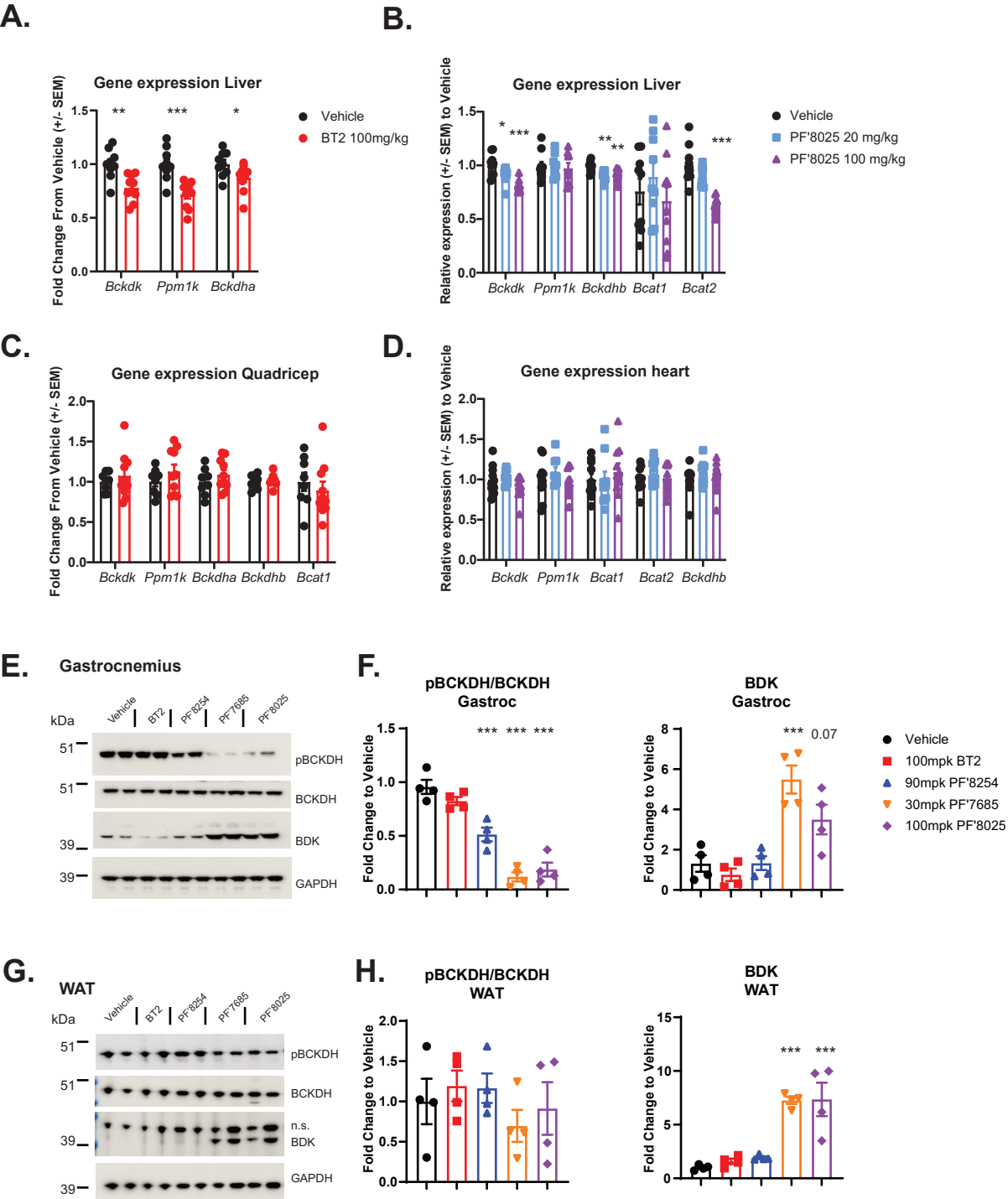
Supplementary Figure 6
Related to Figure 4

Supplementary Figure 6. Thiazole PF-07247685 does not improve glycemia but inhibits BDK and acutely lowers BCKA in plasma and tissues. Mice were fed HFD for 10 weeks, at which time animals were randomized into groups and treated BID with vehicle or PF-07247685 for 18 days. **A.** Study design. **B-C.** An oral glucose tolerance test (oGTT) was performed on day 2 (N=9-10 animals/group; one-way ANOVA with Tukey HSD test was performed on AUC, **, $p=0.008$). **B.** oGTT, **C.** oGTT AUC. **D-P.** PK/PD assessments were performed on days 3 and 17, in which mice were dosed with compound, and timed bleeds were performed to measure drug levels and BCKA levels (N=5 animals/group; one-way ANOVA with Tukey HSD test was performed on AUC in D-O). **D.** Day 3 Leucine, **E.** Day 17 Leucine, **F.** Day 3 Ketoleucine (**; $p=0.006$, #; $p<0.0001$), **G.** Day 17 Ketoleucine (#; $p<0.0001$), **H.** Day 3 Isoleucine (*; $p=0.02$), **I.** Day 17 Isoleucine (*; $p=0.028$), **J.** Day 3 Ketoisoleucine (**; $p=0.001$, #; $p<0.0001$), **K.** Day 17 Ketoisoleucine (*; $p=0.012$, 0.019, #; $p<0.0001$), **L.** Day 3 Valine, **M.** Day 17 Valine, **N.** Day 3 Ketovaline (#; $p=0.0000$), **O.** Day 17 Ketovaline (*; $p=0.01$, 0.023, #; $p<0.0001$), **P.** Total PF-07247685 levels on days 3 and 17. **Q-S.** Mice were fed HFD for 10 weeks, at which time animals were randomized into groups and treated QD with vehicle or PF-07247685 for 9 days. **Q.** Study design. **R-S.** Muscle was harvested one hour post final compound dose, and **R.** BCAA (#; $p<0.0001$, ***, $p=0.001$) and **S.** BCKA (#; $p<0.0001$) were assessed by mass spectrometry (N=2-4 animals/group; one-way ANOVA with Tukey HSD test was performed for statistics). Data represent the mean \pm SEM. Source data are provided as a Source Data file.

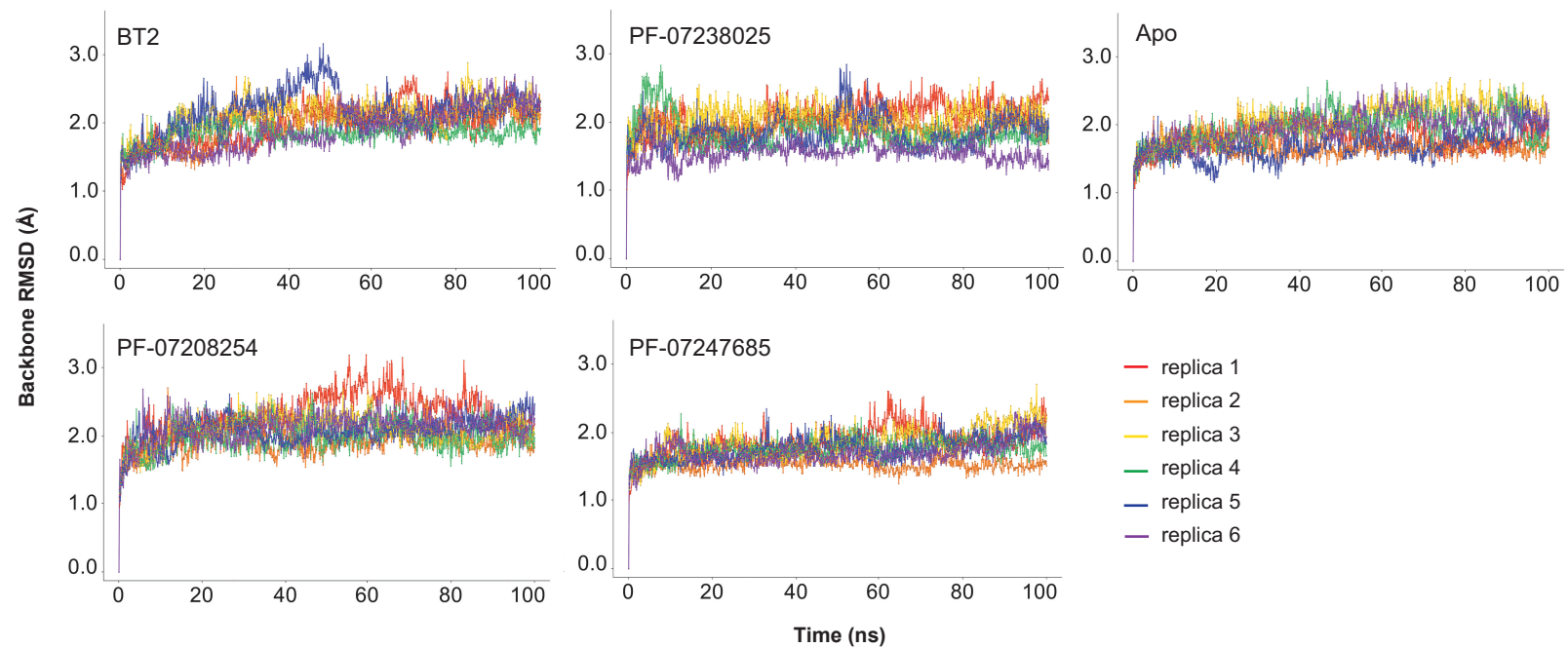
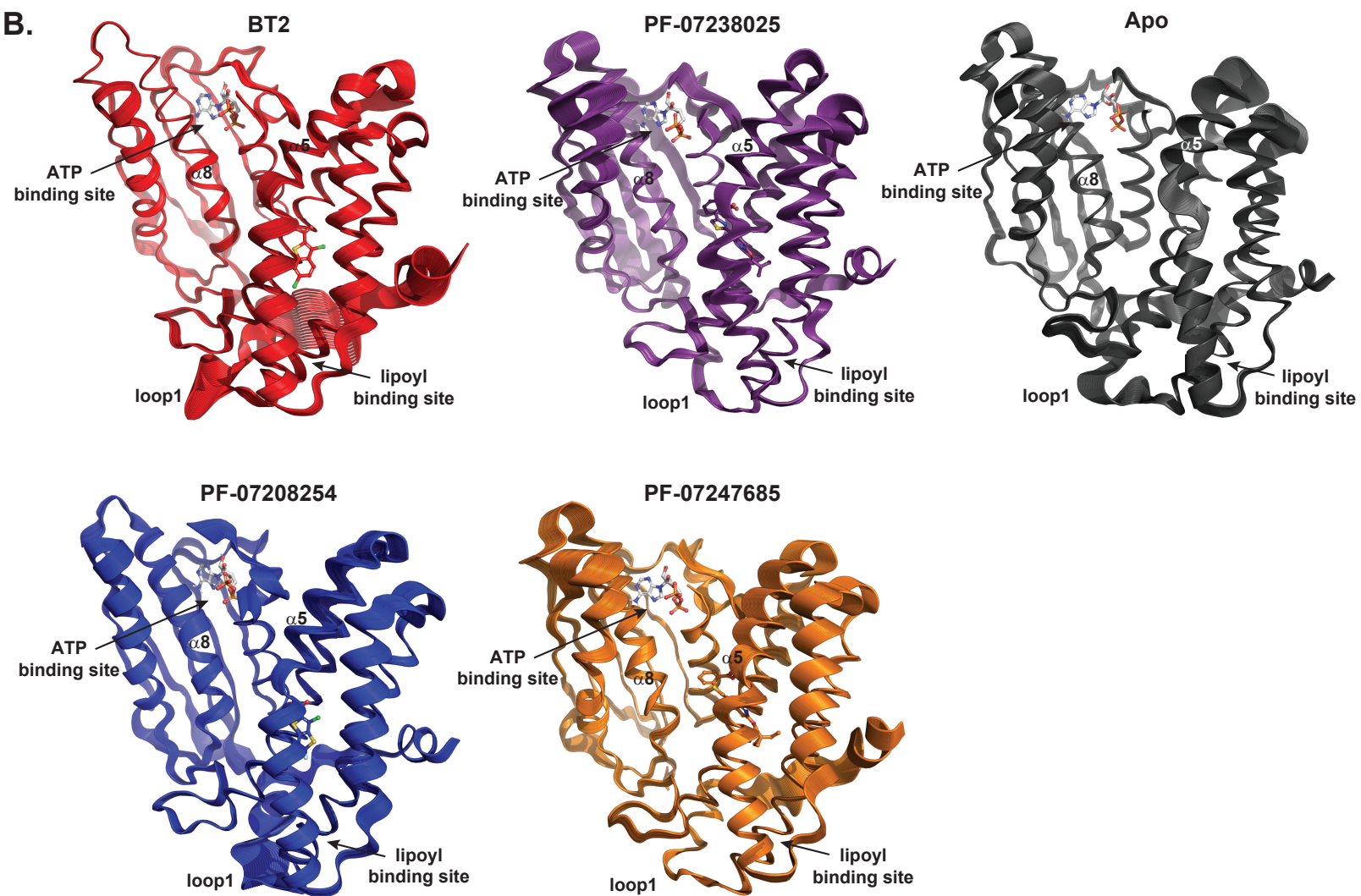


Supplementary Figure 7; Related to Figure 5

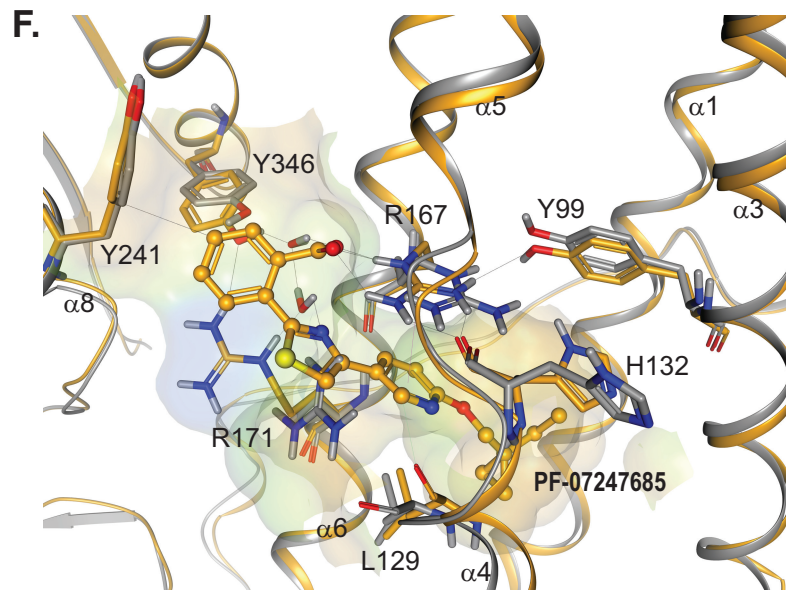
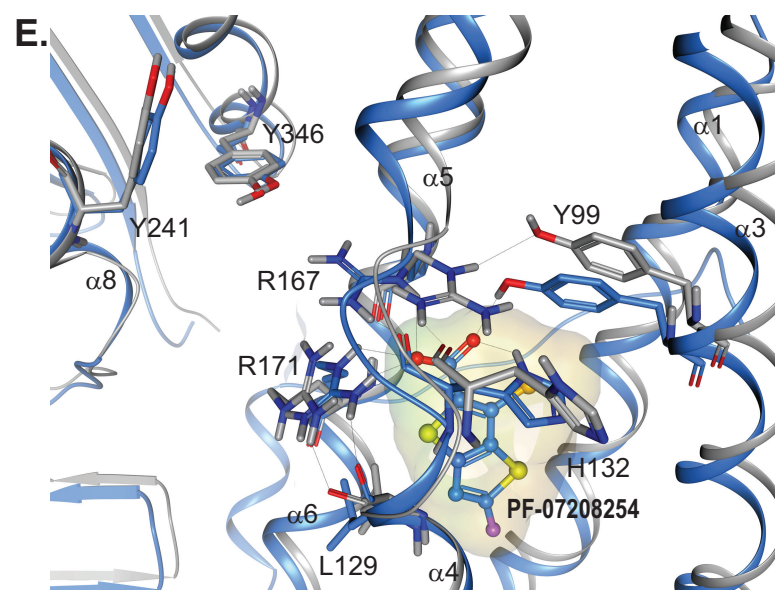
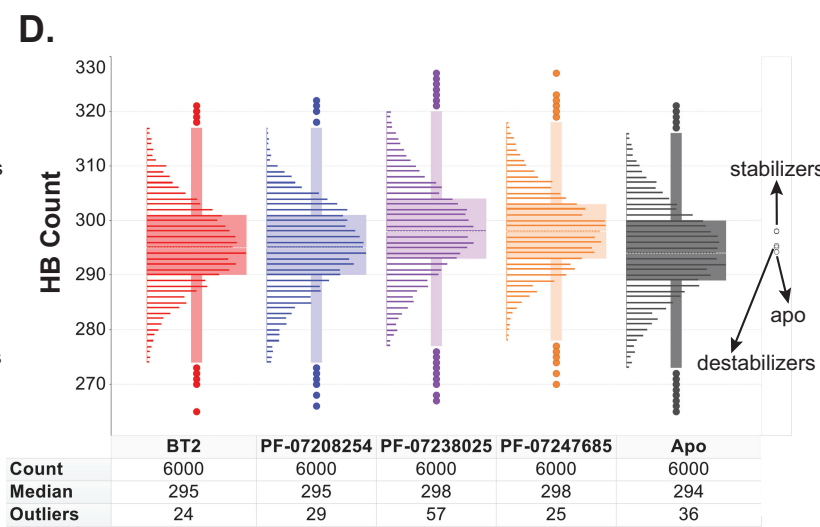
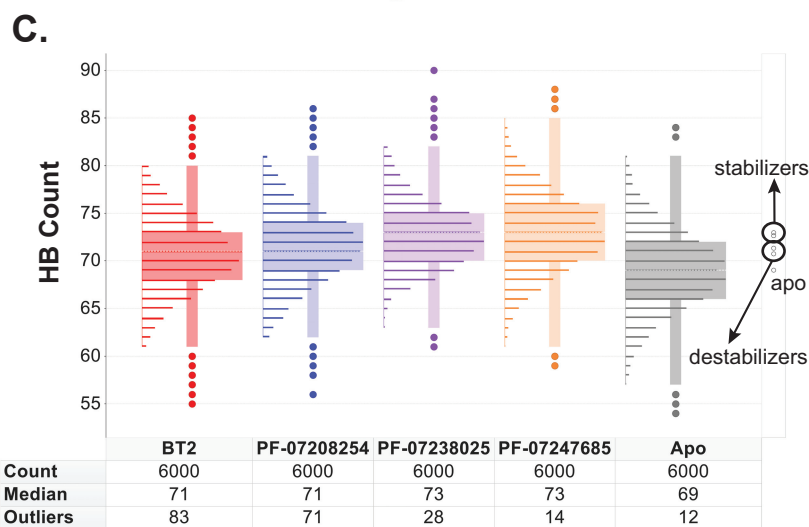
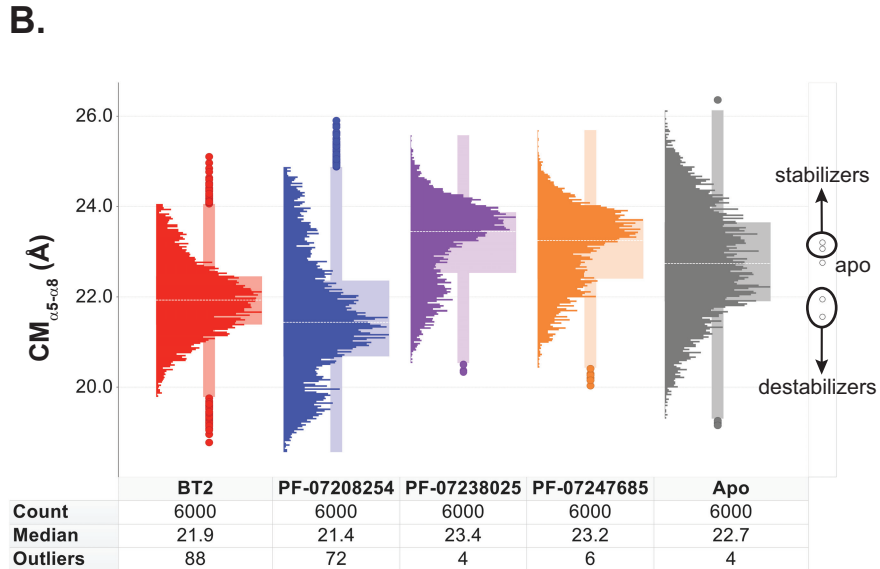
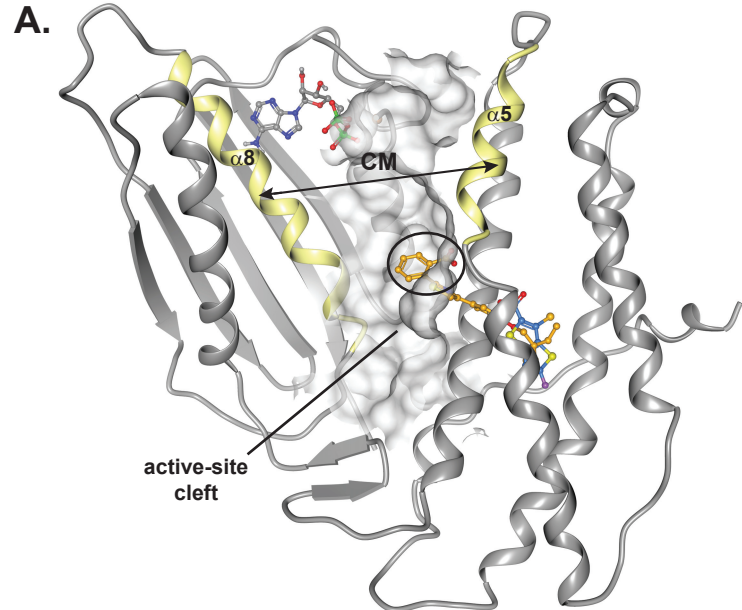
Supplementary Figure 7. Additional BCAA/BCKA and drug levels during study described in Figure 5. Mice were fed HFD for 10 weeks, at which time animals were randomized into groups, and treated BID or QD as indicated with vehicle, BT2, PF-07208254, PF-07247685, or PF-07238025 at maximal inhibitory doses. Mice were bled immediately prior to dosing compound, 1 hour post compound dose, 4 hours post compound dose, 7 hours post compound dose (immediately prior to 2nd daily compound dose if BID dosed), and 24 hours after first compound dose on day 3 and day 17 (N=8-9 animals/group). Washout bleeds were performed at 24, 36, 45 and 68 hours post final compound dose on days 20-22 (N=5 animals/group; a one way ANOVA with Tukey post hoc test was used for statistics on A-L for AUC and 24, 36, 45, 68 h time points). **A.** Isoleucine was measured on day 3 (**; $p=0.008$, #; $p<0.0001$), **B.** day 17 (#; $p<0.0001$), and **C.** upon compound washout (*; $p=0.03$, **; $p=0.001$). **D.** Ketoisoleucine was measured on day 3 (#; $p<0.0001$), **E.** day 17 (#; $p<0.0001$), and **F.** upon compound washout (AUC #; $p<0.0001$, *; $p=0.010$, per time point $p<0.0001$, *; $p=0.010$, 0.018, **; $p=0.003$). **G.** Valine was measured on day 3 (**; $p=0.001$, #; $p<0.0001$), **H.** day 17 (#; $p<0.0001$), and **I.** upon compound washout. **J.** Ketovaline was measured on day 3 (#; $p<0.0001$), **K.** day 17 (#; $p<0.0001$), and **L.** upon compound washout (AUC #; $p<0.0001$, per time point #; $p<0.0001$, **; $p=0.001$, $p=0.002$, *; $p=0.022$, 0.007, 0.03). Dashed lines in panels C,F,I & L represent the 0-7 hour time points from panels B, E, H & K for visualization purposes. Data represent the mean \pm SEM. **M-P.** Drug levels throughout study. **M.** PF-07247685, **N.** PF-07238025, **O.** PF-07208254, **P.** BT2. Solid lines represent day 3, dashed lines day 17, dotted lines are washout days 20-21. Data represent the mean \pm SD. Source data are provided as a Source Data file.



Supplementary Figure 8. BDK mRNA levels not driving BDK protein changes with BT2 or PF-07238025 and BDK protein is upregulated in multiple tissues with thiazoles. A-D. One hour post final compound dose, tissue was harvested. mRNA was isolated, and qPCR was performed from HFD-fed animals that had been treated with BT2 or PF-07238025 (N=8-10 animals/group; a Welch two-sample t-test was performed for statistics). **A.** Liver after BT2 treatment (**; $p=0.001$, ***; $p=0.00047$, *; $p=0.03$). **B.** Liver after PF-07238025 treatment (*; $p=0.041$, **; $p=0.005$, 0.008 ***; $p<0.0001$). **C.** Quadriceps after BT2 treatment. **D.** Heart after PF-07238025 treatment. **E-H.** One hour post final compound dose, tissue was harvested and lysed, and Western blots were performed from HFD-fed animals that had been treated with BT2, PF-07208254, PF-07238025 or PF-07247685 (N=4 animals/group; a one-way ANOVA with Tukey HSD test was performed for statistics). **E.** Gastrocnemius tissue, **F.** Densitometry of **E.** (***; $p<0.0001$) **G.** White adipose tissue (WAT). **H.** Densitometry of **G.** (***; $p<0.0001$) Data represent the mean \pm SEM. *; $p<0.05$; **; $p<0.01$, ***; $p<0.005$. Source data are provided as a Source Data file.

A.**B.**

Supplementary Figure 9. BDK MD trajectories are stable over the course of the simulations; Loop 1 shows dynamic differences. A. Root-mean-square deviation (RMSD) of BDK backbone atoms with respect to the starting structure over six replicas of 100 ns when bound to BT2, PF-07208254, PF-07238025, PF-07247685 and apo. **B.** Visualizations of the first principal component of BDK bound to destabilizers BT2 (red) and PF-07208254 (blue), stabilizers PF-07238025 (purple) and PF-07247685 (orange), and apo (black).

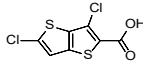
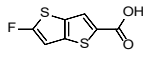
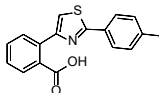


Supplementary Figure 10. BDK active-site cleft narrows and fewer hydrogen bonds are observed with binding of destabilizers and widens with binding of stabilizers. A.

Illustration of active-site cleft (gray surface) where E1 binds and is phosphorylated by BDK, and center-of-mass (CM) distance between helices $\alpha 5$ and $\alpha 8$ (yellow). Stabilizers PF-07238025 (not shown) and PF-07247685 (orange) protrude into the active-site cleft, physically blocking E1 from binding. **B.** Distribution of BDK $CM_{\alpha 5-\alpha 8}$ over MD simulations. **C.** Distribution of the number of hydrogen bonds formed by residues in the BDK lipoyl-binding pocket over the course of MD simulations. **D.** Distribution of the number of hydrogen bonds formed by all BDK residues over the course of MD simulations. **E.** Differences in protein-protein and protein-ligand interactions when BDK is bound to a destabilizer (PF-07208254, blue) compared to apo structure (gray). **F.** Differences in protein-protein and protein-ligand interactions when BDK is bound to a stabilizer (PF-07247685, orange) compared to apo structure (gray).

1 **Supplementary Tables**

2 **Supplementary Table 1. Potency of BDK inhibitors**

Compound	Structure	BDK in vitro IC ₅₀ (nM) ^a	BDK SPR K _D (nM) ^a	Human skeletal myocyte IC ₅₀ (nM) ^a
S1		600 ± 51	75 ± 2.0 ^b	ND ^c
S2		210 ± 10	270 ± 31	930 ± 120
S3		1200 ± 490	5800 ± 4400	>60,000

3 ^aPotency values are ± standard error with an N ≥ 3 except where noted.

4 ^bN = 2

5 ^cNot Determined

6
7

8

9 **Supplementary Table 2. Cerep Bioprint Off-Target Panel**

Target	Format	Single Point Compound Test Concentration (uM) or IC ₅₀ /EC ₅₀	% Inhibition or IC ₅₀ /EC ₅₀		
			PF-07208254	PF-07238025	PF-07247685
Abl Kinase	Kinase Inhibition	10		9	11
Abl Kinase	Kinase Inhibition	100	42		
Acetylcholinesterase	Enzyme Inhibition	10		11	-4
Acetylcholinesterase	Enzyme Inhibition	100	-4		
Adenosine A1 Receptor	Agonism	10		-1	0
Adenosine A1 Receptor	Agonism	100	0		
Adenosine A2a Receptor	Agonism	10		1	1
Adenosine A2a Receptor	Agonism	100	0		
Adrenergic Alpha 1a Adrenoceptor	Agonism	10		-1	1
Adrenergic Alpha 1a Adrenoceptor	Agonism	100	8		
Adrenergic Alpha 1a Adrenoceptor	Antagonism	10		13	14
Adrenergic Alpha 1a Adrenoceptor	Antagonism	100	21		
Adrenergic Alpha 2a receptor	Agonism	10		-2	0
Adrenergic Alpha 2a receptor	Agonism	100	-1		
Adrenergic Alpha 2b Adrenoceptor	Agonism	10		0	-1
Adrenergic Alpha 2b Adrenoceptor	Agonism	100	-4		
Adrenergic Alpha 2b Adrenoceptor	Antagonism	10		9	-1
Adrenergic Alpha 2b Adrenoceptor	Antagonism	100	-2		
Adrenergic Beta 1 Adrenoceptor	Agonism	10		3	6
Adrenergic Beta 1 Adrenoceptor	Agonism	100	2		
Adrenergic Beta 1 Adrenoceptor	Antagonism	10		20	27

Adrenergic Beta 1 Adrenoceptor	Antagonism	100	8		
Adrenergic Beta 2 Adrenoceptor	Agonism	10		4	-6
Adrenergic Beta 2 Adrenoceptor	Agonism	100	-5		
Adrenergic Beta 2 Adrenoceptor	Antagonism	10		8	3
Adrenergic Beta 2 Adrenoceptor	Antagonism	100	10		
AMPA Receptor	Ion Channel Binding	10		-13	5
AMPA Receptor	Ion Channel Binding	100	7		
Androgen Receptor	NHR Binding	10		-6	-8
Androgen Receptor	NHR Binding	100	-4		
Angiotensin 1	Agonism	10		-4	-8
Angiotensin 1	Agonism	100	3		
Angiotensin 1	Antagonism	10		-1	5
Angiotensin 1	Antagonism	100	18		
Angiotensin Converting Enzyme	Enzyme Inhibition	10		-33	-31
Angiotensin Converting Enzyme	Enzyme Inhibition	100	-4		
Aurora A Kinase	Kinase Inhibition	10		-8	-7
Aurora A Kinase	Kinase Inhibition	100	15		
Cannabinoid CB1	Agonism	10		32	39
Cannabinoid CB1	Agonism	100	55		
Cannabinoid CB1	Agonism	EC ₅₀	180,000 nM		
Cannabinoid CB1	Antagonism	10		-1	-4
Cannabinoid CB1	Antagonism	100	-10		
Cholecystokinin 2	Agonism	10		2	-8
Cholecystokinin 2	Agonism	100	0		
Choline Transporter	Transporter Binding	10		-8	-12
Choline Transporter	Transporter Binding	100	-15		
Corticotrophin Releasing Factor 1 (CRF1) Receptor	Agonism	10		-1	4
Corticotrophin Releasing Factor 1 (CRF1) Receptor	Agonism	100	-2		
Corticotrophin Releasing Factor 1 (CRF1) Receptor	Antagonism	10		32	11
Corticotrophin Releasing Factor 1 (CRF1) Receptor	Antagonism	100	39		
Cyclooxygenase 2	Enzyme Inhibition	10		3	4
Cyclooxygenase 2	Enzyme Inhibition	100	0		
Delta Opioid Receptor	Agonism	10		-2	-1
Delta Opioid Receptor	Agonism	100	-2		
Dopamine 2S	Agonism	10		-6	-17
Dopamine 2S	Agonism	100	-29		
Dopamine 2S	Antagonism	10		3	-7
Dopamine 2S	Antagonism	100	-7		
Dopamine D1	Agonism	10		1	4
Dopamine D1	Agonism	100	-4		
Dopamine D1	Antagonism	10		10	5
Dopamine D1	Antagonism	100	-5		
Dopamine Transporter	Transporter Binding	10		-4	-1
Dopamine Transporter	Transporter Binding	100	7		
EGFR Kinase	Kinase Inhibition	10		-1	-6
EGFR Kinase	Kinase Inhibition	100	19		
Endothelin A	Agonism	10		-1	-4
Endothelin A	Agonism	100	4		
GABA Transporter	Transporter Binding	10		-9	-8
GABA Transporter	Transporter Binding	100	0		
GABAa (benzodiazepine site)	Ion Channel Binding	10		-14	13

GABAa (benzodiazepine site)	Ion Channel Binding	100	-9		
GABAa (Cl Channel)	Ion Channel Binding	10		11	19
GABAa (Cl Channel)	Ion Channel Binding	100	19		
GABAa1 Receptor	Ion Channel Binding	10		-28	-21
GABAa1 Receptor	Ion Channel Binding	100	-12		
Glucocorticoid Receptor	NHR Binding	10		-2	0
Glucocorticoid Receptor	NHR Binding	100	4		
Histamine H1	Agonism	10		-4	-5
Histamine H1	Agonism	100	-1		
Histamine H1	Antagonism	10		13	-2
Histamine H1	Antagonism	100	17		
Histamine H2	Agonism	10		2	1
Histamine H2	Agonism	100	0		
Histamine H3	Agonism	10		28	4
Histamine H3	Agonism	100	15		
Kappa Opioid	Agonism	10		-18	-7
Kappa Opioid	Agonism	100	-3		
Kdr Kinase (VEGFR2)	Kinase Inhibition	10		5	-11
Kdr Kinase (VEGFR2)	Kinase Inhibition	100	57		
Kdr Kinase (VEGFR2)	Kinase Inhibition	IC ₅₀	76,000 nM		
LCK Kinase	Kinase Inhibition	10		0	-2
LCK Kinase	Kinase Inhibition	100	-4		
L-Type Ca2+ Channel (dihydropyridine site)	Ion Channel Binding	10		-8	-2
L-Type Ca2+ Channel (dihydropyridine site)	Ion Channel Binding	100	1		
L-Type Ca2+ Channel (diltiazem site)	Ion Channel Binding	10		-30	24
L-Type Ca2+ Channel (diltiazem site)	Ion Channel Binding	100	-8		
L-Type Ca2+ Channel (verapamil site)	Ion Channel Binding	10		-3	1
L-Type Ca2+ Channel (verapamil site)	Ion Channel Binding	100	-6		
Melanocortin MC2 Receptor	Agonism	10		0	0
Melanocortin MC2 Receptor	Agonism	100	0		
Melanocortin MC2 Receptor	Antagonism	10		39	18
Melanocortin MC2 Receptor	Antagonism	100	-4		
Monoamine Oxidase A	Enzyme Inhibition	10		13	12
Monoamine Oxidase A	Enzyme Inhibition	100	0		
Mu Opioid	Antagonism	10		-9	-3
Mu Opioid	Antagonism	100	2		
Mu Opioid	Agonism	10		-1	-3
Mu Opioid	Agonism	100	16		
Muscarinic 1	Agonism	10		-1	1
Muscarinic 1	Agonism	100	-1		
Muscarinic 1	Antagonism	10		14	9
Muscarinic 1	Antagonism	100	0		
Muscarinic 2	Agonism	10		21	3
Muscarinic 2	Agonism	100	39		
Muscarinic 2	Antagonism	10		-12	2
Muscarinic 2	Antagonism	100	-7		
Muscarinic 3	Agonism	10		-5	-1
Muscarinic 3	Agonism	100	0		
Muscarinic 3	Antagonism	10		7	3
Muscarinic 3	Antagonism	100	18		

Na+ Channel (site 2)	Ion Channel Binding	10		-2	31
Na+ Channel (site 2)	Ion Channel Binding	100	-2		
Neurokinin Nk1	Agonism	10		-2	-4
Neurokinin Nk1	Agonism	100	-3		
Nicotinic Acetylcholine Receptor	Ion Channel Binding	10		1	-1
Nicotinic Acetylcholine Receptor	Ion Channel Binding	100	-12		
Nicotinic Acetylcholine Receptor (alpha4, beta2 subunit containing)	Ion Channel Binding	10		-2	-4
Nicotinic Acetylcholine Receptor (alpha4, beta2 subunit containing)	Ion Channel Binding	100	-6		
NMDA Receptor (glutamate site)	Ion Channel Binding	10		-2	-5
NMDA Receptor (glutamate site)	Ion Channel Binding	100	3		
NMDA Receptor (PCP binding site)	Ion Channel Binding	10		-2	0
NMDA Receptor (PCP binding site)	Ion Channel Binding	100	-13		
Norepinephrine Transporter	Transporter Binding	10		-11	6
Norepinephrine Transporter	Transporter Binding	100	-15		
P38alpha MAP Kinase	Kinase Inhibition	10		2	3
P38alpha MAP Kinase	Kinase Inhibition	100	35		
Phosphodiesterase 3B	Enzyme Inhibition	10		5	-16
Phosphodiesterase 3B	Enzyme Inhibition	100	-9		
Phosphodiesterase 4D2	Enzyme Inhibition	10		12	-24
Phosphodiesterase 4D2	Enzyme Inhibition	100	-11		
PPAR-gamma	NHR Binding	10		10	21
PPAR-gamma	NHR Binding	100	62		
PPAR-gamma	NHR Binding	IC ₅₀	86,000 nM	26,000 nM	50,000 nM
Serotonin 5-HT1a Receptor	Agonism	10		-2	-1
Serotonin 5-HT1a Receptor	Agonism	100	-1		
Serotonin 5-HT1b Receptor	Agonism	10		-3	34
Serotonin 5-HT1b Receptor	Agonism	100	39		
Serotonin 5-HT2a	Agonism	10		0	3
Serotonin 5-HT2a	Agonism	100	-5		
Serotonin 5-HT2b	Agonism	10		4	-5
Serotonin 5-HT2b	Agonism	100	-5		
Serotonin 5-HT3	Ion Channel Binding	10		-9	0
Serotonin 5-HT3	Ion Channel Binding	100	-14		
Serotonin 5-HT4e	Agonism	10		2	0
Serotonin 5-HT4e	Agonism	100	6		
Serotonin Transporter	Transporter Binding	10		-10	2
Serotonin Transporter	Transporter Binding	100	-3		
Src Kinase	Kinase Inhibition	10		5	-8
Src Kinase	Kinase Inhibition	100	11		
Thyrotropin Releasing Hormone 1 (TRH1) Receptor	Agonism	10		-2	4
Thyrotropin Releasing Hormone 1 (TRH1) Receptor	Agonism	100	4		
Thyrotropin Releasing Hormone 1 (TRH1) Receptor	Antagonism	10		20	10
Thyrotropin Releasing Hormone 1 (TRH1) Receptor	Antagonism	100	-5		
Vasopressin 1a	Agonism	10		-1	-1
Vasopressin 1a	Agonism	100	16		

10

11 Key compounds were tested against a broad off-target panel to determine selectivity for BDK
12 activity. PF-07238025 and PF-07247685 were tested in single point at 10 µM. Because of its
13 weaker activity PF-07208254 was tested in single point at 100 µM. No targets showed >50%

14 activity for PF-07238025 and PF-07247685. Three targets (shaded in table) showed >50% activity
 15 @ 100 μ M for PF-07208254. These were followed up with dose response curves and
 16 demonstrated high micromolar activity. Because of the weak activity and large margins between
 17 BDK potency and these off-target potencies, pharmacology due to these off-targets in not
 18 anticipated within the context of the included experiments.

19

20 **Supplementary Table 3. Kinase Off-Target Panel**

Target	ATP = Km % Inhibition @ 10 μ M			ATP = 1 mM % Inhibition @ 10 μ M		
	PF-07208254	PF-07238025	PF-07247685	PF-07208254	PF-07238025	PF-07247685
ABL Proto-Oncogene 1 Non-receptor Tyrosine Kinase (ABL1)	9.0	7.0	5.1	-0.5	3.8	0.9
Aurora Kinase A (AURKA)	9.4	5.8	8.9	-2.6	0.6	2.2
Bruton agammaglobulinemia Tyrosine Kinase (BTK)	5.9	5.4	-0.7	0.8	-3.6	3.1
Cyclin Dependent Kinase 1 (CDK2/Cyclin-A)	14.6	3.4	1.2	-1.2	2.9	-1.4
Checkpoint Kinase 1 (CHEK1)	4.6	3.8	-3.1	4.3	1.5	4.5
Checkpoint Kinase 2 (CHEK2)	6.7	-2.7	3.8	-0.7	1.0	-0.2
Casein Kinase 1 delta (CKI-delta)	9.1	2.3	6.0	NT	NT	NT
MAP Kinase Interacting serine/threonine Kinase 1 (MKNK1)	15.1	-2.3	0.5	NT	NT	NT
NUAK family, SNF1-like kinase, 1 (NUAK1)	10.3	1.4	-18.2	NT	NT	NT
DNA-activated, catalytic polypeptide protein kinase (PRKDC)	8.3	-4.7	5.4	NT	NT	NT
CSK tyrosine Kinase	2.9	4.8	4.3	NT	NT	NT
C-terminal Src Kinase (v-src sarcoma (Schmidt-Ruppin A-2) viral oncogene homolog (avian) (SRC)	5.6	6.6	17.3	-4.8	7.8	-1.0
Epidermal Growth Factor Receptor (erythroblastic leukemia viral (v-erb)	-0.9	3.9	-2.6	-7.2	-2.3	1.2
EPH Receptor A2 (EPHA2)	0.5	7.0	0.6	-5.6	4.7	5.6
ERBB-4 receptor protein tyrosine kinase (Tyrosine kinase-type cell surface receptor HER4)	-11.4	1.4	7.2	NT	NT	NT
Fibroblast Growth Factor Receptor 1 (FGFR1)	-0.5	6.4	8.8	-0.5	3.3	2.1
Glycogen Synthase Kinase 3 Beta (GSK3B)	9.7	4.0	11.0	0.7	1.6	3.7
Tyrosine-protein kinase HCK (Haemopoietic cell kinase)	9.9	5.6	4.5	NT	NT	NT
I κ B kinase beta subunit (IKK BETA)	4.8	1.0	-0.0	NT	NT	NT
Insulin Receptor (INSR)	3.1	5.9	3.4	0.0	4.4	-0.4
Interleukin 1 Receptor Associated Kinase 4 (IRAK4)	6.2	3.4	-0.9	-2.1	5.7	2.9
Janus Kinase 3 (JAK3)	0.9	0.4	0.8	-4.1	-1.7	-0.0
Kinase Insert Domain Receptor (a type III receptor tyrosine kinase) (KDR, VEGFR2)	1.1	4.1	2.0	5.6	3.0	0.1
LCK Proto-Oncogene Src Family Tyrosine Kinase, lymphocyte-specific protein kinase (LCK)	20.6	8.1	5.9	9.9	8.5	3.0
Mitogen-Activated Protein Kinase 1 (MAPK1)	9.4	0.3	7.0	2.8	5.2	2.4

Mitogen-Activated Protein Kinase-Activated Protein Kinase 2 (MAPKAPK2)	3.4	-0.3	2.2	-1.5	4.4	3.3
MAP/Microtubule Affinity Regulating Kinase 1 (MARK1)	2.1	6.0	4.3	8.4	2.4	7.5
MET Proto-Oncogene Receptor Tyrosine Kinase (hepatocyte growth factor receptor) (MET)	-3.1	2.8	-0.3	-10.2	-2.7	-2.2
Misshapen-like Kinase 1 (zebrafish)	-3.3	19.7	21.9	NT	NT	NT
Mitogen and stress-activated protein kinase-1 (MSK1)	2.7	1.5	-1.4	NT	NT	NT
Serine/Threonine Kinase 3 (STE20 homolog, yeast) (STK3)	5.5	-9.3	-1.8	-2.3	-1.7	-7.6
NEK6	7.1	6.5	1.2	NT	NT	NT
Ribosomal protein S6 kinase	2.5	3.5	2.7	NT	NT	NT
p21 protein (Cdc42/Tac)-activated kinase 4 (PAK4)	6.0	4.2	8.3	0.9	2.8	3.7
Proto-oncogene kinase PIM-1	44.5	-2.6	-2.6	NT	NT	NT
Pim-2 Proto-Oncogene Serine/Threonine Kinase (PIM2)	22.3	-8.4	0.1	-5.2	1.3	0.9
Protein Kinase cAMP-dependent, Catalytic Subunit Alpha (PRKACA)	2.7	3.2	2.3	-2.4	2.6	0.3
AKT Kinase (Protein Kinase B), v-akt murine thymoma viral oncogene homolog 1 (AKT1)	6.7	2.2	2.4	-0.8	-0.6	-0.8
MAP kinase activated protein kinase 5 (MAPKAPK5)	6.6	1.4	2.3	NT	NT	NT
Rho Associated, Coiled-Coil Containing Protein Kinase 1 (ROCK1)	3.6	-0.8	2.4	0.8	-1.1	-0.9
Rho kinase (ROCK2)	-5.8	-3.5	5.5	NT	NT	NT
Ribosomal protein S6 kinase II alpha 1 (Rsk1)	3.3	1.2	2.4	NT	NT	NT
Ribosomal protein S6 kinase II alpha 3 (Rsk2)	-0.7	-11.1	-1.6	NT	NT	NT
Mitogen-activated protein kinase 12 (MAPK12/ERK6/P38 gamma)	13.3	5.6	4.6	NT	NT	NT
Mitogen-activated protein kinase 13 (MAPK13/P38 gamma)	3.6	0.1	-0.7	NT	NT	NT
Serum/Glucocorticoid Regulated Kinase 1 (SGK1)	-0.1	-11.1	0.7	1.9	-12.3	-5.1
Serine kinase SRPK1	2.8	30.4	12.6	NT	NT	NT
TEK Receptor Tyrosine Kinase, endothelial (TEK)	0.3	3.6	0.6	0.7	3.6	8.6
Neurotrophic Receptor Tyrosine Kinase, type 1 (NTRK1)	5.6	9.6	14.5	5.8	15.5	10.0
Eukaryotic elongation factor-2 kinase	2.3	0.9	-1.5	NT	NT	NT
Mitogen-activated protein kinase kinase kinase 9 (MAPK3K9) (mixed lineage kinase 1)	3.2	-1.1	6.3	NT	NT	NT
RAC-beta serine/threonine kinase (AKT2 kinase)	0.2	1.5	5.5	NT	NT	NT
TAO Kinase 2 (TAOK2)	-2.5	-0.4	-4.7	1.4	-1.0	-1.8
Aurora kinase B (AURKB)	3.0	9.9	17.3	NT	NT	NT
Calcium/Calmodulin Dependent Protein Kinase II Alpha (CAMK2A)	6.8	-0.5	2.8	-0.3	-0.8	3.5
Casein Kinase 1 Alpha 1 (CSNK1A1)	9.2	1.6	3.1	-0.6	3.8	2.1
Casein Kinase 2 Alpha prime polypeptide (CSNK2A2)	24.5	2.1	7.5	7.3	0.9	1.9
Dual-specificity tyrosine-(Y)-phosphorylation regulated kinase (DYRK)	11.8	7.1	2.1	NT	NT	NT
FKBP-rapamycin associated protein (FRAP, mTOR)	5.1	-0.1	0.4	NT	NT	NT

Mitogen-Activated Protein Kinase Kinase Kinase 4 (MAPK4K4)	11.9	17.2	25.5	-7.5	-0.7	3.2
Serine/Threonine-Protein Kinase MASK (MST4)	16.7	5.9	2.9	3.7	0.1	-2.9
Myosin Light Chain Kinase 2 (MYLK2)	-3.6	1.1	1.4	-0.1	-1.6	1.7
Phosphorylase B kinase gamma catalytic chain skeletal muscle isoform	1.8	0.8	2.2	NT	NT	NT
PLK1 kinase	1.8	3.0	10.1	NT	NT	NT
Phosphatidylinositol 4-kinase, catalytic, beta (PI4KB)	7.9	3.1	7.1	NT	NT	NT
Phosphatidylinositol-3-kinase, class 3 (PIK3C3)	7.3	4.0	3.0	NT	NT	NT
Phosphatidylinositol-3-kinase, catalytic, delta polypeptide (PIK3CD)	6.4	12.2	-7.0	NT	NT	NT
Sphingosine kinase 1 (SPHK1)	-15.9	-86.4	-82.5	NT	NT	NT
3-phosphoinositide dependent protein kinase-1 (PDPK1)	-3.2	1.3	-0.6	-3.1	0.8	2.0
Phosphatidylinositol-3-kinase, class 2, alpha polypeptide (PIK3C2A)	2.6	-11.1	-4.2	NT	NT	NT
Phosphatidylinositol-3-kinase, catalytic, beta polypeptide (PIK3CB)	3.1	-3.0	-3.5	NT	NT	NT
Phosphatidylinositol-3-kinase, catalytic, gamma polypeptide (PIK3CG)	4.8	-1.5	-4.6	NT	NT	NT
Phosphatidylinositol-3-kinase, class 2, alpha polypeptide (PIK3C2A)	1.6	-6.3	5.5	NT	NT	NT
Mitogen-Activated Protein Kinase 14 (MAPK14)	3.0	0.5	3.5	4.0	-3.7	7.1
MAP/microtubule affinity-regulating kinase 3 (MARK3)	5.0	3.1	2.1	NT	NT	NT
Protein kinase, DNA-activated, catalytic polypeptide (PRKDC)	8.3	-4.7	5.4	NT	NT	NT
Protein kinase C, alpha (PRKCA)	3.8	-2.0	14.8	NT	NT	NT
Protein kinase C, beta II isoform (PRKCB2)	-1.7	2.6	9.4	1.9	-1.7	4.0
ATP = 10 uM						
% Inhibition @ 10 uM						
Target	PF-07208254	PF-07238025	PF-07247685			
Phosphatidylinositol 4-kinase, catalytic, alpha (PI4KA)	8.2	2.6	-3.1			
Phosphatidylinositol-3-kinase, class 2, beta polypeptide (PIK3C2B)	3.5	-6.7	2.0			
Sphingosine kinase 2 (SPHK2)	-11.8	-9.4	3.9			
ATP = 100 uM						
% Inhibition @ 10 uM						
Mitogen-activated protein kinase 8 (MAPK8 / JNK1)	-0.6	-0.2	2.1			
Mitogen-activated protein kinase 9 (MAPK9 / JNK2)	-3.0	5.4	4.3			
MEK1	4.1	10.1	11.2			
Calcium/calmodulin-dependent protein kinase I (CAMK1)	-7.9	-3.7	-5.1			
Lantha Binding						
% Inhibition @ 10 uM						
TTK protein kinase (TTK)	16.2	4.1	3.6			

Calcium/calmodulin-dependent protein kinase kinase 2, beta (CAMKK2)	7.8	1.8	1.8
Myosin light chain kinase (MYLK)	3.3	1.0	1.3
MAP kinase interacting serine/threonine kinase 2 (MKNK2)	11.8	-2.1	1.2
TGF-beta activated kinase 1/MAP3K7 binding protein 1 (MAP3K7IP1)	2.6	3.6	-1.9
Mitogen-activated protein kinase kinase kinase 11 (MAP3K11)	6.8	-3.5	-2.2
Protein kinase N2 (PKN2)	8.1	4.1	-1.7
Protein kinase, AMP-activated, alpha 1 beta 1 gamma 2 complex (PRKA A1)	5.9	-1.8	0.5
Dual-specificity tyrosine-(Y)-phosphorylation regulated kinase 2 (DYRK)	29.2	13.3	1.9
Mitogen-activated protein kinase 15 (MAPK15)	18.3	-4.9	2.4
Transforming growth factor, beta receptor II (70/80kDa) (TGFB2)	15.9	4.7	15.1

21

22 Key compounds were tested against multiple Invitrogen kinase panels, which included 96 kinases,
 23 to determine kinase selectivity. PF-07208254, PF-07238025, and PF-07247685 were tested at
 24 10 μ M compound concentration for % inhibition of select protein and lipid kinases at the ATP
 25 concentrations noted in the table. Several other kinases were probed for inhibition of binding in a
 26 Lantha screen format assay as noted in the table. All % inhibition values were < 30% with the
 27 exceptions (shaded in table) of PF-07208254 showing 44.5% inhibition of PIM-1 at K_m ATP and
 28 PF-07238025 showing 30.4% inhibition of Serine Kinase SRPK1 at K_m ATP. In a follow-up dose
 29 response, PF-07208254 demonstrated an IC_{50} = 14.4 μ M for PIM-1. Because of this weak activity
 30 and large margins between BDK potency (PF-07208254 BDK IC_{50} = 110 nM) and PF-07238025
 31 BDK IC_{50} = 4.5 nM), and these off-target potencies, pharmacology due to these off-targets is not
 32 anticipated within the context of the included experiments.

33

34

35 X-ray Crystal Structures:

36

37 **Supplementary Table 4. Data collection and refinement statistics (molecular replacement)**

	PF-07208254	S3	PF-07247685
Data collection			
Space group	P6 ₄ 22	P4 ₁ 22	P4 ₁ 22
Cell dimensions			
<i>a</i> , <i>b</i> , <i>c</i> (Å)	132.27, 132.27, 121.70	117.8, 117.8, 154.8	118.370, 118.370, 156.230
α , β , γ (°)	90, 90, 120	90, 90, 90	90, 90, 90
Resolution (Å)	114.5-2.55 (2.70-2.55) *	117.8-2.79 (3.08-2.79)	47.7-3.15(3.23-3.15)
R_{merge}	0.15(2.49)	0.112(2.74)	0.113(2.07)
$I / \sigma I$	13.5(1.2)	17.3(1.7)	17.7(1.6)
Completeness (spherical, %)	86.2(28.3)	63.1(12.7)	93.3(54.7)
Completeness (ellipsoidal, %)	90.4(39.9)	86.0(73.5)	96.0(89.2)
Redundancy	18.0(13.9)	12.8(12.5)	13.1(13.2)

Refinement

Resolution (Å)	114.5-2.54	117.8(2.79)	47.7(3.15)
No. reflections	18,176	17,480	18,537
$R_{\text{work}} / R_{\text{free}}$	0.231/0.270	0.248/0.296	0.240/0.279
No. atoms			
Protein	2,564	5,042	5,163
Ligand/ion	42	124	121
Water	28	12	13
B -factors [‡]			
Protein	80.7	97.2/163	99.9/142
Ligand	81.3	79.8/155	95.3/119
Solvent	63.9	64.02/132	74.5
Wilson Plot	83.56	92.4	102.3
R.m.s. deviations			
Bond lengths (Å)	0.008	0.009	0.008
Bond angles (°)	0.91	0.92	0.91

38 *One crystal was used for each data set. Values in parentheses are for the highest-resolution shell. Anisotropic
39 resolution cutoff was used during data merging and scaling, and both spherical and ellipsoidal completeness are
40 reported.

41 [‡]For **S3** and PF-07247685, the average B factors of protein and bound inhibitors are listed separately for chain A and
42 B in the asymmetric unit. Chain A is more ordered than chain B, and chain B was tightly restrained to chain A
43 during model building and refinements. There is only one chain in the PF-07208254 crystal.

44
45

46 **Supplementary Methods**

47

48 **Chemical Synthesis:**

49

50 BT2 was obtained from Enamine in 95% purity (Monmouth Junction, NJ, USA); Catalog number
51 EN300-00845. Compound **S1** can be synthesized according to a literature procedure, and
52 showed 98.2% purity as determined by LCMS.¹¹ Compound **S2** is commercially available from
53 multiple vendors including Aurora Fine Chemicals LLC (San Diego, CA); catalog number
54 182.043.609. Material used herein was 96.5% pure as determined by LCMS. Compound **S3** is
55 commercially available from multiple vendors including Aurora Fine Chemicals LLC (San Diego,
56 CA); catalog number 100.479.432. Material used herein was 95.7% pure as determined by LCMS.
57 The synthesis of all other included compounds is below.

58 **Methods:**

59 Reactions were performed in air or, when oxygen- or moisture-sensitive reagents or
60 intermediates were employed, under an inert atmosphere (nitrogen or argon). When appropriate,
61 reaction apparatuses were dried under dynamic vacuum using a heat gun, and anhydrous
62 solvents (Sure-Seal™ products from Aldrich Chemical Company, Milwaukee, Wisconsin or
63 DriSolv™ products from EMD Chemicals, Gibbstown, NJ) were employed. Commercial solvents
64 and reagents were used without further purification. When indicated, reactions were heated by
65 microwave irradiation using Biotage Initiator or Personal Chemistry Emrys Optimizer microwaves
66 or the like. Reaction progress was monitored using thin-layer chromatography (TLC), liquid
67 chromatography-mass spectrometry (LCMS) and high-performance liquid chromatography
68 (HPLC) analyses. TLC was performed on pre-coated silica gel plates with a fluorescence
69 indicator (254 nm excitation wavelength) and visualized under UV light and/or with I₂, KMnO₄,
70 CoCl₂, phosphomolybdic acid, and/or ceric ammonium molybdate stains. LCMS data were
71 acquired on an Agilent 1100 Series instrument with a Leap Technologies autosampler, Gemini
72 C18 columns, acetonitrile/water gradients, and either trifluoroacetic acid, formic acid, or
73 ammonium hydroxide modifiers or similar equipment. The column eluent was analyzed using a
74 Waters ZQ mass spectrometer scanning in both positive and negative ion modes from 100 to
75 1200 Da. Other similar instruments were also used. HPLC data were acquired on an Agilent 1100
76 Series instrument using Gemini or XBridge C18 columns, acetonitrile/water gradients, and either
77 trifluoroacetic acid or ammonium hydroxide modifiers and comparable equipment. Purifications
78 were performed by medium performance liquid chromatography (MPLC) using Isco CombiFlash
79 Companion, AnaLogix IntelliFlash 280, Biotage SP1, or Biotage Isolera One instruments and pre-
80 packed Isco RediSep or Biotage Snap silica cartridges and the like. Chiral purifications were
81 performed by chiral supercritical fluid chromatography (SFC) using Berger or Thar instruments
82 and similar instruments; ChiralPAK-AD, -AS, -IC, Chiralcel-OD, or -OJ columns; and CO₂
83 mixtures with methanol, ethanol, isopropanol, or acetonitrile, alone or modified using
84 trifluoroacetic acid or iPrNH₂. UV detection was used to trigger fraction collection.

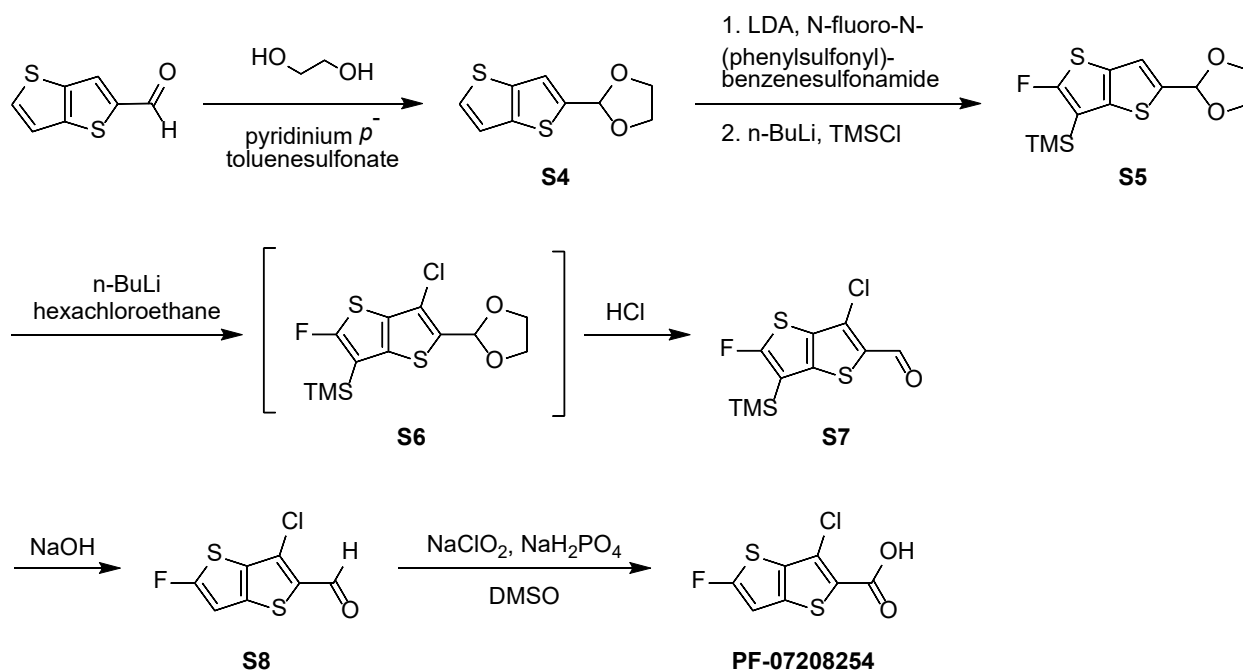
85 Mass spectrometry data are reported from LCMS analyses. Mass spectrometry (MS) was
86 performed via atmospheric pressure chemical ionization (APCI), electrospray ionization (ESI),
87 electron impact ionization (EI) or electron scatter (ES) ionization sources. High resolution mass
88 spectrometry (HRMS) was performed on a Sciex TripleTOF 5600+ (Sciex, Ontario, Canada) with
89 DuoSpray ionization source. The LC instrument includes an Agilent (Agilent Technologies,
90 Wilmington, DE) 1200 binary pump, Agilent 1200 autosampler, Agilent 1200 column
91 compartment, and Agilent 1200 DAD. The instrument acquisition and data handling were done
92 with Sciex Analyst TF version 1.7.1. Prior to acquisition, instrument was calibrated with less than
93 5 ppm accuracy. During acquisition, a calibration run was performed initially and after every 5
94 injections using the Sciex positive polarity tuning mix. Elution Conditions: Column: Waters XSelect

95 HSS T3, 2.1 x 50mm, 2.5 μm particle size; Column Temperature 60 $^{\circ}\text{C}$; Solvent A: Water (0.1%
 96 formic acid); Solvent B: Acetonitrile (0.1% formic acid); Gradient: Initial 5% B, hold for 0.10 min,
 97 5-95% B in 2.8 min, 95-5% B in 0.20 min, 3.5 min total runtime; Flow rate 0.8 mL/min. TOF
 98 Conditions: ESI in Positive Mode; The spray chamber: Gas 1 and 2 at 60, curtain gas at 40,
 99 temperature 600 $^{\circ}\text{C}$, IonSpray voltage 5500 V, declustering potential 100, collision energy 10.
 100 The acquisition was done in TOF MS mode with range of 100-2000 amu with accumulation time
 101 of 0.20 sec. ESI in Negative Mode; The spray chamber: Gas 1 and 2 at 60, curtain gas at 40,
 102 temperature 600 $^{\circ}\text{C}$, IonSpray voltage -4500 V, declustering potential -100, collision energy -10.
 103 The acquisition is done in TOF MS mode with range of 100-2000 amu with accumulation time of
 104 0.20 sec. Proton, carbon, and fluorine nuclear magnetic spectroscopy (^1H NMR, ^{13}C NMR, ^{19}F
 105 NMR) chemical shifts are given in parts per million downfield from tetramethylsilane and were
 106 recorded on 101, 300, 400, 500, or 600 MHz Varian spectrometers. Chemical shifts are expressed
 107 in parts per million (ppm, δ) referenced to the deuterated solvent residual peaks. The peak shapes
 108 are described as follows: s, singlet; d, doublet; t, triplet; q, quartet; quin, quintet; m, multiplet; br
 109 s, broad singlet; app, apparent. Analytical SFC data were acquired on a Berger analytical
 110 instrument as described above. Optical rotation data were acquired on a PerkinElmer model 343
 111 polarimeter using a 1 dm cell. Silica gel chromatography was performed primarily using a medium
 112 pressure Biotage or ISCO systems using columns pre-packaged by various commercial vendors
 113 including Biotage and ISCO.

114 Unless otherwise noted, chemical reactions were performed at room temperature (about
 115 23 degrees Celsius). HPLC, UPLC, LCMS, and SFC retention times were measured using the
 116 methods noted in the procedures. Products were generally dried under vacuum before being
 117 carried on to further reactions or submitted for biological testing. Mass spectrometry data is
 118 reported from liquid chromatography-mass spectrometry (LCMS), atmospheric pressure
 119 chemical ionization (APCI) instrumentation. Chemical shifts for nuclear magnetic resonance
 120 (NMR) data are expressed in parts per million (ppm, δ) referenced to residual peaks from the
 121 deuterated solvents employed.

122

123 Synthesis of 3-chloro-5-fluorothiopheno[3,2-b]thiophene-2-carboxylic acid (**PF-07208254**)



124

125

126 Step 1. Synthesis of 2-(thieno[3,2-*b*]thiophen-2-yl)-1,3-dioxolane (**S4**)

127 To a solution of thieno[3,2-*b*]thiophene-2-carbaldehyde (180 g, 1.07 mol) in cyclohexane (3 L,
128 0.36 M) was added pyridinium *p*-toluenesulfonate (26.9 g, 0.107 mol) and ethylene glycol (597
129 mL, 10.7 mol). The reaction mixture was heated to 90 °C for 40 hours, in an apparatus equipped
130 with a Dean-Stark trap. The resulting mixture was diluted with sodium chloride (aq., 2 L) and the
131 resulting organic layer was separated. The aqueous layer was extracted with ethyl acetate (3 x
132 1 L) and the combined organic layers were dried over sodium sulfate, filtered, and concentrated
133 *in vacuo* to afford **S4** as a light brown solid (230 g). This material was used for next step directly.
134 ¹H NMR (400 MHz, DMSO-*d*₆) δ 7.68 (d, *J* = 5.3 Hz, 1H), 7.57 (s, 1H), 7.43 (dd, *J* = 5.3, 0.7 Hz,
135 1H), 6.10 (s, 1H), 4.07 – 4.00 (m, 2H), 4.00 – 3.93 (m, 2H); HRMS (*m/z*): [M+H]⁺ calcd. for
136 C₉H₉O₂S₂⁺, 213.0038; found, 213.0038; 2.01 min; 96%. HPLC: 8.649 min, 95% pure.

137

138 Step 2. Synthesis of [5-(1,3-dioxolan-2-yl)-2-fluorothieno[3,2-*b*]thiophen-3-yl](trimethyl)silane
139 (**S5**).

140 A solution of **S4** (120.0 g, 564 mmol) in a mixture of toluene (1.5 L) and tetrahydrofuran (0.9 L)
141 was cooled to –78 °C. Lithium diisopropylamide (2.0 M solution in tetrahydrofuran / heptane /
142 ethylbenzene, 367 mL, 1.3 eq.) was added in a drop-wise manner at a rate such that the internal
143 temperature of the reaction mixture remained below –72 °C. The reaction mixture was stirred at
144 this temperature over 1 hour followed by dropwise addition of a *N*-fluoro-*N*-
145 (phenylsulfonyl)benzenesulfonamide (231.7 g, 734 mmol) solution in tetrahydrofuran (5 volumes)
146 at –78 °C. The reaction mixture was stirred at this temperature for 1 hour followed by addition of
147 sodium hydroxide (15%, 20 volumes). Once at ambient temperature, the aqueous phase was
148 extracted with isopropyl acetate (5 volumes). The combined organic layers were dried over
149 sodium sulfate, filtered, and concentrated *in vacuo* to afford 120 g of a crude brown solid. This
150 material was used for next step directly.

151 This solid (120 g) was dissolved in tetrahydrofuran (2.3 L), cooled to –78 °C, and treated in a
152 drop-wise manner with *n*-butyllithium (2.5 M solution in hexanes; 417 mL, 2 eq.) at a rate that
153 maintained the internal reaction temperature below –72 °C. After the reaction mixture had been
154 stirred at –78 °C for 1 hour, a solution of trimethylsilyl chloride (113.2 g, 2 eq.) in tetrahydrofuran
155 (1 volume) was added, while again maintaining the internal reaction temperature below –72 °C.
156 The reaction mixture was then stirred at –78 °C for 1 hour, whereupon an aliquot was partitioned
157 between diethyl ether and saturated aqueous sodium bicarbonate solution. GCMS analysis of
158 the organic layer of this aliquot indicated conversion to **S5**: GCMS *m/z* 302.1 [M⁺]. The reaction
159 mixture was quenched at –78 °C by addition of saturated aqueous sodium bicarbonate solution
160 (10 volumes), and the resulting mixture was allowed to warm to room temperature. The aqueous
161 phase was extracted with isopropyl acetate (5 volumes). The organic layer was concentrated and
162 purified by silica gel (3 g/g), eluted with heptanes : methyl *tert*-butyl ether (10:1). The organic
163 phase was concentrated to 2-3 volumes, then slurried with heptanes (3 volumes). The mixture
164 was filtered, and the residue dried under nitrogen to give **S5** as a yellowish solid (150 g, 88%
165 yield). ¹H NMR (400 MHz, methanol-*d*₄) δ 7.24 (s, 1H), 6.00 (s, 1H), 4.04 – 3.96 (m, 2H), 3.95 –
166 3.86 (m, 2H), 0.29 (s, 9H); ¹⁹F NMR (400 MHz, methanol-*d*₄) δ -113.92 (s, 1H).

167

168 Step 3. Synthesis of 3-chloro-5-fluoro-6-(trimethylsilyl)thieno[3,2-*b*]thiophene-2-carbaldehyde
169 (**S7**)

170 A tetrahydrofuran (1.8 L, 15 volumes) solution of **S5** (150 g, 1 eq.) was cooled down to $-78\text{ }^{\circ}\text{C}$
171 followed by dropwise addition of *n*-BuLi (2.5 M solution in hexanes, 260 mL, 1.3 eq), at a rate
172 that maintained the internal temperature below $-72\text{ }^{\circ}\text{C}$. After completion of the addition, the
173 reaction mixture was allowed to stir at $-78\text{ }^{\circ}\text{C}$ for 1 hour, whereupon a solution of
174 hexachloroethane (165.7 g, 1.4 eq.) in tetrahydrofuran (5 volumes) was added dropwise, in a
175 manner that maintained the internal reaction temperature below $-72\text{ }^{\circ}\text{C}$. The reaction mixture
176 was stirred for a further 1 hour at $-78\text{ }^{\circ}\text{C}$. The reaction mixture, containing **S6**, was quenched
177 with HCl (4 N, 5 volumes) and stirred at room temperature for 6 hours. The aqueous mixture was
178 extracted with isopropyl acetate (5 volumes). The organic phase was concentrated to 2-3
179 volumes, then slurried with isopropyl alcohol (3 volumes). The mixture was filtered, and the
180 residue was dried under nitrogen to give crude material as a yellowish solid. The crude product
181 was slurried with a tetrahydrofuran : water co-mixture (1/1; 20 volumes) and the residue was then
182 dried under nitrogen to afford **S7** as a yellowish solid (87 g, 60% yield). ^1H NMR (400 MHz,
183 DMSO- d_6) δ 9.87 (s, 1H), 0.26 (s, 9H); ^{13}C NMR (101 MHz, DMSO- d_6) δ 182.36, 174.04, 171.07,
184 134.64 (d, $J = 4.8$ Hz), 127.40, 115.98, 115.75, -0.51 (d, $J = 1.8$ Hz); ^{19}F NMR (400 MHz, DMSO-
185 d_6) δ -100.08 (s, 1H); HRMS (m/z): $[\text{M}+\text{H}]^+$ calcd. for $\text{C}_{10}\text{H}_{11}\text{ClFOS}_2\text{Si}^+$, 292.9688; found,
186 292.9688; 3.01 min; 100%. HPLC: 11.806 min, 100% pure.

187

188 Step 4. Synthesis of 3-chloro-5-fluorothieno[3,2-b]thiophene-2-carbaldehyde (**S8**)

189 To a methanol (30 mL) : water (30 mL) solution of **S7** (2.96 g, 10.1 mmol) was added an aqueous
190 solution of sodium hydroxide (1 M, 0.20 mL). The resulting solution was stirred at $50\text{ }^{\circ}\text{C}$ for 1 h.
191 After that time additional water was added to yield a thick slurry. The beige precipitated solid was
192 filtered, rinsed with a methanol : water (1:1 ratio; 12 mL) solution to yield **S8** (2.17 g 89% yield)
193 as a beige solid after drying at $50\text{ }^{\circ}\text{C}$ over 16 h. ^1H NMR (400 MHz, DMSO- d_6) δ 9.99 (s, 1H),
194 7.49 (d, $J = 1.7$ Hz, 1H); ^{13}C NMR (400 MHz, DMSO- d_6) δ 182.08, 169.83, 166.85, 139.70,
195 134.83, 126.90, 105.75; ^{19}F NMR (400 MHz, DMSO- d_6) δ -111.67 (s, 1H); HRMS (m/z): $[\text{M}+\text{H}]^+$
196 calcd. for $\text{C}_7\text{H}_3\text{ClFOS}_2^+$, 220.9292; found, 220.9290; 2.26 min; 94%; HPLC: 9.393 min, 90%
197 pure; LC/MS: 0.817 min / 220.7 $[\text{M}+\text{H}]$.

198

199 Step 5. Synthesis of 3-chloro-5-fluorothieno[3,2-b]thiophene-2-carboxylic acid (**PF-07208254**)

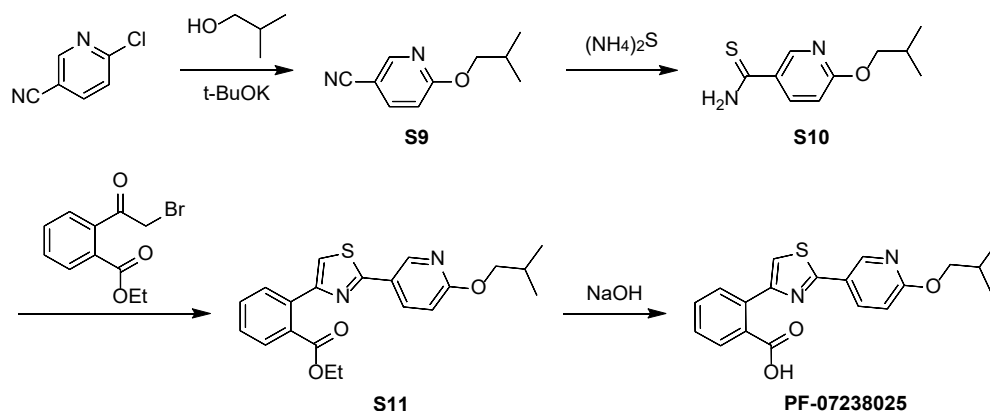
200 A solution of sodium chlorite (20.5 g, 227 mmol) and sodium dihydrogen phosphate (27.5 g, 229
201 mmol) in water (100 mL) was added slowly, in a drop-wise manner, to a $0\text{ }^{\circ}\text{C}$ solution of **S8** (10.0
202 g, 45.3 mmol) in a mixture of dimethyl sulfoxide (56 mL) and 2-methyltetrahydrofuran (100 mL).
203 The reaction mixture was then allowed to warm to room temperature and was stirred at that
204 temperature until the starting material had been completely consumed, as assessed by LCMS
205 analysis (approximately 2 hours). The reaction mixture was then poured in portions into a cold (0
206 $^{\circ}\text{C}$) saturated aqueous solution of sodium thiosulfate pentahydrate (300 mL), at a rate that
207 maintained the temperature of the resulting mixture below $15\text{ }^{\circ}\text{C}$. After stirring at $10\text{ }^{\circ}\text{C}$ for 20
208 minutes, the mixture was diluted with ethyl acetate (200 mL). The aqueous layer was extracted
209 with ethyl acetate (2 x 200 mL), and the combined organic layers were washed with saturated
210 aqueous sodium chloride solution, dried over magnesium sulfate, filtered, and concentrated *in*
211 *vacuo*. The residue was stirred in a mixture of heptane and ethyl acetate (9:1, 50 mL) for about
212 1 hour. The resulting solid was collected via filtration and washed with a mixture of heptane and
213 ethyl acetate (9:1, 2 x 20 mL), providing a white solid (10.58 g). This was stirred in
214 dichloromethane for 20 minutes and filtered; the filter cake was washed with dichloromethane (2
215 x 20 mL) to afford 3-chloro-5-fluorothieno[3,2-b]thiophene-2-carboxylic acid (**PF-07208254**) as a
216 white solid. Yield: 10.0 g, 42.2 mmol, 93%. ^1H NMR (400 MHz, DMSO- d_6) δ 13.7 (br s, 1H), 7.40

217 (d, $J = 1.7$ Hz, 1H), ^{19}F NMR (400 MHz, $\text{DMSO-}d_6$) δ -116.0 (d, 1H); ^{13}C NMR (400 MHz, DMSO-
218 d_6): δ 168.6, 165.64, 161.79, 127.86, 125.20, 122.73, 105.03.; HRMS (m/z): $[\text{M}+\text{H}]^+$ calcd. for
219 $\text{C}_7\text{H}_3\text{ClFO}_2\text{S}_2^+$, 236.9242; found, 236.9242; 2.01 min; 100%; HPLC: 4.668 min. (99% pure).

220

221 Synthesis of 2-{2-[6-(2-methylpropoxy)pyridin-3-yl]-1,3-thiazol-4-yl}benzoic acid (**PF-07238025**)

222



223

224 Step 1. Synthesis of 6-(2-methylpropoxy)pyridine-3-carbonitrile (**S9**)

225 A solution of 2-methylpropan-1-ol (32.1 g, 433 mmol) in tetrahydrofuran (100 mL) was added over
226 3 minutes to a 0 °C suspension of potassium *tert*-butoxide (48.6 g, 433 mmol) in tetrahydrofuran
227 (600 mL). After the reaction mixture had been stirred for 15 minutes, a slurry of 6-chloropyridine-
228 3-carbonitrile (40 g, 290 mmol) in tetrahydrofuran (200 mL) was added in several portions, at a
229 rate that maintained the reaction temperature below 20 °C. When the reaction mixture had cooled
230 to 15 °C, the ice bath was removed and the reaction mixture was allowed to stir at room
231 temperature. After 1 hour, water (700 mL) was added, and the resulting mixture was extracted
232 with ethyl acetate (2 x 800 mL). The combined organic layers were washed with saturated
233 aqueous sodium chloride solution, dried over magnesium sulfate, filtered, and concentrated in
234 vacuo; stirring of the resulting oil caused it to begin to solidify. Heptanes (800 mL) were added,
235 and the mixture was stirred for 20 minutes, whereupon it was filtered to provide **S9**, and the filtrate
236 was concentrated in vacuo to provide a pale-yellow oil. Some of this solid **S9** was used to seed
237 the pale-yellow oil which further solidified upon being subjected to high vacuum to yield in total
238 45.9 g (260 mmol, 90% yield) of **S9** as a yellow solid. ^1H NMR (400 MHz, $\text{DMSO-}d_6$) δ 8.68 (dd,
239 $J = 2.4, 0.8$ Hz, 1H), 8.14 (dd, $J = 8.7, 2.4$ Hz, 1H), 7.01 (dd, $J = 8.8, 0.8$ Hz, 1H), 4.12 (d, $J = 6.7$
240 Hz, 2H), 2.12 – 1.97 (m, 1H), 0.97 (d, $J = 6.7$ Hz, 6H); ^{13}C NMR (101 MHz, $\text{DMSO-}d_6$) δ 165.94,
241 152.66, 142.48, 117.87, 112.06, 102.18, 73.00, 27.76, 19.34. HRMS (m/z): $[\text{M}+\text{H}]^+$ calcd. for
242 $\text{C}_{10}\text{H}_{13}\text{N}_2\text{O}^+$, 177.1022; found, 177.1022; 2.24 min; 99%; HPLC: 8.798 min / 100% pure.

243

244

245 Step 2. Synthesis of 6-(2-methylpropoxy)pyridine-3-carbothioamide (**S10**)

246 This experiment was carried out in two equal batches. Aqueous ammonium sulfide solution (40%,
247 56 g, 330 mmol) was added to a solution of **S9** (28.8 g, 163 mmol) in methanol (350 mL), and the
248 reaction mixture was allowed to stir at room temperature overnight. After the two reactions had
249 been combined, they were concentrated in vacuo to approximately one-half of the original volume,

250 and treated with water (500 mL). The resulting precipitate was collected via filtration, washed with
251 water and air-dried for 1 hour using house vacuum. The yellow solid was then stirred for 10
252 minutes in heptane (700 mL), and again collected via filtration. The filter cake was washed with
253 heptane (2 x 300 mL) to afford **S10** as a solid. Combined yield: 56.36 g, 268.0 mmol, 82%. ¹H
254 NMR (400 MHz, DMSO-*d*₆) δ 9.82 (br s, 1H), 9.50 (br s, 1H), 8.71 (d, *J* = 2.6 Hz, 1H), 8.23 (dd,
255 *J* = 8.8, 2.6 Hz, 1H), 6.90-6.77 (m, 1H), 4.10 (d, *J* = 6.7 Hz, 2H), 2.04 (hept., 1H), 0.97 (d, *J* = 6.7
256 Hz, 6H). ¹³C NMR (101 MHz, DMSO-*d*₆) δ 197.18, 165.63, 146.65, 139.29, 128.97, 110.03, 72.62,
257 27.89, 19.47. HRMS (*m/z*): [M+H]⁺ calcd. for C₁₀H₁₅N₂OS⁺, 211.0900; found, 211.0900; 1.72
258 min; 98%; HPLC: 7.421 min / 100% pure.

259

260 Step 3. Synthesis of ethyl 2-{2-[6-(2-methylpropoxy)pyridin-3-yl]-1,3-thiazol-4-yl}benzoate (**S11**)

261 A mixture of ethyl 2-(bromoacetyl)benzoate (35.2 g, 130 mmol) and **S10** (27.3 g, 130 mmol) in
262 ethanol (350 mL) was heated to 75 °C for 1.5 hours, whereupon it was allowed to cool to room
263 temperature and concentrated in vacuo. The resulting oil was subjected to silica gel
264 chromatography (Eluent: 20% ethyl acetate in heptane); the product was combined with the
265 product of a similar reaction carried out using **S10** (23.3 g, 111 mmol), and the combined waxy
266 solids were granulated into a powder. After this had been stirred in heptane (500 mL) for 30
267 minutes, the solid was collected via filtration, washed with heptane, and resuspended in fresh
268 heptane (500 mL). This mixture was stirred at room temperature over the weekend, and then
269 filtered; the filter cake was washed with heptane to provide **S11** as a colorless solid (58.5 g).

270 The impure column fractions were combined and chromatographed on silica gel (Eluent: 20%
271 ethyl acetate in heptane) to yield additional **S11** as an oil, which solidified to a waxy solid upon
272 drying at high vacuum. This material was suspended in heptane (40 mL) and the collected solid
273 was granulated to a powder and again suspended in heptane (60 mL). After the mixture had been
274 stirred 1 hour, the solid was collected by filtration, washed with heptane (20 mL), suspended in
275 fresh heptane (60 mL), and stirred at room temperature overnight. Filtration provided a filter cake,
276 which was washed with heptane (20 mL) to afford additional **S11** as a colorless solid (12.6 g).
277 Combined yield: 71.1 g, 186 mmol, 77%. ¹H NMR (400 MHz, chloroform-*d*) δ 8.72 (br d, *J* = 2.3
278 Hz, 1H), 8.19 (dd, *J* = 8.7, 2.5 Hz, 1H), 7.76 (dd, *J* = 7.7, 1.4 Hz, 1H), 7.64 (dd, *J* = 7.7, 1.3 Hz,
279 1H), 7.53 (ddd, *J* = 7.6, 7.5, 1.4 Hz, 1H), 7.45 (ddd, *J* = 7.5, 7.5, 1.3 Hz, 1H), 7.31 (s, 1H), 6.81
280 (br d, *J* = 8.7 Hz, 1H), 4.18 (q, *J* = 7.2 Hz, 2H), 4.13 (d, *J* = 6.7 Hz, 2H), 2.19 – 2.04 (m, 1H), 1.09
281 (t, *J* = 7.2 Hz, 3H), 1.04 (d, *J* = 6.7 Hz, 6H); HPLC: 11.082 min, 97% pure; LC/MS (*m/z*): 383.1
282 [M+H], 1.090 min.

283

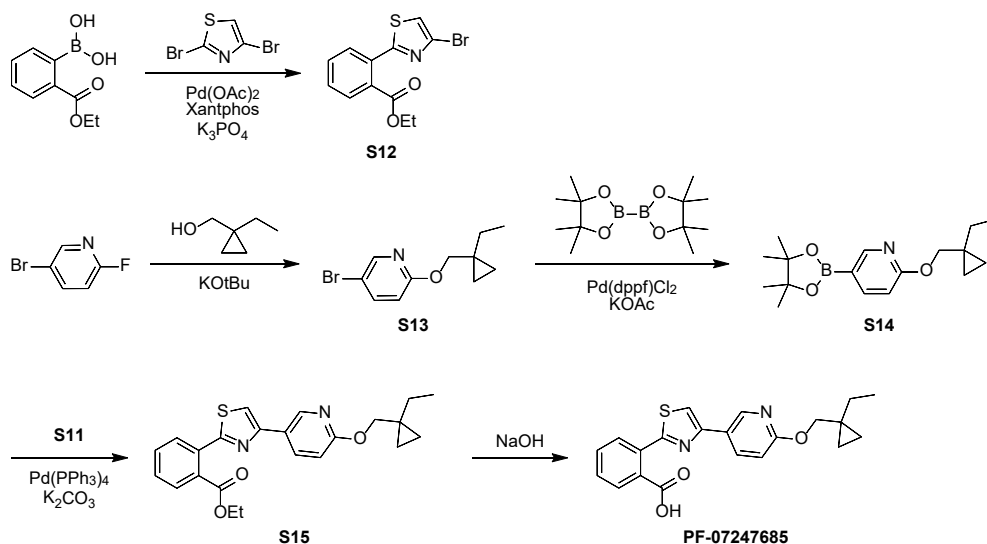
284 Step 4. Synthesis of 2-{2-[6-(2-methylpropoxy)pyridin-3-yl]-1,3-thiazol-4-yl}benzoic acid (**PF-** 285 **07238025**)

286 An aqueous solution of sodium hydroxide (3.0 M; 100 mL, 300 mmol) was added to a suspension
287 of **S11** (58.5 g, 153 mmol) in ethanol (500 mL), and the reaction mixture was heated to 75 °C for
288 2 hours. After the reaction mixture had cooled, it was diluted with water (500 mL), and acidified to
289 a pH of approximately 5 to 6 by addition of 1 M hydrochloric acid. The resulting mixture was
290 allowed to stir for 30 minutes at room temperature, whereupon the precipitate was collected via
291 filtration and washed with water to afford **PF-07238025** as a colorless solid. Yield: 51.3 g, 145
292 mmol, 95%. ¹H NMR (400 MHz, DMSO-*d*₆) δ 12.79 (s, 1H), 8.74 (d, *J* = 2.5 Hz, 1H), 8.21 (dd, *J*
293 = 8.7, 2.5 Hz, 1H), 7.91 (s, 1H), 7.75 (br d, *J* = 7.7 Hz, 1H), 7.62 (br d, *J* = 7.6 Hz, 1H), 7.57 (ddd,
294 *J* = 7.6, 7.5, 1.3 Hz, 1H), 7.48 (ddd, *J* = 7.5, 7.5, 1.0 Hz, 1H), 6.97 (d, *J* = 8.7 Hz, 1H), 4.12 (d, *J*
295 = 6.7 Hz, 2H), 2.14 – 1.99 (m, 1H), 0.99 (d, *J* = 6.7 Hz, 6H). ¹³C NMR (101 MHz, DMSO-*d*₆) δ

296 170.73, 164.99, 163.50, 154.93, 145.43, 137.45, 133.16, 130.76, 129.60, 128.86, 128.65, 123.59,
297 116.52, 111.62, 72.59, 27.91, 19.51; HRMS (m/z): [M+H]⁺ calcd. for C₁₉H₁₉N₂O₃S⁺, 355.1111;
298 found, 355.1111; 2.39 min; 98%; HPLC: 9.149 min / 100% pure.

299

300 Synthesis of 2-(4-{6-[(1-ethylcyclopropyl)methoxy]pyridin-3-yl}-1,3-thiazol-2-yl)benzoic acid (**PF-**
301 **07247685**)



302

303 Step 1. Synthesis of ethyl 2-(4-bromo-1,3-thiazol-2-yl)benzoate (**S12**)

304 A reaction vessel containing a mixture of 2,4-dibromo-1,3-thiazole (10.0 g, 41.2 mmol), [2-
305 (ethoxycarbonyl)phenyl]boronic acid (8.78 g, 45.3 mmol), palladium(II) acetate (462 mg, 2.06
306 mmol), 4,5-bis(diphenylphosphino)-9,9-dimethylxanthene (Xantphos; 1.19 g, 2.06 mmol),
307 potassium phosphate monohydrate (28.4 g, 123 mmol), and tetrahydrofuran (206 mL) was
308 evacuated and charged with nitrogen; this evacuation cycle was carried out a total of 3 times.
309 After the reaction mixture had been heated at 70 °C for 3 days, it was cooled and partitioned
310 between water and ethyl acetate. The aqueous layer was extracted twice with ethyl acetate, and
311 the combined organic layers were washed with saturated aqueous sodium chloride solution, dried
312 over sodium sulfate, filtered, and concentrated in vacuo. Silica gel chromatography was carried
313 out twice: #1 (Eluent: dichloromethane); #2 (Gradient: 0% to 20% ethyl acetate in heptane). The
314 purified material was triturated in heptane, while it still contained a small amount of ethyl acetate
315 from concentration of the column fractions; this afforded **S12** as a yellow solid. Yield: 8.67 g,
316 27.8 mmol, 67%. LCMS 0.89 min / *m/z* 313.9 (bromine isotope pattern observed) [M+H]⁺. ¹H NMR (400
317 MHz, chloroform-*d*) δ 7.88 – 7.79 (m, 1H), 7.68 – 7.60 (m, 1H), 7.63 – 7.51 (m, 2H), 7.33 (s, 1H),
318 4.29 (q, *J* = 7.2 Hz, 2H), 1.24 (t, *J* = 7.1 Hz, 3H); ¹³C NMR (101 MHz, DMSO-*d*₆) δ 168.09, 167.16,
319 132.28, 131.93, 131.25, 131.00, 130.12, 129.65, 124.83, 120.29, 61.53, 14.16; HRMS (m/z):
320 [M+H]⁺, Br isotopic pattern, calcd. for C₁₂H₁₁BrNO₂S⁺, 355.9688; found, 355.9688; 2.26 min;
321 99%; HPLC: 8.780 min / 97% pure.

322

323 Step 2. Synthesis of 5-bromo-2-[(1-ethylcyclopropyl)methoxy]pyridine (**S13**)

324 Potassium *tert*-butoxide (38.3 g, 341 mmol) was added to a 0 °C solution of (1-
325 ethylcyclopropyl)methanol (25.0 g, 250 mmol) in tetrahydrofuran (630 mL). The reaction mixture

326 was stirred for 15 minutes, whereupon a solution of 5-bromo-2-fluoropyridine (40.0 g, 227 mmol)
327 in tetrahydrofuran (60 mL) was added as a single portion. The ice bath was then removed, and
328 the reaction mixture was allowed to stir for 6 hours. After slow addition of water, the resulting
329 mixture was extracted three times with ethyl acetate, and the combined organic layers were
330 washed with saturated aqueous sodium chloride solution, dried over sodium sulfate, filtered, and
331 concentrated in vacuo. Chromatography on silica gel (Gradient: 0% to 10% ethyl acetate in
332 heptane) afforded **S13** as a colorless oil. Yield: 56.1 g, 219 mmol, 96%. ¹H NMR (400 MHz,
333 chloroform-*d*) δ 7.92 (br d, *J* = 2.6 Hz, 1H), 7.40 (dd, *J* = 8.8, 2.6 Hz, 1H), 6.45 (dd, *J* = 8.8 Hz,
334 1H), 3.86 (s, 2H), 1.25 (q, *J* = 7.4 Hz, 2H), 0.72 (t, *J* = 7.5 Hz, 3H), 0.28 (d, *J* = 2.1 Hz, 2H), 0.26
335 – 0.16 (m, 2H); ¹³C NMR (101 MHz, DMSO-*d*₆) δ 163.03, 147.51, 141.94, 113.33, 111.60, 71.38,
336 27.11, 20.83, 11.06, 10.36; HRMS (m/z): [M+H]⁺, Br isotopic pattern, calcd. for C₁₁H₁₅BrNOS⁺,
337 256.0332; found, 256.0333; 2.74 min; 96%; HPLC: 10.631 min / 96% pure.

338

339 Step 3. Synthesis of 2-[(1-ethylcyclopropyl)methoxy]-5-(4,4,5,5-tetramethyl-1,3,2-dioxaborolan-2-
340 yl)pyridine (**S14**)

341 A reaction vessel containing a mixture of **S13** (56.1 g, 219 mmol), 4,4,4',4',5,5,5',5'-octamethyl-
342 2,2'-bi-1,3,2-dioxaborolane (66.7 g, 263 mmol), [1,1'-
343 bis(diphenylphosphino)ferrocene]dichloropalladium(II) (16.0 g, 21.9 mmol), and potassium
344 acetate (KOAc; 64.5 g, 657 mmol) in toluene (706 mL) was evacuated and charged with nitrogen.
345 This evacuation cycle was repeated twice, whereupon the reaction mixture was heated at 100 °C
346 overnight. It was then filtered; the filtrate was washed with toluene and concentrated under
347 reduced pressure, providing **S14** as a black gum. This material was progressed directly to the
348 following step.

349

350 Step 4. Synthesis of ethyl 2-(4-{6-[(1-ethylcyclopropyl)methoxy]pyridin-3-yl}-1,3-thiazol-2-
351 yl)benzoate (**S15**)

352 A reaction vessel containing a mixture of **S12** (57.0 g, 183 mmol), **S14** (from the previous step;
353 ≤219 mmol), potassium carbonate (75.7 g, 548 mmol), and
354 tetrakis(triphenylphosphine)palladium(0) (21.1 g, 18.3 mmol) in 1,4-dioxane (550.0 mL) and water
355 (220 mL) was evacuated and charged with nitrogen. This evacuation cycle was repeated twice,
356 whereupon the reaction mixture was heated to 90 °C for 2 hours. It was then cooled and
357 partitioned between saturated aqueous sodium bicarbonate solution and ethyl acetate. After the
358 aqueous layer had been extracted twice with ethyl acetate, the combined organic layers were
359 washed with saturated aqueous sodium chloride solution, dried over sodium sulfate, filtered, and
360 concentrated in vacuo. Purification was carried out first using silica gel chromatography (Gradient:
361 10% to 20% ethyl acetate in heptane), and then via a second chromatography on silica gel
362 (Eluent: 10% dichloromethane, followed by 20% methanol in dichloromethane) to yield **S15**. Yield:
363 42.8 g, 105 mmol, 57%. ¹H NMR (400 MHz, chloroform-*d*) δ 8.70 (dd, *J* = 2.5, 0.8 Hz, 1H), 8.14
364 (dd, *J* = 8.6, 2.5 Hz, 1H), 7.83 – 7.76 (m, 1H), 7.75 – 7.69 (m, 1H), 7.63 – 7.51 (m, 2H), 7.49 (s,
365 1H), 6.85 (dd, *J* = 8.7, 0.8 Hz, 1H), 4.25 (d, *J* = 7.2 Hz, 1H), 4.21 (d, *J* = 13.1 Hz, 3H), 1.59 (s,
366 3H), 1.53 (t, *J* = 7.4 Hz, 2H), 1.29 (s, 3H), 1.12 (t, *J* = 7.1 Hz, 3H), 1.00 (t, *J* = 7.4 Hz, 3H), 0.90
367 (t, *J* = 6.9 Hz, 2H), 0.56 (t, *J* = 3.0 Hz, 2H), 0.49 – 0.42 (m, 2H). LC/MS (1.08 min / calc'd. 408.52,
368 found 409.3 (M+H)).

369

370 Step 5. Synthesis of 2-(4-{6-[(1-ethylcyclopropyl)methoxy]pyridin-3-yl}-1,3-thiazol-2-yl)benzoic
371 acid (**PF-07247685**)

372 To a solution of **S15** (42.8 g, 105 mmol) in ethanol (1.1 L) was added an aqueous solution of
373 sodium hydroxide (4.0 M; 131 mL, 524 mmol). The reaction mixture was heated at 80 °C for 2
374 hours, whereupon it was concentrated in vacuo to approximately one-half of the original volume
375 and then added to a mixture of 1 M hydrochloric acid and ethyl acetate. The aqueous layer was
376 extracted twice with ethyl acetate, and the combined organic layers were washed sequentially
377 with water and with saturated aqueous sodium chloride solution, dried over sodium sulfate,
378 filtered, and concentrated under reduced pressure. The residue was dissolved in heptane
379 containing a small amount of ethyl acetate, and a small quantity of inorganic material was
380 removed via filtration. The filtrate was diluted with ethyl acetate, washed twice with water and
381 once with saturated aqueous sodium chloride solution, dried over sodium sulfate, filtered, and
382 concentrated in vacuo. The residue was dissolved in a small amount of ethyl acetate; upon
383 swirling of the flask, a solid began to form. heptane was added until the mixture became cloudy,
384 and swirling was continued while additional material precipitated. When it appeared that solid was
385 no longer forming, heptane was added, and the mixture was stirred for 2 hours. Filtration, followed
386 by washing of the filter cake with heptane, provided **PF-07247685** as a white solid. Yield: 34.9 g,
387 91.7 mmol, 87%. ¹H NMR (400 MHz, DMSO-*d*₆) δ 13.05 (s, 1H), 8.77 (dd, *J* = 2.5, 0.7 Hz, 1H),
388 8.25 (dd, *J* = 8.6, 2.5 Hz, 1H), 8.18 (s, 1H), 7.82 – 7.76 (m, 1H), 7.72 – 7.56 (m, 3H), 6.94 (dd, *J*
389 = 8.6, 0.7 Hz, 1H), 4.17 (s, 2H), 1.46 (q, *J* = 7.4 Hz, 2H), 0.93 (t, *J* = 7.4 Hz, 3H), 0.56 – 0.46 (m,
390 2H), 0.48 – 0.38 (m, 2H). ¹³C NMR (101 MHz, DMSO-*d*₆) δ 170.13, 166.04, 163.81, 152.54,
391 145.20, 137.35, 133.84, 131.59, 131.11, 130.40, 129.97, 129.14, 124.17, 115.06, 111.17, 71.11,
392 27.18, 20.99, 11.16, 10.42.; HRMS (m/z): [M+H]⁺ calcd. for C₂₁H₂₁N₂O₃S⁺, 381.1267; found,
393 381.1267; 2.44 min; 100%; HPLC: 9.024 min / 100% pure.

394
395
396
397
398

X-ray Crystal Structure Methods:

399 **Protein Purification and crystallization:** Based on previously published BDK purification
400 strategies^{2,3} an MBP-TEV-humanBDK-His construct was co-expressed with GroEL/ES (pGro7)
401 in *E. coli* BL21 (DE3) cells. Harvested cells were resuspended in 100 mM potassium phosphate,
402 1 mM TCEP, 500 mM KCl, 0.1 mM EDTA, 10% glycerol, 1% Tween-20, 0.25% Triton X-100, pH
403 7.5 supplemented with Roche EDTA-free protease inhibitor tablets and benzonase. After lysis by
404 Microfluidizer (Microfluidics), cellular debris was pelleted by centrifugation at 40,000 xg. The
405 supernatant was applied to a 14 mL column of Amylose Resin High Flow (New England Biolabs),
406 washed with 50 mM HEPES, 1 mM TCEP, 2 mM MgCl₂, 250 mM KCl, 300 mM arginine, 10%
407 glycerol, pH 7.5 and eluted with buffer containing 10 mM maltose. Due to phosphorylation of the
408 protein at the TEV cleavage site, the pooled protein was dephosphorylated with lambda
409 phosphatase (NEB) while simultaneously removing the MBP by TEV protease. Cleaved,
410 dephosphorylated BDK was applied to a Superdex 200 column (Cytiva Life Sciences) equilibrated
411 in 50 mM HEPES, 1 mM TCEP, 2 mM MgCl₂, 1 M NaCl, 250 mM KCl, 300 mM arginine, 10%
412 glycerol, pH 7.5. Fractions containing BDK were pooled and concentrated to at least 30 mg/mL.
413 Crystals of dephosphorylated BDK diffracted poorly. To restore phosphorylation levels closer to
414 pre-dephosphorylation levels, two cycles of autophosphorylation were performed. For each cycle,
415 human BDK protein (25 mg/mL) was incubated overnight with 25 mM ATP and 65 mM MgCl₂,
416 followed by another round of SEC to remove nucleotide. Autophosphorylation was verified by
417 mass spectrometry.

418 Phosphorylated human BDK (20 mg/mL) was incubated with 25 mM ADP and 1 mM ligand and
419 crystals were grown by sitting drop vapor diffusion. For the thiophene PF-07208254, crystals were
420 grown with a well solution of 0.1 M MES pH 5.4, 0.2 M magnesium chloride, and 10% PEG-3350.
421 Crystals were cryoprotected by gradually increasing the glycerol concentration to 25% before
422 flash freezing in liquid nitrogen. For the thiazoles **S3** and PF-07247685, crystals were grown with
423 a well solution of 0.2 M ammonium sulfate and 17-22% PEG-3350 and cryoprotected with 20%
424 glycerol.

425 **Data collection, structure determinations and refinements:**

426
427 Crystal data sets were collected at beamline 17-ID at IMCA CAT (Advanced Photon Source,
428 Argonne National Laboratory, Chicago). The wavelength used was 1 Å. Crystals were kept at 100
429 K using cryo stream. Data were processed using the program autoPROC⁴⁴. Compared to the
430 reported rat BDK complex crystals, our human BDK complex crystals diffracted weaker and
431 showed strong anisotropical diffractions. Data sets were scaled and merged using anisotropic
432 resolution cut off, and both spherical and ellipsoidal data completeness were reported.
433

434 The initial human BDK structure complex with PF-07208254 was determined using published rat
435 BDK/BT2 complex structure (PDB ID, 4E01). Structure refinements were carried out using the
436 program Buster⁵⁵. Protein manual building was carried out using program Coot⁶⁶ and automatic
437 ligand fitting was done using the program RhoFit⁷⁷. There is one human BDK/PF-07208254
438 complex in the crystallographic asymmetric unit, and two human BDK/**S3** and BDK/PF-07247685
439 complexes in the crystallographic asymmetric unit, respectively. In the latter two crystals, complex
440 B is significantly more disordered with weaker electron densities for both the protein and ligands.
441 The percentages of residues in Ramachandran plot favored regions are 96.5%, 95.5%, 95.8%
442 respectively, and in unfavored regions are 0.32%, 0.32% and 0.16% respectively.
443

444 **Computational Methods:**

445
446
447 **Structure Preparation.** Structure preparation was performed using Protein Preparation Wizard
448 defaults in Schrodinger 2021-2⁸⁻¹²⁸⁻¹² unless otherwise stated. X-ray co-crystal structures of rat
449 BCKDK (rBDK) with BT2, PF-07208254, PF-07238025 and PF-07247685 in the allosteric binding
450 site and apo were internally generated (2.1 – 2.9 Å resolution) and used as initial coordinates for
451 MD simulations (human structures were not available at the time). Rat and human BDK protein
452 sequences are 95.6% identical and the 3-dimensional structures are highly similar between the
453 two species (RMSD = 0.63 Å over all heavy atoms). Most of the species differences occur in the
454 N-terminus, which is unresolved in the X-ray crystal structures. There are no residue differences
455 between rat and human within 9 Å of BT2, PF-07208254, PF-07238025 or PF-07247685;
456 therefore, it is expected that the conclusions drawn from analysis of MD results based on the rat
457 structures will translate to human. Two loops were not resolved in the structures. Loop 1 residues
458 R50 – Q52 (numbering based on the signal peptide processed, mature protein) were built using
459 Prime¹²⁻¹⁴¹²⁻¹⁴. The ATP lid (loop 12, residues A306 – G335) was not modeled due to its size and
460 was capped at residues T305 and F336. ADP, two crystallographic ions, Mg²⁺ and K⁺, and one
461 crystallographic water molecule that forms a hydrogen bond network between ADP, D285
462 sidechain and G289 backbone were present in the ATP binding site for all simulations. Consistent
463 zero-order bonds to Mg²⁺ and K⁺ were employed. Two additional crystallographic waters were
464 retained in the structures of PF-07238025 and PF-07247685, one of which forms a hydrogen
465 bond network from the carboxylic acid of the ligand to the L164 backbone, Y346 sidechain, and
466 water #2, and the other of which forms a hydrogen bond network to the thiazole N of the ligand,

467 the R171 sidechain, and water #1. Protonation states were optimized using PROPKA at pH 7.0
468 and checked for consistency across all systems.

469 **System Preparation, MD Simulations, Analysis.** Desmond System Builder in Schrodinger
470 2021-2¹⁵⁻¹⁷¹⁵⁻¹⁷ was used to prepare the systems for simulation. The OPLS4 force field¹⁸¹⁸ was
471 used following customization using the Force Field Builder panel for missing ligand torsion
472 parameters along with the TIP3P water model¹⁹¹⁹. An orthorhombic periodic box was set up with
473 12 Å of water on all sides of the system and neutralizing ions added. Default Desmond
474 minimization and equilibration protocols were employed. Recent work has suggested that analysis
475 of multiple MD replicas leads to more reliable conclusions than those drawn based on a single
476 long simulation²⁰²⁰⁻²³; therefore following equilibration, six independent NPT production
477 simulations of 100 ns each were run for all five systems using Desmond, starting with the same
478 equilibrated structure and using new initial randomized velocities. The independent trajectories
479 were combined for subsequent analysis, giving a total production time of 600 ns for each system.
480 Schrodinger 2021-2 software was used to perform RMSD, RMSF, essential dynamics, CM, and
481 hydrogen bond analyses. BDK lipoyl-binding pocket residues were identified based on overlay
482 with the asymmetric PDK3-L2 complex (PDB ID: 1Y8P)²¹²⁴ and selection of residues within 6 Å of
483 the L2 group.

484

485

486 **Supporting computational details and analysis.**

487 All MD trajectories stabilized by 50 ns based on the backbone root-mean-square deviation
488 (RMSD) from the initial structures (Supplementary Figure 9A). The dynamics of loop 1 and the
489 lipoyl-binding pocket residues upon inhibitor binding seem to play a role in destabilization or
490 stabilization of BDK on the BCKDH complex as described in the main text. As detailed in Tso et
491 al.²³²⁵ there is a network of interactions connecting helices $\alpha 4$ and $\alpha 5$ to the lipoyl-binding pocket,
492 and the inhibitor (S)-CPP perturbs the lipoyl-binding pocket residues. In support of this, the MD
493 simulations suggest there is an overall increase in dynamic flexibility of the BDK lipoyl-binding
494 pocket when bound to destabilizers BT2 and PF-07208254, and an overall decrease in dynamic
495 flexibility of the lipoyl-binding pocket when bound to stabilizers PF-07238025 and PF-07247685.
496 This observation can be explained by an increase in the overall number of hydrogen bonds formed
497 over the course of the MD simulations when BDK is bound to stabilizers PF-07238025 and PF-
498 07247685, 73 and 298 on average for the lipoyl-binding pocket and overall, respectively,
499 compared to when BDK is bound to destabilizers BT2 and PF-07208254, 71 and 295 on average
500 (Supplementary Figure 10C-D).

501

502 The width of the active-site cleft seems to play an important role in the ability of BDK to
503 phosphorylate E1 as described in the main text. When destabilizers BT2 or PF-07208254 are
504 bound to BDK, the width of the active-site cleft is narrowed as measured by CM _{$\alpha 5-\alpha 8$} , preventing
505 E1 from positioning itself for phosphorylation (Supplementary Figure 10A-B). In the apo structure,
506 Y99, L129, H132, R167, and R171 form an intricate hydrogen bond (HB) network: Y99 forms a
507 HB with R167 via sidechain interactions, R167 sidechain forms a HB with the H132 backbone,
508 and R171 sidechain forms a HB with the backbone of L129 (Supplementary Figure 10E-F). Upon
509 binding of a destabilizer, BT2 or PF-07208254, this HB network is rearranged, as previously
510 described by Tso et al.^{25, 26} The acid moiety of the inhibitor binds in between Y99 and R167,
511 forming HB interactions with the sidechains and forcing the R167 sidechain toward the active-site
512 cleft. The HB between the R167 sidechain and H132 backbone is maintained, which pulls the
513 loop in between helices $\alpha 4$ and $\alpha 5$ toward the active-site cleft, and places the H132 sidechain into
514 position to interact with the acid moiety of the inhibitor (Supplementary Figure 10E). The

515 importance of H132 was previously shown in the study of a p.His162Gln variant by Maguolo et
516 al.,²⁵²⁷ and the current results further highlight the importance of this residue and its interactions.
517 The R171 sidechain maintains its HB with the L129 backbone and forms an additional HB
518 interaction with the acid of the ligand. These changes in interactions induced by ligand binding
519 cause a subtle movement in the positions of helix $\alpha 5$ and $\alpha 3$, leading to a narrowing of the active-
520 site cleft.

521
522 In contrast, when stabilizers PF-07238025 or PF-07247685 are bound to BDK, the active-
523 site cleft widens as measured by $CM_{\alpha 5-\alpha 8}$. Upon binding of a stabilizer, PF-07238025 or PF-
524 07247685, the R167 sidechain flips in order to make 2 HBs to the acid moiety of the inhibitor
525 (Supplementary Figure 10F). This causes H132 to adjust to maintain the HBs between its
526 backbone and the R167 sidechain, pulling the loop between helices $\alpha 4$ and $\alpha 5$ away from the
527 active-site cleft. A HB can still be maintained between Y99 and R167 sidechains with the inhibitor
528 bound as in the apo structure. The sidechain of R171 is forced to change conformation upon
529 binding of a stabilizer and forms a HB with the sidechain of Y346 in addition to participating in a
530 water-mediated HB network with the acid and thiazole nitrogen of the inhibitor. The terminal
531 phenyl of the inhibitor, which is positioned in the active-site cleft and blocks E1 from binding,
532 interacts with Y241 through van der Waals (VDW) interactions and pushes the sidechain slightly
533 away, causing the cleft to widen further.

534

535 **Western Blot antibodies:** The following antibodies and concentrations were used for Western
536 blotting. pBCKDH phospho S292 (Bethyl A304-672A 1:1000), total BCKDH (Yenzym 037 1:1000),
537 BDK (abcam ab128935 1:1000), GAPDH (CST 14C10 1:10000), α -tubulin (CST 2144 1:10,000).
538 Secondary antibodies were anti-rabbit IgG HRP-Conjugated-(CST 7074P2 1:10000) Anti-mouse
539 IgG (CST HRP-linked Antibody #7076).

540 **In vivo compound measurements:** Compounds were quantitatively measured in plasma and
541 tissue samples using liquid chromatography–tandem mass spectrometry (LC-MS/MS). All
542 standards were made in blank mouse plasma and were typically prepared at 1-50,000 ng/mL.
543 Tissues were homogenized using a 1:4 dilution in 60:40 isopropanol:water and 2 hours of shaking
544 in the bead beater using zirconia beads. For tissue analysis, a mixed matrix approach was used
545 where an equal volume of blank tissue homogenate was added to plasma standards, and blank
546 plasma was added to tissue samples. Samples were prepared by protein precipitation using
547 acetonitrile containing 150 ng/mL indomethacin, 25 ng/mL diclofenac and 5 ng/mL tolbutamide
548 as internal standards, vortexed and centrifuged, then transferred and diluted with water for LC-
549 MS/MS analysis. Chromatography was performed on a Waters Acquity iClass UPLC System
550 (Milford, MA). Separation was achieved with an Acquity UPLC HSS T3 column (2.1x50 mm, 1.8
551 μ m), and a gradient of 0.1% formic acid in water (Mobile Phase A) and 0.1% formic acid in
552 acetonitrile (Mobile Phase B) at a flow rate of 0.600 mL/min. The gradient increased from 5%B to
553 95%B over 2.0 minutes and the entire run time was 3 minutes. Data was collected on an AB Sciex
554 API6500 mass spectrometer (Foster City, CA, USA) using Turbo IonSpray™ electrospray
555 ionization (ESI) and multiple reaction monitoring (MRM) mode. Typical source conditions (heated
556 capillary temperature, gas1, gas2, and curtain gas) were set at 500C, 40, 60 and 20, respectively.
557 Data acquisition and quantitative processing was carried out with Analyst software version 1.6.2
558 (Applied Biosystems/MDS Sciex, Canada).

559 MRM transitions were optimized for each compound. BT2 (Negative Ion Mode): Q1 245.0; Q3
560 201.0; DP -60; CE -15; IS=Diclofenac. PF-07208254 (Negative Ion Mode): Q1 235.0; Q3 191.0;
561 DP -65; CE -18; IS=Tolbutamide. PF-07238025 (Positive Ion Mode): Q1 355.1; Q3 281.1; DP 60;
562 CE 34; IS=Indomethacin. PF-07247685 (Positive Ion Mode): Q1 381.2; Q3 281.1; DP 80; CE 45;
563 IS=Indomethacin. IS Transitions: Diclofenac (Negative Ion Mode): Q1 294.1; Q3 250.0; DP -40;
564 CE -15. Tolbutamide (Negative Ion Mode): Q1 269.0; Q3 170.0; DP -60; CE -30. Indomethacin
565 (Positive Ion Mode): Q1 358.3; Q3 139.2; DP 46; CE 26.

566 **Plasma BCAA/BCKA quantification:** Plasma BCAA and BCKA were analyzed using a
567 standardized method at Pfizer or at Q² solutions, Ithaca, NY. Two methods were used for
568 BCAA/BCKA quantitation. *Pfizer (Groton, CT):* A surrogate analyte approach was utilized with
569 ¹³C₅ D₈¹⁵N valine, D₁₀ leucine, ¹³C₆ D₁₀¹⁵N isoleucine, ¹³C₄ D₄ ketovaline, D₇ ketoleucine and
570 ¹³C₆ ketoisoleucine as surrogate analytes and ¹³C₅ valine, D₇ leucine, ¹³C₆ isoleucine, ¹³C₅
571 ketovaline and D₃ ketoleucine as internal standards (ketoleucine and ketoisoleucine shared the
572 same IS). Surrogate standard curves were typically prepared at 10 – 50,000 ng/mL in control
573 mouse plasma. Samples and standards were subjected to protein precipitation with methanol
574 containing internal standards, vortexed and centrifuged to obtain supernatant. An aliquot of the
575 supernatant was transferred to a new 96-well block, dried down under nitrogen, and reconstituted
576 in water containing 0.1% acetic acid for injection. Chromatography was performed on a Shimadzu
577 Nexera UPLC System (Kyoto, Japan). Separation of structural isomers was achieved with an
578 Acquity UPLC HSS T3 column (2.1x100 mm, 1.8 μm, Waters Corporation, Milford MA) using 0.1%
579 acetic acid in water (Mobile Phase A) and methanol (Mobile Phase B) at a flow rate of 0.400
580 mL/min. The gradient increased from 3%B to 85%B over 6.1 minutes and the entire run time was
581 10 minutes. Data was collected on an AB Sciex Triple TOF 6600 mass spectrometer (Foster City,
582 CA, USA) using negative ion electrospray ionization (ESI) and TOF MS with a mass range of 60-
583 1060. Extracted ion chromatograms were integrated at a mass tolerance of 10 ppm. Surrogate
584 standard calibration curves were obtained by fitting the normalized intensities of the surrogate
585 standards vs. their concentrations using a linear fit with 1/x² weighting factor. The endogenous
586 concentrations were obtained by converting normalized intensities to concentrations according to
587 the corresponding surrogate standard curve fitting equations. Data acquisition was performed
588 with Analyst software version 1.6.2, peak integrations were performed in MultiQuant and either
589 Multiquant or Watson LIMS 7.5 was used for regression and quantitation.

590 **Tissue BCAA/BCKA quantitation:** Mouse muscle tissue BCAA/BCKA were analyzed using a
591 standardized method at Q² solutions, Ithaca, NY. Briefly, mouse muscle tissue was pounded to
592 powder under liquid N₂ and homogenized and sonicated in working internal standard solution
593 (WISS) containing Leucine D₁₀, Isoleucine D₁₀, Valine D₈, Ketoleucine D₃, Ketoisoleucine D₈,
594 Ketovaline ¹³C₄ D₄ in 4:1 methanol/water at a ratio of 50 mg tissue/1 mL WISS. Samples were
595 spun, and the supernatant was collected and transferred to a deep well injection plate followed
596 by drying under nitrogen at 40 °C. Residue was resuspended in 50 μL water containing 0.2%
597 acetic acid. Samples were run on a Dionex Ultimate 3000 with a Waters HSS T3 1.8 μm, 2.1 x
598 100 mm column. The mobile phase was A:1000:2 water/acetic acid and B: methanol. Gradient
599 separation began at 1.8% B for 2 minutes then increased to 5.5% B over 0.5 minutes, then to
600 6.5% B over 2.75 minutes, then to 100% B over 1.75 minutes and held for 1 minute followed by
601 a return to 1.8%B and held for 1 minute. Data was acquired on a Thermo Q-Exactive mass
602 spectrometer within a scan range of 100 – 160 m/z. A surrogate analyte approach was utilized for
603 quantitation with ¹³C₅¹⁵N valine, ¹³C₆ leucine, ¹³C₆ isoleucine, ¹³C₅ ketovaline, ¹³C₆ ketoleucine
604 and ¹³C₆ ketoisoleucine as surrogate analytes. Surrogate standard curves were typically prepared
605 at 25 – 4000 nM for amino acids and 0.8 – 64 nM for keto acids in pooled mouse tissue extract.
606 The mono-isotopic mass was monitored for all analytes and standards except for leucine,
607 isoleucine and valine, for which the M+1 isotopologue was measured and a correction factor

608 based on the natural isotope abundance was applied. Surrogate standard calibration curves were
609 obtained by fitting the normalized intensities of the surrogate standards vs. their concentrations
610 using a linear fit. The endogenous concentrations were obtained by converting normalized
611 intensities to concentrations according to the corresponding surrogate standard curve fitting
612 equations.

613 **Transverse Aortic Constriction:** Two rounds of equivalent surgeries were performed. The
614 afternoon prior to surgery a subcutaneous dose of SR Meloxicam was administered to ensure
615 adequate pre-operative analgesia coverage. Meloxicam was slowly released over 72 hours. All
616 surgical instruments were sterilized with vaporized hydrogen peroxide. The surgeon and all
617 surgical personnel donned a bonnet, masks, gowns, and gloves. Instruments were sterilized
618 between each animal using a hot bead sterilizer and sterile tip technique. On the day of surgery,
619 anesthesia was induced by administering an anesthetic cocktail IP (Ketamine 25 mg/mL @ 100
620 mg/kg + xylazine 2 mg/mL @ 8 mg/kg). Once at an acceptable plane of anesthesia, the animal
621 was prepped for surgery. A pre-operative dose of LRS was administered subcutaneously at 20
622 mL/kg. Nails were clipped, and fur was shaved from the chin to the xyphoid process. The skin
623 was prepped with 2 consecutive scrubs of Chloraprep swabs. The animal was intubated using
624 polyethylene 60 tubing and placed on a ventilator. End tidal volume was set at 250 μ L/min, and
625 the respiration was set at 140 breaths per minute. A final scrub with a Chloraprep swab was
626 applied. Isoflurane was administered at rate of 0.5 to 2% throughout the procedure.

627 A toe pinch was performed to ensure an adequate plane of anesthesia for surgery. A midline skin
628 incision was made above the 1st and 2nd rib, approximately 0.5-1 cm in length. A local analgesic
629 block (Bupivacaine @ 1 mg/kg + Buprenorphine @ 0.003 mg/kg) was administered to the
630 intercostal muscles along the 1st and 2nd ribs. Using blunt dissection, a 3 mm muscle incision
631 was made between the 1st and 2nd rib. The thymus was gently manipulated and placed on either
632 side of the incision to expose the aortic arch beneath. A retractor was placed on each side of the
633 incision to secure the thymus and create a clear surgical window of the aortic arch. The tissue of
634 the aortic arch was gently isolated, between the brachiocephalic artery and the left common
635 artery. A 6-0 Silk suture was passed under the aortic arch, and a 4 mm stainless steel pin (0.38
636 mm diameter) was placed across the aorta. The suture was tied around the needle and secured
637 using a surgeon's knot. Immediately, the stainless steel pin was removed from under the suture
638 and the suture remained in place to produce a defined constriction of the vessel. For sham
639 surgery, the aortic arch was isolated, and a suture was passed under the aortic arch, no ligation
640 was made, and the suture was removed. The retractor was carefully removed, and the ribs were
641 closed with 2 simple interrupted sutures using 6-0 Prolene. To prevent atelectasis, before
642 completely closing the muscle incision, positive pressure was applied to the exhaust tubing of the
643 ventilator to assist in evacuating any excess air from the chest cavity. A small amount of saline
644 was applied to the muscle tissue, and the skin was closed with 5-0 Prolene using 2 single external
645 horizontal mattress pattern sutures. The mouse was slowly weaned off the ventilator. An
646 intraperitoneal dose of Antisedan (0.5 mg/mL @ 1 mg/kg) was administered to reverse the effects
647 of xylazine. When the animal was removed from the ventilator, they were placed in a warm oxygen
648 chamber until they were ambulatory. Once ambulatory the mice were returned to a clean warm
649 cage and a subcutaneous dose of diluted buprenorphine was administered. During day 0 PM
650 post-operative assessments, a subcutaneous dose of LRS (20 mL/kg) and diluted buprenorphine
651 was administered. Another dose of subcutaneous LRS and diluted buprenorphine was
652 administered during day 1 AM post-operative assessments. During day 1 PM post-operative
653 assessments through day 2 PM assessments, diluted buprenorphine was administered
654 subcutaneously. Animals were given Nutra Gel support for 4 days post surgery. After the 72-hour
655 post-op period animals were monitored daily until post-op day 7. Food consumption was
656 monitored throughout the study to ensure similar food consumption across groups. Three animals

657 that did not consume at least 1.5 g/day compound chow for 3 consecutive days and consequently
658 had very low plasma levels of PF-07208254 for a sustained time period were excluded from the
659 study. Animals that lost 20% of body weight or greater from the start of surgery were humanely
660 euthanized. At euthanasia, hearts were excised, excess blood within the chamber was drained,
661 hearts were weighed, the atria were removed, and the ventricles were immediately snap frozen
662 in liquid nitrogen. Lungs were blotted briefly on a napkin and weighed.

663
664 **Echocardiography:** Ultrasounds were acquired in a blinded fashion at 4 weeks post-surgery on
665 the Vevo3100 using the MX550D probe. Prior to the imaging studies, animals were anesthetized
666 with 2% isoflurane in an induction chamber. Once asleep, animals were placed onto a heated
667 platform set to 34 °C to maintain body temperature. Heart rates were monitored and maintained
668 above 400 bpm for all measurements. Electrode gel was applied to the four paws and taped to
669 the ECG electrodes on the heated platform. Hair was removed from the chest with Nair, and
670 isoflurane was set to 0.5-1.0% for systolic function acquisition. Warm echo gel was placed on the
671 shaved chest, and the MX550D probe was used for recordings. For recording of the pasternal
672 long axis (LV long axis view), the “notch” of the MX550D transducer was placed towards the head
673 of the animal and rotated approximately 30-45 degrees clockwise. When heart structures were
674 visualized clearly, a B-mode image of the heart was recorded. The MX550D probe was turned 90
675 degrees clockwise to the left side of the mouse to obtain a pasternal short axis view (LV short
676 axis view). Once the ventricular structures were clear, the M-mode cursor was set in the middle
677 of the ventricle and an M-mode image of the ventricle was recorded. After scanning was finished,
678 residual echo gel was removed, and the mouse was returned to the cage for recovery.
679 Echocardiography images were analyzed using Vevo Lab 3.20 software. At least three beats were
680 measured, and the mean was calculated. Images were analyzed blindly after acquisition.

681 **Hek293 Cell experiments:** Human embryonic kidney (HEK293) cells were purchased from
682 American Type Culture Collection (ATCC) (CRL-1573™) and were cultured at 37 °C in Eagle’s
683 Minimal Essential Medium (EMEM) supplemented with 10% Hi-FBS (Gibco) and 100 units/mL
684 Penicillin/Streptomycin (ThermoFisher Scientific). BT2 (100 and 300 µM), PF-07208254 (3, 10, 30
685 or 300 µM), PF-07238025 (0.2, 0.6, 2 or 6 µM), PF-07247685 (0.01, 0.03, 0.1 or 0.3 µM) or DMSO
686 (0.01%) was added to HEK293 cells and incubated for 48 hours at 37 °C. Whole cell lysates were
687 lysed in 200 µL of Cell Signaling lysis buffer containing HALT protease inhibitors (ThermoFisher
688 Scientific) 48 hours post-treatment. Cells were lysed by sonication. Samples were then spun at
689 16,260 x g for 10 minutes, and the supernatant was placed in new tubes. Total protein
690 quantification was calculated using Pierce BCA assay. All samples were boiled at 95 °C for 5
691 minutes with Invitrogen LDS buffer and Reducing Agent at a concentration of 2 mg/mL of total
692 protein based on the BCA assay results. 20 µg of each sample was loaded into NuPage 4-12%
693 Bis-Tris gels and samples were run at 160V for 2 hours using the BioRad system. The proteins
694 were then transferred to a PVDF membrane using the iBlot2 system. Membranes were blocked
695 in 5% milk in TBS plus 0.05% Tween 20. The membranes were exposed using the Amersham
696 800 imager, and Imagequant software and Microsoft Excel 365 was used to analyze densitometry
697 of each band. Primary antibodies used are detailed above.

698

699 **In vitro BDK FRET activity assay:** Initially, 5 µL of 2X BDK enzyme (5 nM final) in assay buffer
700 (20 mM Tris·HCl (pH 7.5), 100 mM KCl, 5 mM MgCl₂, 0.5 mM DTT, 0.02% (vol/vol) Tween-20,
701 and 0.01% BSA) was added to the compound plates and pre-incubated for 15 min at room
702 temperature. Final enzyme concentration was optimized to reflect the linear range of enzyme
703 activity with less than 30% substrate conversion. This was followed by addition of 5 µL of 2X LBD-
704 Tev-PhosphoPep+Lipoyl substrate/ATP mix in assay buffer to initiate the reaction. Plates were

705 covered with a lid and allowed to incubate at room temperature for 90 min. Final concentration of
706 LBD-E1 substrate was 50 nM and final concentration of ATP was 15 μ M. Following incubation,
707 the enzyme reactions were stopped by adding 5 μ L of 4X stop/primary antibody solution
708 containing 100 mM (final) EDTA, 2 nM (final) anti-His Eu antibody, and 1:1000 anti-pE1 antibody
709 in assay buffer. The plates were covered and incubated at room temperature for 30 min. Finally,
710 5 μ L of 4X detection reagent consisting of 20 nM (final) anti-rabbit Ulight antibody and 1X LANCE
711 detection buffer in dH₂O was then added. The plates were centrifuged for 30 seconds at 113 x g.
712 After a 60 min incubation, the plates were read on an EnVision® MultiReader in TR-FRET mode
713 (excitation 320 nm: emissions 665 nm). The raw data from the EnVision® MultiReader was
714 expressed as a ratio and was analyzed using proprietary software (Activity Base). The percent
715 effect at each concentration of compound was calculated relative to the values for the uninhibited
716 control wells (100% DMSO) and fully inhibited control wells (600 μ M radicicol) on each assay
717 plate. IC₅₀ values were determined from the percent effect data using a 4-parameter logistic dose
718 response model (Activity Base).

719
720 **Human skeletal muscle BDK activity assay:** BDK activity and inhibition in human skeletal
721 muscle cells was monitored by measuring BDK dependent phosphorylation of endogenous
722 BCKDHA using a custom AlphaLISA SureFire Ultra assay system. Prior to the assay, the total
723 BCKDHA antibody (Bethyl Laboratories - A303-790A) was biotinylated using the ChromaLink™
724 One-Shot Antibody Biotinylation Kit (Trilink Technologies B-9007-009K) and a phospho (S293)
725 BCKDHA antibody (Bethyl Laboratories A304-672A) was CaptSure tagged using the Lightning-
726 Link® CaptSure™ Conjugation Kit (TGR BioSciences 6300007). Human skeletal myocytes
727 (Gibco A11440) were previously immortalized via the introduction of hTERT into the cells.
728 Immortalized human skeletal muscle cells were plated at 15,000 cells/well and grown in skeletal
729 muscle growth media containing the media supplement and chick embryo extract (Promocell C-
730 23060 and C-23160, MP92850145) in 384-well CulturPlate plates. After overnight incubation,
731 media was removed, and compound treatments were performed in growth media diluted 10X in
732 PBS for 60 minutes. Cells were washed with PBS and lysed in 1X lysis buffer (Cell Signaling
733 9803) containing 2 nM biotinylated total BCKDHA Antibody and 1X protease/phosphatase
734 inhibitor cocktail (Cell Signaling 5872). After an hour incubation at room temperature, a 1X
735 immunoassay buffer (Perkin Elmer AL000F) mix containing 1:400 CaptSure tagged Phospho
736 BCKDHA Antibody and 40 μ g/ μ L Anti CaptSure acceptor beads (Perkin Elmer ALSU-ACAB) was
737 added to the lysates and allowed to incubate for 60 minutes. The signal was then generated by
738 the addition of streptavidin donor beads (Perkin Elmer ALSU-ASDB) at 40 μ g/ μ L in 1X
739 immunoassay buffer and incubating at room temperature for an additional 30 minutes. The
740 phospho BCKDHA signal was developed using EnVision® multilabel reader (Perkin Elmer) using
741 Alphascreen settings (excitation 680 nm, emission 570 nm). The fluorescence emission was used
742 to calculate the % effect relative to the HPE (30 μ M BT2) and ZPE (DMSO). IC₅₀ curves were
743 generated using ActivityBase software.

744 **RNA Isolation:** Frozen tissues were placed in Matrix D Lysis Tubes (2 mL) and homogenized in
745 1 mL of Qiazol and 200 μ L of chloroform (Sigma). Samples were then spun for 10 min at 11,292
746 x g for phase separation, and the upper aqueous phase of each sample was mixed in a 1:1 ratio
747 with 70% ethanol. The samples were then washed in Qiagen RNEasy spin columns and reagents
748 according to the manufacturer's protocol. Total RNA was quantified using NanoDrop. qPCR was
749 performed using the RNA to CT one step kit (Invitrogen) according to manufacturer's instructions
750 and the Taqman Probes (Fisher) used are listed in Supplementary Table 5.

751 **Supplementary Table 5. RT-PCR Probes**

Gene	Catalog ID
------	------------

Tnfa	Mm00443258_m1
Ccl2	Mm00441242_m1
Cd68	Mm03047343_m1
Ccr2	Mm99999051_gH
Col1a1	Mm00801666_g1
Col1a2	Mm00483888_m1
Bckdk	Mm00437777_m1
Ppia	Mm02342430_g1
Hprt	Mm03024075_m1
Gapdh	Mm99999915_g1
Itgam	Mm00434455_m1
Bckdha	Mm00476112_m1
Bckdhb	Mm01177077_m1
Bcat1	Mm00500289_m1
Bcat2	Mm00802192_m1
Dbt	Mm00501651_m1

752

753

754 **Plasma analysis and ELISA:** Whole blood samples were collected in K₂ EDTA tubes and placed
755 on ice. Samples were then spun in a microcentrifuge at 4 °C for 10 min at 11,292 x g. Plasma
756 was aliquoted into separate tubes, and ALPCO Ultrasensitive Insulin ELISA (80-INSMSU-E01,
757 E10) was utilized according to manufacturers' instructions.

758 **Liver triglyceride assessment:** Frozen livers were pulverized on a cooled aluminum block in
759 liquid nitrogen. Approximately 50 mg of pulverized tissue was added to a pre-weighed 2 mL lysing
760 matrix D tube. After the tissue was added, these tubes were weighed again to determine the exact
761 weight of the tissues. 1 mL of homogenization buffer, containing 10 mM TRIS pH 7.4, 0.9% NaCl
762 and 0.2% Triton X100, was added to each sample. Samples were immediately homogenized using
763 MP FastPrep 5G with the following parameters: (speed: 6, time: 40 seconds, cycles: 1). The
764 samples were then vortexed for 20 seconds. and then transferred to 1.1 mL tubes and
765 immediately analyzed on a Siemens Chemistry XPT clinical analyzer using Triglycerides_2
766 reagents.

767 **Histopathology Evaluation:** The left lateral lobe of the liver was fixed in 10% formalin, embedded
768 in paraffin, and sectioned; 5 mm sections were mounted to positively charged slides for H&E
769 staining. A board-certified veterinary pathologist who was familiar with the animal models graded
770 H&E sections for hepatic lipid vacuolation (steatosis) and inflammation (inflammatory cell
771 infiltrates) in a blinded fashion on a scale of 0-4.

772 **Interaction proteome:**

773 **Lysis and digestion.** Mouse hearts were lysed from mice that were treated with vehicle, 10 mg/kg
774 PF-07247685 BID (described in Extended data Fig. 5), or 100 mg/kg BT2 QD for 18 days. BDK
775 was immunoprecipitated from 5 mg of heart lysate with 15 µL BDK antibody (N=3/group) or 5 µL
776 IgG (N=3 total). Immunoprecipitates were performed overnight, protein A magnetic beads were
777 added, and Ips were washed 3x using lysis buffer. The beads were subsequently washed 3
778 additional times in PBS and resuspended in denaturing buffer (8 M urea and 0.1 M Tris, pH 8.5).

779 The proteins were reduced with dithiothreitol (DTT) 1 mM final concentration for 30 min at 55 °C
780 and alkylated with iodoacetamide (55 mM final concentration) for 30 min at RT in the dark. Lys-C
781 protease (Wako Chemicals, Richmond, VA, USA) was added at a ratio 1:100 to the total protein
782 amount and incubated at room temperature for 2 h in a Thermomixer. Urea was diluted to 2 M
783 with 50 mM Tris pH 8.5, and the samples were incubated with trypsin (1:50 w/w) (Pierce
784 Biotechnology, USA) overnight at 37 °C at 41 x g.

785 **Elution and desalting of peptides.** The peptide mixtures were acidified with formic acid (FA) to
786 1% final concentration (pH <3) and centrifuged at 4000 x g for 5 min. Peptides were desalted in
787 2-plug C18 (Empore C18 extraction disks). The stage tips were sequentially conditioned with
788 methanol (MeOH), 100% acetonitrile (ACN), 50% (vol/vol) ACN / 0.1% (vol/vol) FA, and 0.1%
789 (vol/vol) FA. The samples were loaded onto the stage tips and centrifuged at 3000–3500 x g for
790 3 min at room temperature. After sample loading, the tips were washed twice with 0.1% FA.
791 Peptides were eluted with 50% ACN/0.1% FA. The eluted peptides were dried in a Speed-Vac
792 centrifuge, reconstituted in 5% ACN, 0.1% FA (vol/vol) and sonicated in a water bath sonicator
793 for 5 min.

794 **MS analyses.** The peptides were loaded on a 50 cm column (Thermo Fisher ES903) and
795 separated by reversed-phase chromatography using a gradient from 5% to 30% B over 2 h (Buffer
796 A: 0.1% FA in HPLC grade water; Buffer B: 80% ACN, 0.1% FA) with a flow rate of 0.25 µL/min
797 using an EASY-nLC 1200 system (Thermo Fisher Scientific). For interaction proteome MS data
798 were acquired on a Q Exactive HF mass spectrometer (Thermo Scientific) using a data-
799 dependent acquisition top 10 method, AGC target 3e6, maximum injection time of 32 msec, scan
800 range of 375-1500 m/z and a resolution of 60K. MS/MS was performed at a resolution of 15K,
801 AGC target 1e5, maximum injection time of 60 msec, isolation window 1.4 m/z. Dynamic exclusion
802 was set to 20 seconds. Raw mass spectrometry data were processed using the MaxQuant
803 software Version 1.6.10.43 (www.maxquant.org) with the Andromeda search engine integrated
804 into MaxQuant environment. The MS/MS spectra were searched against the mouse UniProt
805 sequence database without spliced isoforms. All MS/MS spectra were searched with the following
806 MaxQuant parameters for peptide identification: acetyl (protein N-terminus) and methionine
807 oxidation, were selected as variable modifications; cysteine carbamidomethylation was selected
808 as fixed modification. A maximum of 2 missed cleavages were allowed. Peptide spectrum
809 matches and proteins were automatically filtered to a 1% false discovery rate based on
810 Andromeda score, peptide length, and individual peptide mass errors. Modified peptides required
811 a minimum peptide length of at least six amino acids (AA).

812 **Quantification.** TMT reporter ion intensity values were quantified from MS2 scans using an
813 integration tolerance of 20 ppm (Orbitrap) with the most confident centroid setting (Maxquant
814 1.6.10.43) for matching peptides. For interactome analysis, raw reporter ion abundance was used
815 for further analysis. MSstatsTMT workflow starts from the peptide intensities reported in
816 Maxquant's evidence.txt file. When a peptide and charge combination was measured multiple
817 times in a sample, only the maximum intensity was kept. The log₂ peptide intensities were median
818 normalized assuming equal input loading of all channels. Peptide intensities were summarized to
819 protein intensities using Tukey's median polish algorithm²²²⁸. MSstatsTMT builds protein-wise
820 linear models based on these protein summaries, which was used for AP-MS proteomics analysis.

821 **SPR binding assay:**

822 The binding affinity and kinetics of binding were measured using Surface Plasmon Resonance
823 based binding assay²⁹. These experiments were carried out on Biacore B3000 (Cytiva Inc) and
824 Sierra Sensors (now Bruker) MASS-1 instruments. There was no significant difference in results
825 obtained on both these instruments. Bap-tagged BDK protein was captured on a Streptavidin
826 coated sensor chip to achieve about 4000 to 4500 RUs of surface density. All the samples were
827 prepared in buffer consisting of 10mM HEPES, pH 7.5, 150 mM NaCl, 2 mM MgCl₂, 0.005%

828 Tween-20 and 2% DMSO. The same buffer was used as the running buffer during the
829 experiments. Compound samples were injected at a flow rate of 30 μ L/min for 120 seconds of
830 association time followed by at least 300 seconds of dissociation period. The compounds were
831 tested in a concentration series consisting of at least 6 samples made with 2-fold dilution. The
832 highest concentration was selected based on compound potency in the biochemical assay or
833 binding affinity observed in a previous experiment. Multiple blank injections were run before and
834 after each compound series to allow double reference subtraction during data processing and
835 analysis. Radicicol was tested in every experiment as a positive control to assess activity of the
836 captured protein on the surface. A DMSO curve was run during each experiment to properly
837 correct for excluded volume. The data were processed and analyzed using Bruker Analyzer,
838 Scrubber and Biaeval softwares to calculate binding affinities and kinetics by fitting the data to
839 1:1 binding model.

840

841

842 **Supplementary References:**

843

- 844 1. Wright, W.B. Preparation of 3-chlorothiopheno[3,2-b]thiophene derivatives from thiophene-2-
845 acrylic acids. *J. Heterocycl. Chem.* **9**, 879-882 (1972).
- 846 2. Davie, J.R. *et al.* Expression and characterization of branched-chain alpha-ketoacid
847 dehydrogenase kinase from the rat. Is it a histidine-protein kinase? *J Biol Chem* **270**, 19861-
848 19867 (1995).
- 849 3. Machius, M., Chuang, J.L., Wynn, R.M., Tomchick, D.R. & Chuang, D.T. Structure of rat BCKD
850 kinase: nucleotide-induced domain communication in a mitochondrial protein kinase. *Proc Natl*
851 *Acad Sci U S A* **98**, 11218-11223 (2001).
- 852 4. Vonrhein, C. *et al.* Data processing and analysis with the autoPROC toolbox. *Acta Crystallogr. D.*
853 *Biol. Crystallogr.* **67**, 293-302 (2011).
- 854 5. Bricogne G., B.E., Brandl M., Flensburg C., Keller P., Paciorek W., Roversi P, Sharff A., Smart O.S.,
855 Vonrhein C., Womack T.O. (Global Phasing Ltd., Cambridge, United Kingdom; 2017).
- 856 6. Emsley P, C.K. (2004).
- 857 7. Smart OS, W., TO, Sharff A, Flensburg C, Keller P, Paciorek W, Vonrhein C and Bricogne G
858 (Global Phasing Ltd., Cambridge, United Kingdom; 2014).
- 859 8. Madhavi Sastry, G., Adzhigirey, M., Day, T., Annabhimoju, R. & Sherman, W. Protein and ligand
860 preparation: parameters, protocols, and influence on virtual screening enrichments. *J. Comput.*
861 *Aided Mol. Des.* **27**, 221-234 (2013).
- 862 9. Schrödinger (
- 863 10. Epik (New York, NY; 2021).
- 864 11. Impact (New York, NY; 2021).
- 865 12. Prime (New York, NY; 2021).
- 866 13. Jacobson, M.P., Friesner, R.A., Xiang, Z. & Honig, B. On the role of the crystal environment in
867 determining protein side-chain conformations. *J. Mol. Biol.* **320**, 597-608 (2002).
- 868 14. Jacobson, M.P. *et al.* A hierarchical approach to all-atom protein loop prediction. *Proteins:*
869 *Structure, Function, and Bioinformatics* **55**, 351-367 (2004).
- 870 15. Bowers, K.J. *et al.* in Proceedings of the ACM/IEEE Conference on Supercomputing (SC06)
871 (Tampa, Florida.
- 872 16. Desmond (New York, NY; 2021).
- 873 17. Schrödinger (New York, NY; 2021).

- 874 18. Lu, C. *et al.* OPLS4: Improving force field accuracy on challenging regimes of chemical space.
875 *Journal of Chemical Theory and Computation* **17**, 4291-4300 (2021).
- 876 19. Jorgensen, W.L., Chandrasekhar, J., Madura, J.D., Impey, R.W. & Klein, M.L. Comparison of
877 simple potential functions for simulating liquid water. *The Journal of Chemical Physics* **79**, 926-
878 935 (1983).
- 879 20. Knapp, B., Ospina, L. & Deane, C.M. Avoiding false positive conclusions in molecular simulation:
880 The importance of replicas. *Journal of Chemical Theory and Computation* **14**, 6127-6138 (2018).
- 881 21. Vassaux, M., Wan, S., Edeling, W. & Coveney, P.V. Ensembles Are Required to Handle Aleatoric
882 and Parametric Uncertainty in Molecular Dynamics Simulation. *J Chem Theory Comput* **17**, 5187-
883 5197 (2021).
- 884 22. Poongavanam, V. *et al.* Linker-Dependent Folding Rationalizes PROTAC Cell Permeability. *J. Med.*
885 *Chem.* **65**, 13029-13040 (2022).
- 886 23. Ball, K.A. *et al.* Conformational Dynamics of the HIV-Vif Protein Complex. *Biophys. J.* **116**, 1432-
887 1445 (2019).
- 888 24. Kato, M., Chuang, J.L., Tso, S.C., Wynn, R.M. & Chuang, D.T. Crystal structure of pyruvate
889 dehydrogenase kinase 3 bound to lipoyl domain 2 of human pyruvate dehydrogenase complex.
890 *EMBO J.* **24**, 1763-1774 (2005).
- 891 25. Tso, S.C. *et al.* Structure-based design and mechanisms of allosteric inhibitors for mitochondrial
892 branched-chain alpha-ketoacid dehydrogenase kinase. *Proc Natl Acad Sci U S A* **110**, 9728-9733
893 (2013).
- 894 26. Tso, S.C. *et al.* Benzothiophene carboxylate derivatives as novel allosteric inhibitors of branched-
895 chain alpha-ketoacid dehydrogenase kinase. *J. Biol. Chem.* **289**, 20583-20593 (2014).
- 896 27. Maguolo, A. *et al.* A gain-of-function mutation on BCKDK gene and its possible pathogenic role in
897 branched-chain amino acid metabolism. *Genes* **13**, 233 (2022).
- 898 28. Huang, T. *et al.* MSstatsTMT: Statistical detection of differentially abundant proteins in
899 experiments with isobaric labeling and multiple mixtures. *Mol Cell Proteomics* **19**, 1706-1723
900 (2020).
- 901 29. Liu, S. *et al.* Structural studies identify angiotensin II receptor blocker-like compounds as
902 branched-chain ketoacid dehydrogenase kinase inhibitors. *J Biol Chem* **299**, 102959 (2023).

903

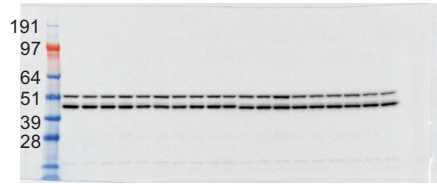
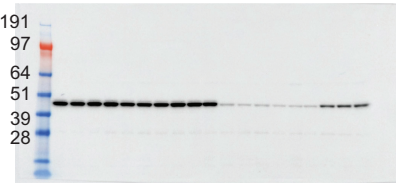
Supplementary Figure 11. Western blots

Related to Figure 1

pBCKDH

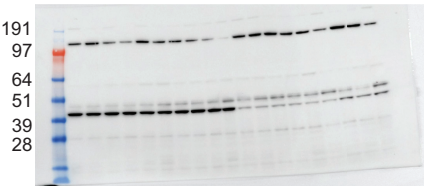
BCKDH

pBCKDH pS292 (Bethyl A304-672A 1:1000)
 total BCKDH (Yenzym 037 1:1000)
 BDK (abcam ab128935 1:1000)
 GAPDH (CST 14C10 1:10000)



BDK

GAPDH



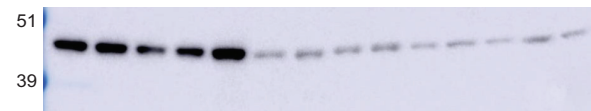
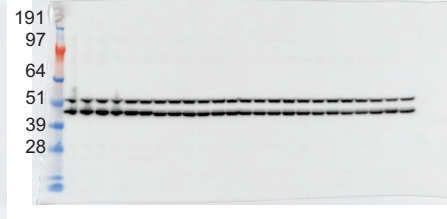
Related to Figure 6A

pBCKDH

BCKDH

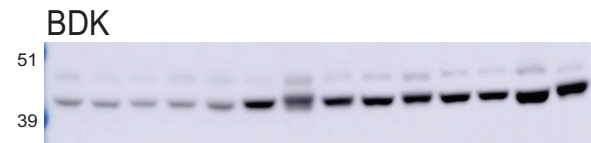
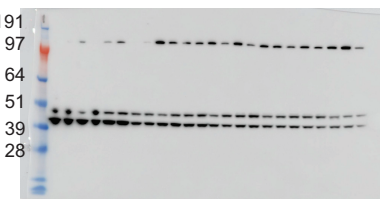
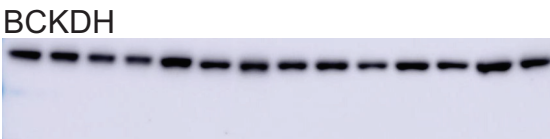
Related to Figure 6C

pBCKDH

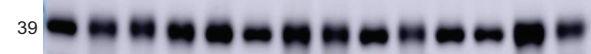


BDK

GAPDH



GAPDH



Related to Figure 6E

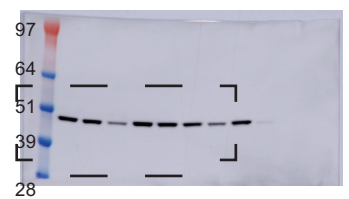
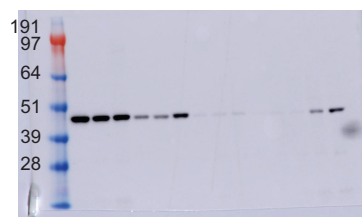
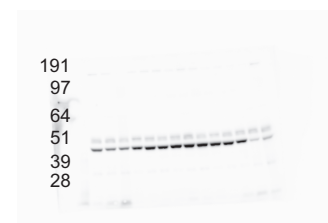
BDK

pBCKDH

Related to Figure 7A

BDK

pBCKDH

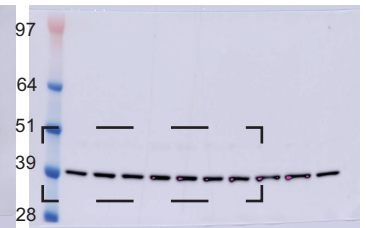
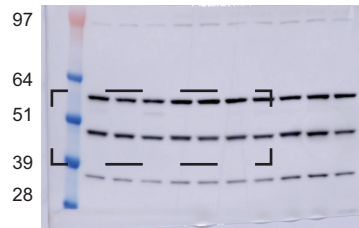
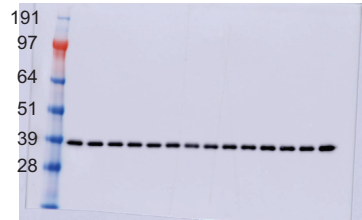
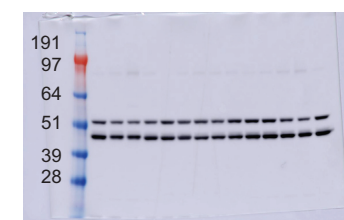


BCKDH

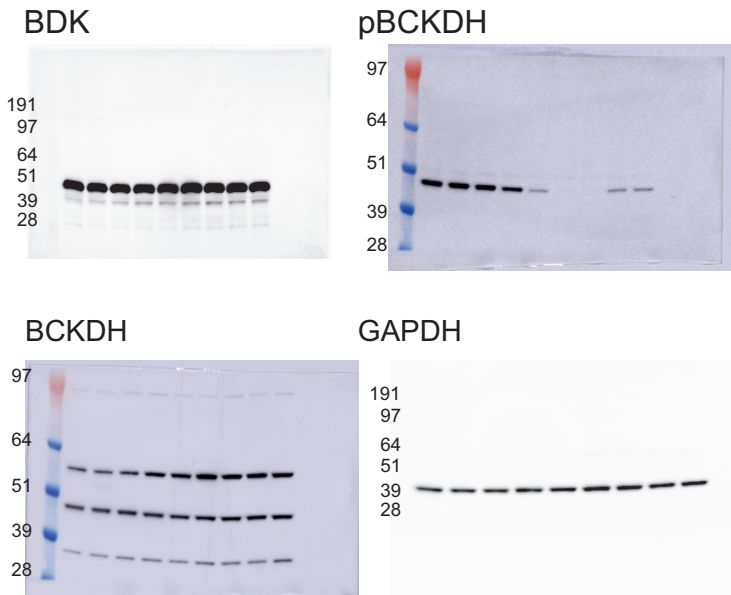
GAPDH

BCKDH

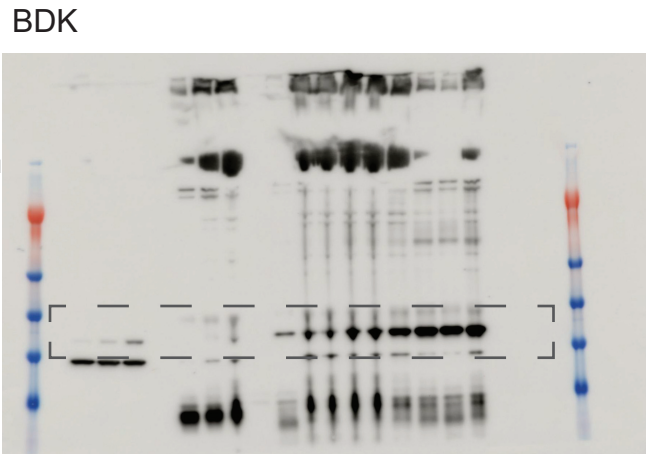
GAPDH



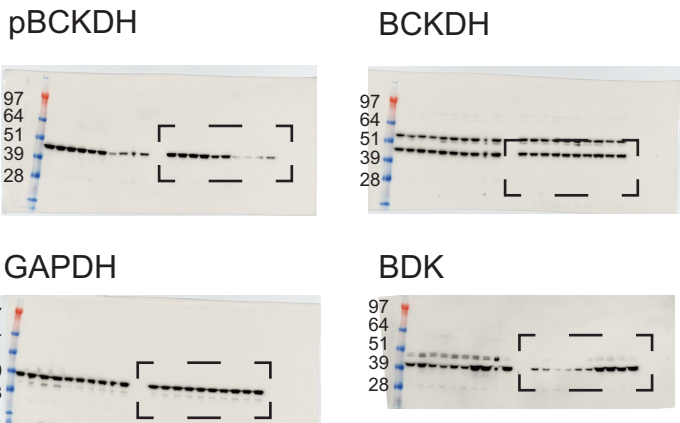
Related to Figure 7C



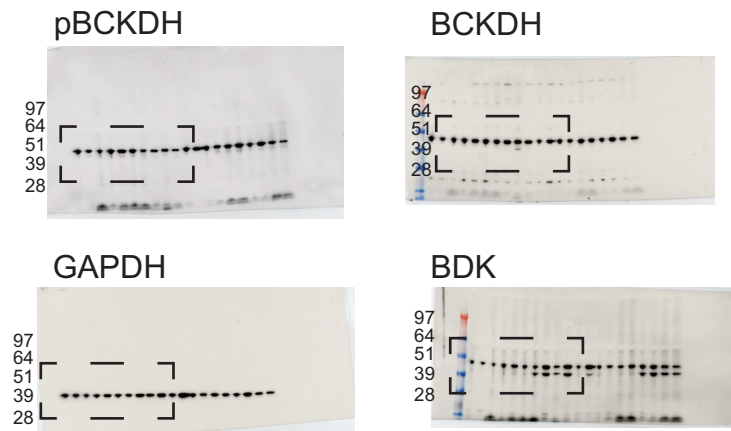
Related to Figure 8B



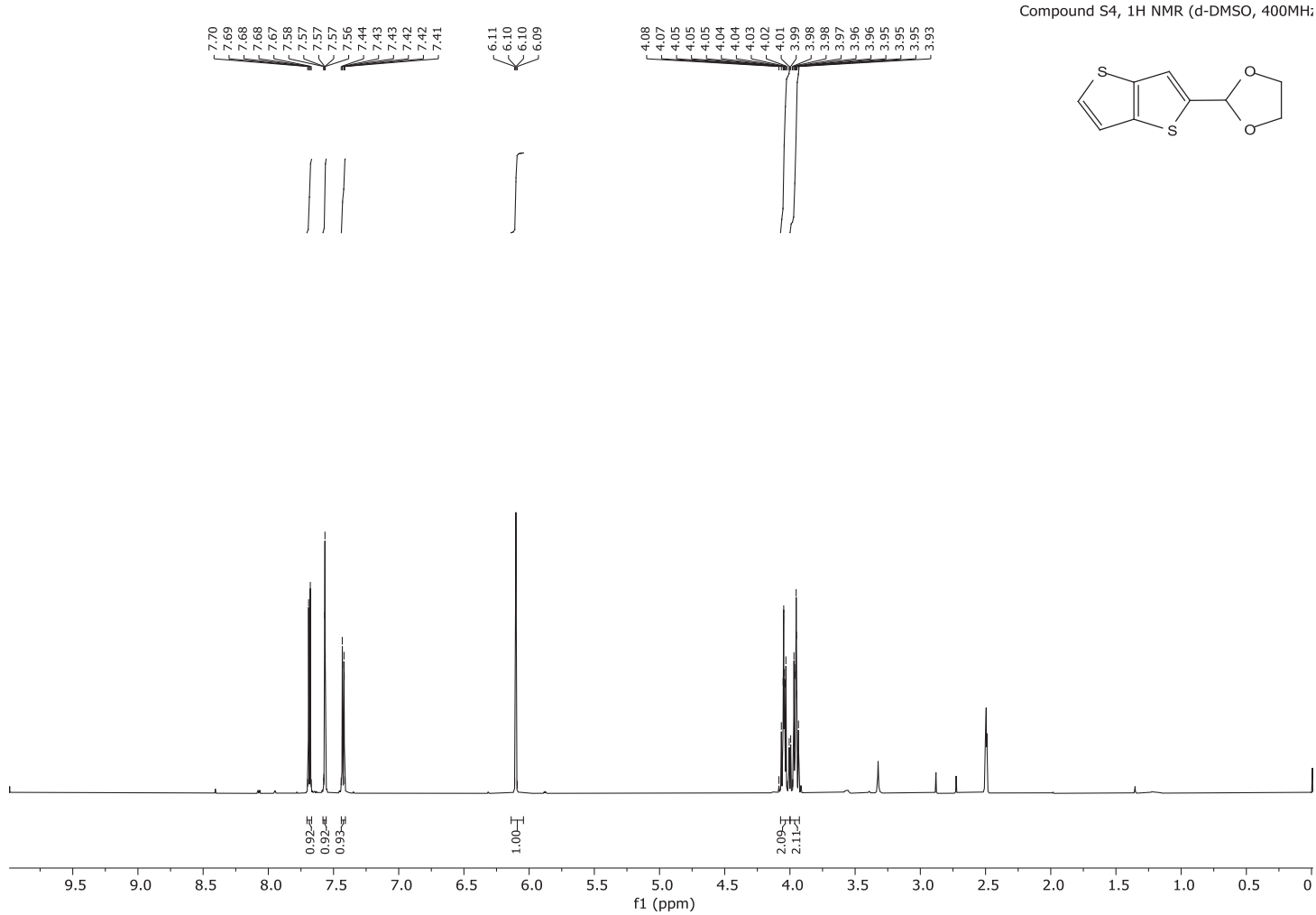
Related to Supplementary Figure 8E



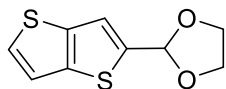
Related to Supplementary Figure 8F



Supplementary Figure 12. 1H NMR of compound S4

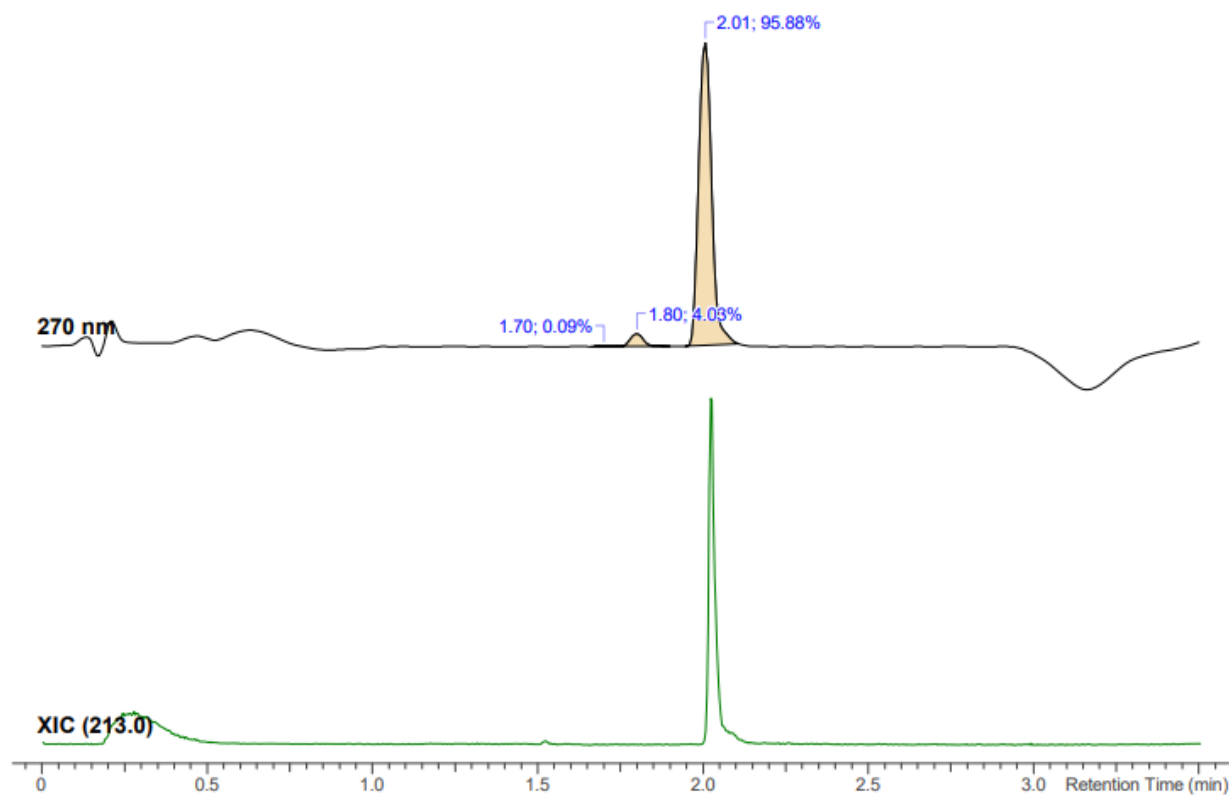


Supplementary Figure 13. HRMS of compound S4



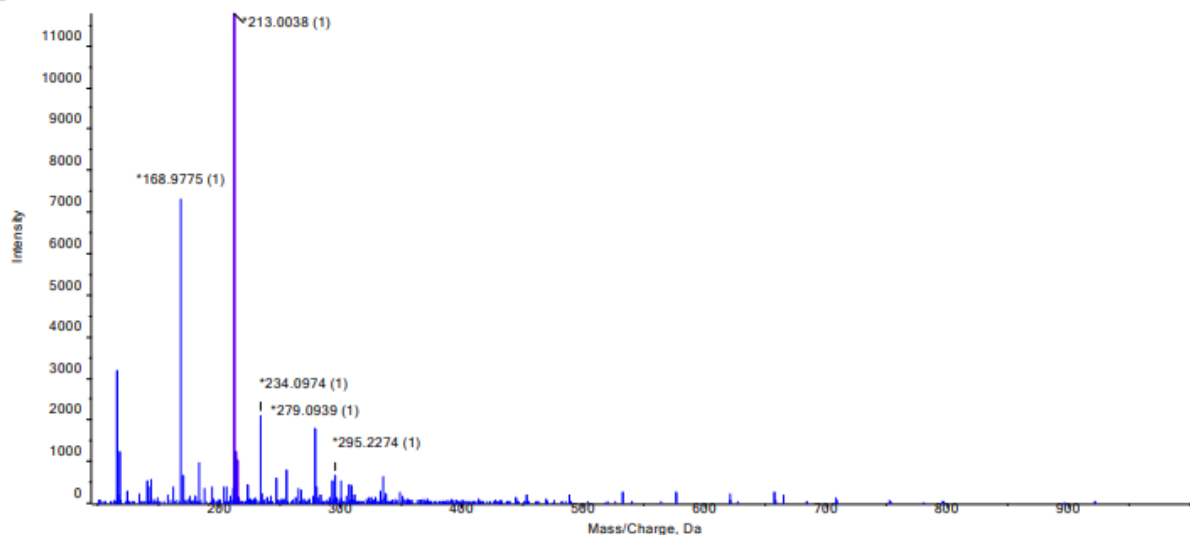
S4

Open Access HRMS Sample Report			
Sample ID	00110407-5465-005	HPLC	Agilent 1200
Molecular Formula	C ₉ H ₈ O ₂ S ₂	Mass Spectrometer	Sciex 5600+ QToF
Submittor	Martinez Alsina, Luis A	DAD	190-400 nm, reported 270nm
Run Date	4/4/2023	MS Scan	100-2000 amu
Analyst	Quinn, Alandra	Acquisition Method	HRMS-3min gradient AQ
Analyst's CeN	00714673-0163	eWB Archive Ref	00713459-0292

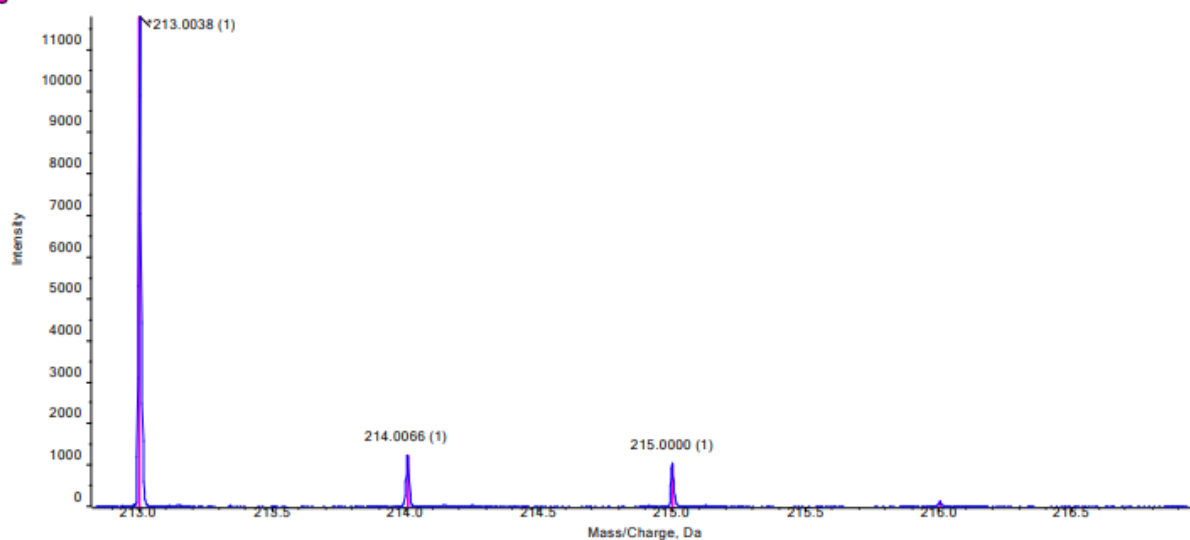


No.	Peak Name	tR (min)	Area (%)
1	unknown	1.70	0.09
2	unknown	1.80	4.03
3	C ₉ H ₈ O ₂ S ₂	2.01	95.88

● Spectrum from 00110407-5465-005.wiff (sample 1) - 00110407-5465-005, +TOF MS (100 - 2000) from 1.981 to 2.076 min
 ● Isotopic Distribution for C₉H₈O₂S₂ H⁺

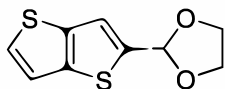


● Spectrum from 00110407-5465-005.wiff (sample 1) - 00110407-5465-005, +TOF MS (100 - 2000) from 1.981 to 2.076 min
 ● Isotopic Distribution for C₉H₈O₂S₂ H⁺



Peak at 2.01 min in UV								
Mass/Charge (Da)	Height	Relative % Height	Compound	Peak Type	Theoretical m/z	Error (ppm)	Theoretical m/z	Theoretical Intensity
213.0038	11774	100.0	C ₉ H ₈ O ₂ S ₂	[M+H] ⁺	213.0039	-0.1	213.0039	100.0
214.0066	1237	10.5					214.0067	11.8
215.0000	1046	8.9					215.0006	9.9
216.0037	128	1.1					216.0033	1.0

Supplementary Figure 14. HPLC of compound S4



S4

Sampl. Name: 00132438-141-05

Acq. Method: D:\Chem32\HPLC-007\DATA\2019\040219\123790-040219-1820 2019-04-02
13-39-26\AM-123790-02-M1.M

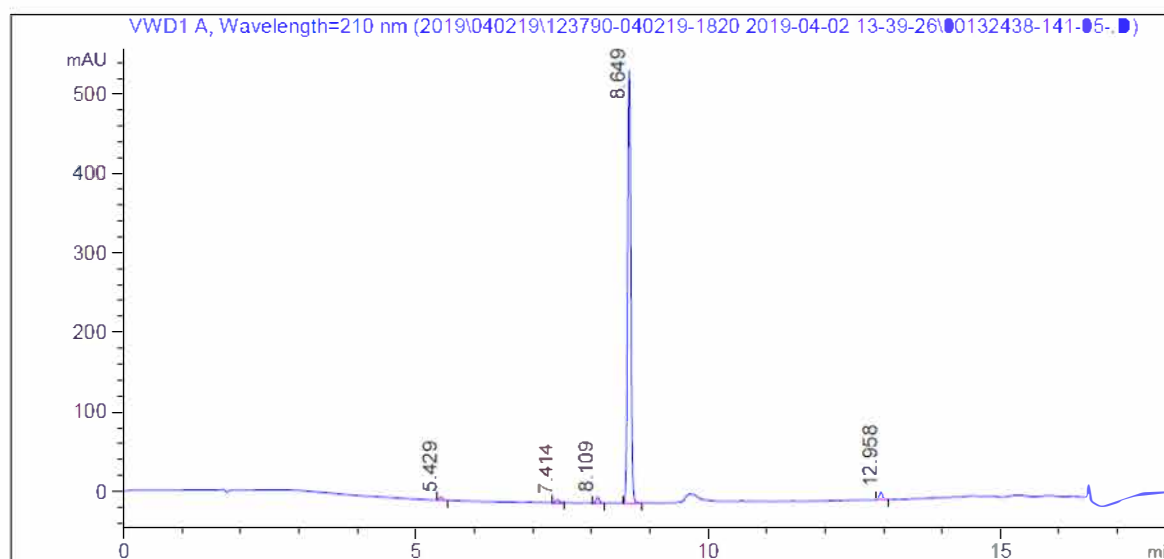
Data File: D:\CHEM32\HPLC-007\DATA\2019\040219\123790-040219-1820 2019-04-02
13-39-26\00132438-141-05-.D

User Name: LN

Acq. Instrument: HPLC-007

Acq. Date: 04/02/2019 18:34:37

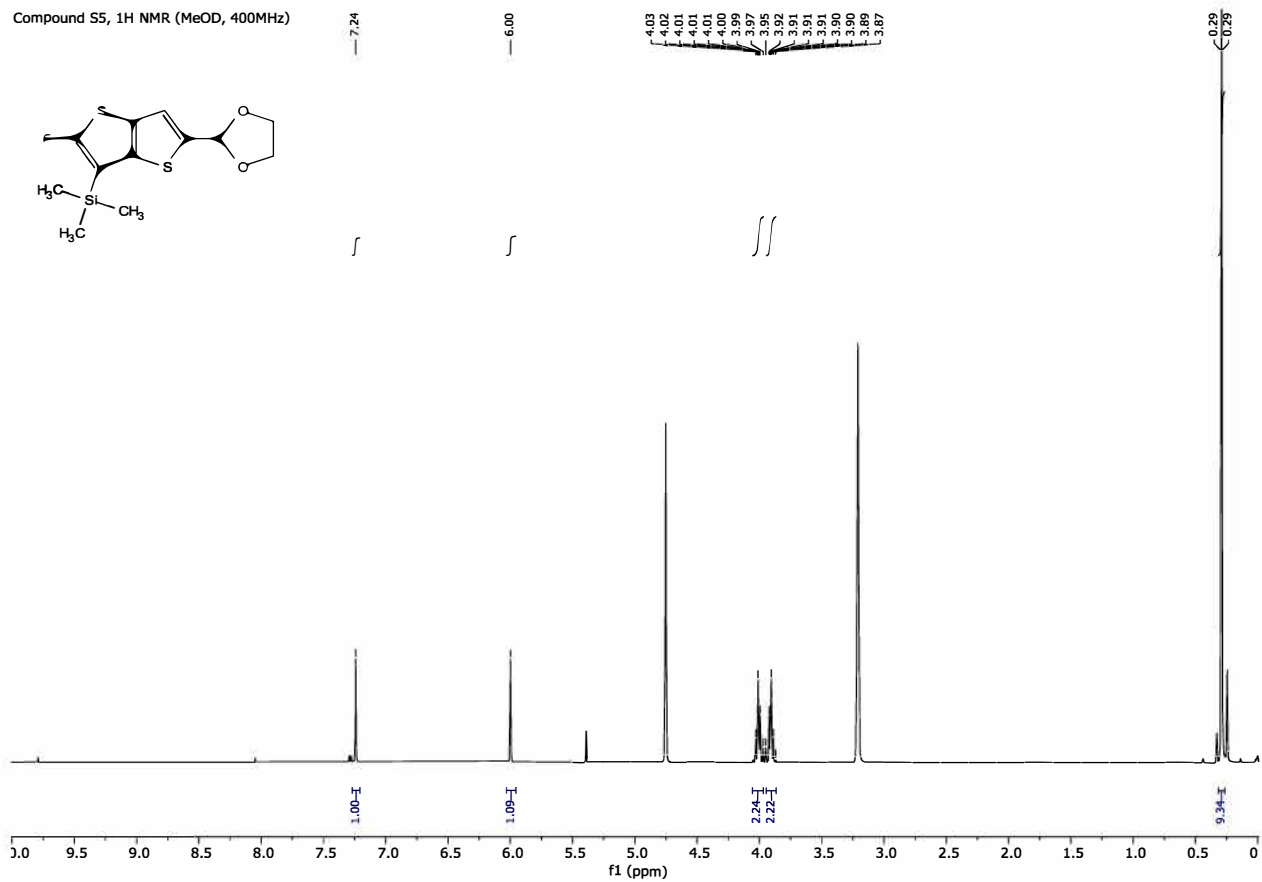
Injection Vol.: 2.0 µl



#	Meas. Ret	Width	Symmetry	Height	Area	Area %
1	5.4291	0.0630	0.8142	3.8512	14.5653	0.6555
2	7.4143	0.0780	0.9469	4.1883	19.5896	0.8816
3	8.1092	0.0639	0.9313	7.0948	27.2131	1.2247
4	8.6492	0.0649	0.9675	545.4932	2123.0632	95.5439
5	12.9580	0.0679	0.9056	9.2360	37.6493	1.6943

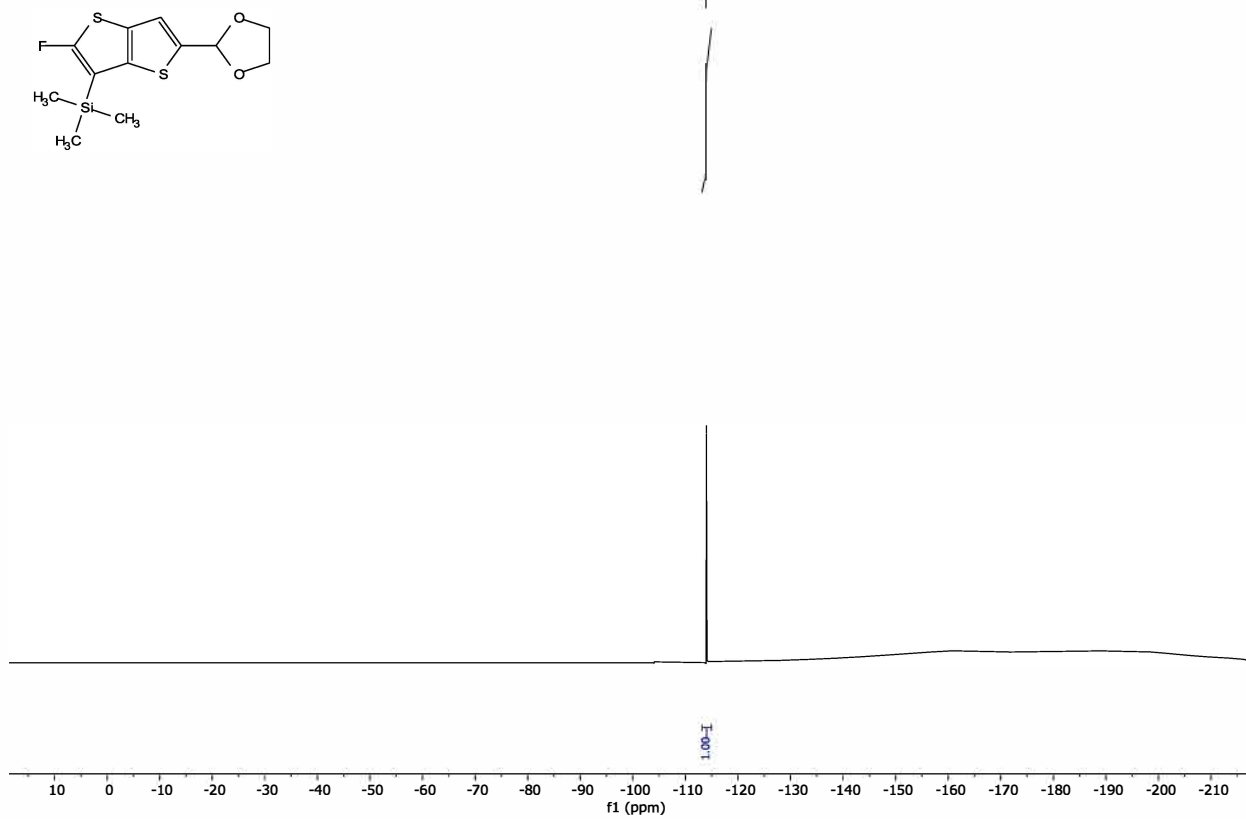
Supplementary Figure 15. ¹H NMR of compound S5

Compound S5, ¹H NMR (MeOD, 400MHz)

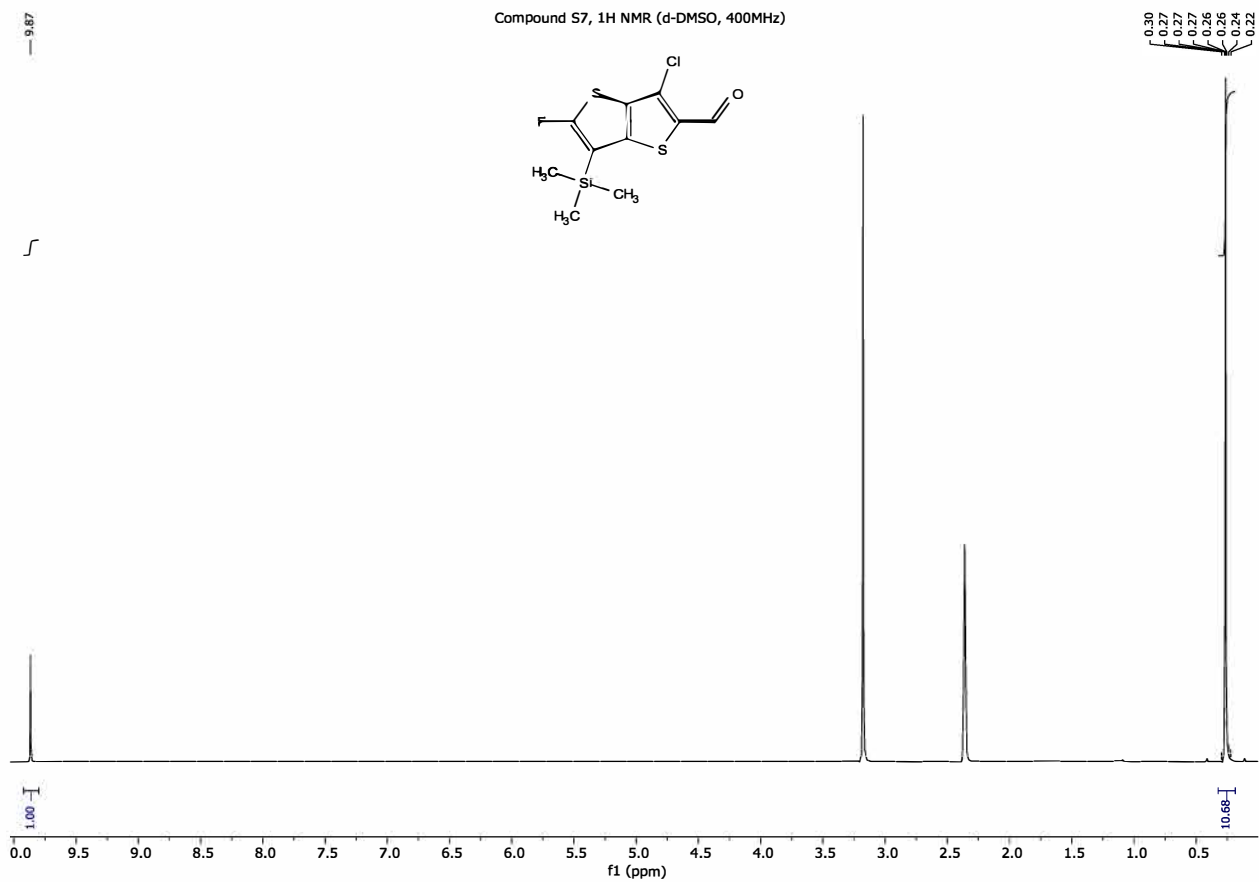


Supplementary Figure 16. ¹⁹F NMR of compound S5

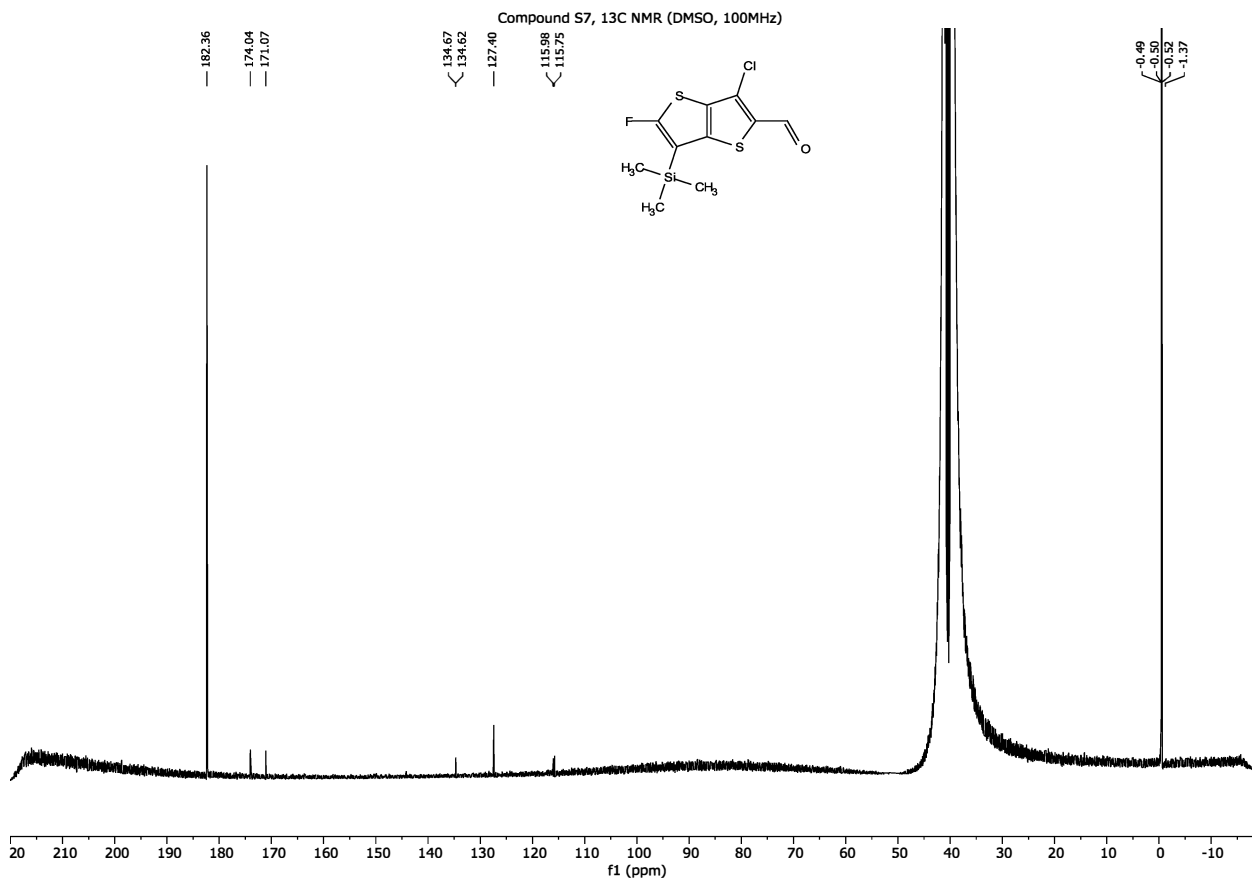
Compound S5, ¹⁹F NMR (MeOD, 400MHz)



Supplementary Figure 17. 1H NMR of compound S7

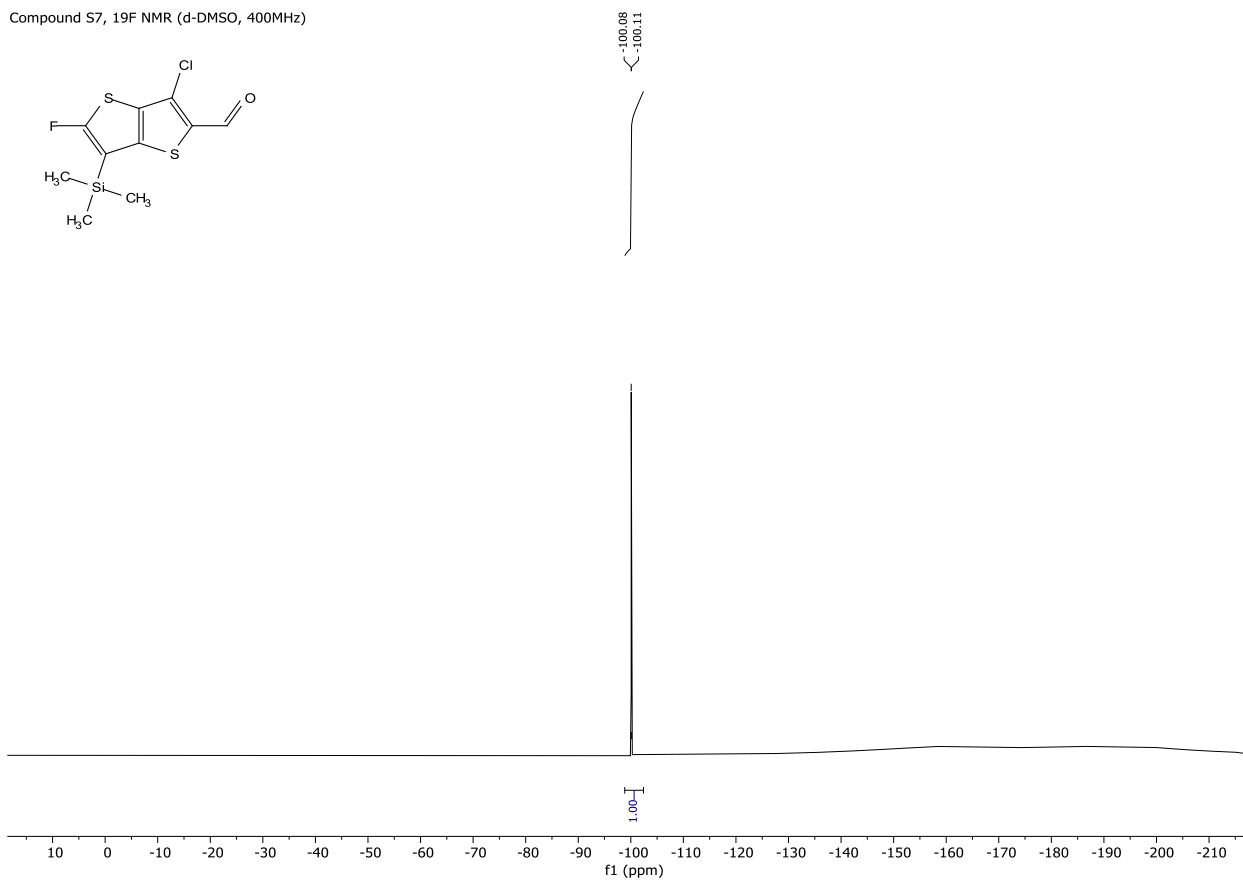
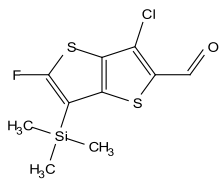


Supplementary Figure 18. ¹³C NMR of compound S7

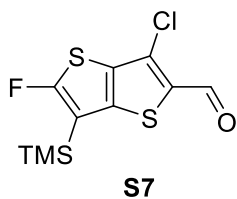


Supplementary Figure 19. 19F NMR of compound S7

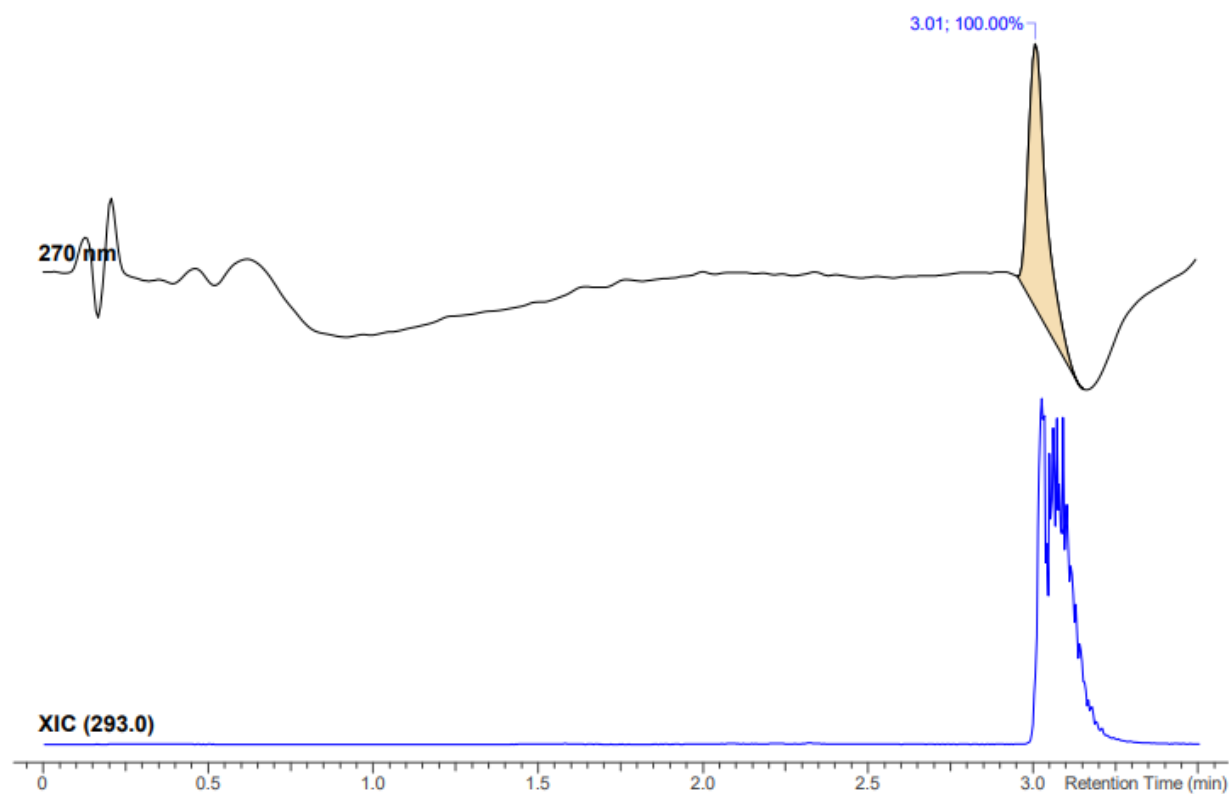
Compound S7, 19F NMR (d-DMSO, 400MHz)



Supplementary Figure 20. HRMS of compound S7

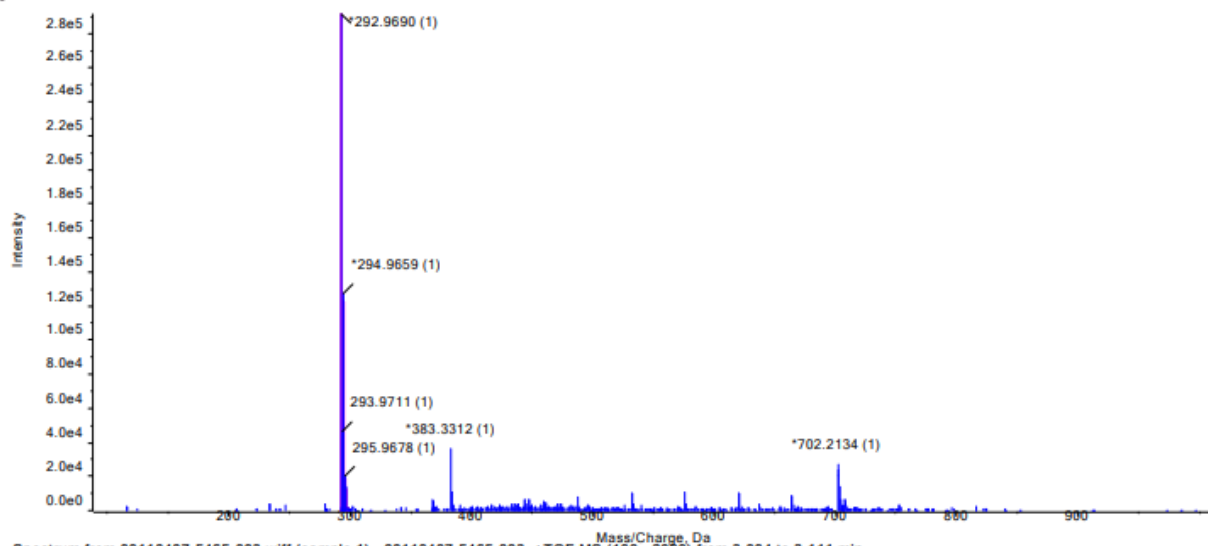


Open Access HRMS Sample Report			
Sample ID	00110407-5465-003	HPLC	Agilent 1200
Molecular Formula	C ₁₀ H ₁₀ ClFOS ₂ Si	Mass Spectrometer	Sciex 5600+ QToF
Submittor	Martinez Alsina, Luis A	DAD	190-400 nm, reported 270nm
Run Date	4/4/2023	MS Scan	100-2000 amu
Analyst	Quinn, Alandra	Acquisition Method	HRMS-3min gradient AQ
Analyst's CeN	00714673-0163	eWB Archive Ref	00713459-0292

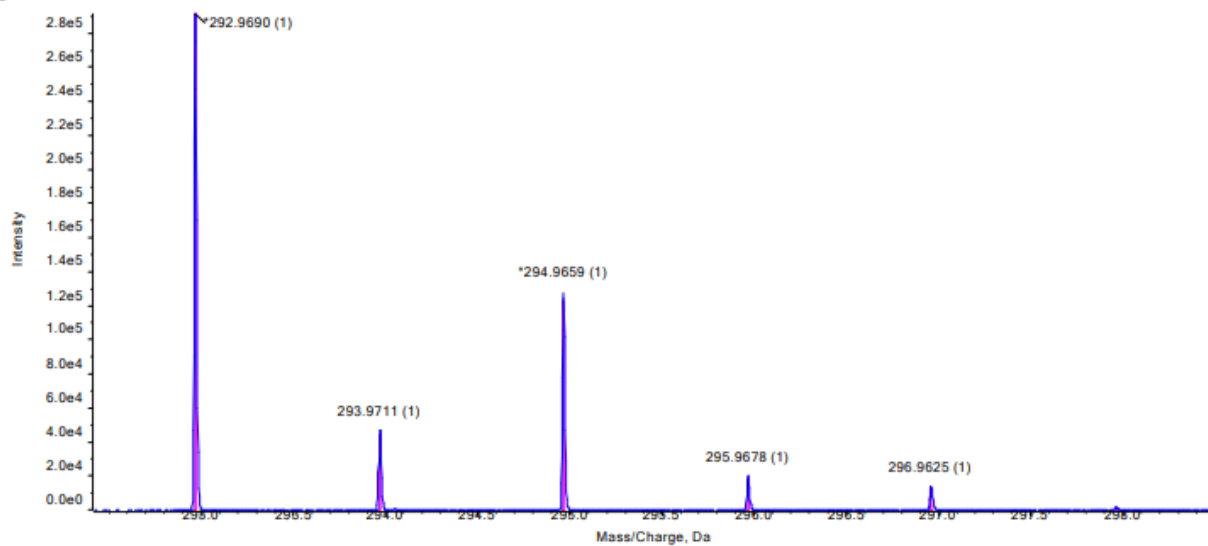


No.	Peak Name	tR (min)	Area (%)
1	C ₁₀ H ₁₀ ClFOS ₂ Si	3.01	100.00

● Spectrum from 00110407-5465-003.wiff (sample 1) - 00110407-5465-003, +TOF MS (100 - 2000) from 3.004 to 3.111 min
 ● Isotopic Distribution for C₁₀H₁₀ClFOS₂Si H⁺

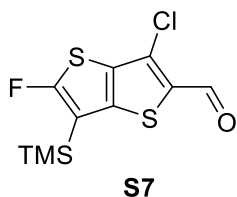


● Spectrum from 00110407-5465-003.wiff (sample 1) - 00110407-5465-003, +TOF MS (100 - 2000) from 3.004 to 3.111 min
 ● Isotopic Distribution for C₁₀H₁₀ClFOS₂Si H⁺

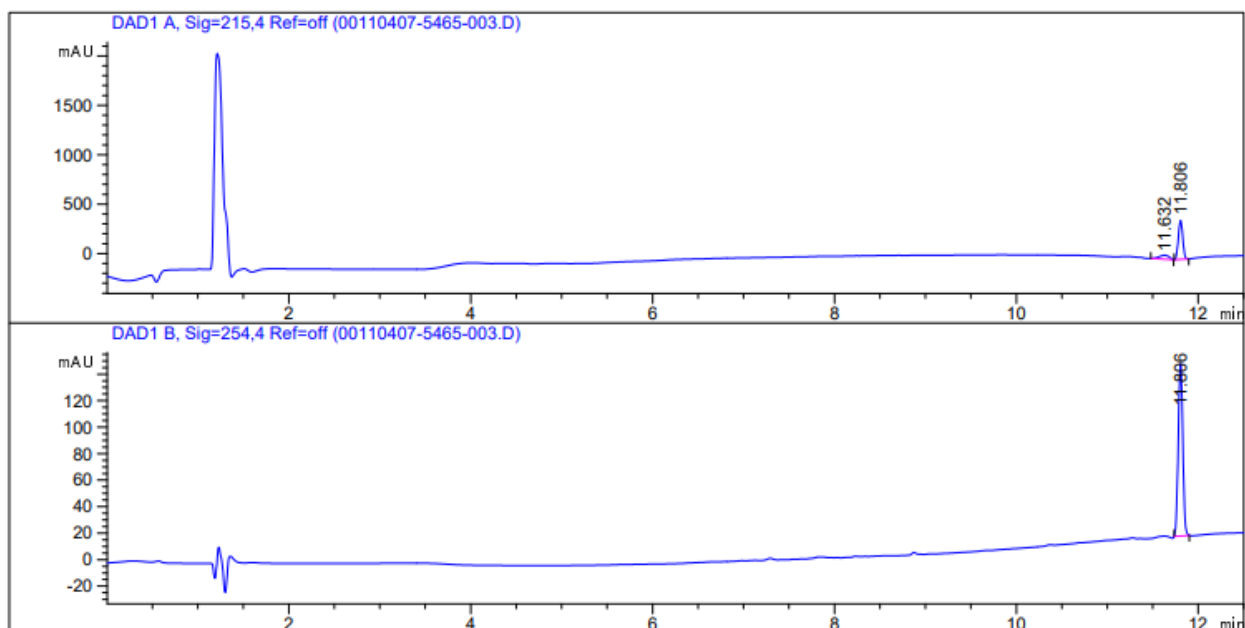


Peak at 3.01 min in UV								
Mass/Charge (Da)	Height	Relative % Height	Compound	Peak Type	Theoretical m/z	Error (ppm)	Theoretical m/z	Theoretical Intensity
292.9690	291363	100.0	C ₁₀ H ₁₀ ClFOS ₂ Si	[M+H] ⁺	292.9688	0.8	292.9688	100.0
293.9711	46906	16.1					293.9707	17.9
294.9659	127292	43.7					294.9658	45.8
295.9678	19914	6.8					295.9677	7.8
296.9625	13923	4.8					296.9629	5.1

Supplementary Figure 21. HPLC of compound S7



```
=====
Acq. Operator   : SYSTEM                      Seq. Line :    3
Sample Operator : SYSTEM
Acq. Instrument : LC-325GF                    Location  :    3
Injection Date  : 3/17/2023 4:12:37 PM       Inj       :    1
                                           Inj Volume: 5.000 µl
Different Inj Volume from Sample Entry! Actual Inj Volume : 10.000 µl
Sequence File   : C:\Users\Public\Documents\ChemStation\1\Data\DEF_LC_2021 2023-03-17 15-41
                 -03\DEF_LC_2021.S
Method          : C:\Users\Public\Documents\ChemStation\1\Data\DEF_LC_2021 2023-03-17 15-41
                 -03\ACID_CLASSIC.M (Sequence Method)
Last changed    : 6/8/2017 9:26:22 AM by SYSTEM
Method Info     : ACID METHOD for classic look on new Chemstation software
                 Column: XBridge C18 5 micron (4.6 mm x 150 mm)
                 Flow rate: 1.500 mL/min with solvents containing 0.1% TFA
                 0-1.5 min: 5% acetonitrile/water
                 1.5-10 min: 5-100% acetonitrile water
                 10-11 min: 100% acetonitrile
                 11-12.5 min: 100-5% acetonitrile/water
=====
```



```
=====
                          Area Percent Report
=====
```

```
Sorted By      :      Signal
Multiplier     :      1.0000
Dilution       :      1.0000
Do not use Multiplier & Dilution Factor with ISTDs
```

Signal 1: DAD1 A, Sig=215,4 Ref=off

Peak #	RetTime [min]	Type	Width [min]	Area [mAU*s]	Height [mAU]	Area %
1	11.632	BB	0.1213	314.89941	42.08999	19.1677
2	11.806	BB	0.0511	1327.96643	396.49451	80.8323

Totals : 1642.86584 438.58450

Signal 2: DAD1 B, Sig=254,4 Ref=off

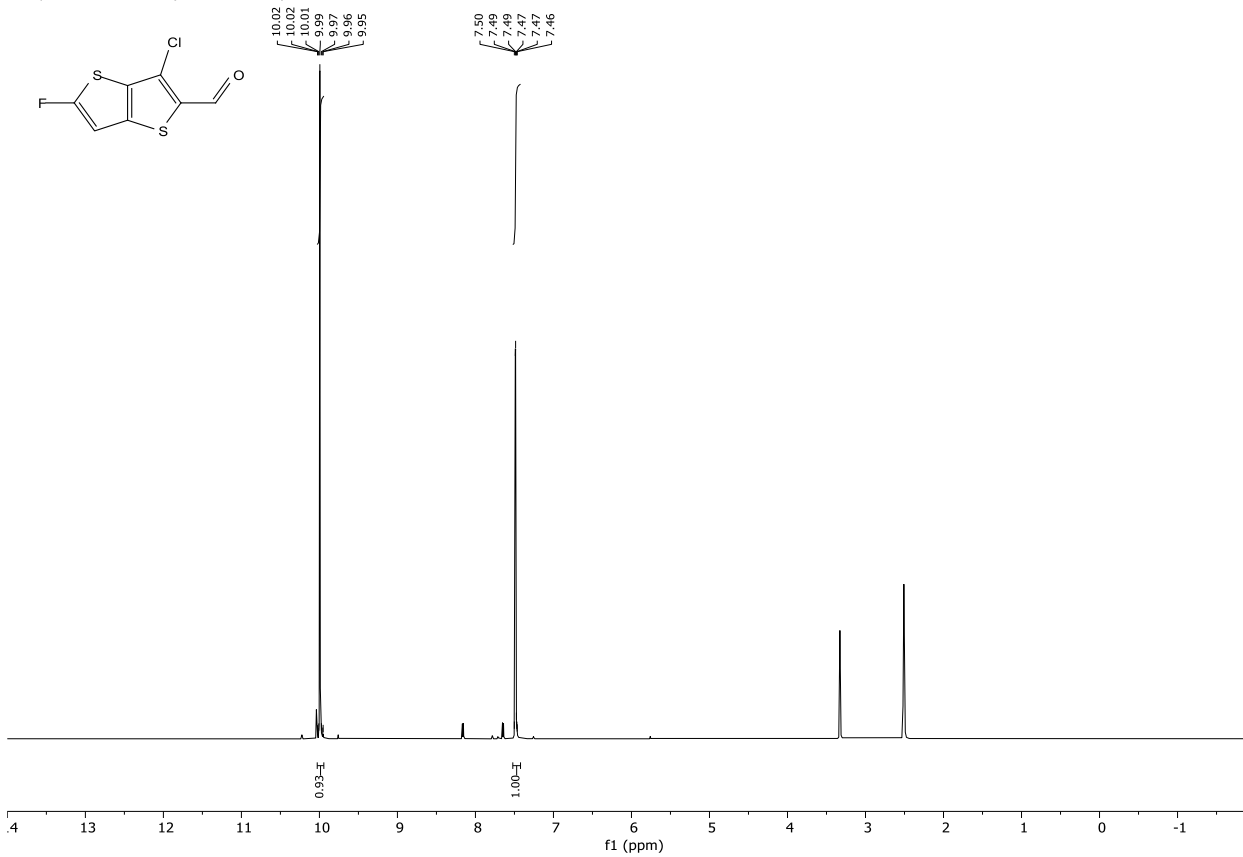
Peak #	RetTime [min]	Type	Width [min]	Area [mAU*s]	Height [mAU]	Area %
1	11.806	BB	0.0523	453.53329	131.35742	100.0000

Totals : 453.53329 131.35742

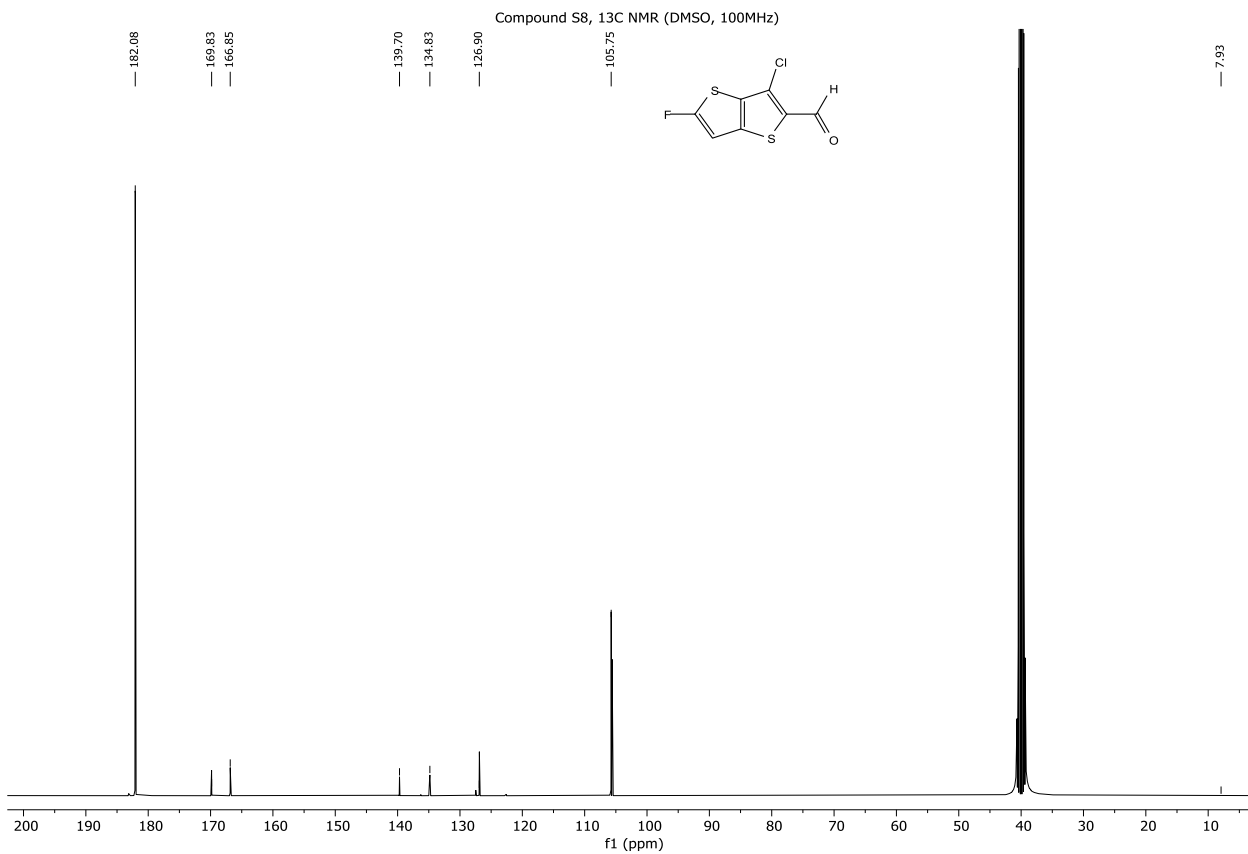
=====
*** End of Report ***

Supplementary Figure 22. ¹H NMR of compound S8

Compound S8, ¹H NMR (DMSO, 400MHz)

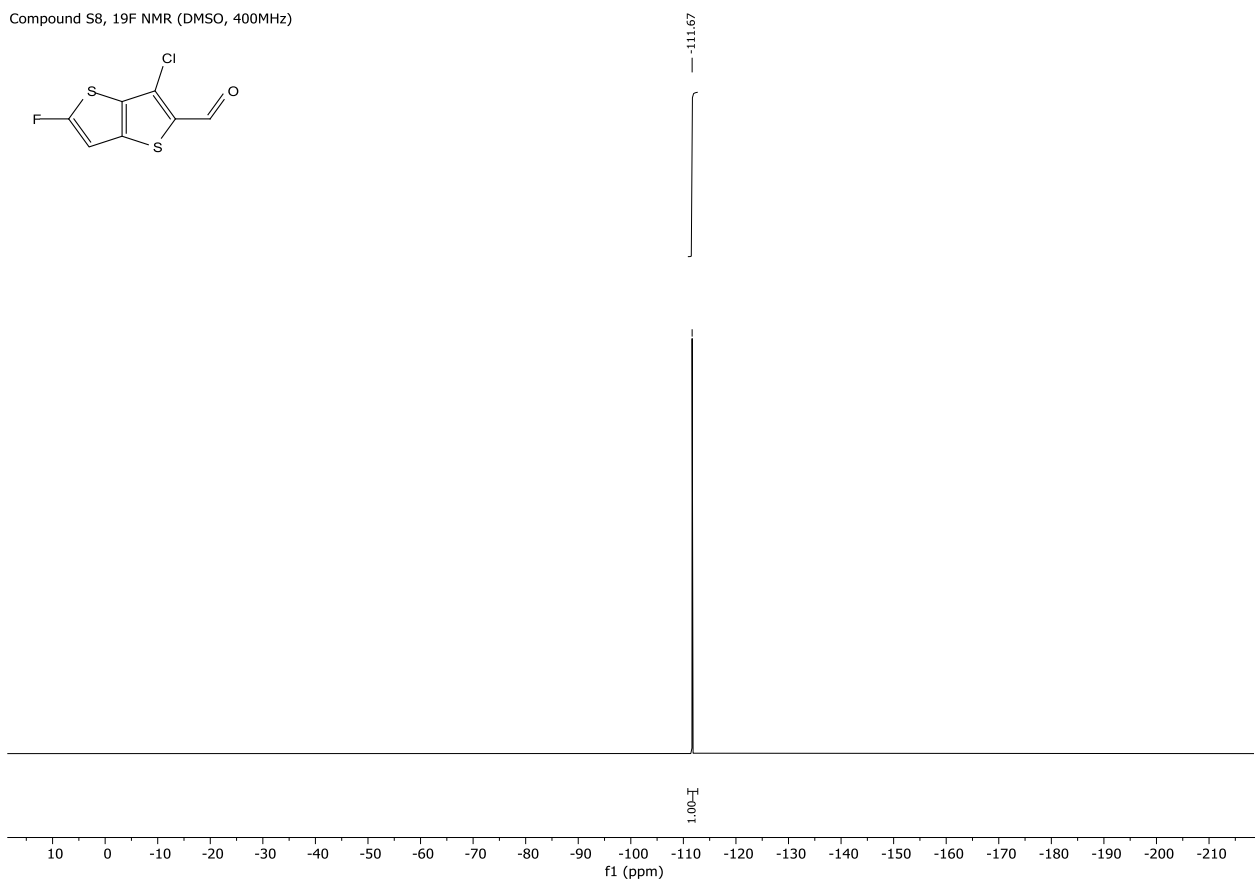
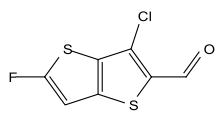


Supplementary Figure 23. ¹³C NMR of compound S8

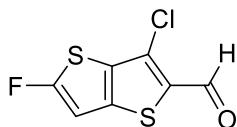


Supplementary Figure 24. ¹⁹F NMR of compound S8

Compound S8, ¹⁹F NMR (DMSO, 400MHz)

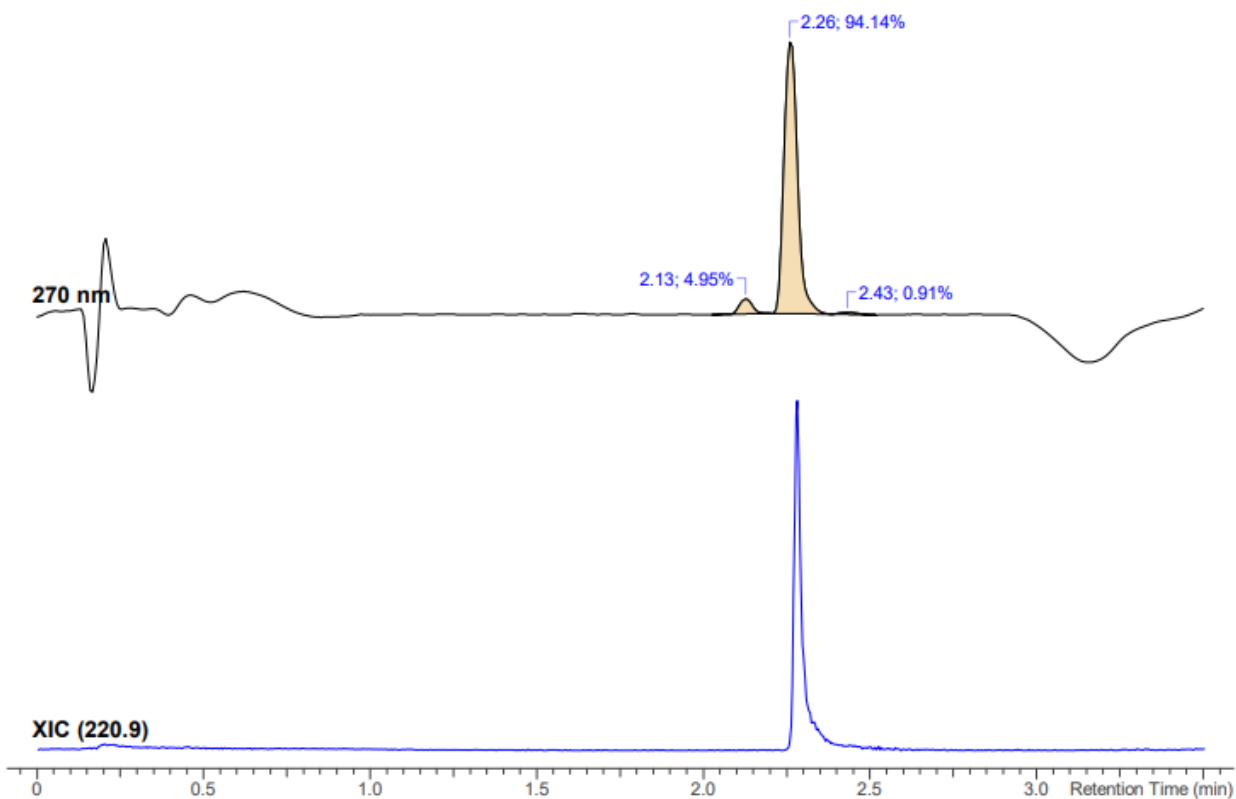


Supplementary Figure 25. HRMS of compound S8



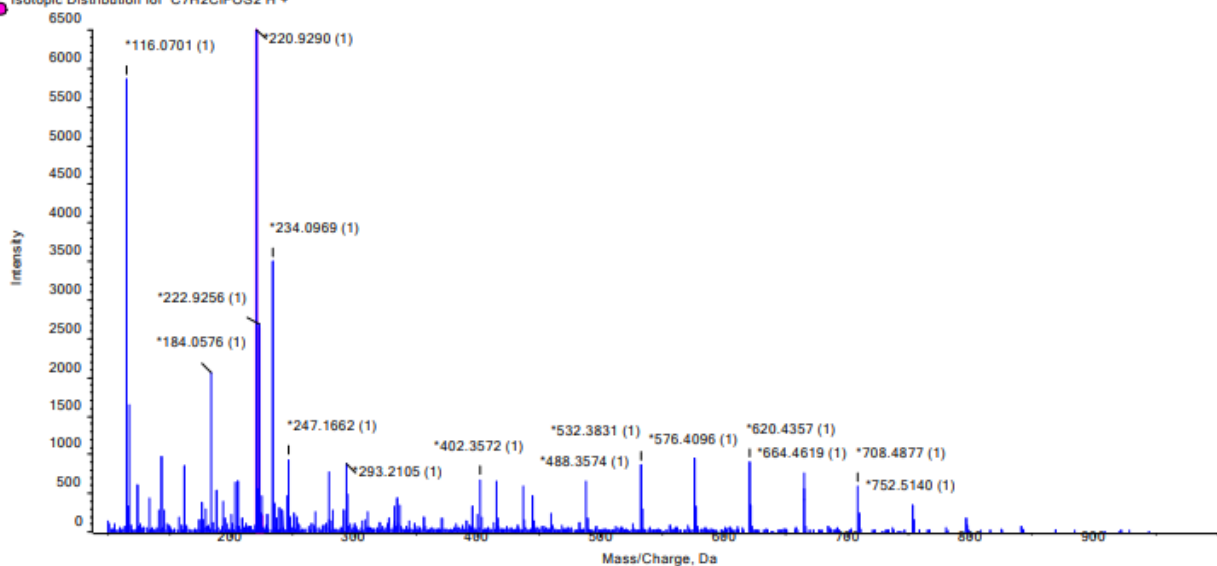
S8

Open Access HRMS Sample Report			
Sample ID	00110407-5465-004	HPLC	Agilent 1200
Molecular Formula	C7H2ClFOS2	Mass Spectrometer	Sciex 5600+ QToF
Submittor	Martinez Alsina, Luis A	DAD	190-400 nm, reported 270nm
Run Date	4/4/2023	MS Scan	100-2000 amu
Analyst	Quinn, Alandra	Acquisition Method	HRMS-3min gradient AQ
Analyst's CeN	00714673-0163	eWB Archive Ref	00713459-0292

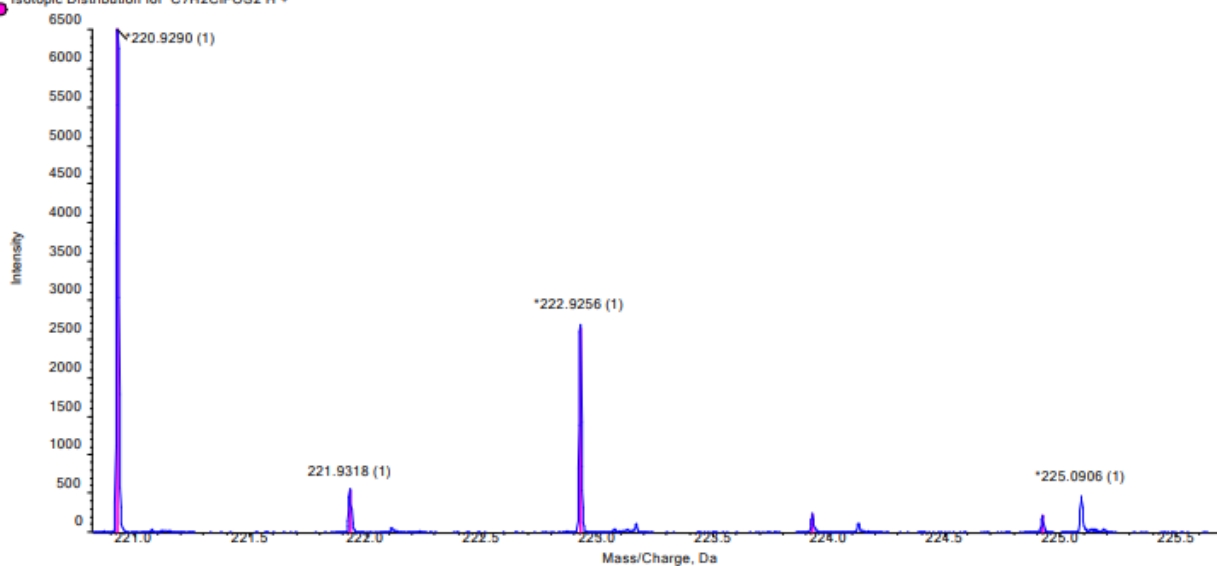


No.	Peak Name	tR (min)	Area (%)
1	unknown	2.13	4.95
2	C7H2ClFOS2	2.26	94.14
3	unknown	2.43	0.91

Spectrum from 00110407-5465-004_2.wiff (sample 1) - 00110407-5465-004, +TOF MS (100 - 2000) from 2.252 to 2.340 min
 Isotopic Distribution for C7H2ClFOS2 H +



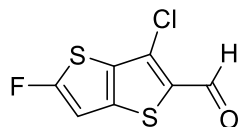
Spectrum from 00110407-5465-004_2.wiff (sample 1) - 00110407-5465-004, +TOF MS (100 - 2000) from 2.252 to 2.340 min
 Isotopic Distribution for C7H2ClFOS2 H +



Peak at 2.26 min in UV

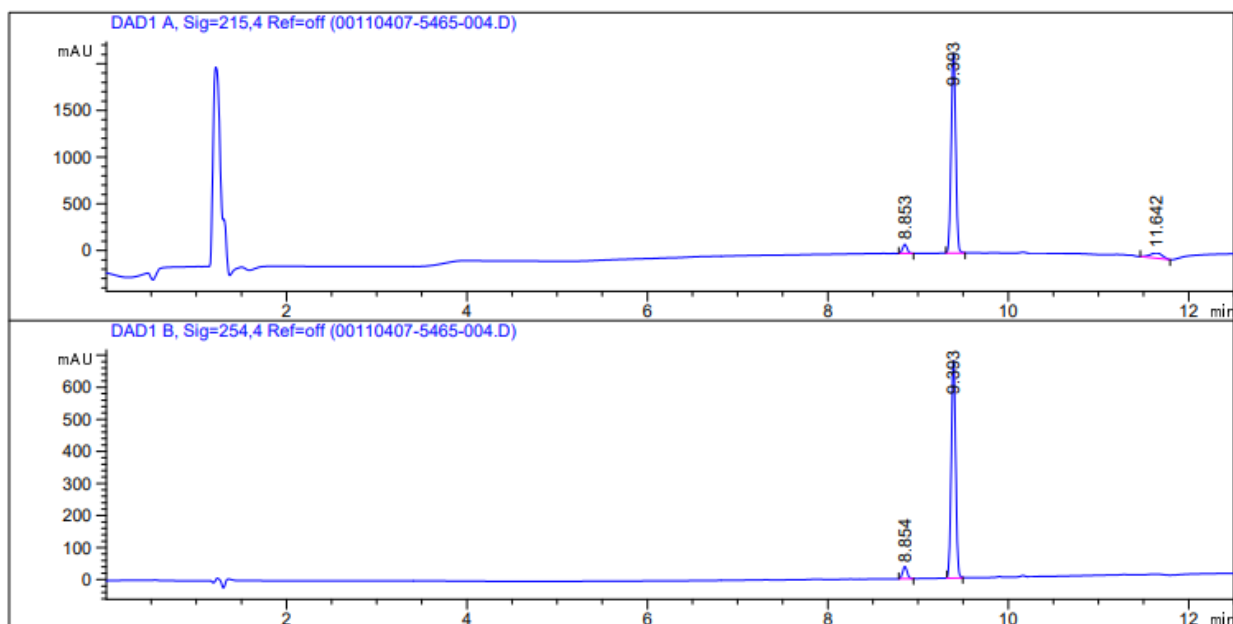
Mass/Charge (Da)	Height	Relative % Height	Compound	Peak Type	Theoretical m/z	Error (ppm)	Theoretical m/z	Theoretical Intensity
220.9290	6500	100.0	C7H2ClFOS2	[M+H] ⁺	220.9292	-1.3	220.9292	100.0
221.9318	548	8.4					221.9319	9.4
222.9256	2689	41.4					222.9261	41.4
223.9283	249	3.8					223.9289	3.8
224.9221	209	3.2					224.9227	3.3

Supplementary Figure 26. HPLC of compound S8



S8

```
=====
Acq. Operator   : SYSTEM                               Seq. Line :    4
Sample Operator : SYSTEM                               Location  :    4
Acq. Instrument : LC-325GF                             Inj       :    1
Injection Date  : 3/17/2023 4:26:47 PM                 Inj Volume: 5.000 µl
                                                    Actual Inj Volume : 10.000 µl
Different Inj Volume from Sample Entry!
Sequence File   : C:\Users\Public\Documents\ChemStation\1\Data\DEF_LC_2021 2023-03-17 15-41
                 -03\DEF_LC_2021.S
Method          : C:\Users\Public\Documents\ChemStation\1\Data\DEF_LC_2021 2023-03-17 15-41
                 -03\ACID_CLASSIC.M (Sequence Method)
Last changed    : 6/8/2017 9:26:22 AM by SYSTEM
Method Info     : ACID METHOD for classic look on new Chemstation software
                 Column: XBridge C18 5 micron (4.6 mm x 150 mm)
                 Flow rate: 1.500 mL/min with solvents containing 0.1% TFA
                 0-1.5 min: 5% acetonitrile/water
                 1.5-10 min: 5-100% acetonitrile water
                 10-11 min: 100% acetonitrile
                 11-12.5 min: 100-5% acetonitrile/water
=====
```



=====
Area Percent Report
=====

```
Sorted By      : Signal
Multiplier     : 1.0000
Dilution      : 1.0000
Do not use Multiplier & Dilution Factor with ISTDs
```

Signal 1: DAD1 A, Sig=215,4 Ref=off

Peak #	RetTime [min]	Type	Width [min]	Area [mAU*s]	Height [mAU]	Area %
1	8.853	BB	0.0546	337.35281	96.83382	4.0003
2	9.393	BB	0.0570	7575.64990	2155.09009	89.8311
3	11.642	BB	0.1470	520.20831	55.69928	6.1686

Totals : 8433.21103 2307.62319

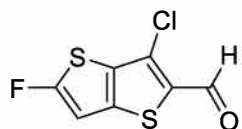
Signal 2: DAD1 B, Sig=254,4 Ref=off

Peak #	RetTime [min]	Type	Width [min]	Area [mAU*s]	Height [mAU]	Area %
1	8.854	BB	0.0550	133.53358	38.03883	5.4395
2	9.393	BB	0.0538	2321.35132	680.88263	94.5605

Totals : 2454.88490 718.92146

=====
*** End of Report ***

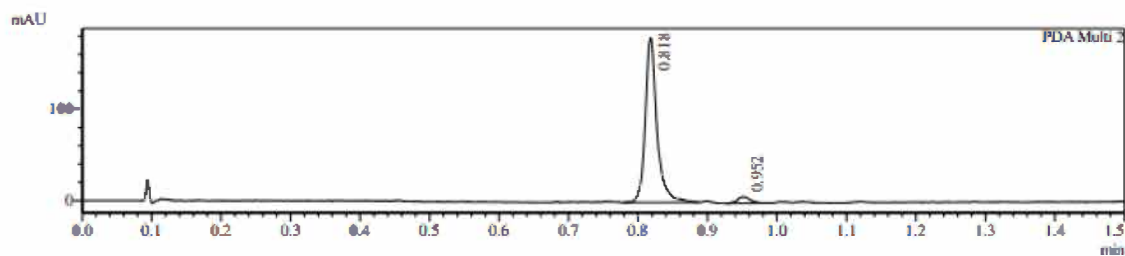
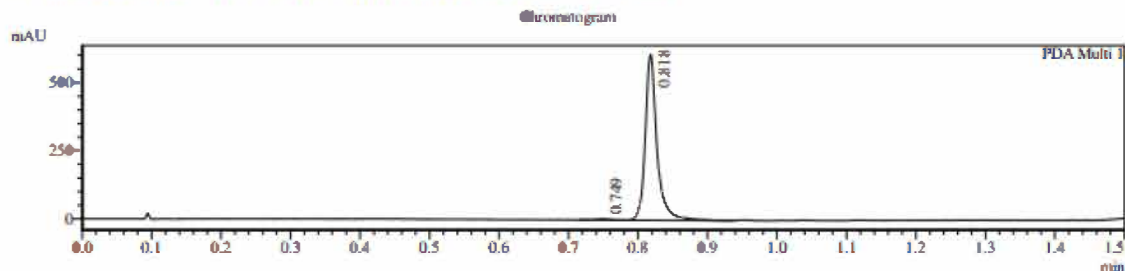
Supplementary Figure 27. LCMS of compound S8



S8

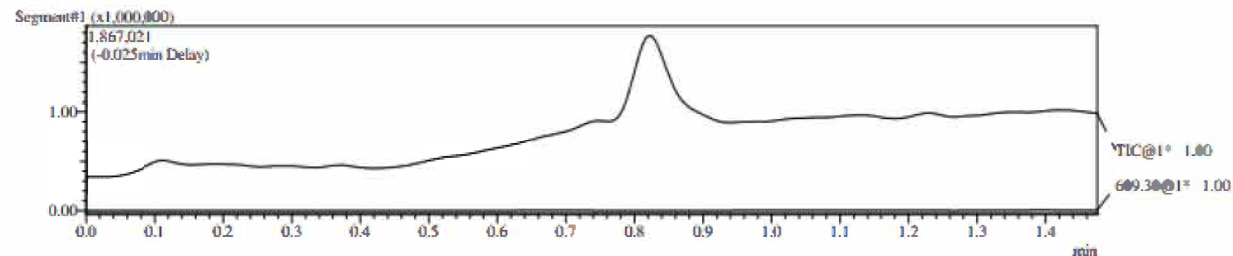
MS Ionization : ESI

Instrument & Column: LCMS-AH(4-302) Chromolith. Flash RP-18e 25-2mm



1 PDA Multi 1 / 220nm 4nm

2 PDA Multi 2 / 254nm 4nm



Integration Result

Ch1 220nm 4nm

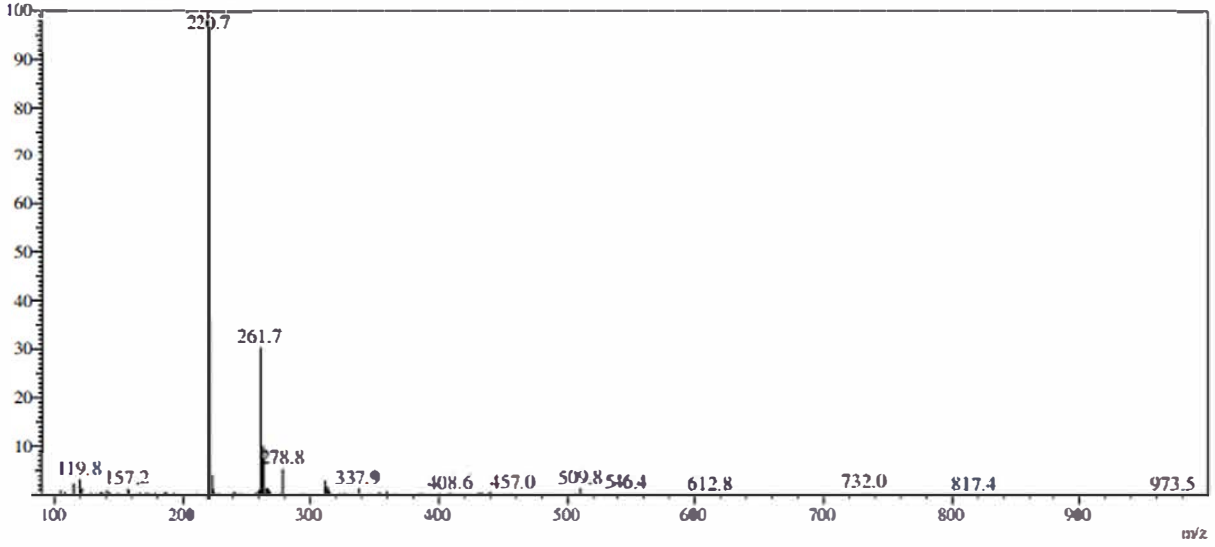
Peak#	Ret. Time	Height	Height %	USP Width	Area	Area %
1	0.749	3232	0.538	0.030	4932	0.683
2	0.818	597822	99.462	0.028	717323	99.317

Ch2 254nm 4nm

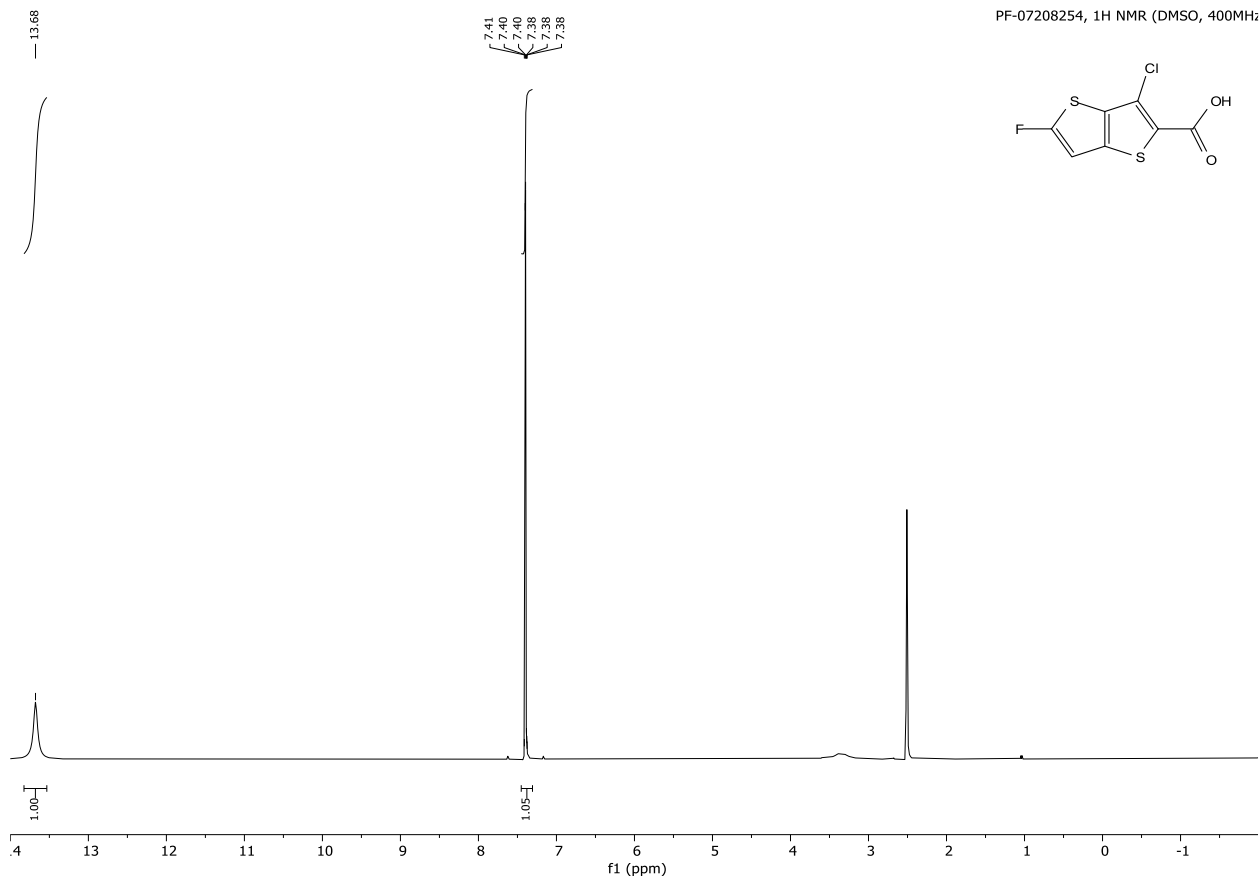
Peak#	Ret. Time	Height	Height %	USP Width	Area	Area %
1	0.818	177973	96.210	0.028	210958	95.975
2	0.952	7011	3.790	0.030	8846	4.025

MS Spectrum Graph

RetTime: 0.817 DataFile: C:\DATA\1901\190115\00711155-1003-001A.tcd

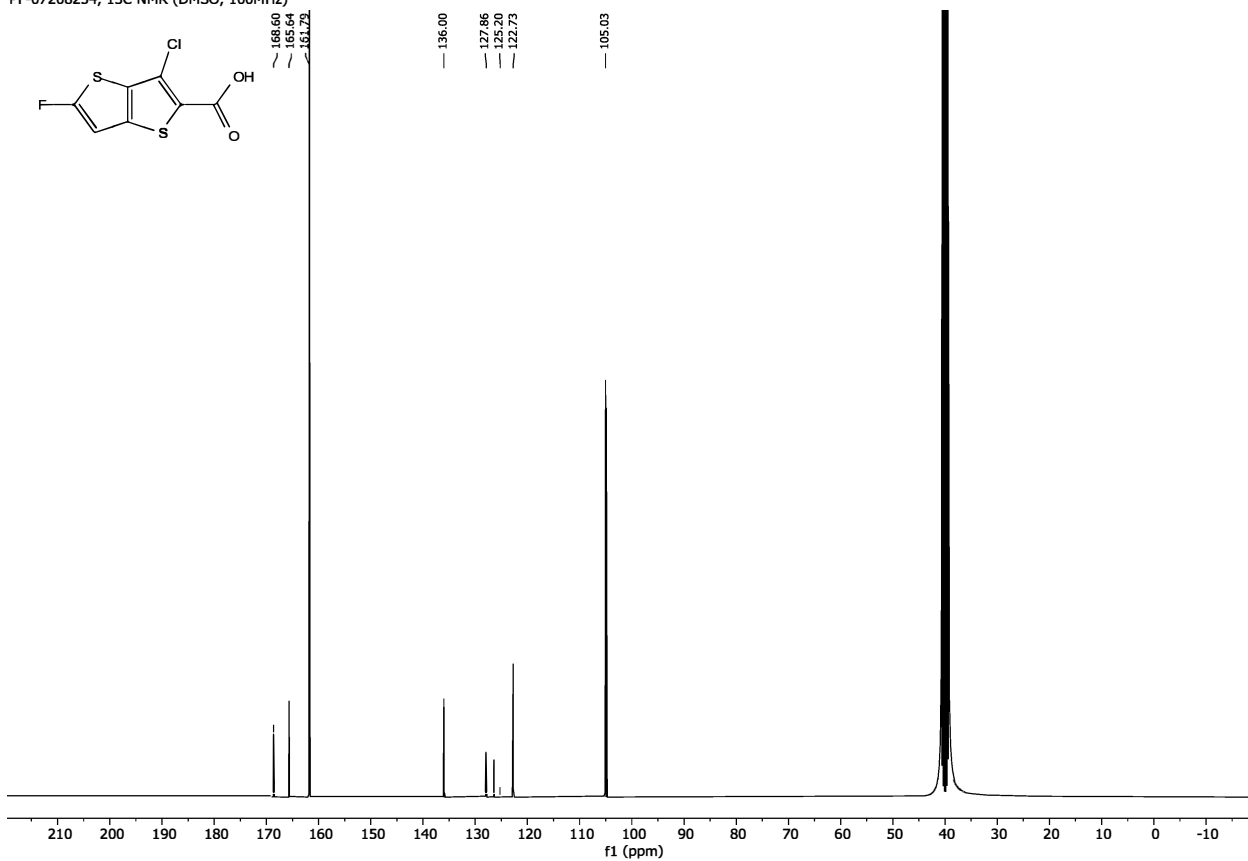
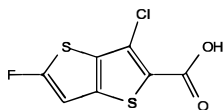


Supplementary Figure 28. 1H NMR of PF-07208254



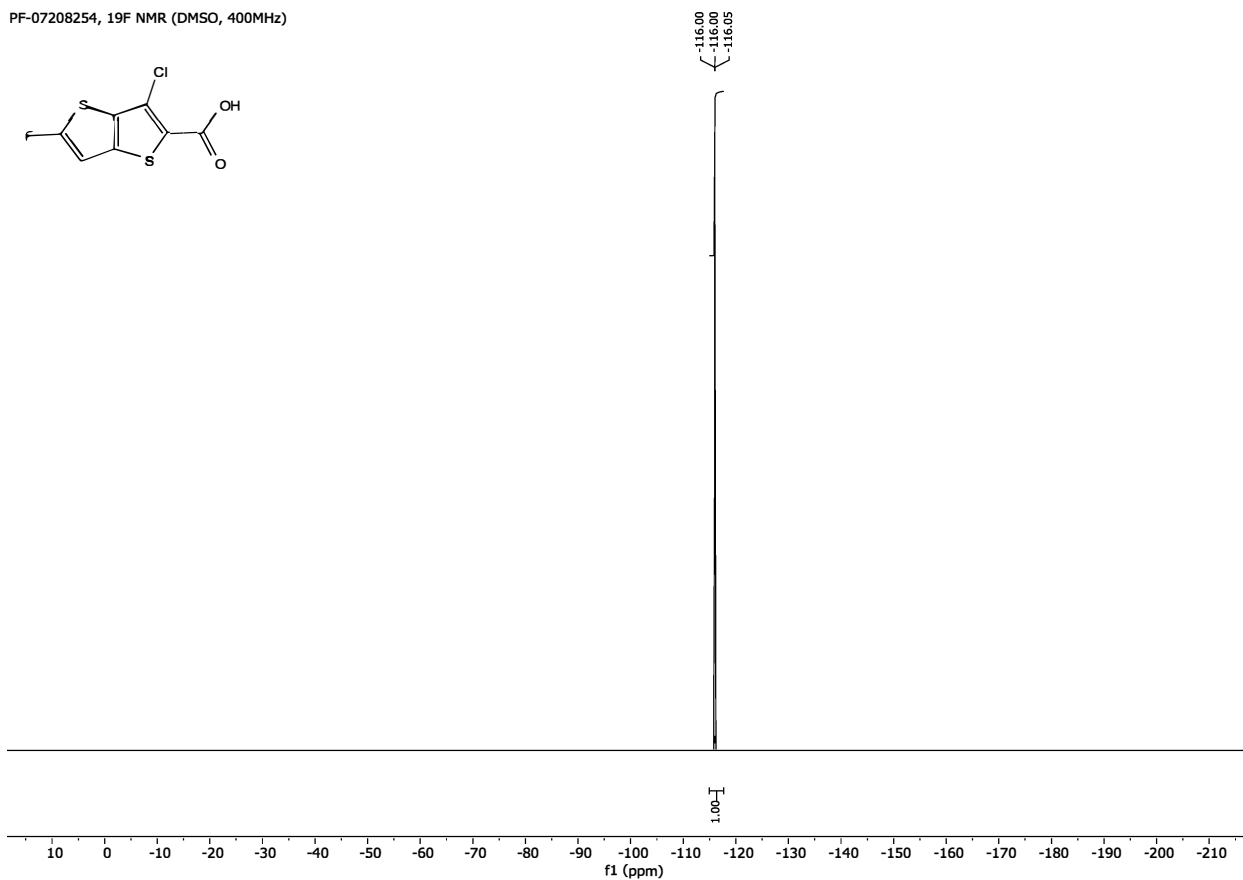
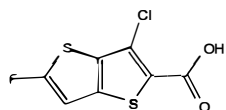
Supplementary Figure 29. ¹³C NMR of PF-07208254

PF-07208254, ¹³C NMR (DMSO, 100MHz)

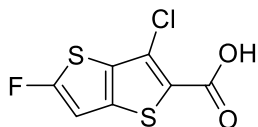


Supplementary Figure 30. ¹⁹F NMR of PF-07208254

PF-07208254, ¹⁹F NMR (DMSO, 400MHz)

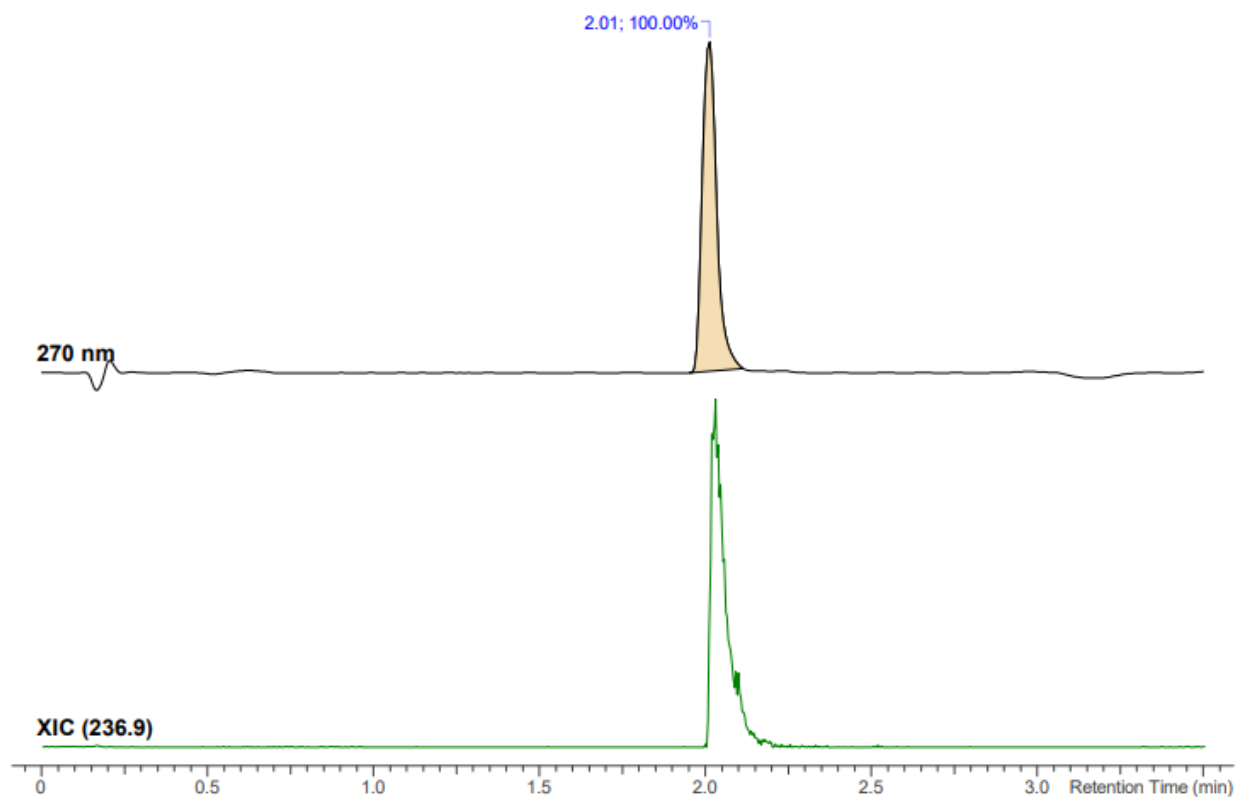


Supplementary Figure 31. HRMS of PF-07208254



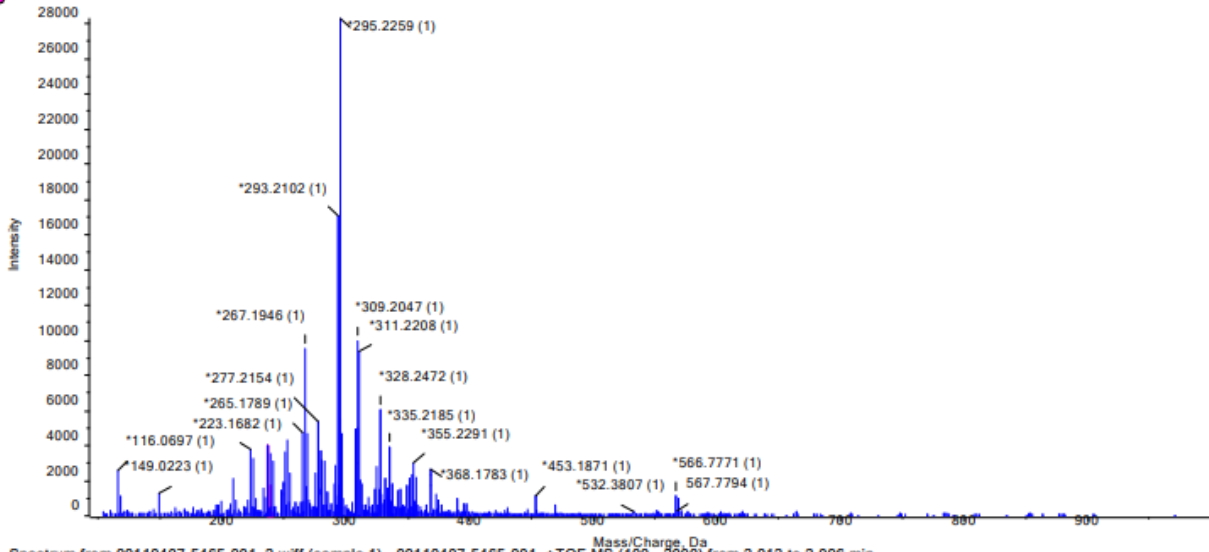
PF-07208254

Open Access HRMS Sample Report			
Sample ID	00110407-5465-001	HPLC	Agilent 1200
Molecular Formula	C7H2ClFO2S2	Mass Spectrometer	Sciex 5600+ QToF
Submittor	Martinez Alsina, Luis A	DAD	190-400 nm, reported 270nm
Run Date	4/4/2023	MS Scan	100-2000 amu
Analyst	Quinn, Alandra	Acquisition Method	HRMS-3min gradient AQ
Analyst's CeN	00714673-0163	eWB Archive Ref	00713459-0292

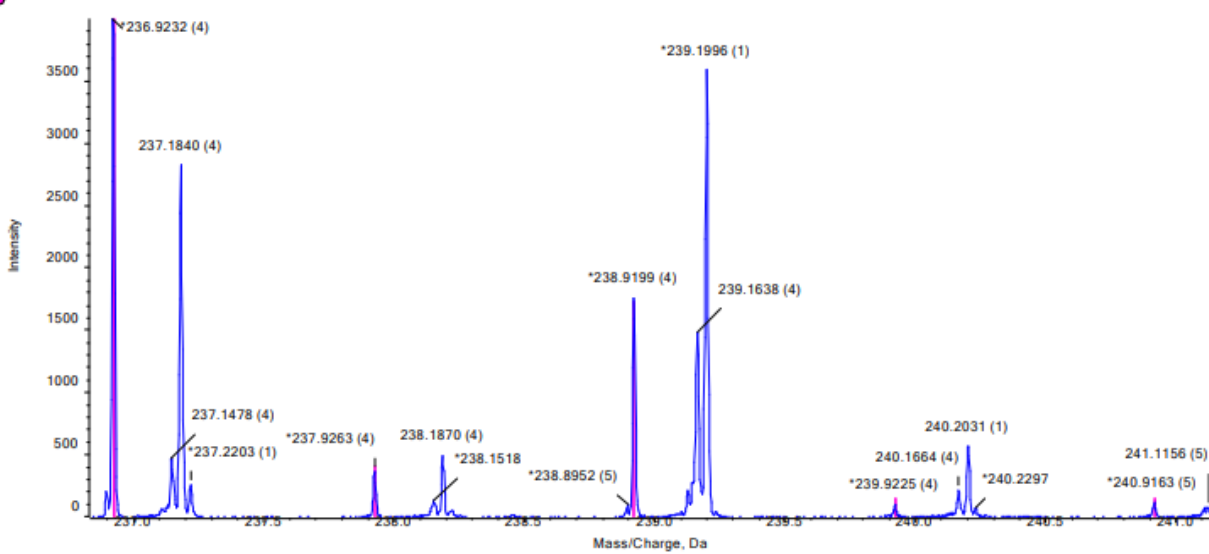


No.	Peak Name	tR (min)	Area (%)
1	C7H2ClFO2S2	2.01	100.00

● Spectrum from 00110407-5465-001_2.wiff (sample 1) - 00110407-5465-001, +TOF MS (100 - 2000) from 2.012 to 2.096 min
 ● Isotopic Distribution for C7H2ClFO2S2 H +

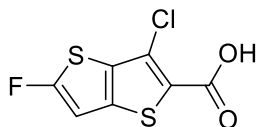


● Spectrum from 00110407-5465-001_2.wiff (sample 1) - 00110407-5465-001, +TOF MS (100 - 2000) from 2.012 to 2.096 min
 ● Isotopic Distribution for C7H2ClFO2S2 H +



Peak at 2.01 min in UV								
Mass/Charge (Da)	Height	Relative % Height	Compound	Peak Type	Theoretical m/z	Error (ppm)	Theoretical m/z	Theoretical Intensity
236.9232	3998	100.0	C7H2ClFO2S2	[M+H] ⁺	236.9242	-4.1	236.9242	100.0
237.9263	367	9.2					237.9269	9.5
238.9199	1760	44.0					238.9211	41.6
239.9225	99	2.5					239.9238	3.8
240.9163	116	2.9					240.9178	3.4

Supplementary Figure 32. HPLC of PF-07208254

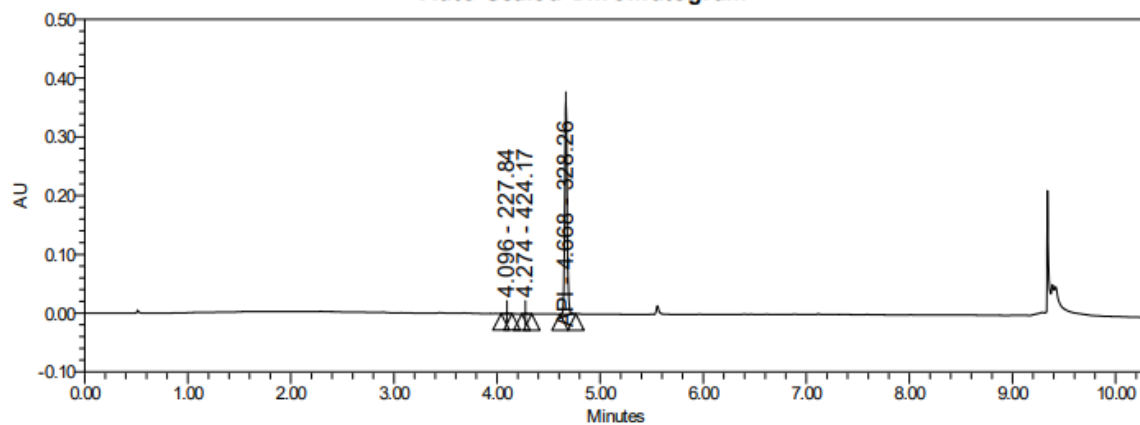


PF-07208254

connecting discovery to pharm sci

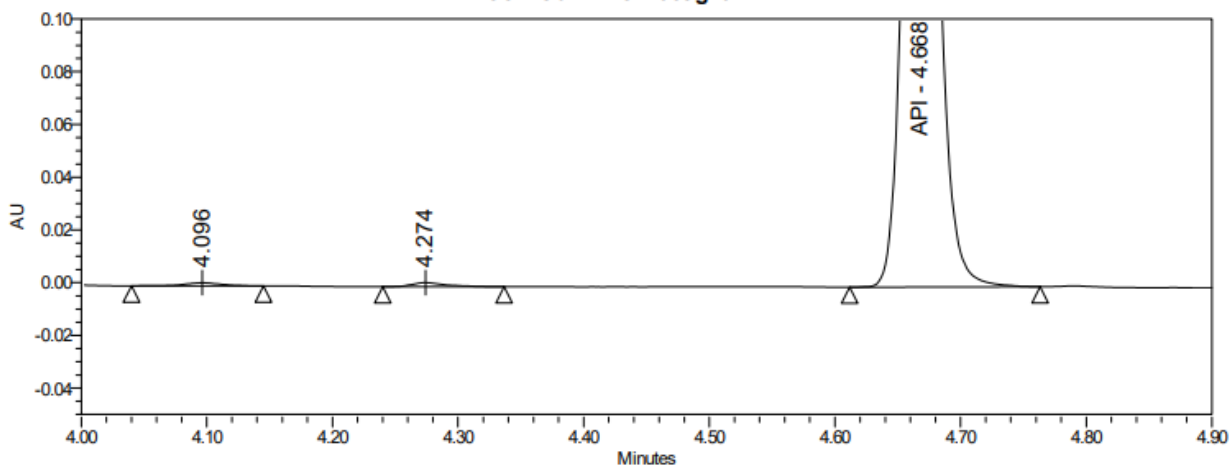
SAMPLE INFORMATION			
Sample Name:	PF-07208254-00-0026	Acquired By:	LiC03
Vial:	1:A,2	Date Acquired:	14-Feb-20 12:40:27 PM EST
Injection #:	1	Acq. Method Set:	GRO343M3_10pt3_MSA_RP18
Injection Volume:	1.00 ul	Date Processed:	14-Feb-20 1:40:28 PM EST
Run Time:	10.3 Minutes	Processing Method:	GRO343_UPLC_PM
Sample Set Name:	GRO343_CL_ETS 02142020 Run1	Channel Name:	PDA 210 nm

Auto-Scaled Chromatogram



Sample Name PF-07208254-00-0026; Vial 1:A,2; Injection 1; Channel PDA Ch1 210nm@4.8nm; Date Acquired 14-Feb-20 12:40:27 PM EST

Zoomed Chromatogram



SAMPLE INFORMATION

Sample Name:	PF-07208254-00-0026	Acquired By:	LiC03
Vial:	1:A,2	Date Acquired:	14-Feb-20 12:40:27 PM EST
Injection #:	1	Acq. Method Set:	GRO343M3_10pt3_MSA_RP18
Injection Volume:	1.00 ul	Date Processed:	14-Feb-20 1:40:28 PM EST
Run Time:	10.3 Minutes	Processing Method:	GRO343_UPLC_PM
Sample Set Name:	GRO343_CL_ETS 02142020 Run1	Channel Name:	PDA 210 nm

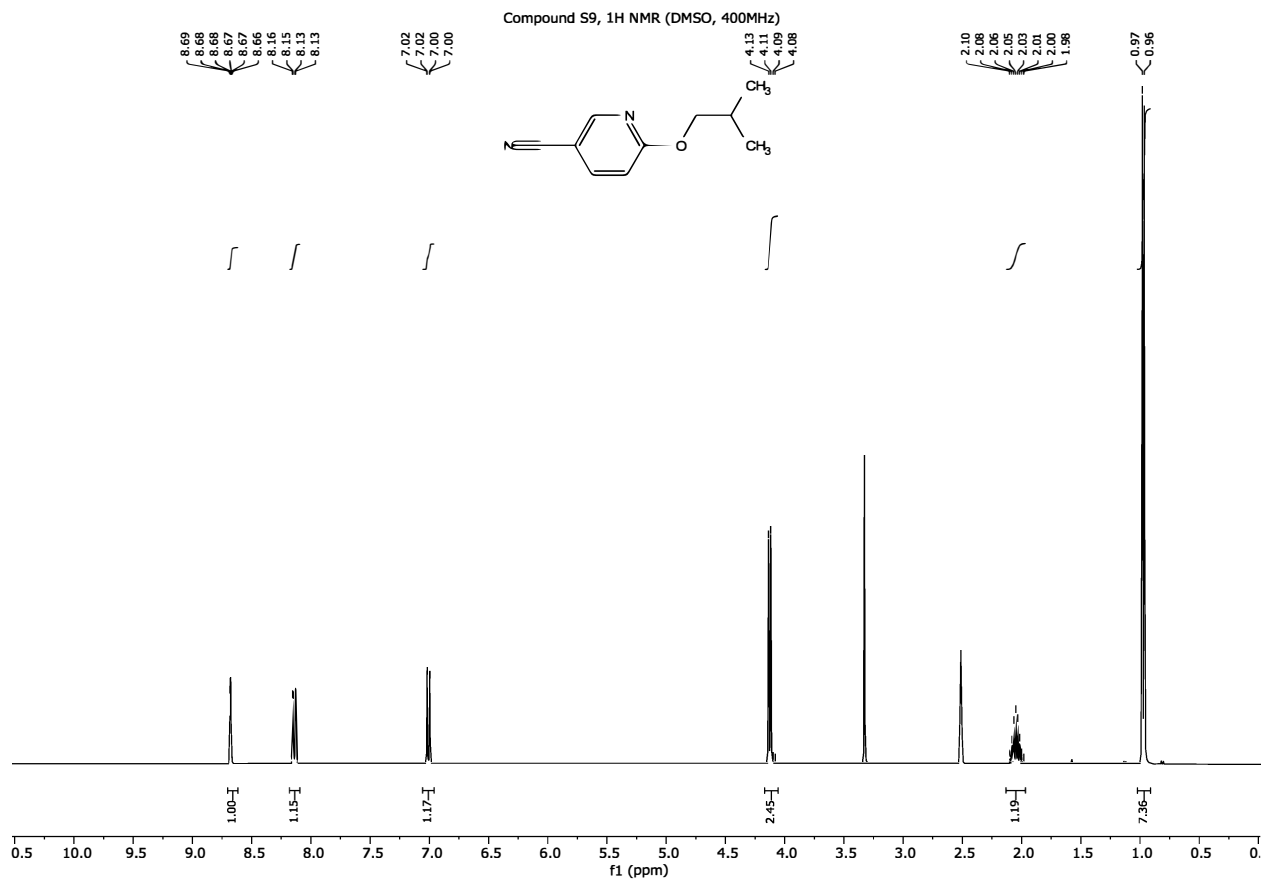
Area % Results

Result Id 95855

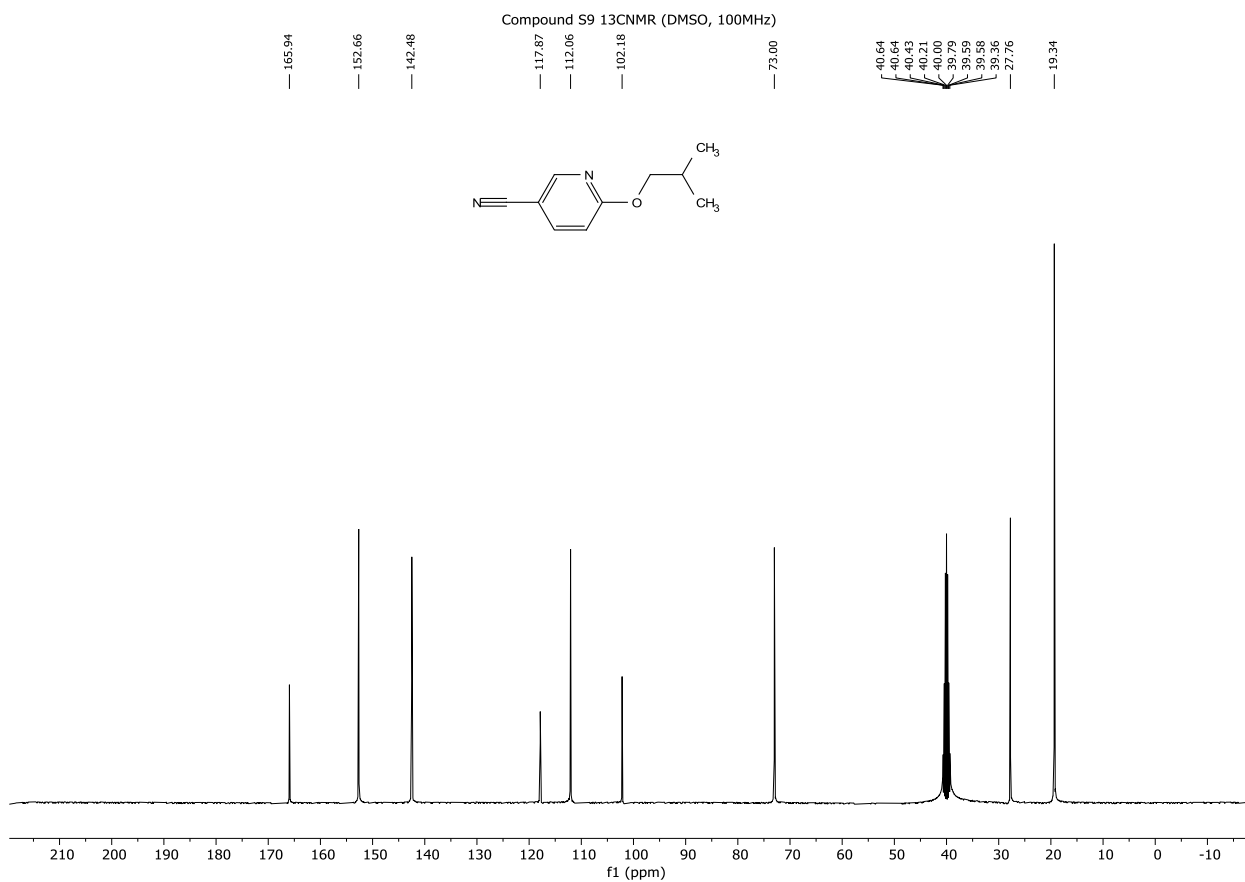
Peak Results

	PeakName	RT	Area	% Area	Height	USP Tailing	s/n	USP s/n	USP Resolution
1		4.096	2416	0.41	1201				
2		4.274	2938	0.50	1560				
3	API	4.668	582040	99.09	360389				

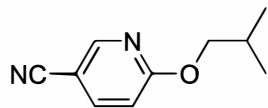
Supplementary Figure 33. 1H NMR of compound S9



Supplementary Figure 34. ¹³C NMR of compound S9

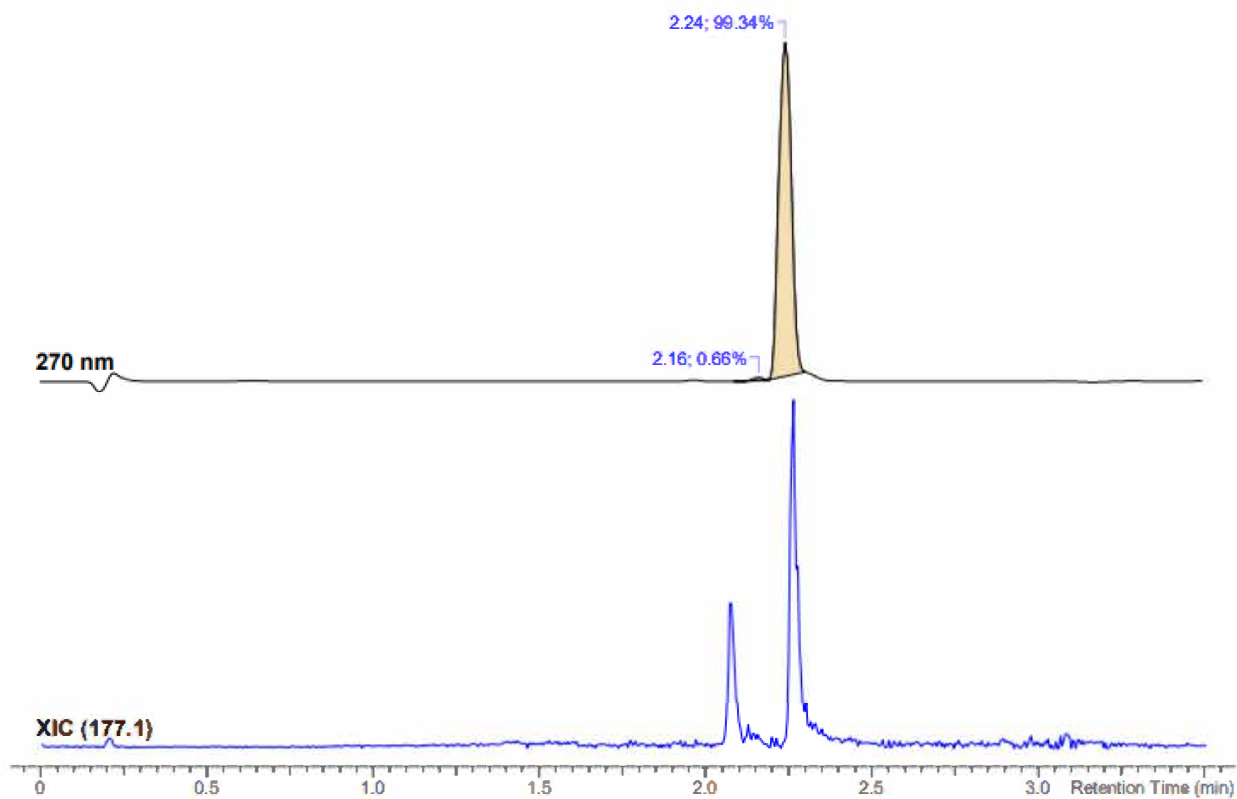


Supplementary Figure 35. HRMS of compound S9



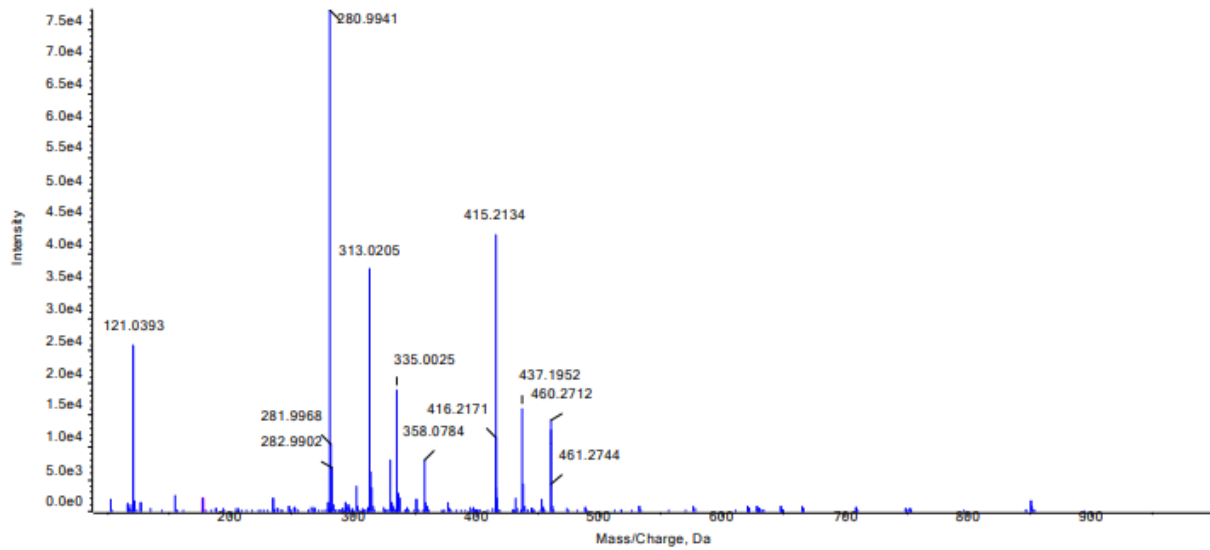
S9

Open Access HRMS Sample Report			
Sample ID	00110580-3414-006	HPLC	Agilent 1200
Molecular Formula	C10H12N2O	Mass Spectrometer	Sciex 5600+ QToF
Submittor	Martinez, Luis	DAD	190-400 nm, reported 270nm
Run Date	4/27/2023	MS Scan	100-2000 amu
Analyst	Quinn, Alandra	Acquisition Method	HRMS-3min gradient AQ
Analyst's CeN	00714673-0166	eWB Archive Ref	00713459-0294

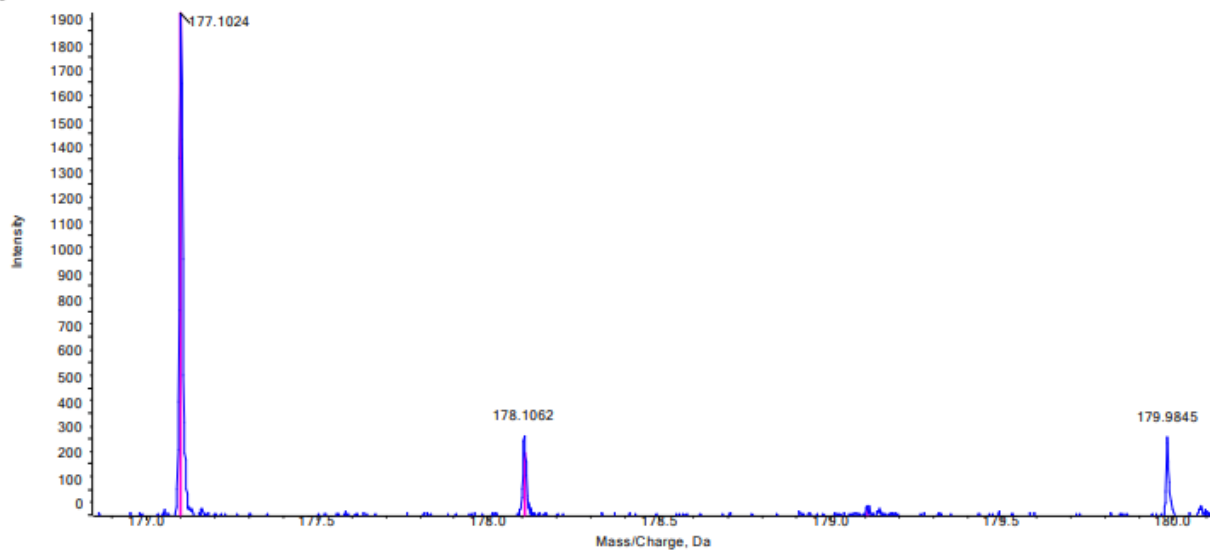


No.	Peak Name	tR (min)	Area (%)
1	unknown	2.16	0.66
2	C10H12N2O	2.24	99.34

Spectrum from 00110580-3414-006_5.wiff (sample 1) - C10H12N2O, +TOF MS (100 - 2000) from 2.241 to 2.306 min
 Isotopic Distribution for C10H12N2O H +



Spectrum from 00110580-3414-006_5.wiff (sample 1) - C10H12N2O, +TOF MS (100 - 2000) from 2.241 to 2.306 min
 Isotopic Distribution for C10H12N2O H +



Peak at 2.24 min in UV								
Mass/Charge (Da)	Height	Relative % Height	Compound	Peak Type	Theoretical m/z	Error (ppm)	Theoretical m/z	Theoretical Intensity
177.1024	1969	100.0	C10H12N2O	[M+H] ⁺	177.1022	0.8	177.1022	100.0
178.1062	310	15.8					178.1052	12.0
179.1076	39	2.0					179.1078	0.9

=====
 Area Percent Report
 =====

Sorted By : Signal
 Multiplier : 1.0000
 Dilution : 1.0000
 Do not use Multiplier & Dilution Factor with ISTDs

Signal 1: DAD1 A, Sig=210,4 Ref=off

Peak #	RetTime [min]	Type	Width [min]	Area [mAU*s]	Height [mAU]	Area %
1	8.798	BB	0.0561	1291.38745	357.88132	100.0000

Totals : 1291.38745 357.88132

Signal 2: DAD1 B, Sig=254,4 Ref=off

Peak #	RetTime [min]	Type	Width [min]	Area [mAU*s]	Height [mAU]	Area %
1	8.798	BB	0.0558	5101.04199	1424.99304	100.0000

Totals : 5101.04199 1424.99304

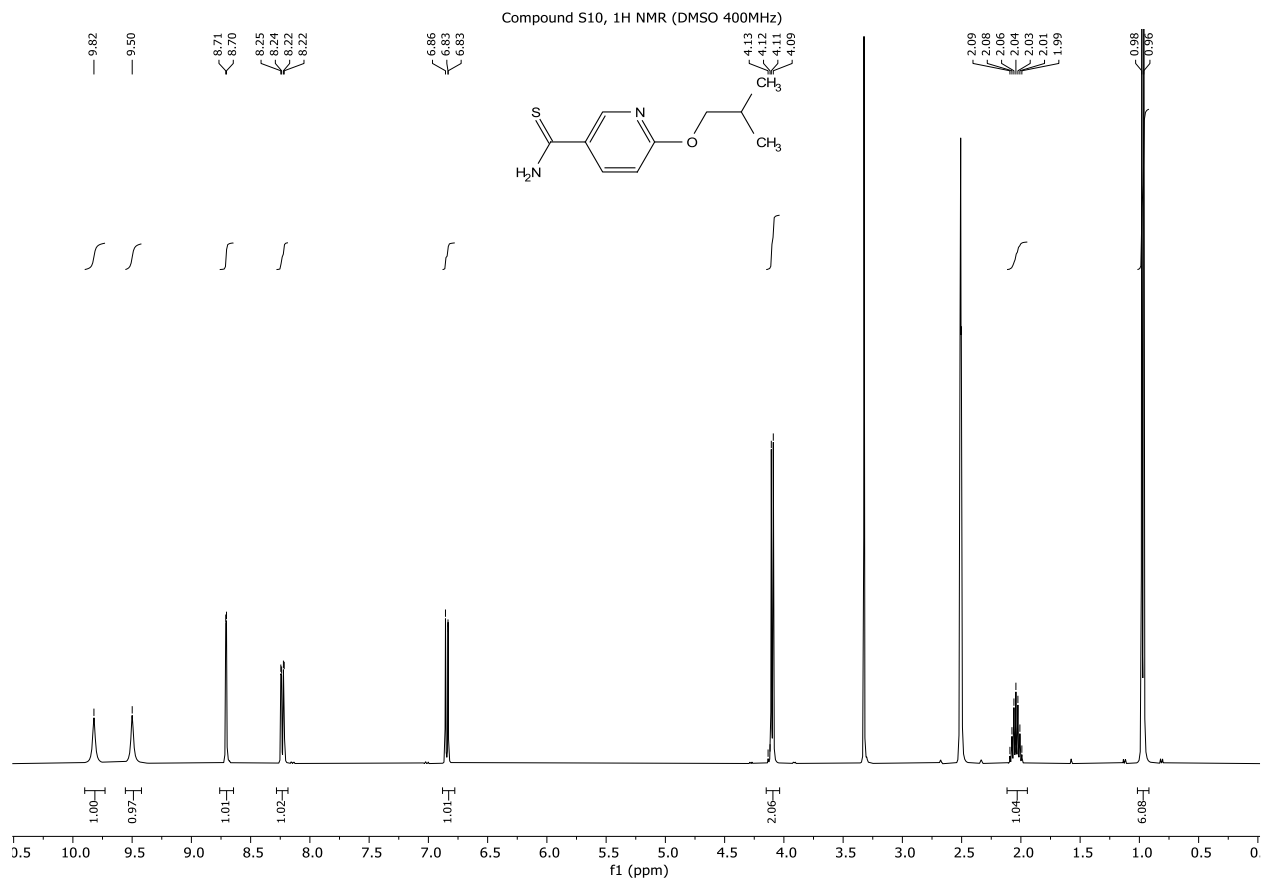
Signal 3: DAD1 C, Sig=280,4 Ref=off

Peak #	RetTime [min]	Type	Width [min]	Area [mAU*s]	Height [mAU]	Area %
1	8.798	BB	0.0553	2957.12744	835.37280	100.0000

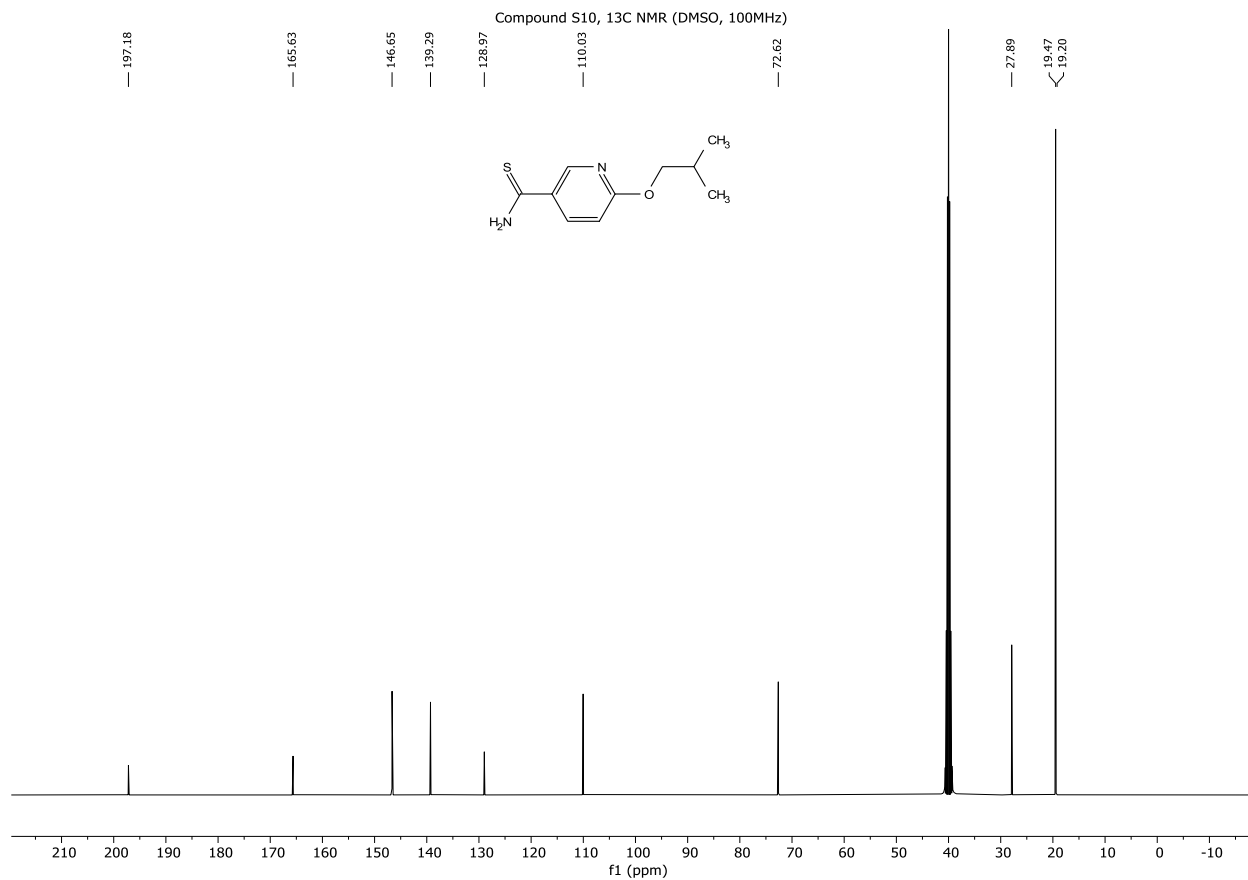
Totals : 2957.12744 835.37280

=====
 *** End of Report ***

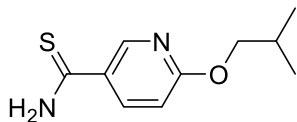
Supplementary Figure 37. 1H NMR of compound S10



Supplementary Figure 38. ¹³C NMR of compound S10



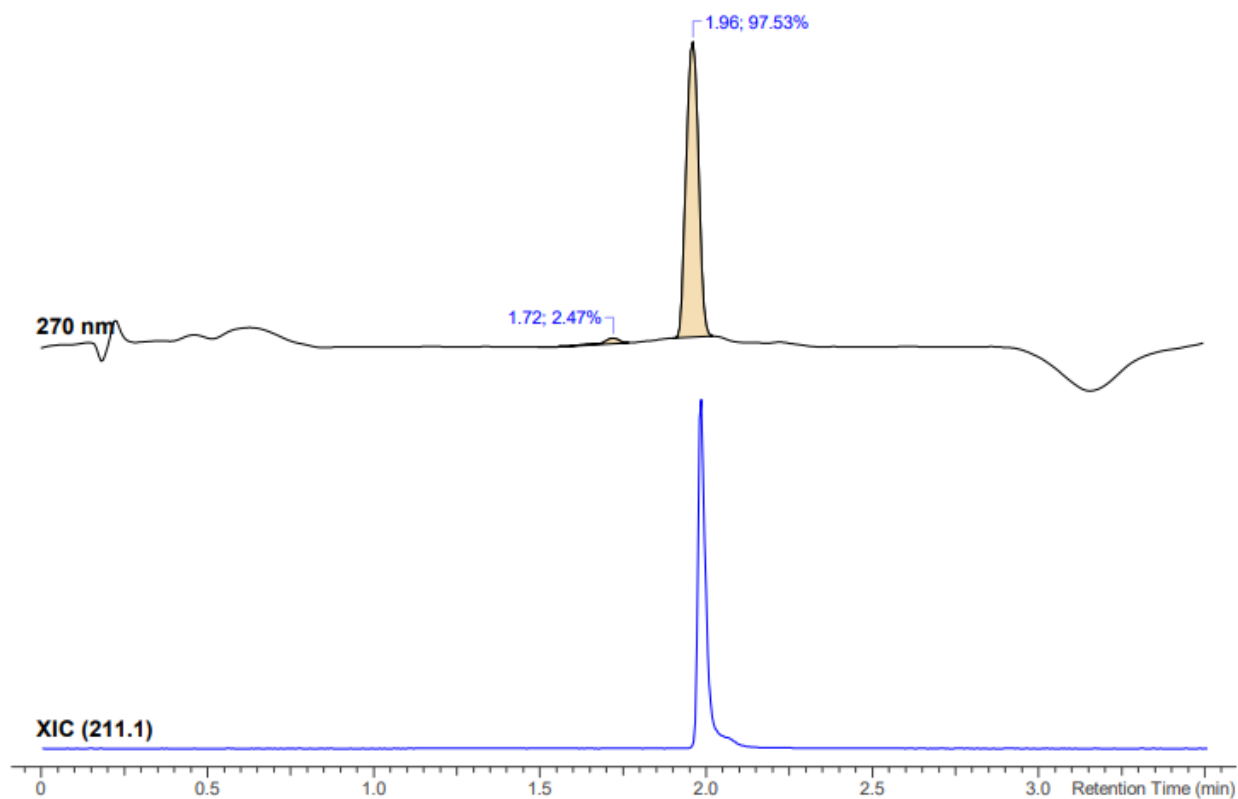
Supplementary Figure 39. HRMS of compound S10



S10

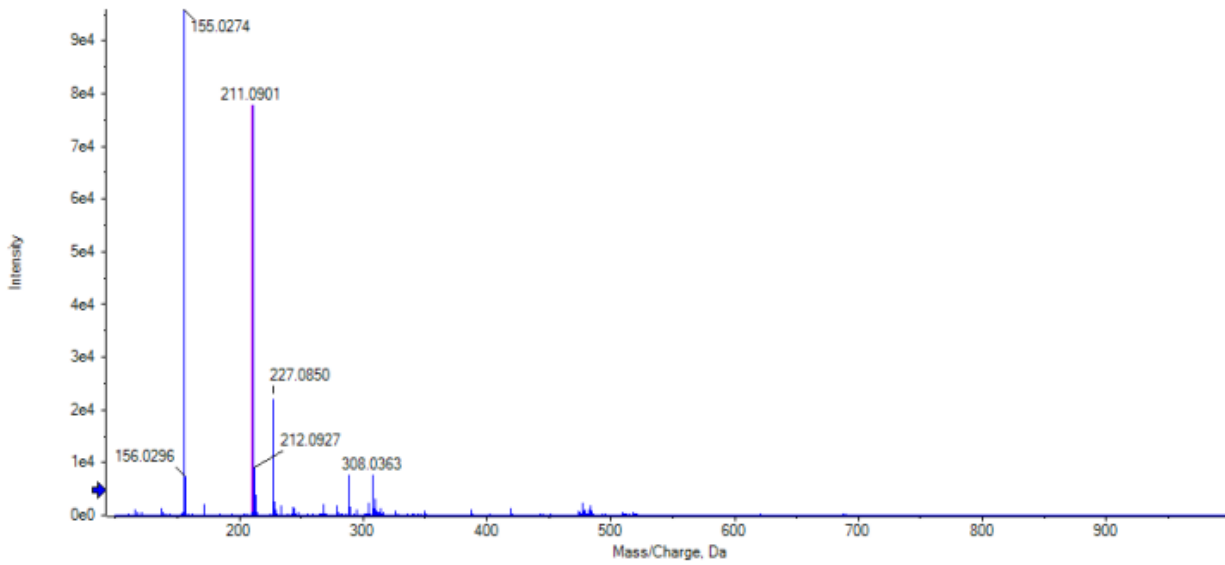
Open Access HRMS Sample Report

Sample ID	00110512-3609-003	HPLC	Agilent 1200
Molecular Formula	C10H14N2OS	Mass Spectrometer	Sciex 5600+ QToF
Submittor	Martinez, Luis	DAD	190-400 nm, reported 270nm
Run Date	4/27/2023	MS Scan	100-2000 amu
Analyst	Quinn, Alandra	Acquisition Method	HRMS-3min gradient AQ
Analyst's CeN	00714673-0166	eWB Archive Ref	00713459-0294

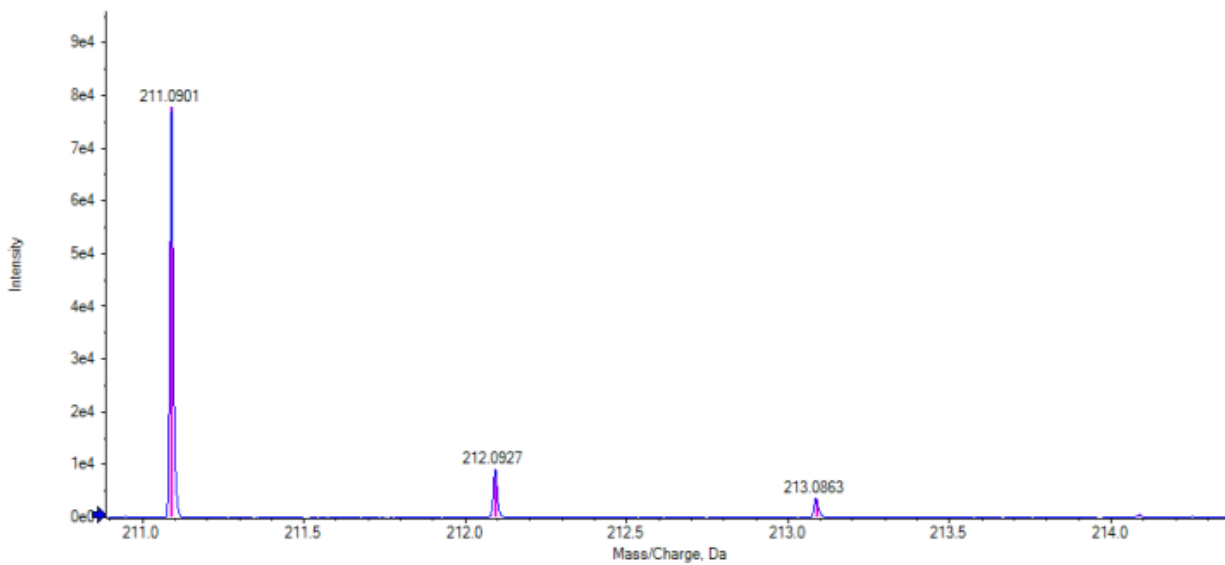


No.	Peak Name	tR (min)	Area (%)
1	unknown	1.72	2.47
2	C10H14N2OS	1.96	97.53

● Spectrum from 00110512-3609-003.wiff (sample 1) - C₁₀H₁₄N₂O₅, +TOF MS (100 - 2000) from 1.934 to 2.027 min
 ● Isotopic Distribution for C₁₀H₁₄N₂O₅ H⁺



● Spectrum from 00110512-3609-003.wiff (sample 1) - C₁₀H₁₄N₂O₅, +TOF MS (100 - 2000) from 1.934 to 2.027 min
 ● Isotopic Distribution for C₁₀H₁₄N₂O₅ H⁺



Peak at 1.96 min in UV								
Mass/Charge (Da)	Height	Relative % Height	Compound	Peak Type	Theoretical m/z	Error (ppm)	Theoretical m/z	Theoretical Intensity
211.0901	77845	100.0	C ₁₀ H ₁₄ N ₂ O ₅	[M+H] ⁺	211.0900	0.5	211.0900	100.0
212.0927	9088	11.7					212.0927	12.8
213.0863	3722	4.8					213.0874	5.4
214.0889	532	0.7					214.0896	0.6

=====
 Area Percent Report
 =====

Sorted By : Signal
 Multiplier : 1.0000
 Dilution : 1.0000
 Do not use Multiplier & Dilution Factor with ISTDs

Signal 1: DAD1 A, Sig=210,4 Ref=off

Peak #	RetTime [min]	Type	Width [min]	Area [mAU*s]	Height [mAU]	Area %
1	7.421	BB	0.0652	1861.47400	441.43124	100.0000

Totals : 1861.47400 441.43124

Signal 2: DAD1 B, Sig=254,4 Ref=off

Peak #	RetTime [min]	Type	Width [min]	Area [mAU*s]	Height [mAU]	Area %
1	7.421	BB	0.0650	1249.24487	297.22464	100.0000

Totals : 1249.24487 297.22464

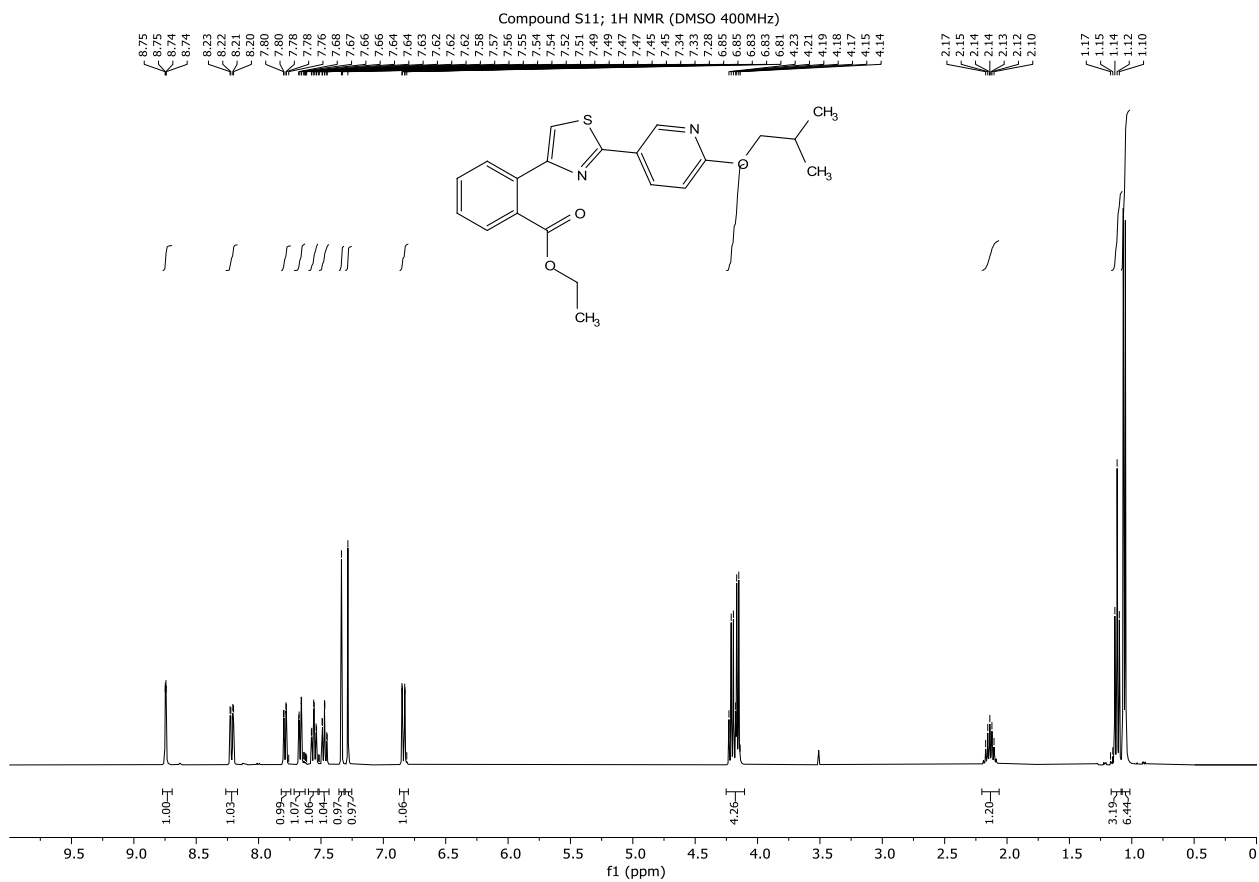
Signal 3: DAD1 C, Sig=280,4 Ref=off

Peak #	RetTime [min]	Type	Width [min]	Area [mAU*s]	Height [mAU]	Area %
1	7.421	BB	0.0650	1533.97607	365.13541	100.0000

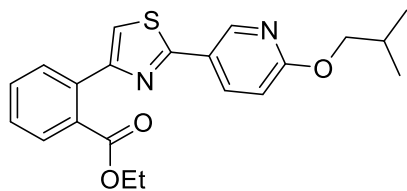
Totals : 1533.97607 365.13541

=====
 *** End of Report ***

Supplementary Figure 41. 1H NMR of compound S11



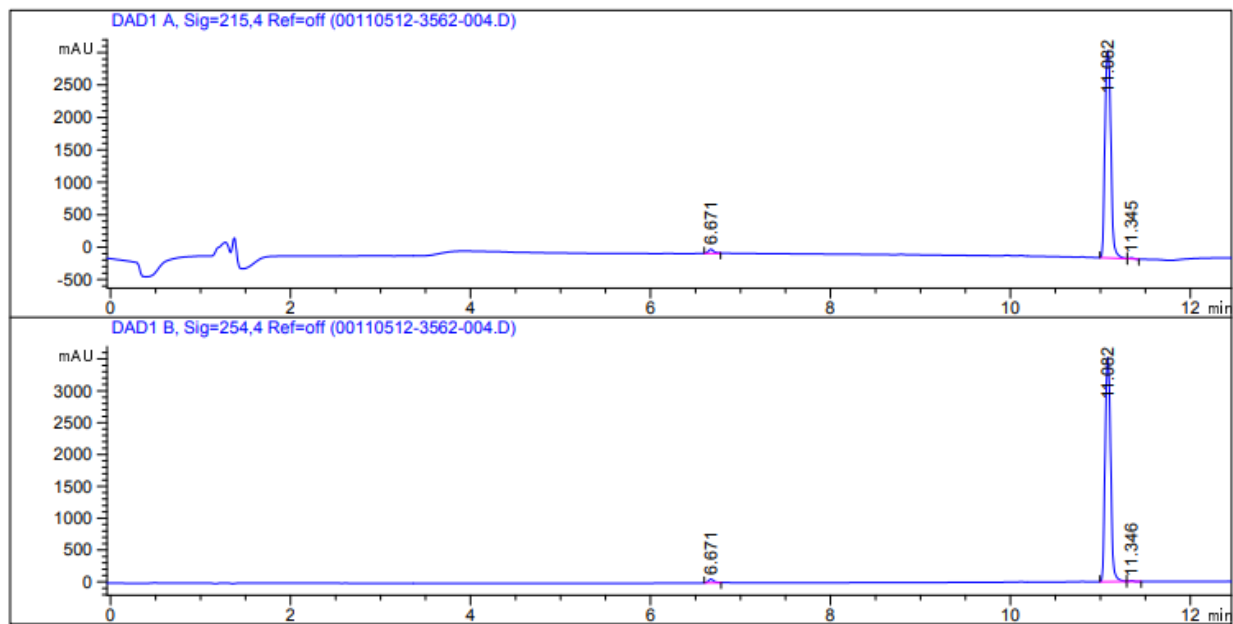
Supplementary Figure 42. HPLC of compound S11



S11

```
=====
Acq. Operator   : SYSTEM                      Seq. Line :    3
Acq. Instrument : LC-235GC                   Location  :    2
Injection Date  : 3/25/2019 6:52:20 AM      Inj       :    1
                                           Inj Volume: 5.0 µl
Different Inj Volume from Sample Entry! Actual Inj Volume : 10.0 µl
Sequence File   : C:\Chem32\1\Data\THERMO\TEST 2019-03-25 06-23-17\TEST.S
Method          : C:\Chem32\1\Data\THERMO\TEST 2019-03-25 06-23-17\ACID_CLASSIC.M (Sequence
Method)
Last changed    : 3/25/2019 6:23:18 AM by SYSTEM
Method Info     : ACID METHOD for classic look on new Chemstation software
                  Column: XBridge C18 5 micron (4.6 mm x 150 mm)
                  Flow rate: 1.500 mL/min with solvents containing 0.1% TFA
                  0-1.5 min: 5% acetonitrile/water
                  1.5-10 min: 5-100% acetonitrile water
                  10-11 min: 100% acetonitrile
                  11-12.5 min: 100-5% acetonitrile/water
=====
```

Sample Info : 00110512-3562-004



Area Percent Report

```
=====
Sorted By      : Signal
Multiplier     : 1.0000
Dilution       : 1.0000
Do not use Multiplier & Dilution Factor with ISTDs
=====
```

Signal 1: DAD1 A, Sig=215,4 Ref=off

Peak #	RetTime [min]	Type	Width [min]	Area [mAU*s]	Height [mAU]	Area %
1	6.671	BB	0.0644	274.95190	63.60682	1.8365
2	11.082	BV	0.0732	1.46410e4	3209.51489	97.7920
3	11.345	VB	0.0533	55.62463	16.49937	0.3715

Totals : 1.49716e4 3289.62108

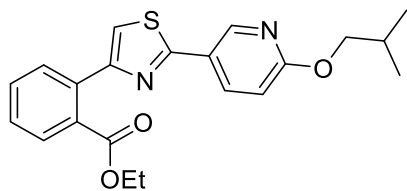
Signal 2: DAD1 B, Sig=254,4 Ref=off

Peak #	RetTime [min]	Type	Width [min]	Area [mAU*s]	Height [mAU]	Area %
1	6.671	BB	0.0644	252.87498	58.50365	1.6504
2	11.082	BB	0.0696	1.50151e4	3532.13159	97.9943
3	11.346	BB	0.0574	54.44085	14.63323	0.3553

Totals : 1.53225e4 3605.26847

=====
*** End of Report ***

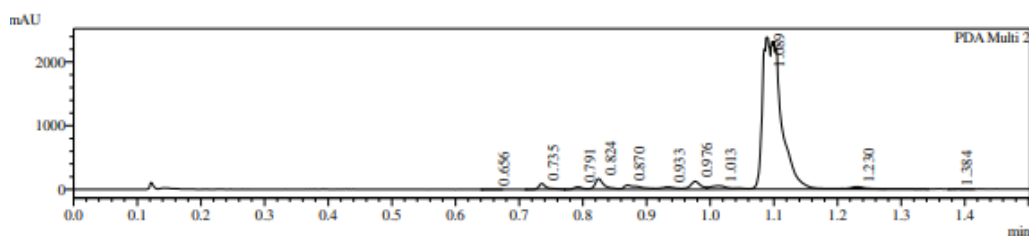
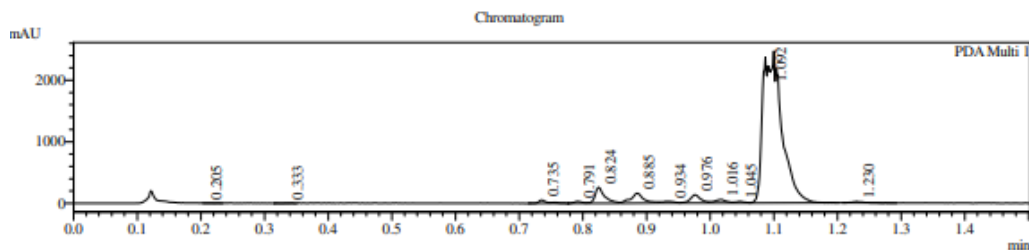
Supplementary Figure 43. LCMS of compound S11



S11

MS Ionization : ESI

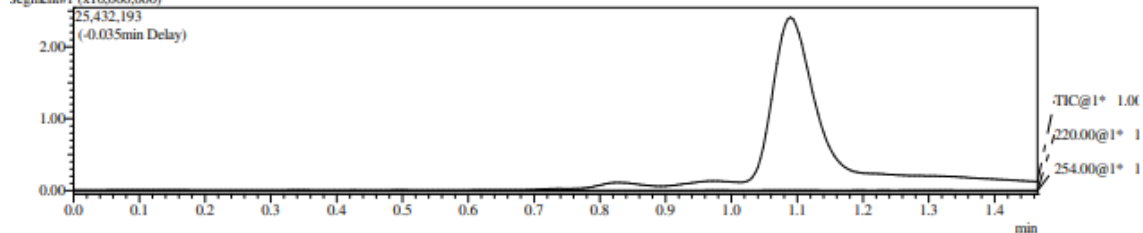
Instrument & Column: LCMS-AO(4-302) Chromolith. Flash RP-18e 25-2mm



1 PDA Multi 1 / 220nm 4nm

2 PDA Multi 2 / 254nm 4nm

Segment#1 (x10,000,000)



Integration Result

PDA Ch1 220nm 4nm

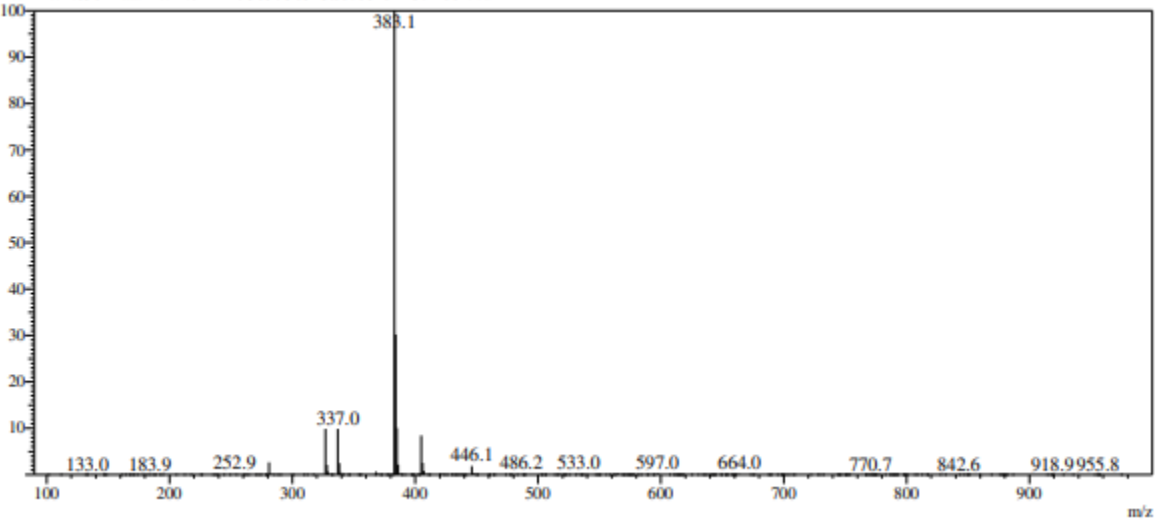
Peak#	Ret. Time	Height	Height %	USP Width	Area	Area %
1	0.205	2209	0.075	0.011	3089	0.052
2	0.333	2421	0.083	0.056	4759	0.080
3	0.735	51657	1.764	0.021	51542	0.864
4	0.791	30427	1.039	0.026	27472	0.461
5	0.824	251295	8.582	0.027	268431	4.501
6	0.885	159999	5.464	0.033	226778	3.802
7	0.934	27653	0.944	0.050	37216	0.624
8	0.976	132772	4.534	0.031	154079	2.583
9	1.016	54021	1.845	0.038	71389	1.197
10	1.045	23064	0.788	0.025	24651	0.413
11	1.092	2174106	74.244	0.046	5066531	84.953
12	1.230	18691	0.638	0.037	28020	0.470

PDA Ch2 254nm 4nm

Peak#	Ret. Time	Height	Height %	USP Width	Area	Area %
1	0.656	2619	0.088	0.090	3035	0.054
2	0.735	90238	3.026	0.021	79163	1.399

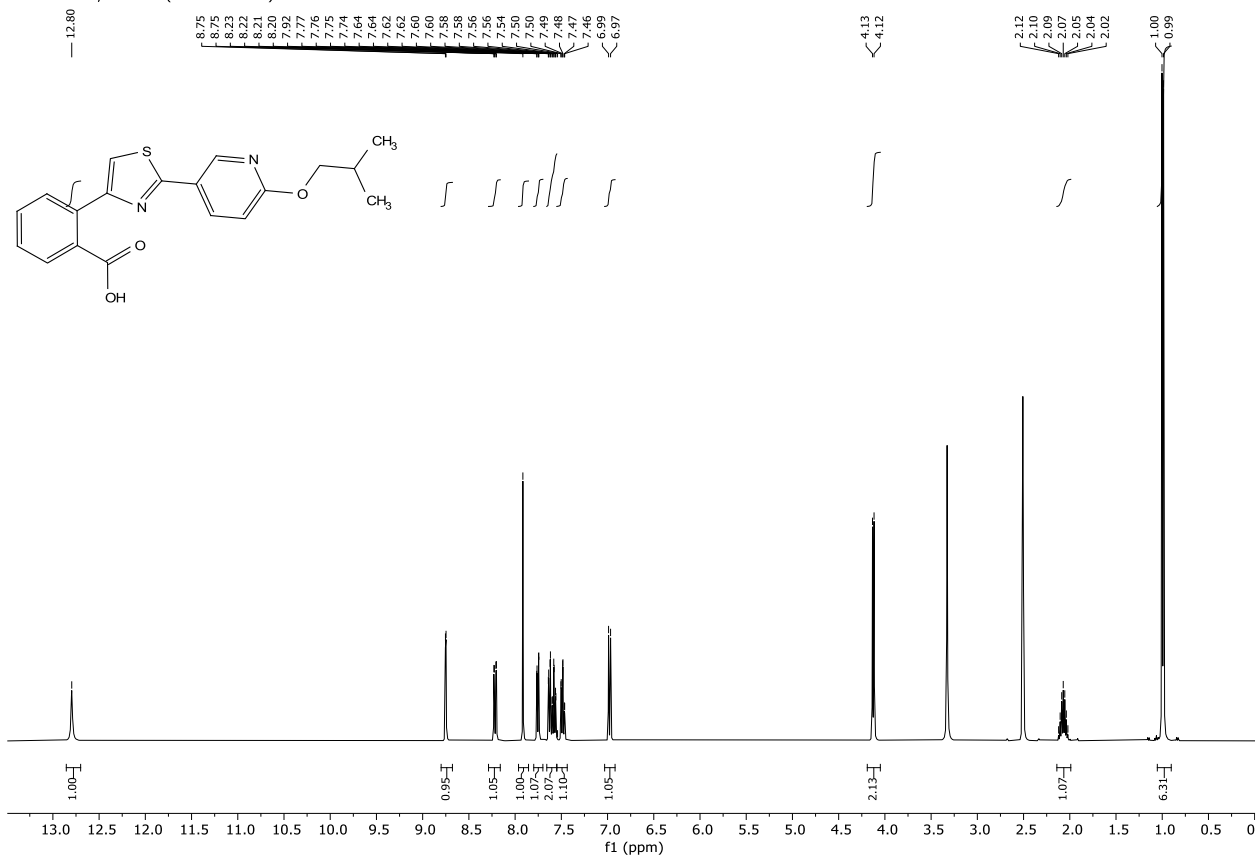
Peak#	Ret. Time	Height	Height %	USP Width	Area	Area %
3	0.791	37896	1.271	0.026	37006	0.654
4	0.824	161148	5.403	0.025	163388	2.888
5	0.870	65664	2.202	0.048	108551	1.919
6	0.933	37046	1.242	0.041	58674	1.037
7	0.976	120552	4.042	0.031	139263	2.461
8	1.013	53342	1.789	0.056	111290	1.967
9	1.089	2380165	79.809	0.043	4911657	86.809
10	1.230	32100	1.076	0.034	42757	0.756
11	1.384	1570	0.053	0.022	3229	0.057

RetTime: 1.090 DataFile: D:\DATA\1903\190328\00708262-1371-001.lcd

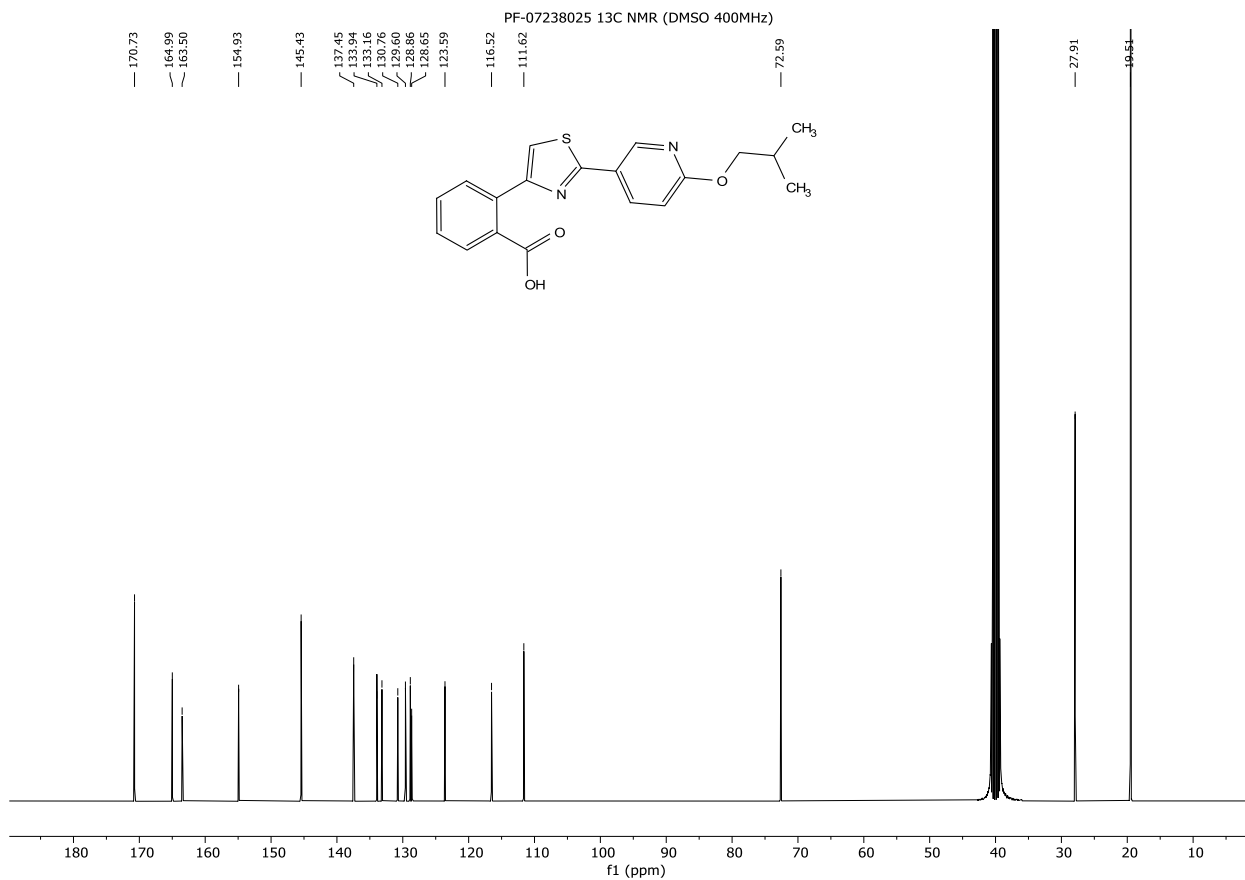


Supplementary Figure 44. 1H NMR of PF-07238025

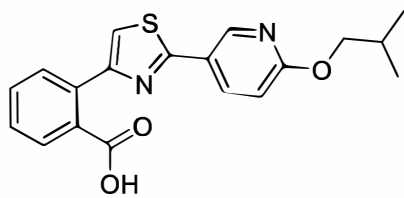
PF-07238025, 1H NMR (DMSO 400MHz)



Supplementary Figure 45. ¹³C NMR of PF-07238025

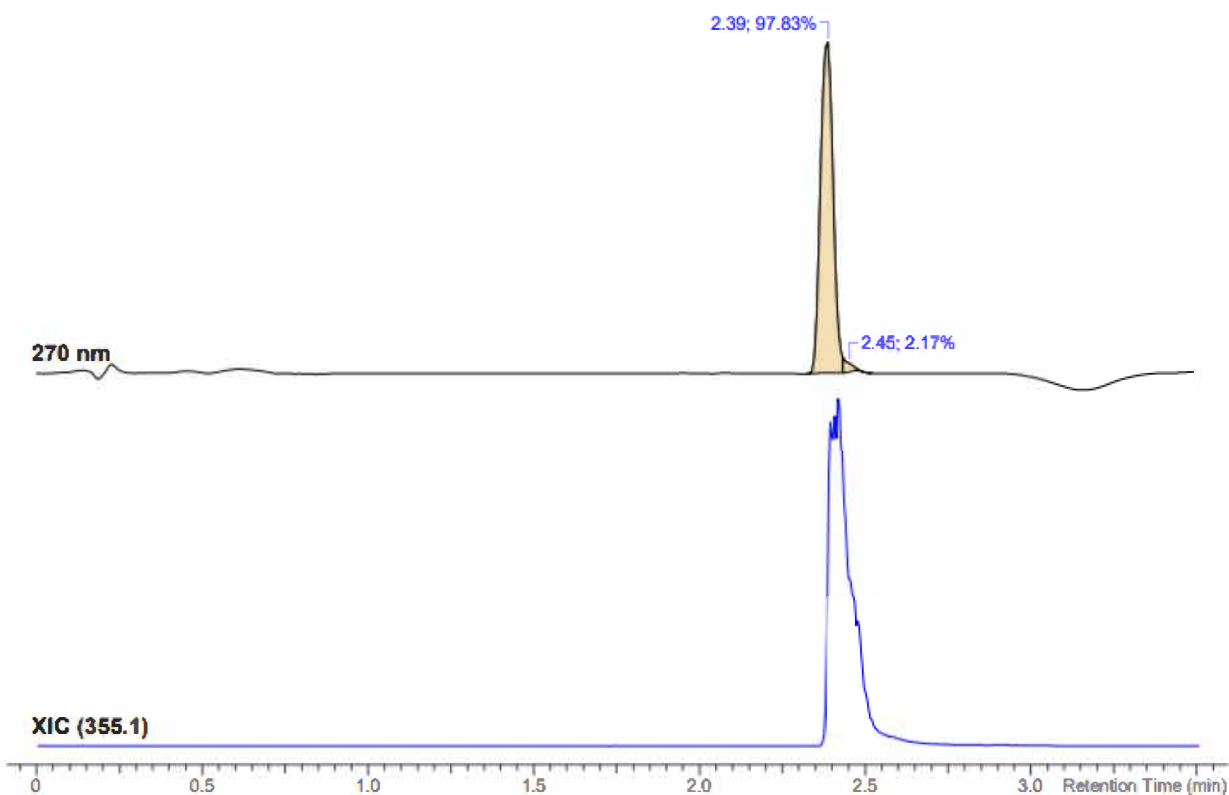


Supplementary Figure 46. HRMS of PF-07238025



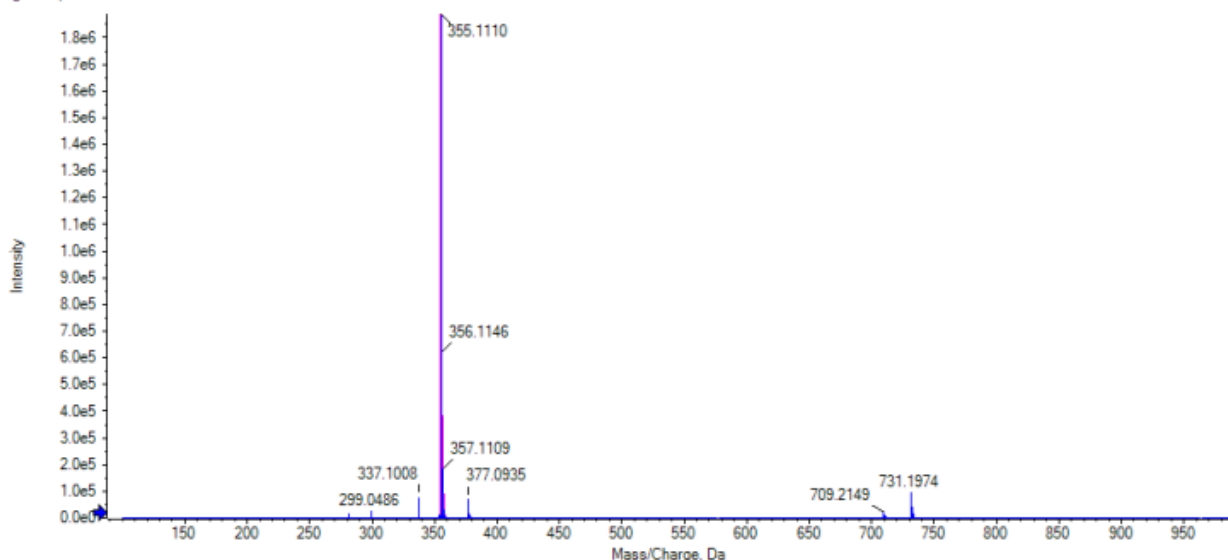
PF-07238025

Open Access HRMS Sample Report			
Sample ID	00110580-3430-001	HPLC	Agilent 1200
Molecular Formula	C ₁₉ H ₁₈ N ₂ O ₃ S	Mass Spectrometer	Sciex 5600+ QToF
Submittor	Martinez, Luis	DAD	190-400 nm, reported 270nm
Run Date	4/27/2023	MS Scan	100-2000 amu
Analyst	Quinn, Alandra	Acquisition Method	HRMS-3min gradient AQ
Analyst's CeN	00714673-0166	eWB Archive Ref	00713459-0294

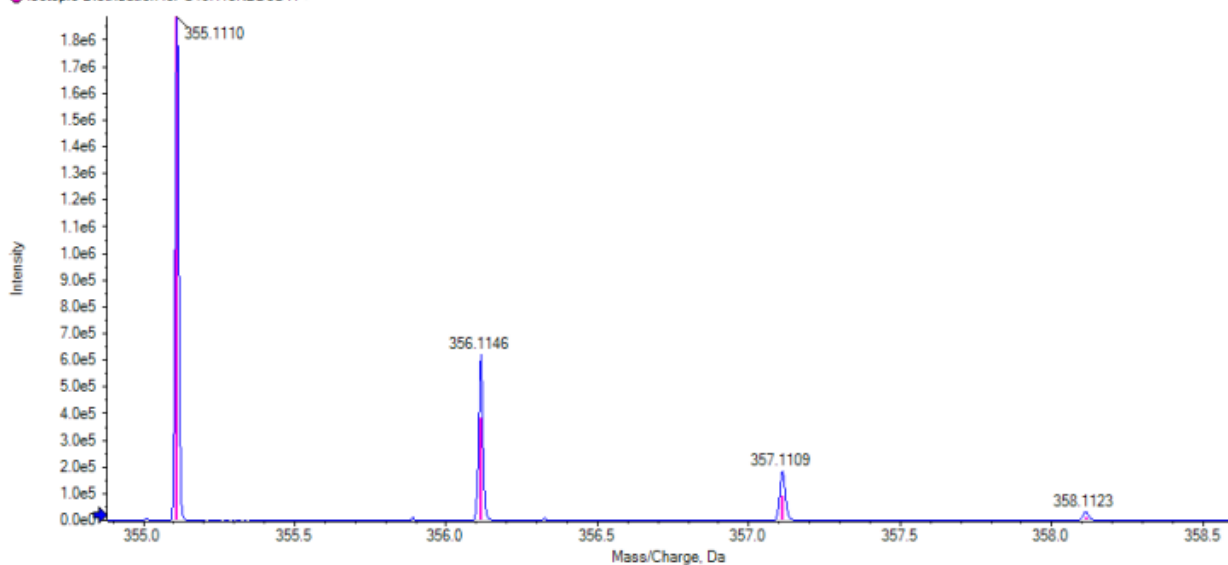


No.	Peak Name	tR (min)	Area (%)
1	C ₁₉ H ₁₈ N ₂ O ₃ S	2.39	97.83
2	unknown	2.45	2.17

● Spectrum from 00110580-3430-001.wiff (sample 1) - C₁₉H₁₈N₂O₃S, +TOF MS (100 - 2000) from 2.381 to 2.455 min
 ● Isotopic Distribution for C₁₉H₁₈N₂O₃S H⁺



● Spectrum from 00110580-3430-001.wiff (sample 1) - C₁₉H₁₈N₂O₃S, +TOF MS (100 - 2000) from 2.381 to 2.455 min
 ● Isotopic Distribution for C₁₉H₁₈N₂O₃S H⁺



Peak at 2.39 min in UV								
Mass/Charge (Da)	Height	Relative % Height	Compound	Peak Type	Theoretical m/z	Error (ppm)	Theoretical m/z	Theoretical Intensity
355.1110	1886716	100.0	C ₁₉ H ₁₈ N ₂ O ₃ S	[M+H] ⁺	355.1111	-0.1	355.1111	100.0
356.1146	622056	33.0					356.1141	23.0
357.1109	184260	9.8					357.1110	7.5
358.1123	32639	1.7					358.1123	1.3

=====
Area Percent Report
=====

Sorted By : Signal
Multiplier : 1.0000
Dilution : 1.0000
Do not use Multiplier & Dilution Factor with ISTDs

Signal 1: DAD1 A, Sig=210,4 Ref=off

Peak #	RetTime [min]	Type	Width [min]	Area [mAU*s]	Height [mAU]	Area %
1	1.521	BB	0.3515	1026.59692	44.11615	10.7388
2	9.149	BB	0.0549	8533.05957	2434.75903	89.2612

Totals : 9559.65649 2478.87518

Signal 2: DAD1 B, Sig=254,4 Ref=off

Peak #	RetTime [min]	Type	Width [min]	Area [mAU*s]	Height [mAU]	Area %
1	9.149	BB	0.0534	6460.28711	1915.08313	100.0000

Totals : 6460.28711 1915.08313

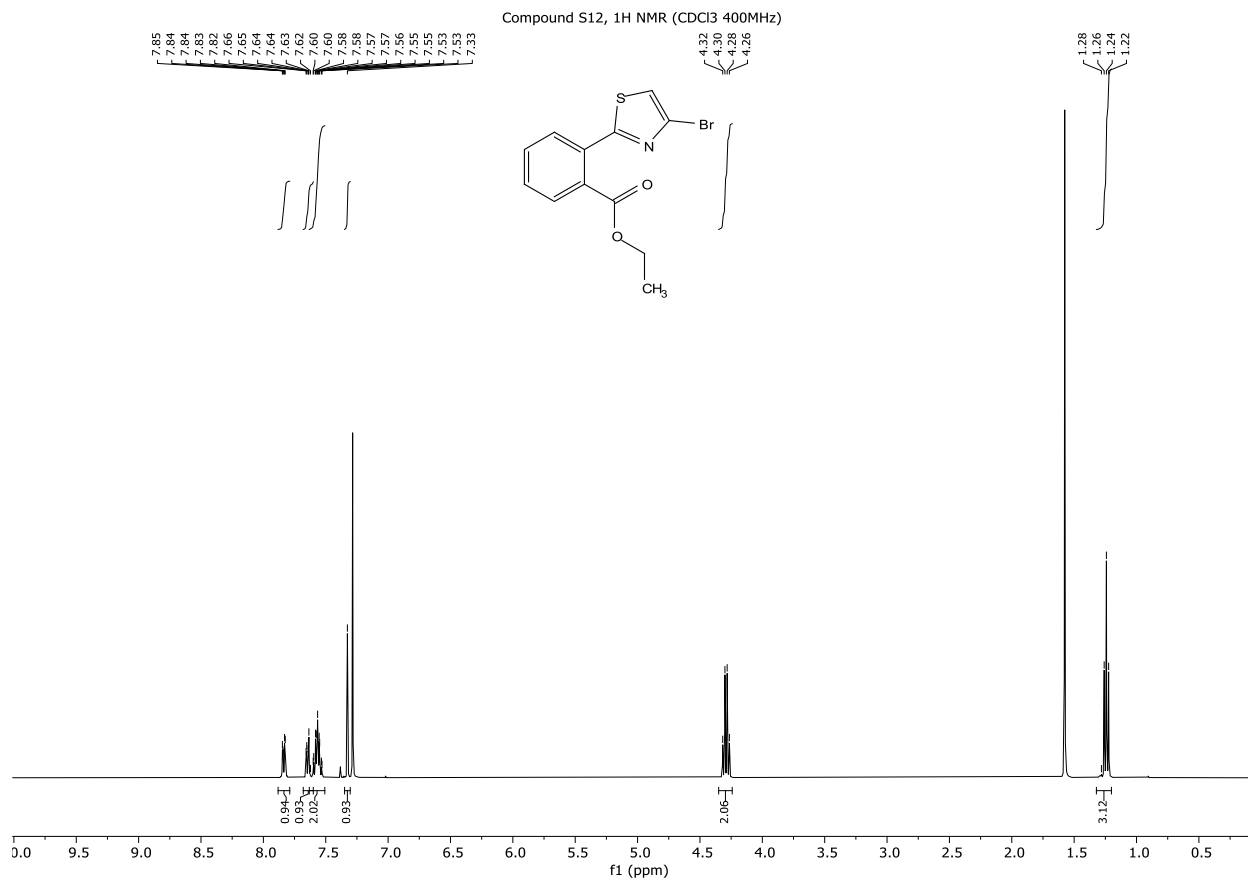
Signal 3: DAD1 C, Sig=280,4 Ref=off

Peak #	RetTime [min]	Type	Width [min]	Area [mAU*s]	Height [mAU]	Area %
1	9.148	BB	0.0533	5073.91406	1506.82288	100.0000

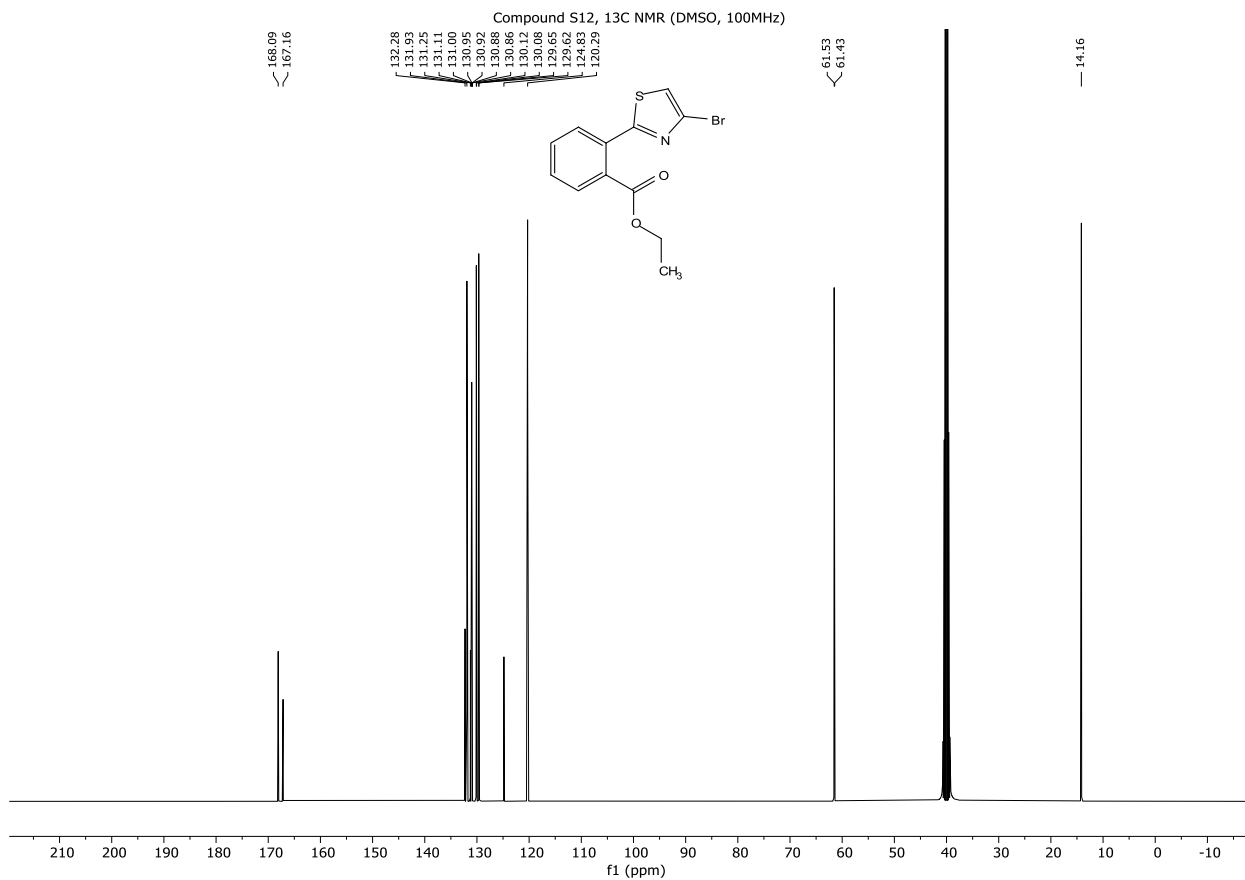
Totals : 5073.91406 1506.82288

=====
*** End of Report ***

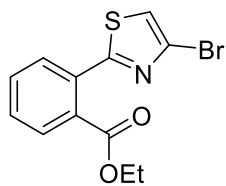
Supplementary Figure 48. 1H NMR of compound S12



Supplementary Figure 49. ¹³C NMR of compound S12

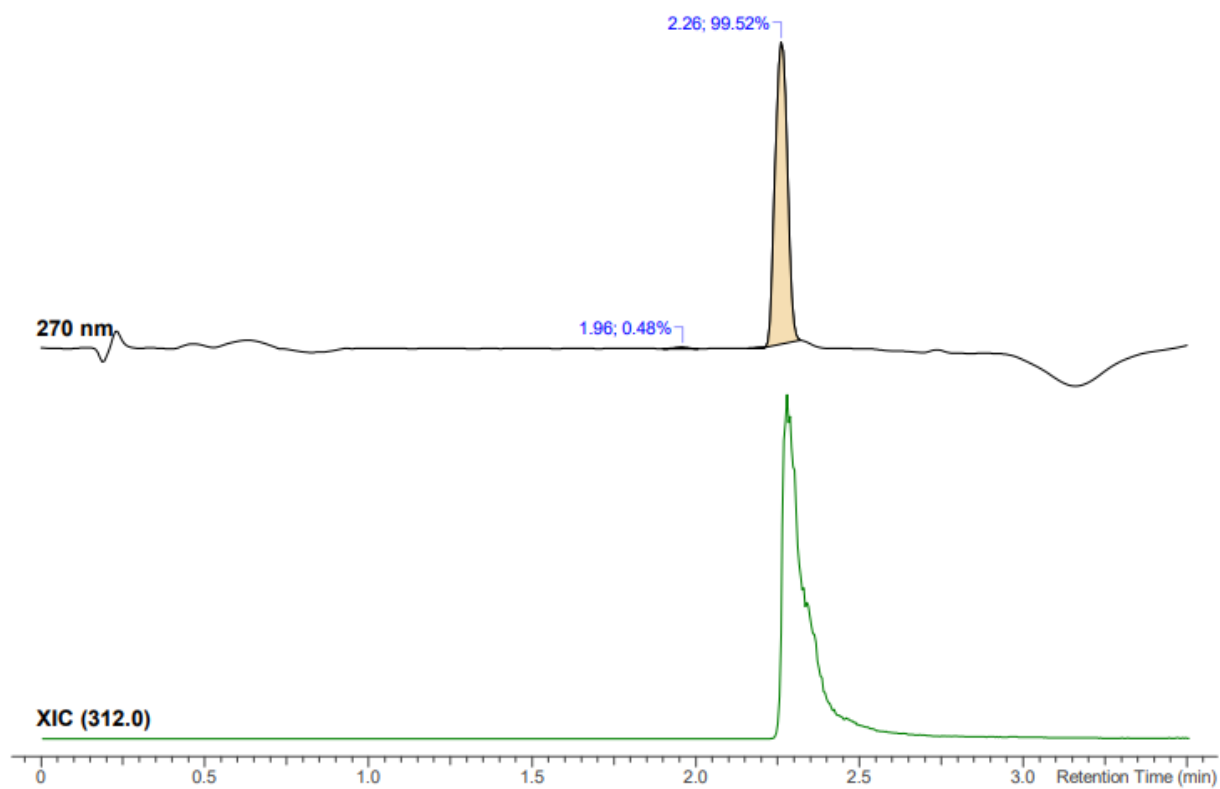


Supplementary Figure 50. HRMS of compound S12



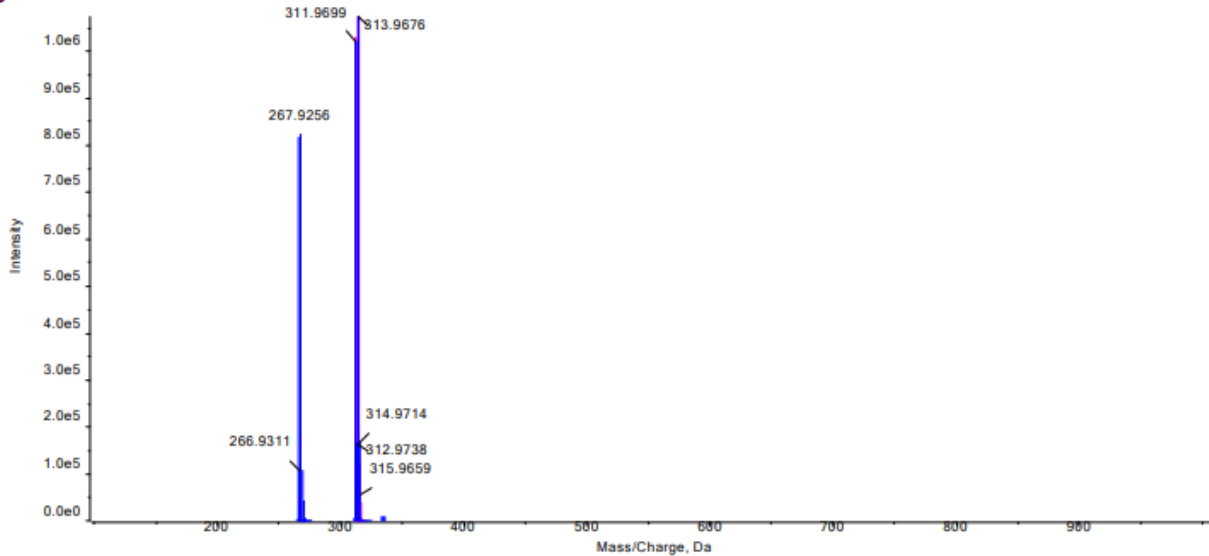
S12

Open Access HRMS Sample Report			
Sample ID	00711867-0388-001	HPLC	Agilent 1200
Molecular Formula	C ₁₂ H ₁₀ BrNO ₂ S	Mass Spectrometer	Sciex 5600+ QToF
Submittor	Martinez, Luis	DAD	190-400 nm, reported 270nm
Run Date	4/27/2023	MS Scan	100-2000 amu
Analyst	Quinn, Alandra	Acquisition Method	HRMS-3min gradient AQ
Analyst's CeN	00714673-0166	eWB Archive Ref	00713459-0294

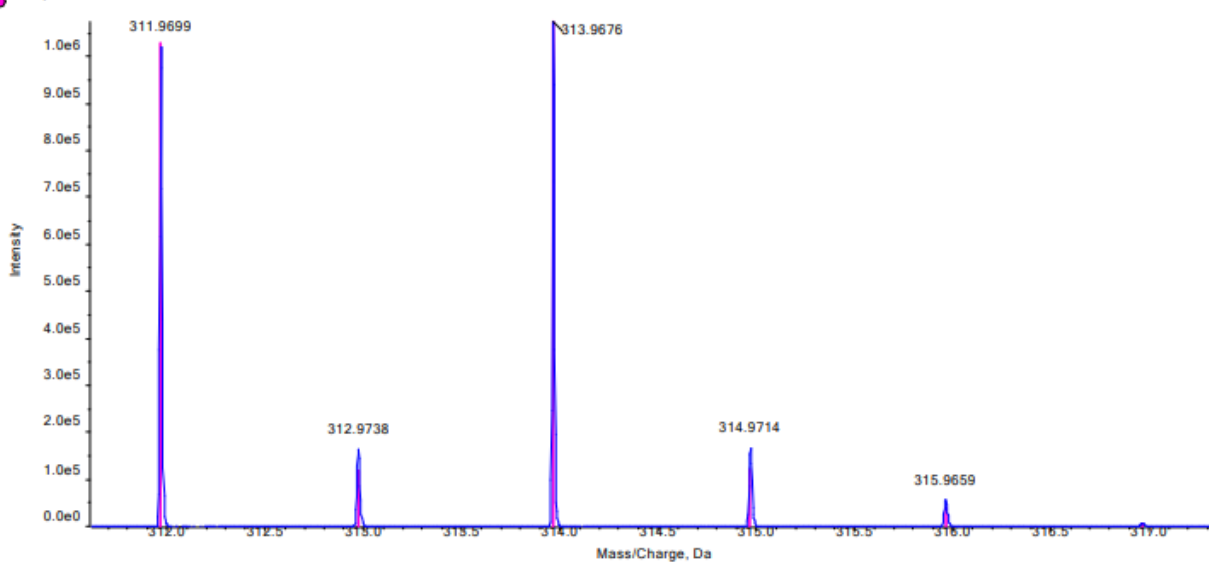


No.	Peak Name	tR (min)	Area (%)
1	unknown	1.96	0.48
2	C ₁₂ H ₁₀ BrNO ₂ S	2.26	99.52

● Spectrum from 00711867-0388-001.wiff (sample 1) - C12H10BrNO2S, +TOF MS (100 - 2000) from 2.264 to 2.325 min
 ● Isotopic Distribution for C12H10BrNO2S H +

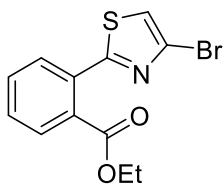


● Spectrum from 00711867-0388-001.wiff (sample 1) - C12H10BrNO2S, +TOF MS (100 - 2000) from 2.264 to 2.325 min
 ● Isotopic Distribution for C12H10BrNO2S H +



Peak at 2.26 min in UV								
Mass/Charge (Da)	Height	Relative % Height	Compound	Peak Type	Theoretical m/z	Error (ppm)	Theoretical m/z	Theoretical Intensity
311.9699	1021812	95.1	C12H10BrNO2S	[M+H] ⁺	311.9688	3.4	311.9688	97.0
312.9738	164442	15.3					312.9719	14.3
313.9676	1073990	100.0					313.9668	100.0
314.9714	166621	15.5					314.9698	14.6
315.9659	57382	5.3					315.9650	5.6

Supplementary Figure 51. HPLC of compound S12



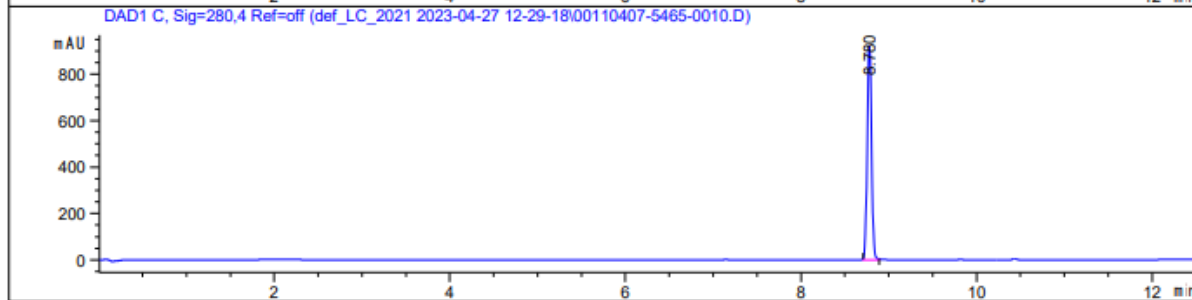
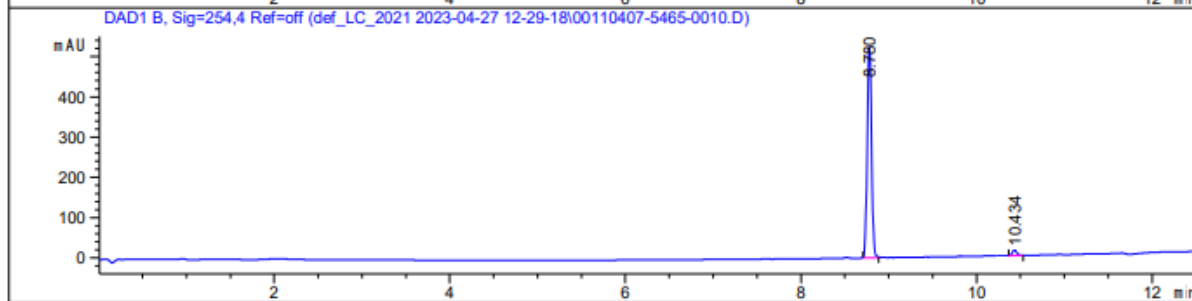
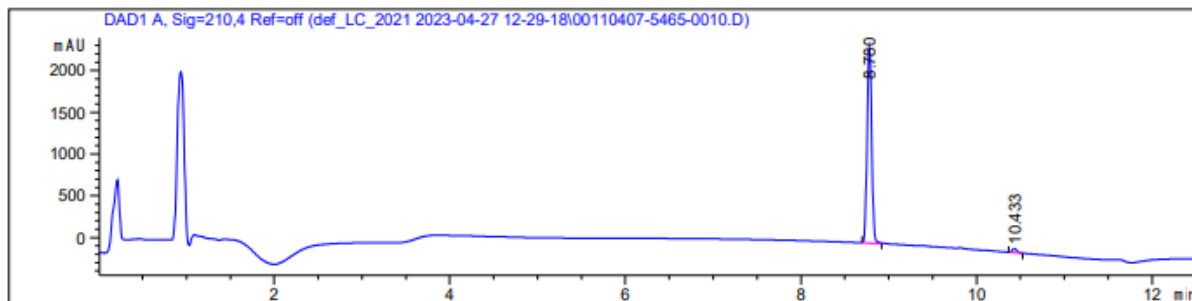
S12

```

=====
Acq. Operator   : SYSTEM                      Seq. Line :    5
Sample Operator : SYSTEM
Acq. Instrument : HPLC-233GA                 Location  :   10
Injection Date  : 4/27/2023 1:30:55 PM       Inj       :    1
                                           Inj Volume: 10.000 µl

Acq. Method     : C:\Users\Public\Documents\ChemStation\1\Data\def_LC_2021 2023-04-27 12-29-18\ACID_GRADIENT.M
Last changed    : 6/9/2021 9:16:24 AM by SYSTEM
Analysis Method : C:\Users\Public\Documents\ChemStation\1\Data\def_LC_2021 2023-04-27 12-29-18\ACID_GRADIENT.M (Sequence Method)
Last changed    : 4/28/2023 2:01:26 PM by SYSTEM
                 (modified after loading)

Method Info     : Column: XBridge C18 5 micron (4.6 mm x 150 mm)
                 Flow rate: 1.500 mL/min with solvents containing 0.1% TFA
                 0-1.5 min: 5% acetonitrile/water
                 1.5-10 min: 5-100% acetonitrile water
                 10-11 min: 100% acetonitrile
                 11-12.5 min: 100-5% acetonitrile/water
    
```



=====
 Area Percent Report
 =====

Sorted By : Signal
 Multiplier : 1.0000
 Dilution : 1.0000
 Do not use Multiplier & Dilution Factor with ISTDs

Signal 1: DAD1 A, Sig=210,4 Ref=off

Peak #	RetTime [min]	Type	Width [min]	Area [mAU*s]	Height [mAU]	Area %
1	8.780	BB	0.0568	8567.22363	2332.77637	97.9666
2	10.433	BB	0.0537	177.82544	52.29279	2.0334

Totals : 8745.04907 2385.06916

Signal 2: DAD1 B, Sig=254,4 Ref=off

Peak #	RetTime [min]	Type	Width [min]	Area [mAU*s]	Height [mAU]	Area %
1	8.780	BB	0.0542	1805.83240	523.63135	97.4147
2	10.434	BB	0.0533	47.92553	14.21884	2.5853

Totals : 1853.75793 537.85019

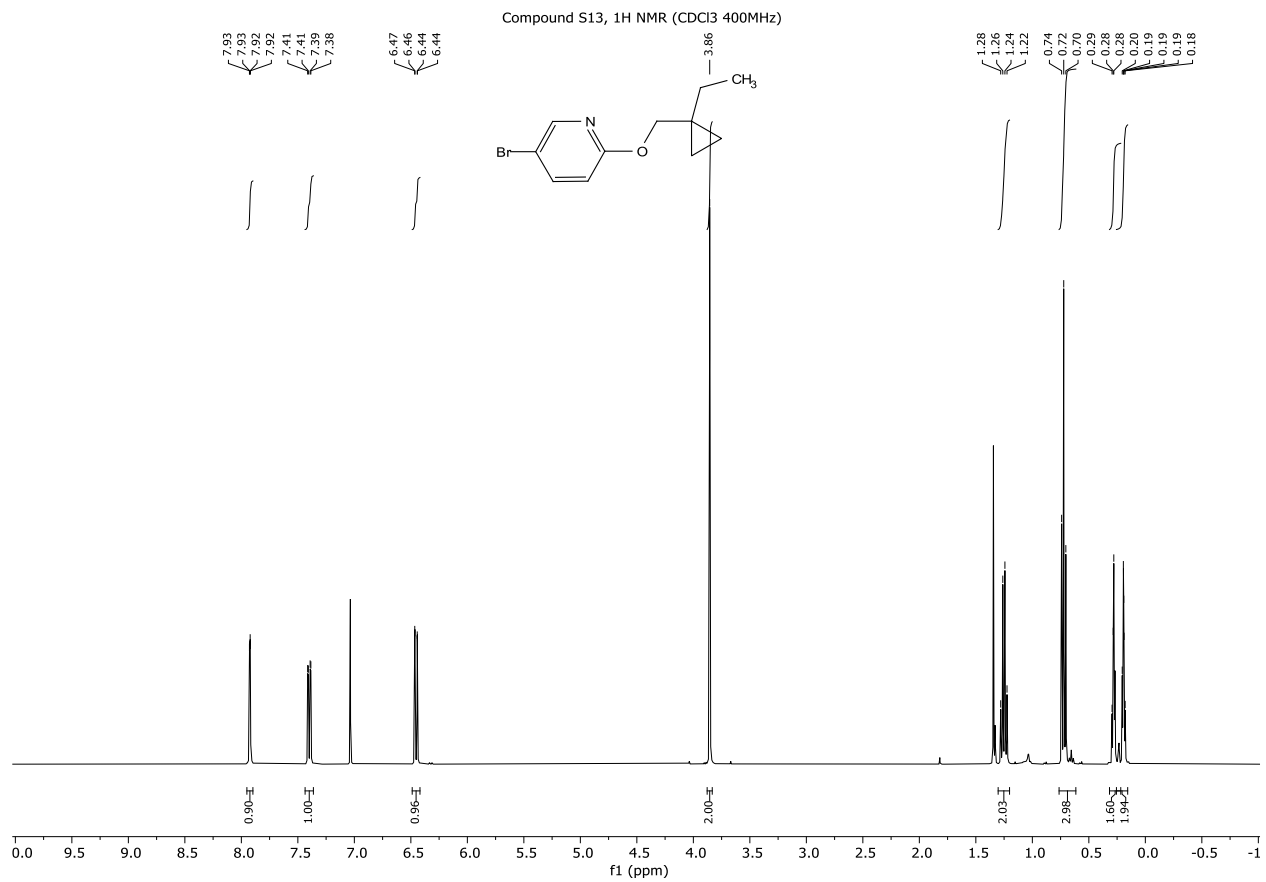
Signal 3: DAD1 C, Sig=280,4 Ref=off

Peak #	RetTime [min]	Type	Width [min]	Area [mAU*s]	Height [mAU]	Area %
1	8.780	BB	0.0543	3189.18506	923.13580	100.0000

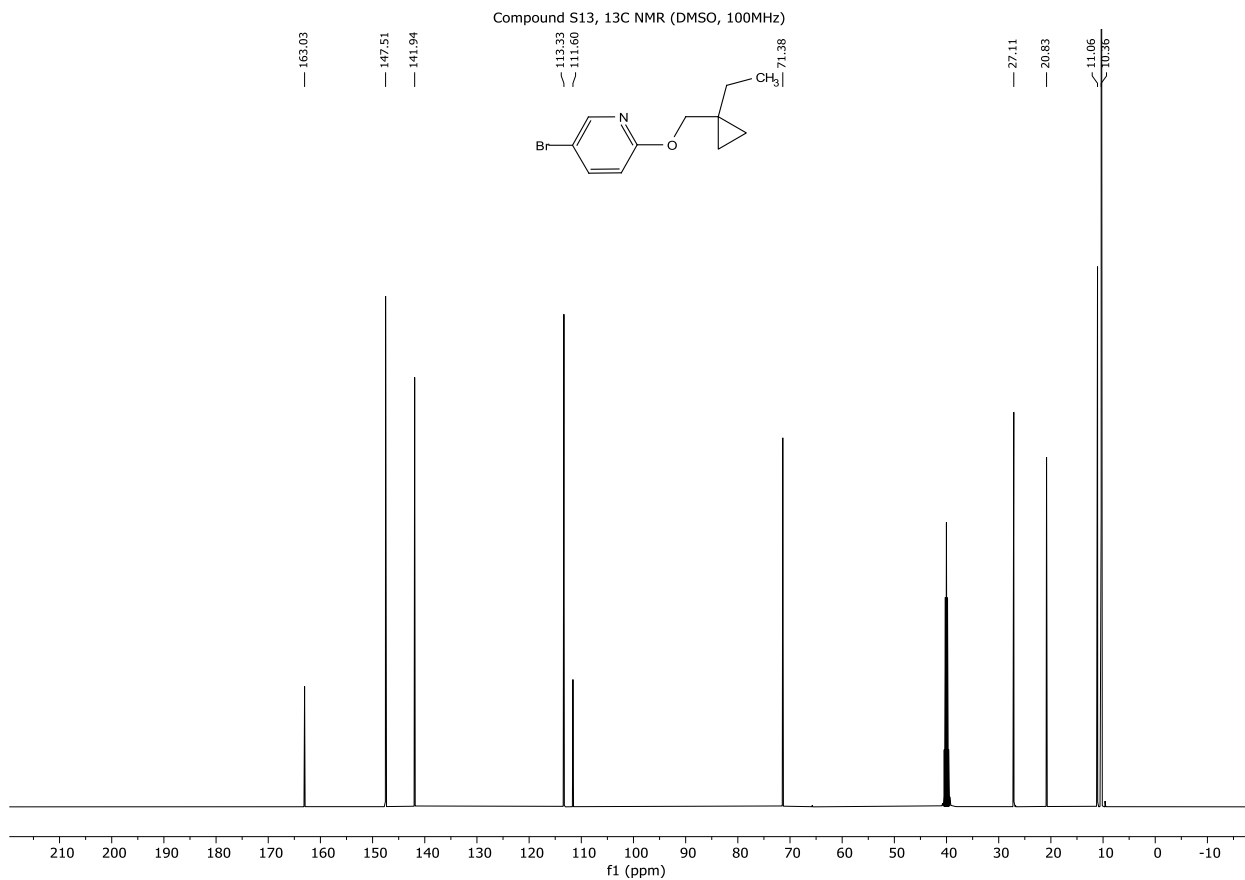
Totals : 3189.18506 923.13580

=====
 *** End of Report ***

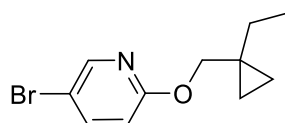
Supplementary Figure 52. 1H NMR of compound S13



Supplementary Figure 53. ¹³C NMR of compound S13

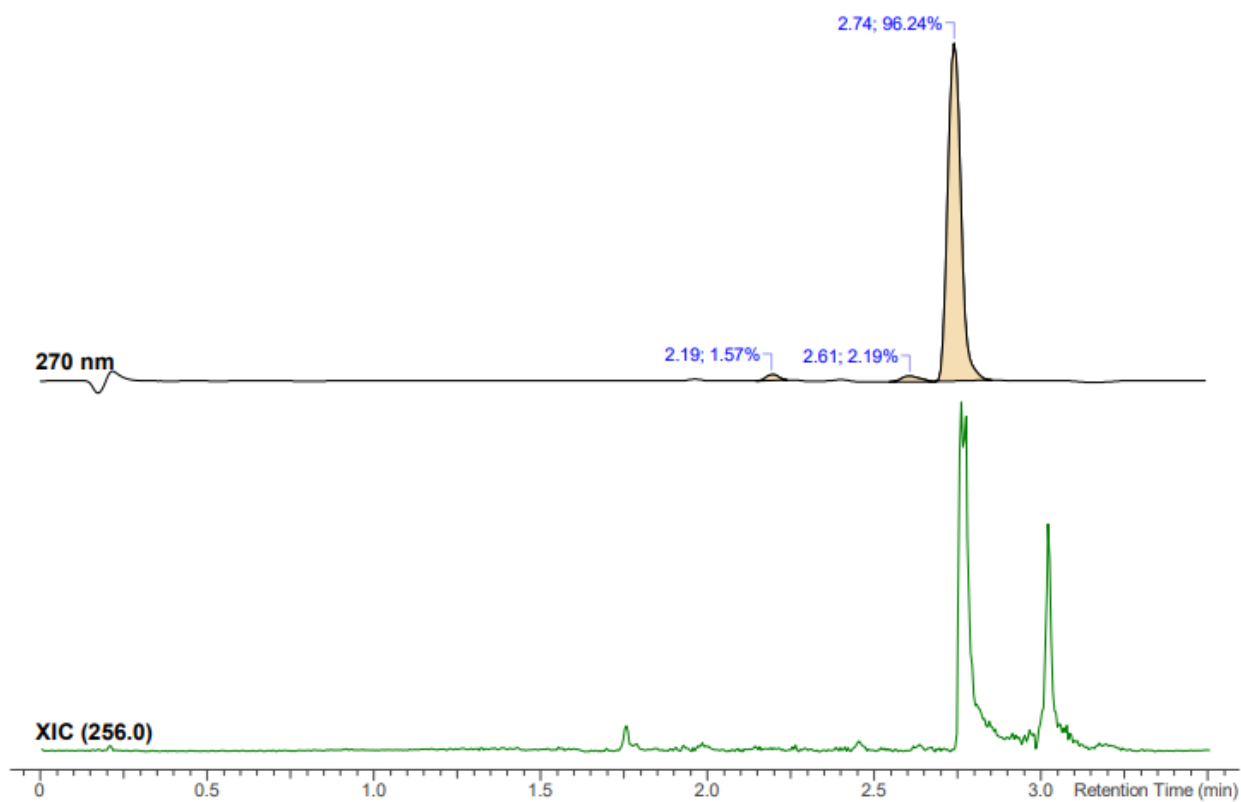


Supplementary Figure 54. HRMS of compound S13



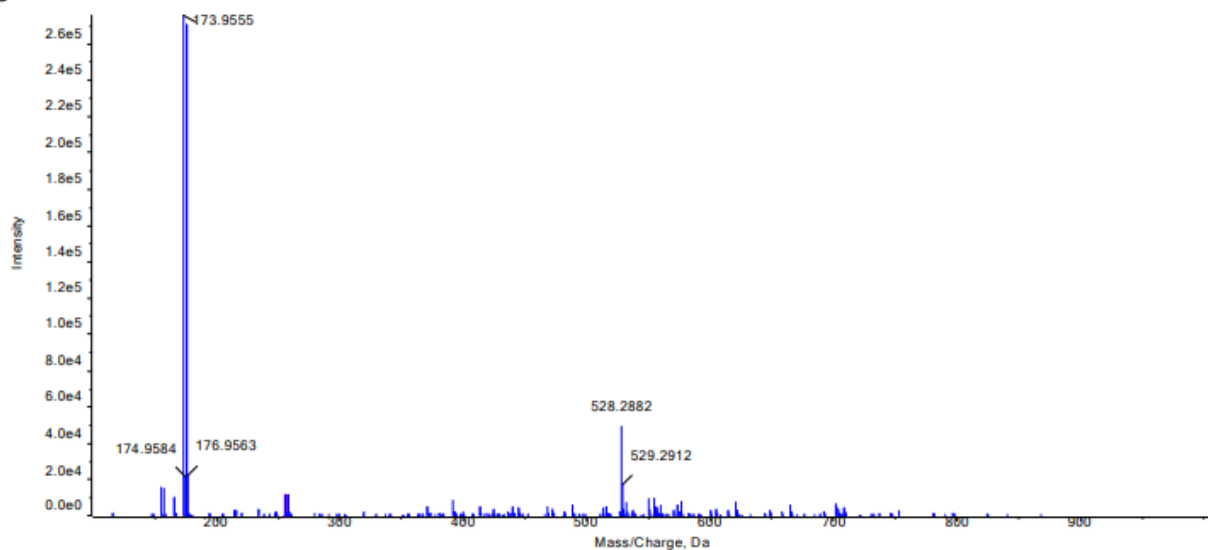
S13

Open Access HRMS Sample Report			
Sample ID	00180155-0098-001	HPLC	Agilent 1200
Molecular Formula	C ₁₁ H ₁₄ BrNO	Mass Spectrometer	Sciex 5600+ QToF
Submittor	Martinez, Luis	DAD	190-400 nm, reported 270nm
Run Date	4/27/2023	MS Scan	100-2000 amu
Analyst	Quinn, Alandra	Acquisition Method	HRMS-3min gradient AQ
Analyst's CeN	00714673-0166	eWB Archive Ref	00713459-0294

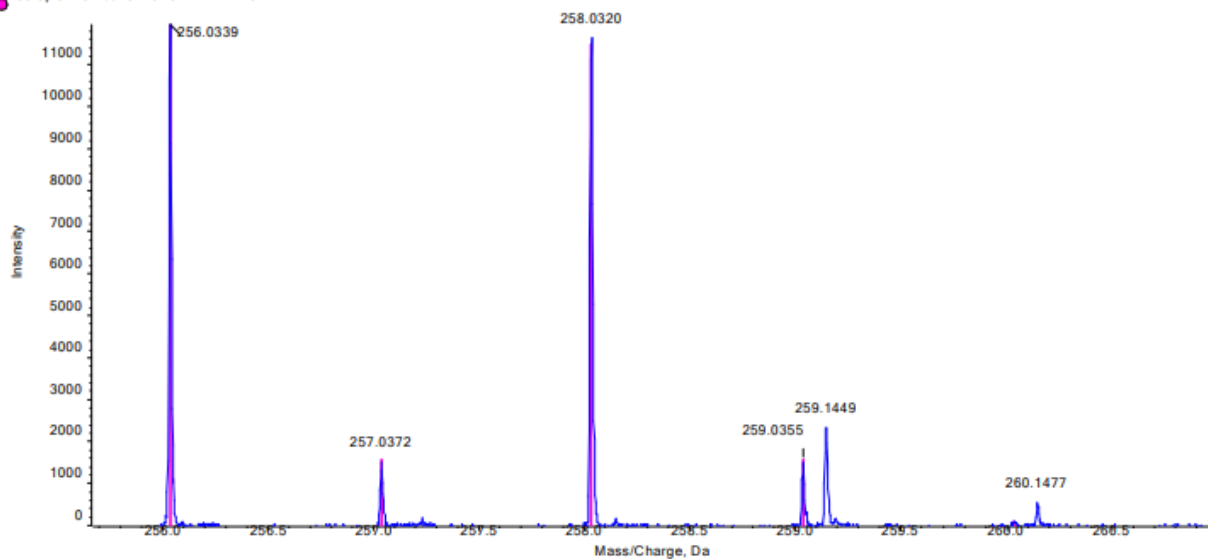


No.	Peak Name	tR (min)	Area (%)
1	unknown	2.19	1.57
2	unknown	2.61	2.19
3	C ₁₁ H ₁₄ BrNO	2.74	96.24

● Spectrum from 00180155-0098-001_5.wiff (sample 1) - C11H12BrNO, +TOF MS (100 - 2000) from 2.748 to 2.794 min
 ● Isotopic Distribution for C11H14BrNO H +



● Spectrum from 00180155-0098-001_5.wiff (sample 1) - C11H12BrNO, +TOF MS (100 - 2000) from 2.748 to 2.794 min
 ● Isotopic Distribution for C11H14BrNO H +



Peak at 2.74 min in UV								
Mass/Charge (Da)	Height	Relative % Height	Compound	Peak Type	Theoretical m/z	Error (ppm)	Theoretical m/z	Theoretical Intensity
256.0339	11951	100.0	C11H14BrNO	[M+H] ⁺	256.0332	2.8	256.0332	100.0
257.0372	1510	12.6					257.0364	12.8
258.0320	11641	97.4					258.0312	98.2
259.0355	1504	12.6					259.0343	12.5
260.0388	93	0.8					258.0214	0.9

=====
 Area Percent Report
 =====

Sorted By : Signal
 Multiplier : 1.0000
 Dilution : 1.0000
 Do not use Multiplier & Dilution Factor with ISTDs

Signal 1: DAD1 A, Sig=210,4 Ref=off

Peak #	RetTime [min]	Type	Width [min]	Area [mAU*s]	Height [mAU]	Area %
1	8.707	BB	0.0581	145.41386	38.43911	1.8333
2	9.411	BB	0.0953	91.78696	12.84769	1.1572
3	10.298	BB	0.0551	45.86970	13.01597	0.5783
4	10.637	BB	0.0550	7648.67236	2175.46094	96.4312

Totals : 7931.74288 2239.76370

Signal 2: DAD1 B, Sig=254,4 Ref=off

Peak #	RetTime [min]	Type	Width [min]	Area [mAU*s]	Height [mAU]	Area %
1	10.637	BB	0.0538	1003.27765	293.85690	100.0000

Totals : 1003.27765 293.85690

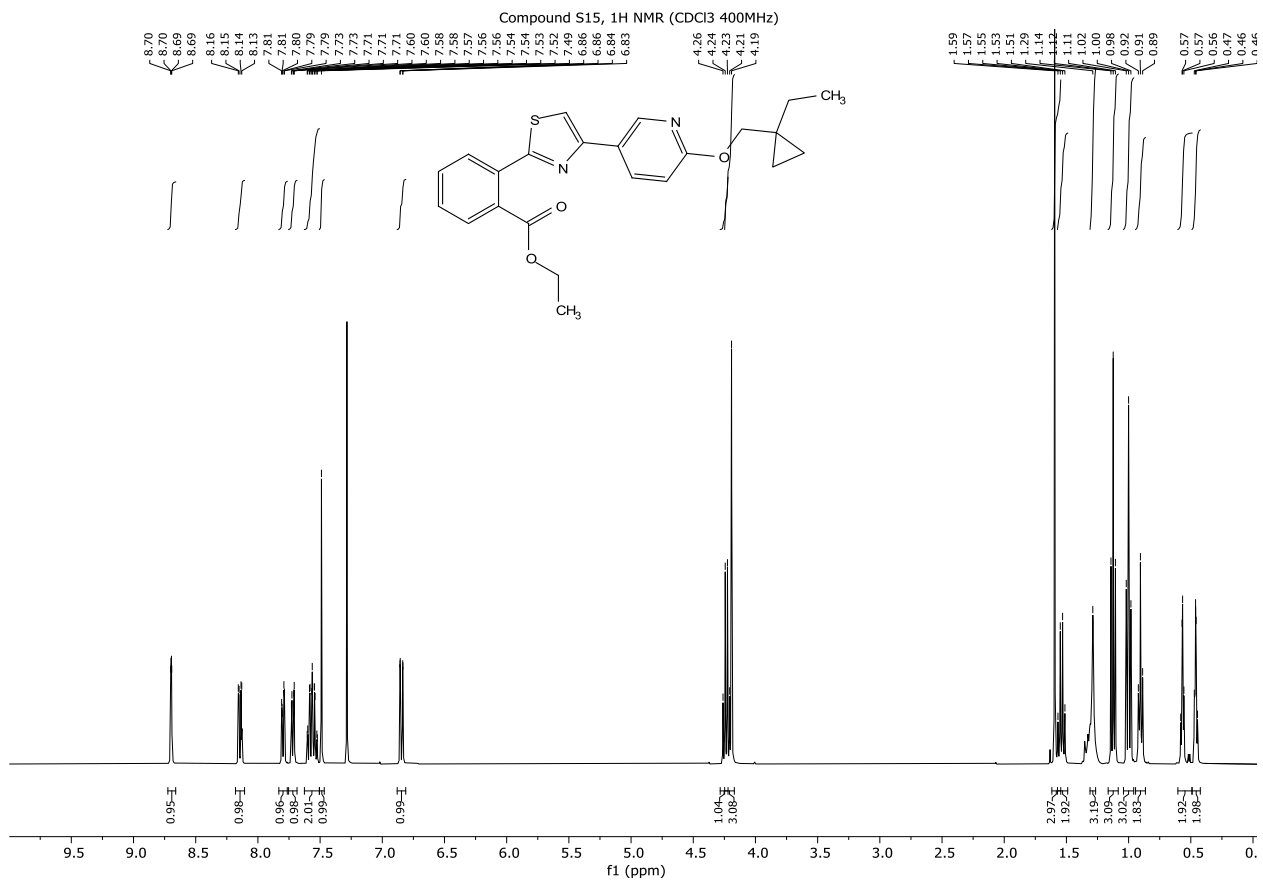
Signal 3: DAD1 C, Sig=280,4 Ref=off

Peak #	RetTime [min]	Type	Width [min]	Area [mAU*s]	Height [mAU]	Area %
1	8.708	BB	0.0569	83.47157	22.68753	1.7387
2	9.246	BB	0.0537	38.49805	11.30905	0.8019
3	10.637	BB	0.0540	4678.93945	1365.01904	97.4594

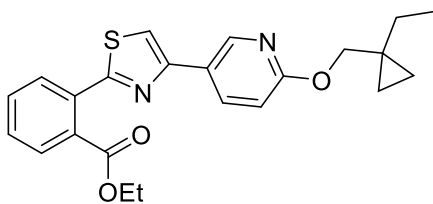
Totals : 4800.90908 1399.01562

=====
 *** End of Report ***

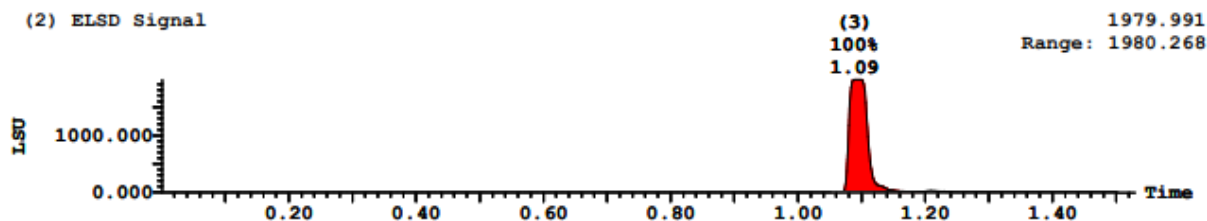
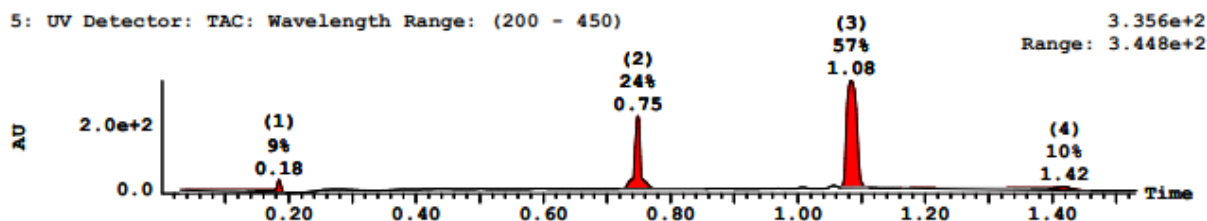
Supplementary Figure 56. 1H NMR of compound S15



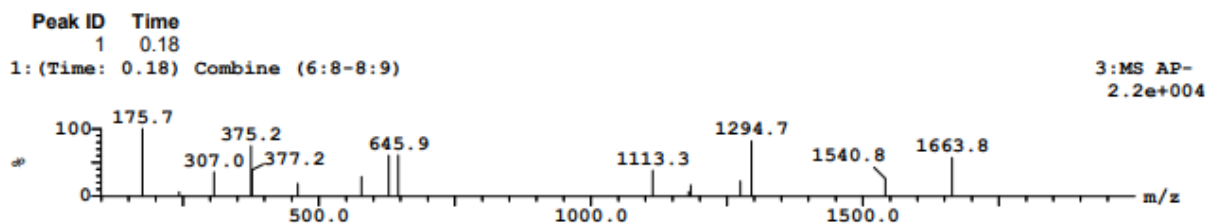
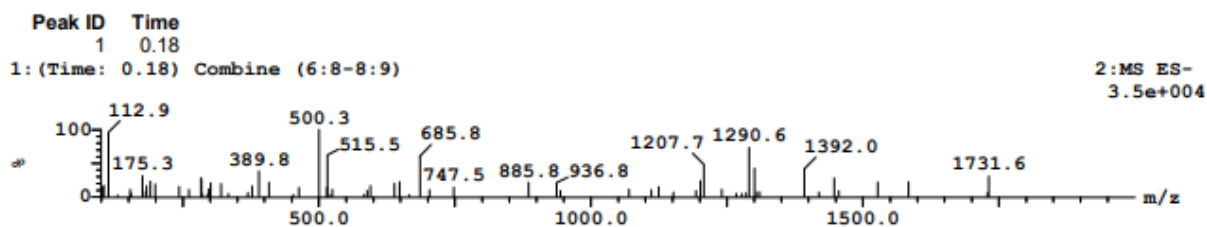
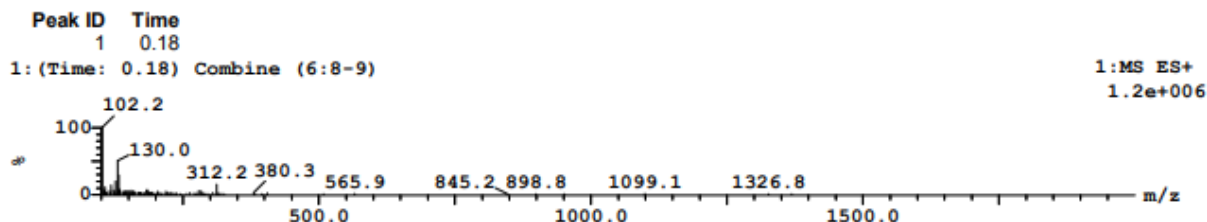
Supplementary Figure 57. LCMS of compound S15



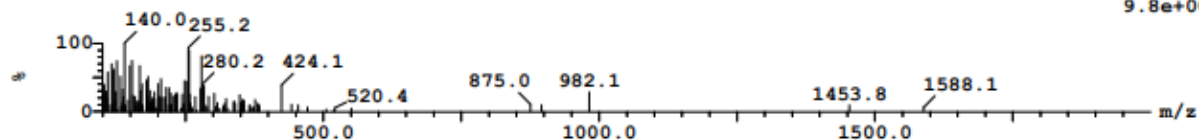
S15



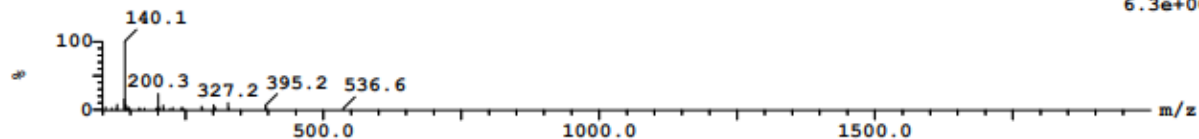
Peak ID	Time	Mass Found	AreaAbs	Area %Total
3	1.09	Not Found	65045	100.00



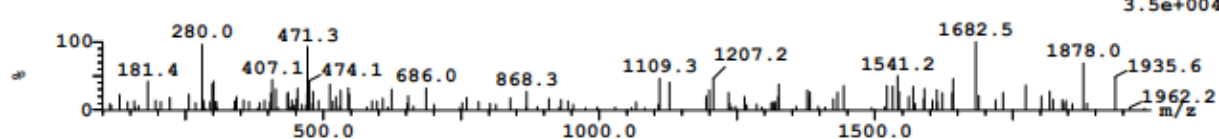
Peak ID Time
1 0.18
1: (Time: 0.18) Combine (6:7-8:9) 4:MS AP+
9.8e+004



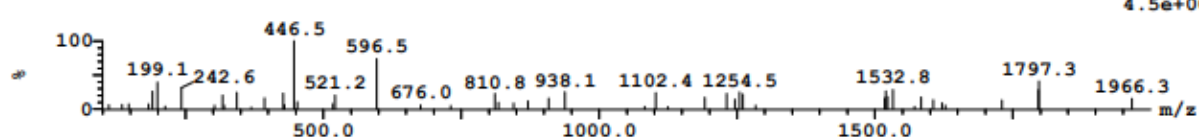
Peak ID Time
2 0.75
2: (Time: 0.75) Combine (26:28-(24:25+32:33)) 1:MS ES+
6.3e+006



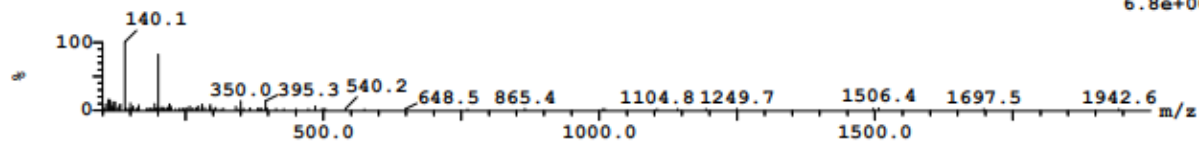
Peak ID Time
2 0.75
2: (Time: 0.75) Combine (26:28-(24:25+31:32)) 2:MS ES-
3.5e+004



Peak ID Time
2 0.75
2: (Time: 0.75) Combine (26:27-(24:25+31:32)) 3:MS AP-
4.5e+004



Peak ID Time
2 0.75
2: (Time: 0.75) Combine (25:27-(24+31:32)) 4:MS AP+
6.8e+005



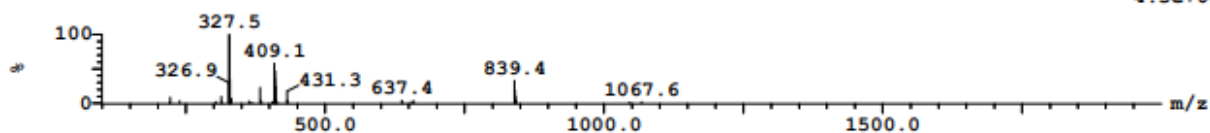
Peak ID Time

3 1.08

3: (Time: 1.09) Combine (38:40-(36:37+44))

1:MS ES+

4.5e+007



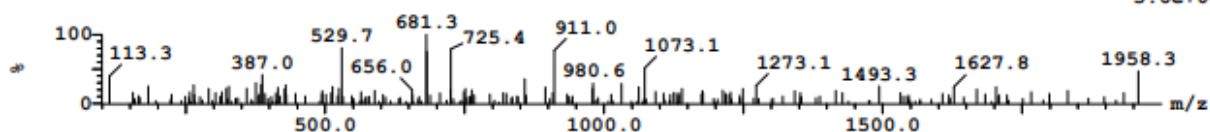
Peak ID Time

3 1.08

3: (Time: 1.09) Combine (38:40-(36:37+43:44))

2:MS ES-

5.6e+004



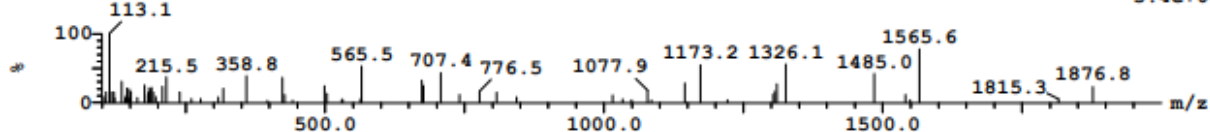
Peak ID Time

3 1.08

3: (Time: 1.09) Combine (38:39-(36+43:44))

3:MS AP-

5.4e+004



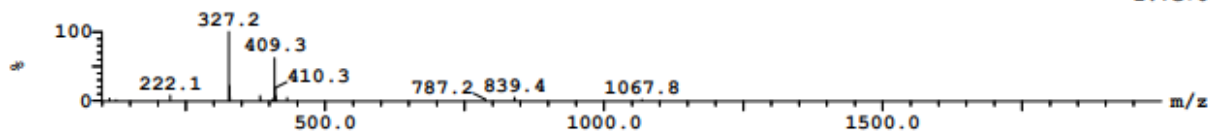
Peak ID Time

3 1.08

3: (Time: 1.09) Combine (37:39-(35:36+43:44))

4:MS AP+

1.7e+007



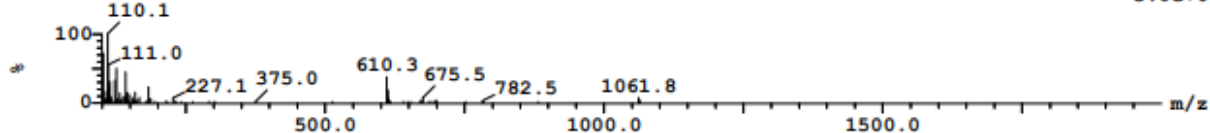
Peak ID Time

4 1.42

4: (Time: 1.42) Combine (50:52-40:41)

1:MS ES+

5.0e+006

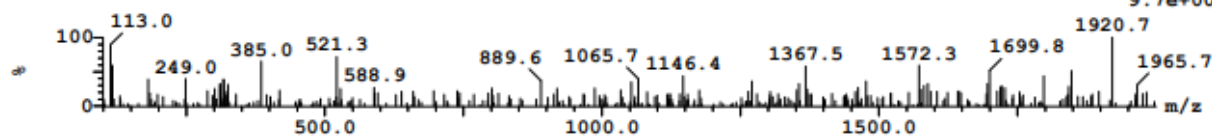


Peak ID Time

4 1.42

4: (Time: 1.42) Combine (50:51-(40+53))

2:MS ES-
9.7e+004

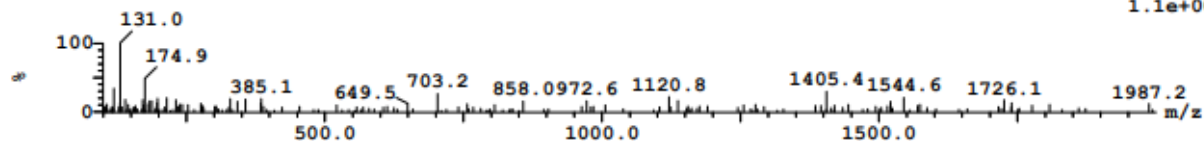


Peak ID Time

4 1.42

4: (Time: 1.42) Combine (49:51-(39:40+53))

3:MS AP-
1.1e+005

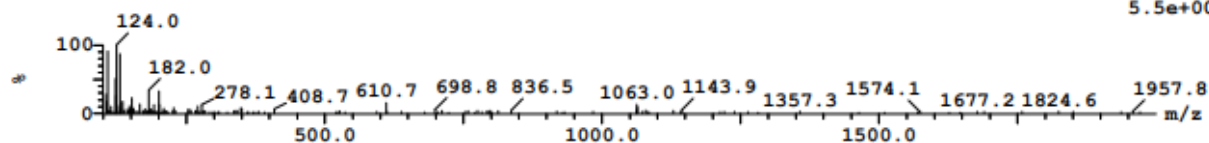


Peak ID Time

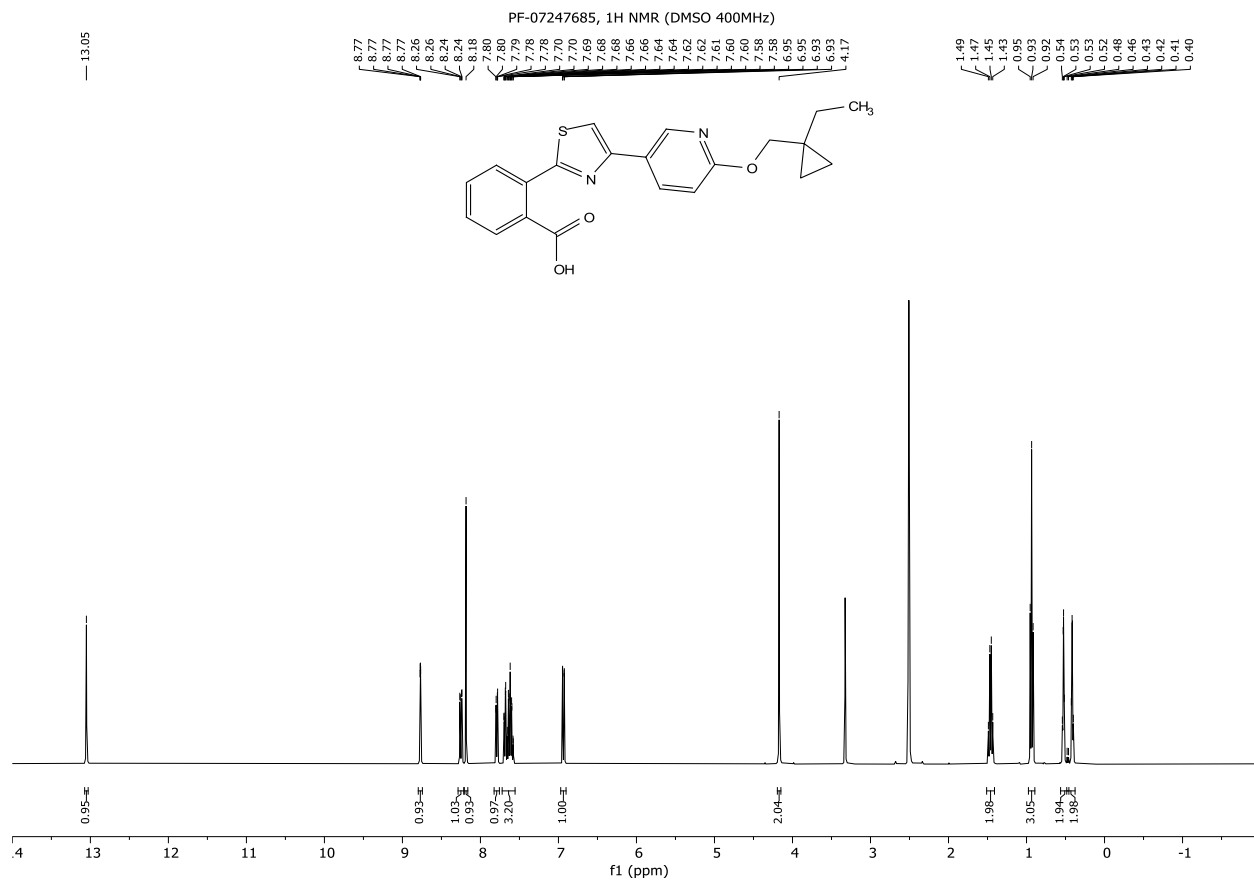
4 1.42

4: (Time: 1.42) Combine (49:51-(39:40+52:53))

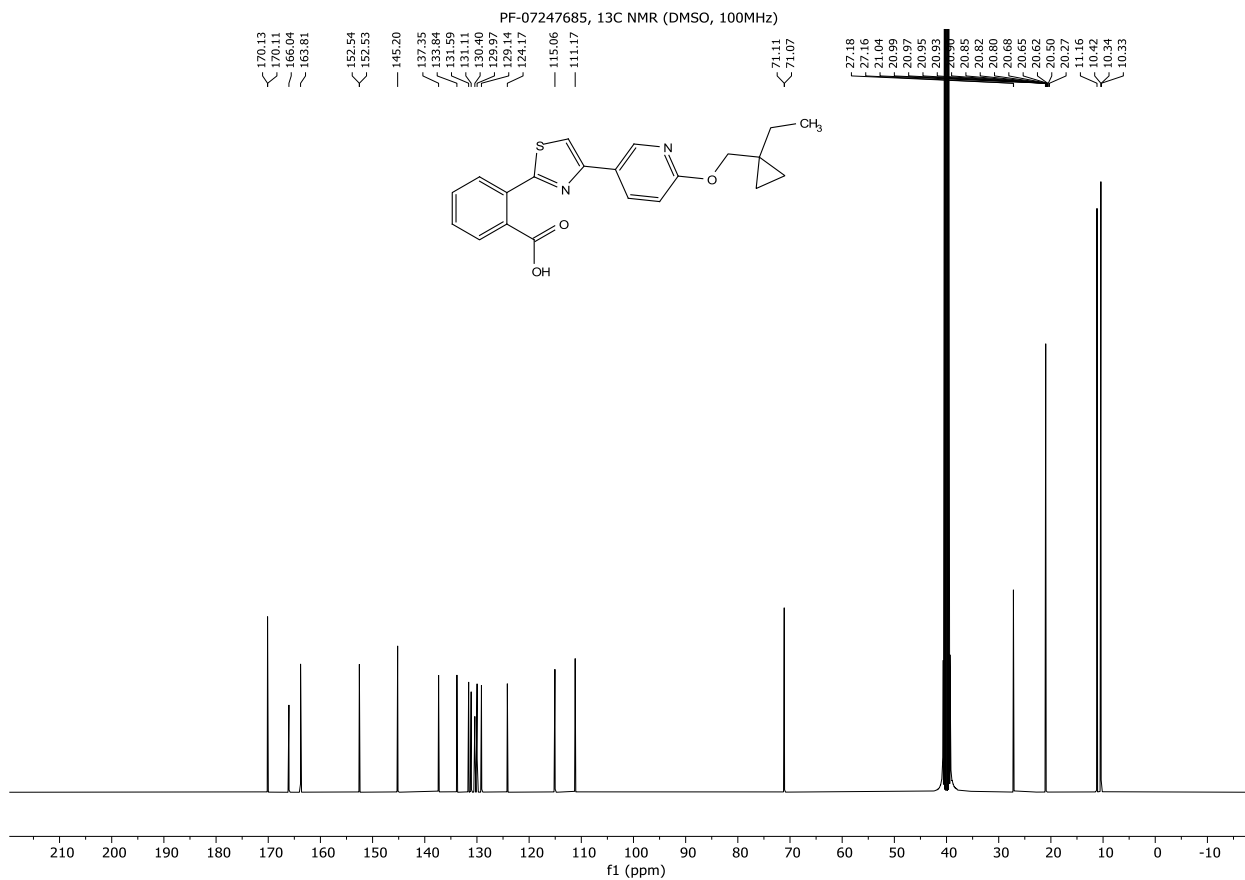
4:MS AP+
5.5e+005



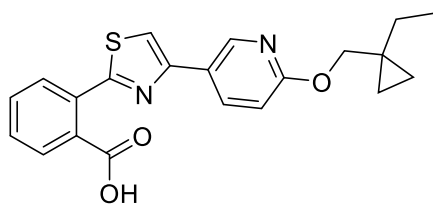
Supplementary Figure 58. 1H NMR of PF-07247685



Supplementary Figure 59. ¹³C NMR of PF-07247685

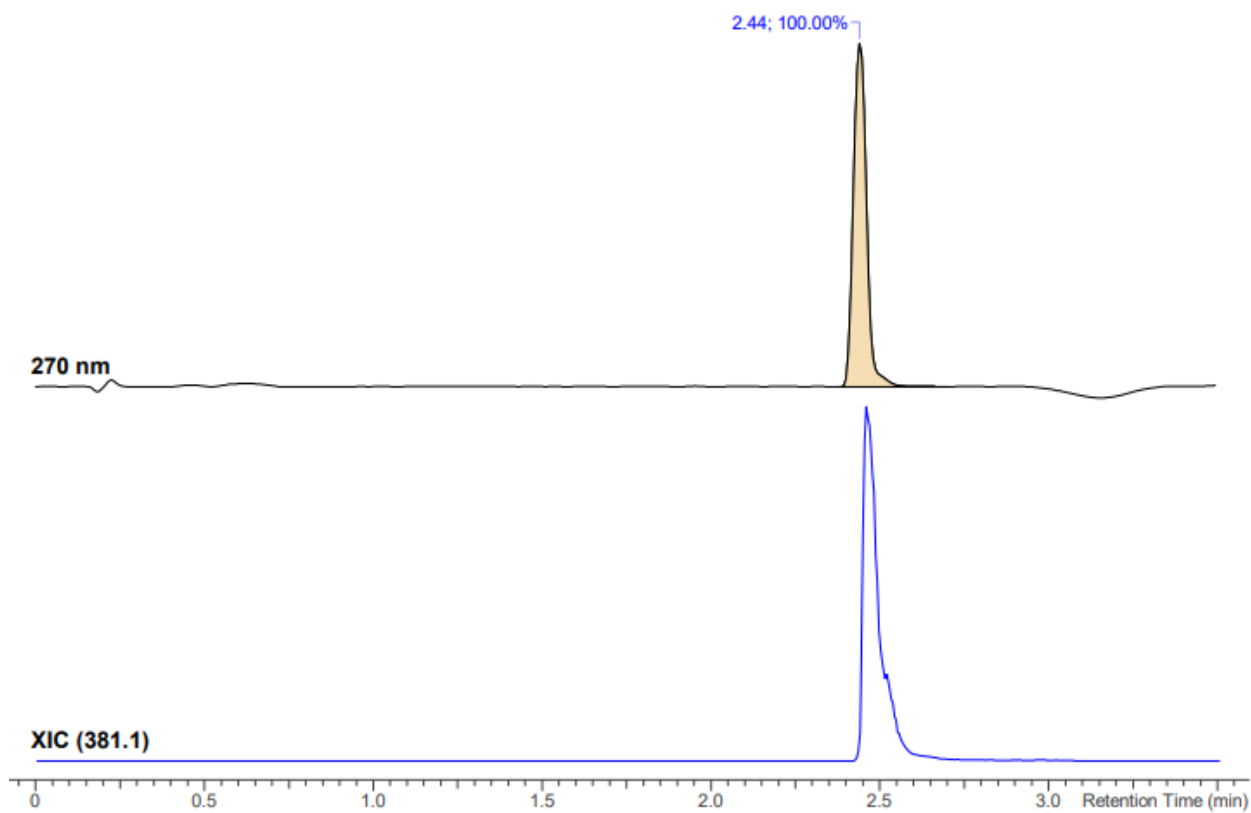


Supplementary Figure 60. HRMS of PF-07247685



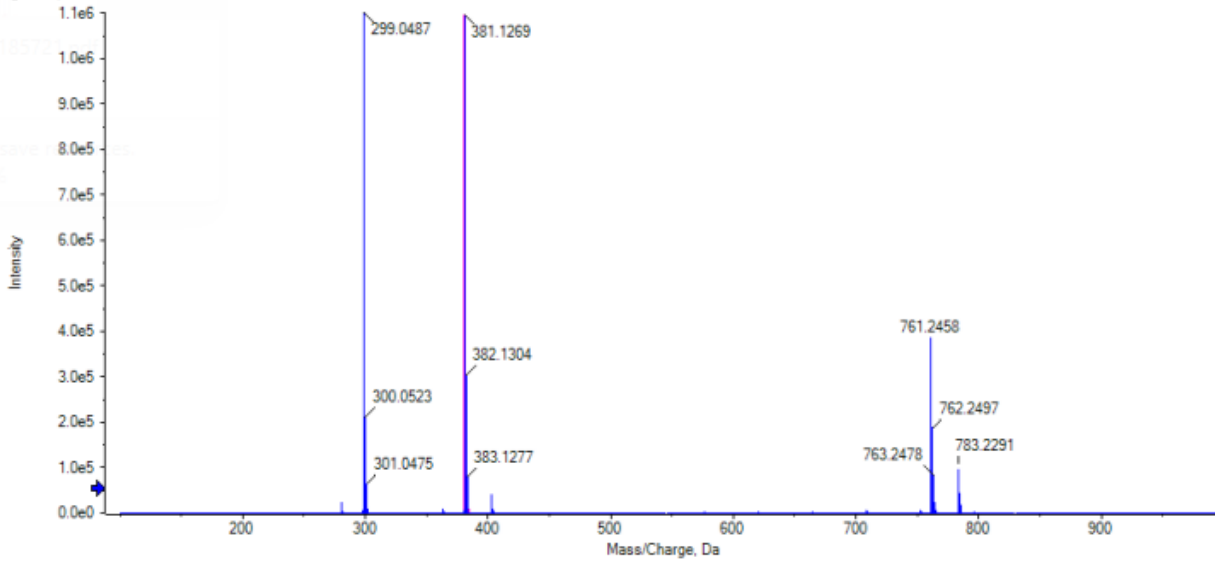
PF-07247685

Open Access HRMS Sample Report			
Sample ID	00712228-0051-001	HPLC	Agilent 1200
Molecular Formula	C ₂₁ H ₂₀ N ₂ O ₃ S	Mass Spectrometer	Sciex 5600+ QToF
Submittor	Martinez, Luis	DAD	190-400 nm, reported 270nm
Run Date	4/27/2023	MS Scan	100-2000 amu
Analyst	Quinn, Alandra	Acquisition Method	HRMS-3min gradient AQ
Analyst's CeN	00714673-0166	eWB Archive Ref	00713459-0294

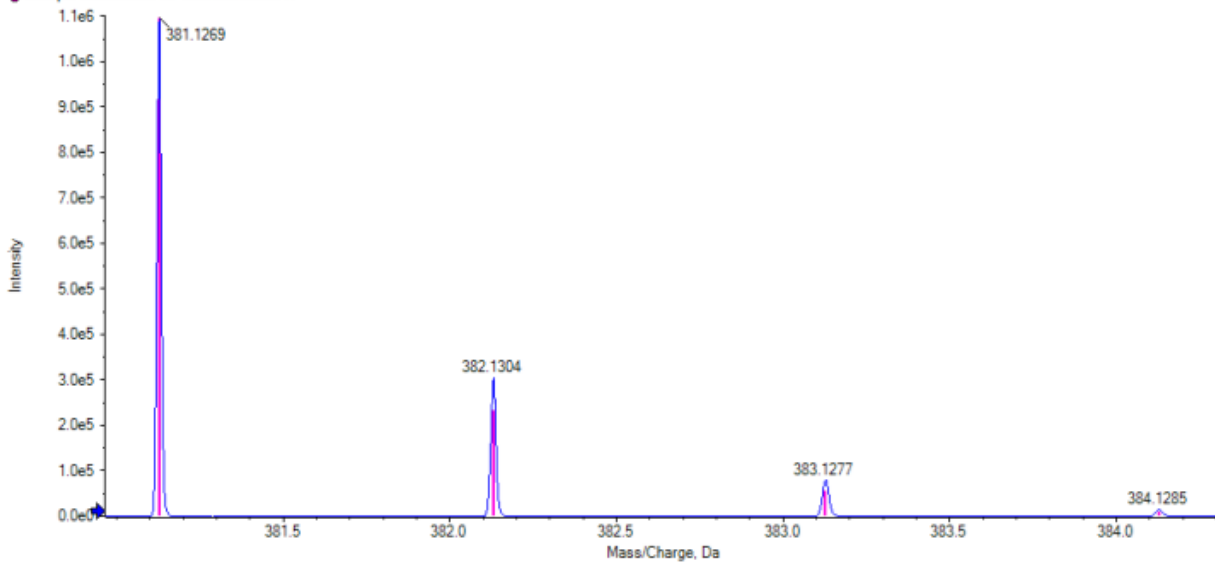


No.	Peak Name	tR (min)	Area (%)
1	C ₂₁ H ₂₀ N ₂ O ₃ S	2.44	100.00

● Spectrum from 00712228-0051-001.wiff (sample 1) - C₂₁H₂₀N₂O₃S, +TOF MS (100 - 2000) from 2.427 to 2.502 min
 ● Isotopic Distribution for C₂₁H₂₀N₂O₃S H⁺



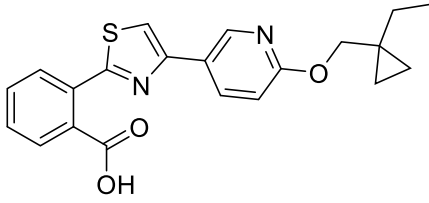
● Spectrum from 00712228-0051-001.wiff (sample 1) - C₂₁H₂₀N₂O₃S, +TOF MS (100 - 2000) from 2.427 to 2.502 min
 ● Isotopic Distribution for C₂₁H₂₀N₂O₃S H⁺



Peak at 2.44 min in UV

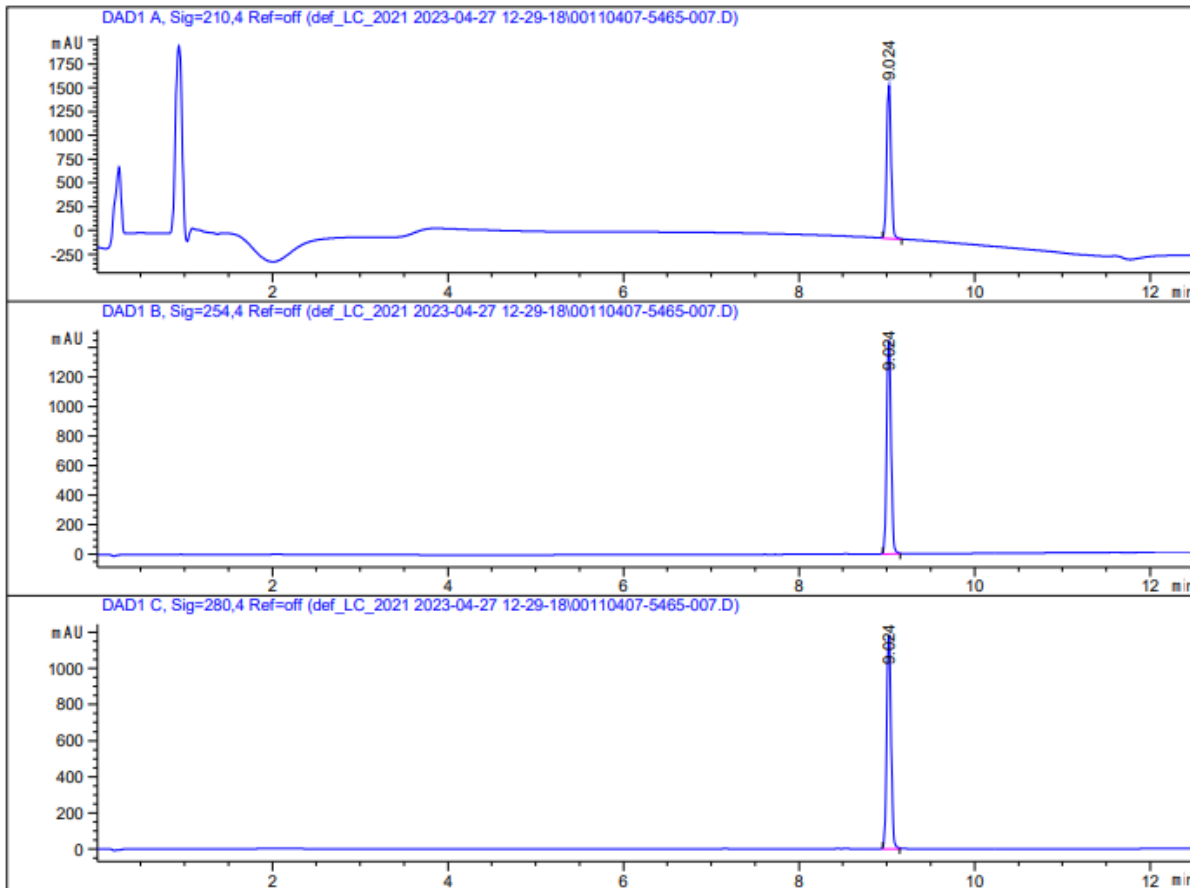
Mass/Charge (Da)	Height	Relative % Height	Compound	Peak Type	Theoretical m/z	Error (ppm)	Theoretical m/z	Theoretical Intensity
381.1269	1097286	100.0	C ₂₁ H ₂₀ N ₂ O ₃ S	[M+H] ⁺	381.1267	0.3	381.1267	100.0
382.1304	304353	27.7					382.1298	25.2
383.1277	79446	7.2					383.1271	8.1
384.1285	14392	1.3					384.1282	1.5

Supplementary Figure 61. HPLC of PF-07247685



PF-07247685

=====
Acq. Operator : SYSTEM Seq. Line : 2
Sample Operator : SYSTEM
Acq. Instrument : HPLC-233GA Location : 7
Injection Date : 4/27/2023 12:48:32 PM Inj : 1
Inj Volume : 10.000 µl
Acq. Method : C:\Users\Public\Documents\ChemStation\1\Data\def_LC_2021 2023-04-27 12-29-18\ACID_GRADIENT.M
Last changed : 6/9/2021 9:16:24 AM by SYSTEM
Analysis Method : C:\Users\Public\Documents\ChemStation\1\Data\def_LC_2021 2023-04-27 12-29-18\ACID_GRADIENT.M (Sequence Method)
Last changed : 4/28/2023 2:01:26 PM by SYSTEM
(modified after loading)
Method Info : Column: XBridge C18 5 micron (4.6 mm x 150 mm)
Flow rate: 1.500 mL/min with solvents containing 0.1% TFA
0-1.5 min: 5% acetonitrile/water
1.5-10 min: 5-100% acetonitrile water
10-11 min: 100% acetonitrile
11-12.5 min: 100-5% acetonitrile/water



=====
Area Percent Report
=====

Sorted By : Signal
Multiplier : 1.0000
Dilution : 1.0000
Do not use Multiplier & Dilution Factor with ISTDs

Signal 1: DAD1 A, Sig=210,4 Ref=off

Peak #	RetTime [min]	Type	Width [min]	Area [mAU*s]	Height [mAU]	Area %
1	9.024	BB	0.0549	5616.75732	1601.76013	100.0000

Totals : 5616.75732 1601.76013

Signal 2: DAD1 B, Sig=254,4 Ref=off

Peak #	RetTime [min]	Type	Width [min]	Area [mAU*s]	Height [mAU]	Area %
1	9.024	BB	0.0546	5052.00098	1450.17712	100.0000

Totals : 5052.00098 1450.17712

Signal 3: DAD1 C, Sig=280,4 Ref=off

Peak #	RetTime [min]	Type	Width [min]	Area [mAU*s]	Height [mAU]	Area %
1	9.024	BB	0.0546	4133.79639	1187.12280	100.0000

Totals : 4133.79639 1187.12280

=====
*** End of Report ***
=====